Hawaii Ocean Time-series
Data Report 7: 1995

November 1996

David Karl
Luis Tupas
Fernando Santiago-Mandujano
Craig Nosse
Dale Hebel
Eric Firing
Roger Lukas

University of Hawaii
School of Ocean and Earth Science and Technology
1000 Pope Road
Honolulu, Hawaii 96822
U. S.A.

SOEST 96-09

PREFACE

Scientists working on the Hawaii Ocean Time-series (HOT) program have been making repeated observations of the hydrography, chemistry and biology of the water column at a station north of Oahu, Hawaii since October 1988. The objective of this research is to provide a comprehensive description of the ocean at a site representative of the North Pacific subtropical gyre. Cruises are made approximately once a month to the HOT deep-water station (22°45'N, 158°00'W) located about 100 km north of Oahu, Hawaii. Measurements of the thermohaline structure, water column chemistry, currents, primary production and particle sedimentation rates are made on each cruise.

This document reports the data collected in 1995. However, we have included some data from 1988-1993 to place the 1995 measurements within the context of our ongoing time-series observations. The data reported here are a screened subset of the complete data set. Summary plots are given for CTD, biogeochemical, optical, meteorological, thermosalinograph, inverted echo sounder and ADCP observations.

In order to provide easy computer access to our data, CTD data at National Oceanographic Data Center (NODC) standard pressures for temperature, potential temperature, salinity, oxygen and potential density are provided in ASCII files on the enclosed diskette. Chemical measurements are also summarized in a set of Lotus-123™ files on the enclosed diskette. The complete data set resides on a Sun workstation at the University of Hawaii. These data are in ASCII format, and can easily be accessed using anonymous file transfer protocol (ftp) via Internet or the World Wide Web (WWW). Instructions for using the Lotus files and for obtaining the data from the network are presented in Chapter 8. The entire data set is available at NODC.

ACKNOWLEDGMENTS

Many people participated in the 1995 cruises sponsored by the HOT program. They are listed in Table 1.6. We gratefully acknowledge their contributions and support. Thanks are due to Lance Fujieki, Daniel Sadler, Terrence Houlihan, Mai Lopez, Molly Lucas, Robert Miller and Jefrey Snyder for participating in most of the 1995 cruises and for the tremendous amount of time and effort they have put into the program. Special thanks are given to Lisa Lum for her excellent administrative support of the program, to Sharon DeCarlo and Lance Fujieki for programming and data management, Carolyn Leong for CTD processing and to June Firing and Xiaomei Zhou for ADCP processing. Ursula Magaard performed many of the core chemical analyses. Ted Walsh, Terry Houlihan and Georgia Tien performed the nutrient analyses, Jinchun Yuan and Molly Lucas performed the salinity measurements and Jason Killam and Tuan Huynh provided additional technical support. We gratefully acknowledge the support from Nordeen Larson and Ken Lawson of Sea-Bird for helping us to maintain the quality of the CTD data throughout the HOT program. We also would like to thank the captain and crew members of the R/V *Moana Wave* and the UH Marine Center staff for their efforts. Without the assistance of these people, the data presented in this report could not have been collected, processed, analyzed and reported.

This data set was acquired with funding from the National Science Foundation (NSF) and State of Hawaii general funds. The specific grants which have supported this work are NSF grants OCE-9303094 (WOCE), and OCE-9301368 (JGOFS). We also acknowledge the contributions of Yuan Hui Li (OCE-9315392), Michael Landry (OCE-9218152) and Robert Bidigare (OCE-9315311) and their staff to the scientific efforts of HOT.

Weather buoy data used in this report were obtained by the NOAA National Data Buoy Center (NDBC) and were provided to us by the National Oceanographic Data Center (NODC). We thank Pat Caldwell for his assistance.

1. INTRODUCTION

1.1. Oceanic Time-series Measurements

Systematic, long-term time-series studies of selected aquatic and terrestrial habitats have yielded significant contributions to earth and ocean sciences through the characterization of climate trends. Important examples include the recognition of acid rain (Hubbard Brook long-term ecological study, Vermont; Likens et al., 1977), the documentation of increasing carbon dioxide (CO_2) in the earth's atmosphere (Mauna Loa Observatory, Hawaii; Keeling et al., 1976) and the description of large scale ocean-atmosphere climate interactions in the equatorial Pacific Ocean (Southern Oscillation index; Troup, 1965).

Long time-series observations of climate-relevant variables in the ocean are extremely important, yet they are rare. Repeated oceanographic measurements are required to gain an understanding of natural processes or phenomena that exhibit slow or irregular change, as well as rapid event-driven variations that are impossible to document reliably from a single field expedition. Time-series studies are also ideally suited for the documentation of complex natural phenomena that are under the combined influence of physical, chemical and biological controls. Examination of data derived from the few long-term oceanic time-series that do exist provides ample incentive and scientific justification to establish additional study sites (Wiebe et al., 1987).

The role of the oceans in climate variability is primarily in the sequestration and transportation of heat and carbon (Barnett, 1978). Both can be introduced into the ocean in one place, only to return to the atmosphere, at a subsequent time, possibly at a distant location. While both heat and carbon can be exchanged with the atmosphere only carbon is lost to the seafloor through sedimentation. The oceans are known to play a central role in regulating the global concentration of CO_2 in the atmosphere (Sarmiento and Toggweiler, 1984; Dymond and Lyle, 1985). It is generally believed that the world ocean has removed a significant portion of anthropogenic CO_2 added to the atmosphere, although the precise partitioning between the ocean and terrestrial spheres is not well constrained (Tans et al., 1990; Quay et al., 1992; Keeling and Shertz, 1992).

The cycling of carbon within the ocean is controlled by a set of reversible, reduction-oxidation reactions involving dissolved inorganic carbon (DIC) and dissolved organic carbon (DOC) with marine biota serving as the critical catalysts. Detailed information on the rates and mechanisms of removal of DIC from the surface ocean by biological processes, the export of biogenic carbon (both as organic and carbonate particles) to the ocean's interior, and the sites of remineralization and burial are all of considerable importance in the carbon cycle. The continuous downward flux of biogenic materials, termed the "biological pump" (Volk and Hoffert, 1985; Longhurst and Harrison, 1989), is a central component of all contemporary studies of biogeochemical cycling in the ocean and, therefore, of all studies of global environmental change.

During the embryonic phase of ocean exploration more than a century ago (Thomson, 1877), it was realized that a comprehensive understanding of the oceanic habitat and its biota would require a multidisciplinary experimental approach and extensive field observations. Progress toward this goal has been limited by natural habitat variability, both in space and time, and by logistical constraints of ship-based sampling. Consequently, our current view of many

complex oceanographic processes is likely biased (e.g., Dickey, 1991; Wiggert et al., 1994). The synoptic and repeat perspective that is now available from research satellites is expected to improve our understanding of oceanic variability, despite certain limitations.

In 1988, two deep ocean time-series hydrostations were established with support from the U.S. National Science Foundation (NSF): one in the western North Atlantic Ocean near the historical Panulirus Station (Bermuda Atlantic Time-series Study [BATS]; Michaels and Knap, 1996) and the other in the subtropical North Pacific Ocean near Hawaii (Hawaii Ocean Time-series [HOT]; Karl and Lukas, 1996). These programs were established and are currently operated by scientists at Bermuda Biological Station for Research and the University of Hawaii, respectively.

The primary research objectives of these ocean measurement programs are to establish and maintain deep-water hydrostations for observing and interpreting physical and biogeochemical variability. The initial design called for repeat measurements of a suite of core parameters at approximately monthly intervals, compilation of the data and rapid distribution to the scientific community.

1.2. HOT Station ALOHA: Roots and Branches

A deep-ocean weather station network was established in the post-World War II period as a ship-based observation program designed to improve global weather prediction capabilities. One of the sites, Station November, was located in the eastern sector of the North Pacific Ocean gyre at 30°N, 140°W and was occupied during 121 cruises between July 1966 and May 1974. The intercruise frequency ranged from a few days to a few weeks with a typical cruise duration of 2-3 weeks, including transits. Water samples were collected from approximately 12-14 depths in the range of 0-1500 m using bottles equipped with deep-sea reversing thermometers. Salinity and, on occasion, dissolved oxygen concentrations were measured from the discrete water samples.

During the 1970s, most of the U.S. weather ship stations were phased out of operation and were eventually replaced with more cost-effective, unattended ocean buoys. These buoys measure standard meteorological parameters as well as basic wave characteristics (e.g., significant wave direction, height, period and spectrum) but few, if any, hydrographic variables.

Physical and biogeochemical time-series investigations of the North Pacific subtropical region are sparse (Figure 1.1) and consist of a series of unrelated research programs including CLIMAX, GOLLUM, NORPAX, VERTEX, ADIOS and most recently HOT. CLIMAX I occupied a series of stations near 28°N, 155°W during August-September 1968 and CLIMAX II reoccupied the site during September of the following year. Since that time, scientists from the Scripps Institution of Oceanography have revisited the "CLIMAX region" (26.5° to 31°N, 150.5°

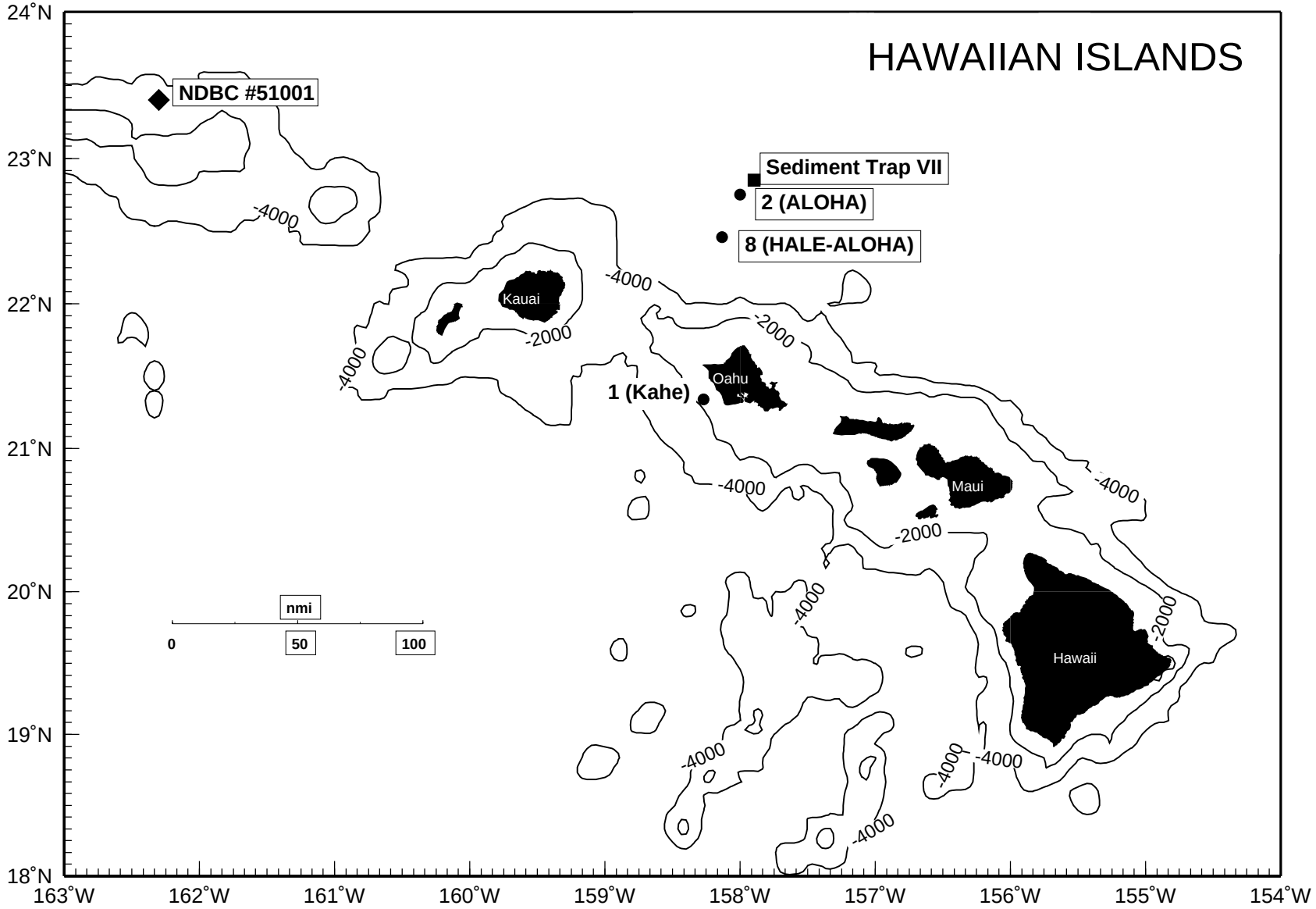

Figure 1.1: [Upper panel] Map of the Hawaiian Islands showing the locations of Stations ALOHA, Kahe and the NDBC weather buoy. [Lower panel] Expanded view of Station ALOHA (a 6 nautical mile radius circle centered at 22°45'N, 158° 00'W) and the past and present locations of the inverted echo sounders (IES) and the bottom-moored sediment traps (ST) relative to the current and retired underwater telephone cables.

to 158°W) on 18 cruises between 1971 and 1985 (Hayward, 1987). It is important to emphasize that the temporal coverage in this time-series is biased with respect to season because approximately 70% of the cruises occurred in summer (June-Sept) and 35% were in August alone. These observations are also aliased by the annual cycle because no cruises were conducted in 1970, 1975, 1978-79, 1981 or 1984. Nevertheless, observations made during this extensive series of cruises, especially the measurements of plankton distributions, nutrient concentrations and rates of primary production, provided an unprecedented view of the oligotrophic North Pacific ecosystem structure and dynamics.

From January 1969 to June 1970, a deep ocean hydrostation (Station GOLLUM; Figure 1.1) was established by scientists at the University of Hawaii at a location 47 km north of Oahu (22°10'N, 158°00'W; Gordon, 1970). The water depth was 4760 m and the location was selected to be beyond the biogeochemical influences of the Hawaiian Ridge (Doty and Oguri, 1956). On approximately monthly intervals, 13 two-day research cruises were conducted to observe and interpret variations in particulate organic matter distributions in the water column and other parameters (Gordon, 1970).

A major advance in our understanding of biogeochemical processes in the sea was made during the NSF International Decade for Ocean Exploration (IDOE)-sponsored Geochemical Ocean Sections Study (GEOSECS) Pacific Ocean expedition (August 1973 - June 1974). Although repeated ocean observations were not made during GEOSECS, the high-precision data, including numerous radioactive and stable isotopic tracers, that were collected from selected stations in the central North Pacific Ocean can be used as the basis for assessing "change," especially for the concentration and ^{13}C isotopic composition of the total dissolved carbon dioxide pool (Quay et al., 1992). In particular, GEOSECS stations #202 (33°6'N, 139°34'W), #204 (31°22'N, 150°2'W), #212 (30°N, 159°50'W) and #235 (16°45'N, 161°19'W) are the most relevant to our current biogeochemical investigations at Station ALOHA (Figure 1.1).

In the early 1970's the North Pacific experiment (NORPAX) was initiated as an additional component of the NSF-IDOE. Research was focused on large scale interactions between the ocean and the atmosphere (e.g., El Niño), and the application of this knowledge to long-range climate forecasting. The Anomaly Dynamics Study was one component of NORPAX aimed at understanding interannual variability of the mid-latitude, North Pacific upper ocean thermal structure. Long-term ocean observation programs were fundamental to the success of NORPAX and, accordingly, the Trans-Pac XBT program and the Pacific Sea Level Network were established. Furthermore, the extensive 15 cruise Hawaii-to-Tahiti Shuttle time-series experiment (January 1979 - June 1980) was conducted to obtain direct measurements of the temporal variations in thermal structure of the equatorial Pacific region (Figure 1.1). These cruises also supported extensive ancillary research programs on chemical and biological oceanography, and provided a rich dataset including measurements of DIC and primary productivity (Wyrtki et al., 1981).

With the abandonment of the central North Pacific Ocean weather ship stations and time-series programs such as Station GOLLUM, there remained very few sites where comprehensive serial measurements of the internal variability of the ocean were continuing. The Intergovernmental Oceanographic Commission (IOC) and World Climate Research Program (WCRP) Committee on Climate Change in the Ocean (CCCO) recognized this deficiency, and in

1981 endorsed the initiation of new ocean observation programs. Reactivation of Station GOLLUM was an explicit recommendation (JSC/CCCO, 1981).

In 1986, a biogeochemical time-series station was established in the northeast Pacific Ocean (33°N, 139°W) as one component of the NSF-sponsored Vertical Transport and Exchange (VERTEX) research program (Figure 1.1). A major objective of the VERTEX time-series project was to investigate seasonality in carbon export from the euphotic zone in relation to contemporaneous primary production. During an 18-month period (October 1986 - May 1988), the station was occupied for seven 1-week periods on approximately 3-month intervals. In addition to standard hydrographic surveys, samples were also collected for the measurement of dissolved inorganic and organic nutrients, particulate matter elemental analysis, primary production, nitrogen assimilation rates, microbial biomass and particle flux (Knauer et al., 1990; Harrison et al., 1992). Significant variability was observed in rates of primary production and particle flux and no clear relationship was found between new production and primary production. Despite the comprehensive scope and intensity of this research project, the sampling frequency was clearly inadequate to resolve much of the natural variability in this oligotrophic oceanic ecosystem.

In response to the growing awareness of the ocean's role in climate and global environmental change, and the need for additional and more comprehensive oceanic time-series measurements, the Board on Ocean Science and Policy (BOSP) of the National Research Council (NRC) sponsored a workshop on "Global Observations and Understanding of the General Circulation of the Oceans" in August 1983. The proceedings of this workshop (National Research Council, 1984a) served as a prospectus for the development of the U.S. component of the World Ocean Circulation Experiment (U.S.-WOCE). U.S.-WOCE has the following objectives: (1) to understand the general circulation of the global ocean, to model with confidence its present state and predict its evolution in relation to long-term changes in the atmosphere and (2) to provide the scientific background for designing an observation system for long-term measurement of the large-scale circulation of the ocean.

In a parallel effort, a separate research program termed Global Ocean Flux Study (GOFS) focused on the ocean's carbon cycle and associated air-sea fluxes of carbon dioxide. In September 1984, NRC-BOSP sponsored a workshop on "Global Ocean Flux Study" which served as an eventual blueprint for the GOFS program (National Research Council, 1984b). In 1986, the International Council of Scientific Unions (ICSU) established the International Geosphere-Biosphere Programme: A Study of Global Change (IGBP), and the following year JGOFS (Joint GOFS) was designed as a Core Project of IGBP. U.S.-JGOFS research efforts focus on the oceanic carbon cycle, its sensitivity to change and the regulation of the atmosphere-ocean CO_2 balance (Brewer et al., 1986).

The broad objectives of U.S.-JGOFS are: (1) to determine and understand on a global scale the time-varying fluxes of carbon and associated biogenic elements in the ocean and (2) to evaluate the related exchanges of these elements with the atmosphere, the sea floor and the continental boundaries (SCOR, 1990, JGOFS Rept. #5). To achieve these goals, four separate program elements were defined: (1) process studies to capture key regular events, (2) long-term time-series observations at strategic sites, (3) a global survey of relevant oceanic properties (e.g., CO_2) and (4) a vigorous data interpretation and modeling effort to disseminate knowledge and to generate testable hypotheses.

In 1987, two separate proposals were submitted to the U.S.-WOCE and U.S.-JGOFS program committees to establish a multi-disciplinary, deep water hydrostation in Hawaiian waters. In July 1988, these proposals were funded by the National Science Foundation and Station ALOHA was officially on the map (Figure 1.1).

1.3. HOT Program Design and Implementation

1.3.1. WOCE and JGOFS objectives for HOT

The primary objective of HOT is to obtain a long time-series of physical and biochemical observations in the North Pacific subtropical gyre that will address the goals of the U.S. Global Change Research Program. The objectives specific to the WOCE program are to:

- document and understand seasonal and interannual variability of water masses
- relate water mass variations to gyre fluctuations
- determine the need and methods for monitoring currents at Station ALOHA
- develop a climatology of short-term physical variability

In addition to these general primary objectives, the physical oceanographic component of HOT provides CTD/rosette sampling support for the JGOFS time-series sampling program, and supports development of new instrumentation for hydrographic observations. To date, HOT has supported research on lowered acoustic profiler measurements of currents in support of WOCE objectives (Firing and Gordon, 1990), and on dissolved oxygen sensor technology (Atkinson et al., 1995), to name a few examples.

The objectives of HOT specific to the JGOFS program are to:

- document and understand seasonal and interannual variability in the rates of primary production, new production and particle export from the surface ocean
- determine the mechanisms and rates of nutrient input and recycling, especially for N and P in the upper 200 m of the water column
- measure the time-varying concentrations of DIC in the upper water column and estimate the annual air-to-sea CO_2 flux

In addition to these general primary objectives (Table 1.1), the biogeochemical component of HOT provides logistical support for numerous complementary research programs (Table 1.2).

Table 1.1: HOT Core Projects

Principal Investigator	Institution	Project Title
Robert Bidigare	Univ. of Hawaii	Core Pigment Measurements
David Karl	Univ. of Hawaii	JGOFS Component
Michael Landry	Univ. of Hawaii	Zooplankton Variability and Particulate Fluxes
Yuan-Hui Li	Univ. of Hawaii	Inorganic Carbon System Measurements
Roger Lukas	Univ. of Hawaii	WOCE Component

Table 1.2: Ancillary Projects Supported by HOT

Principal Investigator	Institution	Agency	Duration	Project Title
Marlin Atkinson	Univ. of Hawaii	NSF	12/88-12/95	Calibration Stability of Two New Oxygen Sensors for CTDs
Lisa Campbell	Univ. of Hawaii	NSF	3/91-2/94	Phytoplankton Population Dynamics at the Hawaii ocean Time-series Station
Lisa Campbell	Univ. of Hawaii	NSF	11/94-10/97	Effects of light and nitrogen source on *Prochlorococcus* growth
James Cowen	Univ. of Hawaii	NSF	8/92-12/94	Studies on the Dynamics of Marine Snow and Particle Aggregation in the North Pacific Central Gyre
Steve Emerson	Univ. of Washington	NSF	10/93-9/96	Ocean Oxygen Fluxes
David Karl / Renate Scharek	Univ. of Hawaii	NSF	1/95-5/96	Diatom population dynamics
Charles Keeling	UCSD, Scripps	NSF	12/88-present	A Study of the Abundance and 13C/12C Ratio of Atmosphere Carbon Dioxide and Oceanic Carbon in Relation to the Global Carbon Cycle
George Luther	Univ. of Delaware	NSF	2/93- 1/96	Iodine Speciation as a Primary Productivity Indicator
Christopher Measures	Univ. of Hawaii	ONR	4/93-12/95	Temporal Variation of Dissolved Trace Element Concentrations in Response to Asian Dust Inputs
Brian Popp	Univ. of Hawaii	NSF	6/91-5/94	Isotopic Analyses of DOC and Cell Concentrates
Paul Quay	Univ. of Washington	NOAA	6/93-present	13C/12C of Dissolved Inorganic Carbon in the Ocean
Hans Thierstein	Geo. Inst. Switzerland	Swiss FIT	1/93-10/96	Calcareous Phytoplankton Dynamics
Jon Zehr	Rensselaer	NSF	1/96-present	Nitrogen fixation genes

1.3.2. Initial HOT program design considerations

There are both scientific and logistical considerations involved with the establishment of any long-term, time-series measurement program. Foremost among these is site selection, choice of variables to be measured and general sampling design, including sampling frequency. Equally important design considerations are those dealing with the choice of analytical methods for a given candidate variable, especially an assessment of the desired accuracy and precision, and availability of suitable reference materials, the hierarchy of sampling replication and, for data collected at a fixed geographical location, mesoscale horizontal variability.

The HOT program was initially conceived as being a deep-ocean, ship- and mooring-based observation experiment that would have an approximately 20-year lifetime. Consequently, we selected a core suite of environmental variables that might be expected to display detectable change on time scales of several days to one decade. Except for the availability of existing satellite and ocean buoy sea surface data, the initial phase of the HOT program (Oct 1988 - Feb 1991) was entirely supported by research vessels. In February 1991, an array of five inverted echo sounders (IES) was deployed in an approximately 150 km^2 network around Station ALOHA (Chiswell, 1996) and in June 1992, a sequencing sediment trap mooring was deployed a few km north of Station ALOHA (Karl, 1994). In 1993, the IES network was replaced with two strategically-positioned instruments: one at Station ALOHA and the other at Station Kaena (Table 1.3). Except for brief service intervals, both the Station ALOHA IES transducer and ALOHA sediment trap mooring have been collecting data since their respective initial deployments.

1.3.3. Station ALOHA site selection

We evaluated several major criteria prior to selection of the site for the HOT oligotrophic ocean benchmark hydrostation. First, the station must be located in deep water (>4000 m), upwind (north-northeast) of the main Hawaiian islands and of sufficient distance from land to be free from coastal ocean dynamics and biogeochemical influences. On the other hand, the station should be close enough to the port of Honolulu to make relatively short duration (<5 d) monthly cruises logistically and financially feasible. A desirable, but less stringent criterion would locate the station at, or near, previously studied regions of the central North Pacific Ocean, in particular Station GOLLUM.

After consideration of these criteria, we established our primary sampling site at 22°45'N, 158°00'W at a location approximately 100 km north of the island of Oahu (Figure 1.1 and Table 1.3), and generally restrict our monthly sampling activities to a circle with a 6 nmi radius around this nominal site. Station ALOHA is in deep water (4750 m) and is more than one Rossby radius (50 km) away from steep topography associated with the Hawaiian Ridge. We also established a coastal station W-SW of the island of Oahu, approximately 10 km off Kahe Point (21°20.6'N, 158°16.4'W) in 1500 m of water. Station Kahe serves as a coastal analogue to our deep-water site and the data collected there provide a near-shore time-series for comparison to our primary open ocean site. Station Kahe is also used to test our equipment each month before departing for Station ALOHA, and to train new personnel at the beginning of each cruise.

Table 1.3: Locations of the HOT Water Column and Bottom Stations

Station	Coordinates	Approximate Depth (m)	Comments
I. Hydrographic Stations			
1 (Kahe)	21° 20.6'N 158° 16.4'W	1,500	HOT Program coastal time-series station
2 (ALOHA)	22° 45'N 158° 00'W	4,800	HOT Program open ocean time-series station
3	23° 25'N 158° 00'W	4,800	One of three onshore to offshore transect sites, established in 1993
4	21° 57.8'N 158° 00'W	4,000	One of three onshore to offshore transect sites, established in 1993
5	21° 46.6'N 158° 00'W	450	One of three onshore to offshore transect sites, established in 1993
II. IES Network			
6 (Kaena)	21° 50.8'N 158° 21.8'W	2,500	May 1993-Jun 1994, Jun 1994-Oct 1995
N	23° 00.7'N 157° 59.9'W	4,800	Feb 1991-Feb 1992, Jun 1992-May 1993
C	22° 44.9'N 157° 59.9'W	4,800	Feb 1991-Feb 1992, Jun 1992-May 1993 May 1993-Jun 1994, Jun 1994-Oct 1995, Oct 1995-Oct 1996
SW	22° 37.0'N 158° 14.7'W	4,800	Feb 1991-Feb 1992, Jun 1992- May 1993
SE	22° 30.0'N 157° 45.2'W	4,800	Feb 1991-Feb 1992, Jun 1992- May 1993
E	22° 44.8'N 157° 54.0'W	4,800	Feb 1991- Feb 1992
III Sediment Traps			
ALOHA-I	22° 57.3'N 158° 06.2'W	4,800	1st deployment of bottom-moored sequencing sediment trap (Jun 1992-Sept 1993)
ALOHA-II	23° 6.7'N 157° 55.8'W	4,800	2nd deployment (Sept 1993 - Oct 1994)
ALOHA-III	22° 50.2'N 157° 55.9'W	4,800	3rd deployment (May 1995 - Oct 1995)
ALOHA-IV	22° 51.7'N 157° 54.3'W	4,800	4th deployment (Nov 1995 - Oct 1996)
IV Weather Buoys			
Buoy #51026	21° 22'N 156° 57'W		NOAA-NDBC meteorological buoy
Buoy #51001	23° 24'N 162° 18'W		NOAA-NDBC meteorological buoy

1.3.4. Field sampling strategy

HOT program cruises are conducted at approximately monthly intervals; the exact timing is dictated by the availability of research vessels. To date, our field observations have not been severely aliased by month, season or year, except perhaps for a slight under representation of data collected during November and December and slight over representation in February and September (Karl and Lukas, 1996). From HOT-1 (October 1988) to HOT-65 (August 1995), with the exception of HOT-42 and HOT-43 (November and December 1992), each cruise was 5 d in duration. Beginning with HOT-66 (September 1995) the standard HOT cruise was reduced by 20% to 4 d in order to accommodate additional mooring-based field programs.

From HOT-1 (October 1988) to HOT-32 (December 1991), underway expendible bathythermograph (XBT; Sippican T-7 probes) surveys were conducted at 7 nmi spacing on the outbound transect from Station Kahe to Station ALOHA. These surveys were later discontinued because the space-time correlation of the energetic, internal semi-diurnal tides made it difficult to interpret these data. In 1995 we added an instrumented, 1.5 m Endeco towfish package (Sea-Bird CTD, optical plankton counter, fluorometer) to our sampling program (see section 2.10). Upper water column currents are measured both underway and on station using a hull-mounted acoustic doppler current profiler (ADCP), when available (Firing, 1996). The majority of our sampling effort, approximately 60-72 hrs per cruise, is spent at Station ALOHA. Underway near-surface measurement of a variety of physical, chemical and biological properties is made possible by sampling seawater through a pumped intake system positioned in the hull of the R/V *Moana Wave*. In 1996, we replaced the existing system with a non-contaminating PVC/ stainless steel system and added several new sensors (see section 2.9).

High vertical resolution environmental data are collected with a Sea-Bird CTD having external temperature (T), conductivity (C), dissolved oxygen (DO), fluorescence (F) and light transmission (LT) sensors, and an internal pressure (P) sensor. A Sea-Bird 24-place carousel and an aluminum rosette that is capable of supporting 24 12-l PVC bottles are used to obtain water samples from desired depths. The CTD and rosette are deployed on a 3-conductor cable allowing for real-time display of data and for tripping the bottles at specific depths of interest.

The CTD system takes 24 samples sec^{-1} and the raw data are stored both on the computer and, for redundancy, on VHS-format video tapes. We also routinely collect "clean" water samples for biological rate measurements using General Oceanics Go-Flo bottles, Kevlar cable, metal-free sheave, Teflon messengers and a stainless steel bottom weight. A free-drifting sediment trap array, identical in design to the VERTEX particle interceptor trap (PIT) mooring (Knauer et al., 1979), is deployed at Station ALOHA for an approximately 2-3 d period to collect sinking particles for chemical and microbiological analyses.

Sampling at Station ALOHA typically begins with sediment trap deployment followed by a deep (>4700 m) CTD cast and a "burst series" of 12-18 consecutive casts, on 3-hr intervals, to 1000 m to span the local inertial period (~31 hr) and three semidiurnal tidal cycles. The repeated CTD casts enable us to calculate an average density profile from which variability on tidal and near-inertial time scales has been removed. These average density profiles are useful for the comparison of dynamic height and for the comparison of the depth distribution of chemical parameters from different casts and at monthly intervals. For example, by fitting the distribution of inorganic nutrients to this average density structure, the depth of the nutricline can be defined

each month, independent from the short time scale changes in the density structure of the upper water column (Dore and Karl, 1996). This sampling strategy is designed to assess variability on time scales of a few hr to a few yr. Very high frequency variability (<6 hr) and variability on time scales of between 3-60 d are not adequately sampled at the present time. Initial results from the IES network suggest that these frequencies might be important at Station ALOHA (Chiswell, 1996). However, no field sampling program, regardless of its intensity, can adequately resolve the entire spectrum of variability that theoretically exists in the ocean (Tabata, 1965). The HOT program is no exception.

Water samples for a variety of chemical and biological measurements are routinely collected from the surface to within 5 m of the seafloor. To the extent possible, we collect samples for complementary biogeochemical measurements from the same or from contiguous casts to minimize aliasing caused by time-dependent changes in the density field. This is especially important for samples collected in the upper 300 m of the water column. Furthermore, we attempt to sample from common depths and specific density horizons each month to facilitate comparisons between cruises. Water samples for salinity determinations are collected from every water bottle to identify sampling errors. Approximately 20% of the water samples are collected and analyzed in duplicate or triplicate to assess and track our analytical precision in sample analysis.

1.3.5. Core measurements, experiments and protocols

Our primary study area is characterized by warm (>23°C) surface waters with low NO_3^- concentrations (<15 nM), seasonally variable surface mixed-layers (10-120 m), low standing stocks (i.e., biomass) of living organisms (10-15 µg C l^{-1}) and a persistent deep (75-140 m) chl *a* maximum layer (DCML). Ideally, the suite of core measurement parameters should provide a data base to validate existing biogeochemical models and to develop improved ones. Our list of core measurements has evolved since the inception of the HOT program in 1988, and now includes both continuous and discrete physical, biological and chemical ship-based measurements, *in situ* biological rate experiments, and observations and sample collections from bottom-moored instruments and buoys (Table 1.4). Continuity in the measurement parameters and their quality, rather than continuity in the methods employed, is of greatest interest. Detailed analytical methods are expected to change over time through technical improvements. In addition to the core data, specialized measurements and process-oriented experiments have also been conducted at Station ALOHA (Table 1.4).

This report presents selected core data collected during the seventh year of the HOT Program (January-December 1995; Table 1.5). During this period, 8 regular HOT cruises were conducted using the University of Hawaii research vessel R/V *Moana Wave* and one was conducted using the R/V *Maurice Ewing*. In addition, a separate R/V *Moana Wave* cruise (ST-4) was conducted for the purpose of annual servicing of the bottom-moored sediment trap array. A total field scientific crew of 49 different HOT staff, students and visiting scientists were involved in our 1995 field work (Table 1.6). These measurements are part of a much larger HOT program

Table 1.4: Parameters Measured at Station ALOHA

Parameter	Depth Range (m)	Analytical Procedure
I. CTD Measurements		
Depth (pressure)	0-4800	Pressure transducer on Sea-Bird CTD-rosette package
Temperature	0-4800	Thermistor on Sea-Bird CTD package with frequent calibration
Salinity	0-4800	Conductivity sensor on Sea-Bird CTD package, standardization with Guildline AutoSal #8400A against Wormley standard seawater
Oxygen	0-4800	Polarographic sensor on Sea-Bird CTD package with Winkler standardization
Fluorescence	0-1000	Sea-Tech flash fluorometer on Sea-Bird CTD package
Beam Transmission	0-1000	Sea-Tech 25 cm path length beam transmissometer on Sea-Bird CTD package
II. Optical Measurements		
Incident Irradiance (PAR)	Surface	LI-COR cosine collector and Biospherical 4 π collector
Underwater Irradiance (PAR)	0-150	Biospherical profiling natural fluorometer 4 π Collector
Solar Stimulated Fluorescence (683nm)	0-150	Biospherical profiling natural fluorometer
III. Water Column Chemical Measurements		
Oxygen	0-4750	Winkler titration
Dissolved Inorganic Carbon	0-4750	Coulometry
Titration Alkalinity	0-4750	Automated titration
pH	0-4750	Spectrophotometric
Nitrate Plus Nitrite	0-4750	Autoanalyzer
Soluble Reactive Phosphorus	0-4750	Autoanalyzer
Silicate	0-4750	Autoanalyzer
Low Level Nitrate Plus Nitrite	0-200	Chemiluminescence
Low Level Phosphorus	0-200	Magnesium-induced coprecipitation
Dissolved Organic Carbon	0-1000	High temperature catalytic oxidation
Total Dissolved Nitrogen	0-1000	U.V. oxidation
Total Dissolved Phosphorus	0-1000	U.V. oxidation
Particulate Carbon	0-1000	High temperature combustion
Particulate Nitrogen	0-1000	High temperature combustion
Particulate Phosphorus	0-1000	High temperature combustion

Table 1.4: continued

Parameter	Depth Range (m)	Analytical Procedure
IV. Water Column Biomass Measurements		
Chlorophyll *a* and Phaeopigments	0-200	Fluorometric analysis
Plant Pigments	0-200	High performance liquid chromatography
Adenosine 5'-Triphosphate	0-1000	Firefly bioluminescence
Bacteria and Cyanobacteria	0-1000	Flow cytometry
V. Carbon Assimilation and Particle Flux		
Primary Production	0-175	"Clean" ^{14}C incubations
Carbon, Nitrogen, Phosphorus and Mass Flux	150, 200, 300, 500	Free-floating particle interceptor traps
VI. Currents		
Acoustic Doppler Current Profiler	0-300	Hull mounted, RDI #VM-150
Acoustic Doppler Current Profiler	0-4750	Lowered
VII. Instrumented Towfish		
Temperature	45	Thermistor on Sea-Bird package
Salinity	45	Conductivity sensor on Sea-Bird package
Zooplankton	45	Optical Plankton Counter
Fluorescence	45	WetLabs SeaStar fluorometer on CTD package
VIII. Bow Intake System		
Temperature	3	Sea-Bird remote temperature sensor in sea chest in bow of the ship with annual calibration
Salinity	3	Sea-Bird temperature and conductivity sensors inside the thermosalinograph package, with similar standardization as for CTD salinity (section I)
Carbon Dioxide	3	Gas equilibration, infrared detection
IX. Moored Instruments		
Inverted Echo Sounder Network (Dynamic height)	100-1000	Acoustic telemetry, CTD calibration
Sequencing Sediment Traps	1500, 3000, 4000	Parflux MK7-21

Table 1.5: Chronology of 1995 HOT Cruises

HOT	Ship	Depart	Return
60	R/V *Moana Wave*	4 February 1995	9 February 1995
61	R/V *Moana Wave*	2 March 1995	7 March 1995
62	R/V *Moana Wave*	4 April 1995	9 April 1995
63	R/V *Moana Wave*	5 May 1995	10 May 1995
64	R/V *Maurice Ewing*	28 July 1995	2 August 1995
65	R/V *Moana Wave*	27 August 1995	1 September 1995
66	R/V *Moana Wave*	25 September 1995	29 September 1995
67	R/V *Moana Wave*	25 October 1995	30 October 1995
ST-4	R/V *Moana Wave*	12 November 1995	14 November 1995
68	R/V *Moana Wave*	15 November 1995	19 November 1995

Table 1.6: 1995 Cruise Personnel (shaded area=cruise participant)

Cruise Participants	60	61	62	63	64	65	66	67	ST-4	68
Principal Investigators										
Dale Hebel	■	■	■	■	■	■	■			■
David Karl				■					■	
Luis Tupas	■	■	■	■	■	■	■	■		■
University of Hawaii Scientists										
Lisa Campbell						■				
Renate Scharek, Postdoctoral Fellow	■	■	■							
SuzannaVink, Postdoctoral Fellow	■	■	■	■						
Visiting Scientists and Technicians										
Giacomo DiTullio					■					
Steven Emerson	■						■			
Mark Huntley	■	■								
David Jones					■	■				
Ricardo Letelier			■							
Mai Lopez		■	■	■	■	■	■	■		■
Bruce Monger					■					
Michael Mulroney								■		
James Richman				■						
Marc Rosen									■	
Charles Stump			■	■	■			■		■
Tania Westby					■					
	60	**61**	**62**	**63**	**64**	**65**	**66**	**67**	**ST-4**	**68**

Table 1.6: continued

Cruise Participants	60	61	62	63	64	65	66	67	ST-4	68
University of Hawaii Research Associates										
Patrick Driscoll						■	■			
Lance Fujieki	■				■	■	■	■		■
Terrence Houlihan	■	■	■	■	■	■	■	■	■	■
Ursula Magaard				■				■		
Craig Nosse	■	■	■	■	■	■	■	■		■
David Pence	■	■	■	■						
Fernando Santiago-Mandujano	■				■		■	■		■
Jefrey Snyder	■	■	■	■	■	■	■	■		■
Jinchun Yuan	■	■	■	■	■					
University of Hawaii Students										
Angela Adams		■								
Mark Baird							■	■		
Jeff Bolestra									■	
Christopher Carrillo								■		
Jim Falter									■	
Shevaun Fennel					■					
Patrick Goda	■			■		■				
Kristi Hanson		■			■					
Hongbin Liu					■	■				
Molly Lucas			■		■	■	■	■		■
Robert Miller			■	■	■	■	■	■		■
Matt Parry									■	
Rebecca Reitmeyer	■									
Gretchen Rollwagen			■							
Daniel Sadler	■	■	■	■	■	■		■		■
Karen Selph	■	■	■							
Ann Tarrant									■	
Angie Thomson					■				■	
Don Wright					■					
Visiting Students										
Karen Casciotti, REU student					■	■				
Peter Kolman							■			
Teri Navarro-Perez		■								
	60	**61**	**62**	**63**	**64**	**65**	**66**	**67**	**ST-4**	**68**

data set on physical and biogeochemical variability at Station ALOHA that has been collected since October 1988. The complete data set is available to the community by several methods that are described in a subsequent section of this report (see Chapter 8).

2. SAMPLING PROCEDURES AND ANALYTICAL METHODS

A comprehensive summary of all sampling and analytical methods currently used in the HOT program along with information on measurement accuracy and precision can be found in the "Hawaii Ocean Time-series Program Field and Laboratory Protocols" manual. This document is available on the World Wide Web (http://hahana.soest.hawaii.edu) or can be obtained in hard copy by contacting D. Karl (phone; 808-956-8964, fax: 808-956-5059; email: dkarl@soest.hawaii.edu). Brief summaries of selected methods as well as calibration specifications and quality control / quality assurance information for CY 1995 are presented in this report. Hydrographic sampling methods are included in "WOCE Hydrographic Sampling Procedure. A primer for ship-board operations at the Hawaii Ocean Time-series Station," also available in the WWW (http://www.soest.hawaii.edu/HOT_WOCE).

2.1. CTD Profiling

Continuous measurements of temperature, salinity, oxygen, fluorescence and beam transmission are made with a Sea-Bird SBE-911 Plus CTD package with dual temperature, salinity and oxygen sensors and fluorometer and transmissometer described in Tupas et al. (1995).

CTD casts are made at Stations Kahe and ALOHA during each cruise, and at Stations 6 and 3 on some. A CTD cast to 1000 m is made at Station Kahe. At Station ALOHA a burst of consecutive CTD casts to 1000 m is made over 36 hours to span the local inertial period and three semi-diurnal tidal cycles. One WOCE standard cast within 5 m of the bottom is made during each cruise. During four cruises in 1995 a second deep cast was obtained at Station ALOHA to observe short time changes in the deep and bottom water (cf. Lukas and Santiago-Mandujano, 1996). Also, Station 6 (Kaena Pt., Figure 1.1) was occupied during most of the cruises to obtain a CTD cast for calibration of the Inverted Echo Sounder (IES) located at this site. During HOT-67, the IES from Station 6 was retrieved, so this station has not been visited since. Station 3 (north of ALOHA) was also occupied during HOT-67.

2.1.1. Data acquisition and processing

CTD data were acquired at a rate of 24 samples per second. Digital data were stored on an IBM-compatible PC and, for redundancy, the analog signal was recorded on VHS video tapes. Backups of CTD data were made onto Bernoulli disks and later onto DAT tapes. The raw CTD data were quality controlled and screened for spikes as described in Winn et al. (1993). Data alignment, averaging, correction and reporting were done as described in Tupas et al. (1993). Salinity spike rejection parameters were modified for some cruises in 1995. Spikes occur when the CTD samples the disturbed water of its wake. Therefore, samples from the downcast were rejected when the CTD was moving upward or when its acceleration exceeded 0.5 m s^{-2} in magnitude. Cruises 61, 62 and 63 were conducted under rough sea conditions, with heavy ship rolling during some of the casts, causing large vertical velocity fluctuation of the CTD package. The acceleration cutoff value had to be increased to between 0.55 and 0.7 m s^{-2} to leave enough points to average in each bin. The data were additionally screened by comparing the primary and secondary sensors. These differences permitted identification of problems in the sensors. Only the data from one pair of sensors, whichever was deemed most reliable, are reported here.

Temperature is reported in the ITS-90 scale. Salinity and all derived units were calculated using the UNESCO (1981) routines; salinity is reported in the practical salinity scale (PSS-78). Oxygen is reported in $\mu mol\ kg^{-1}$.

2.1.2. Sensor corrections and calibrations

2.1.2.1. pressure

The pressure calibration strategy employed a high-quality quartz pressure transducer as a transfer standard. Periodic recalibrations of this lab standard were performed with a primary pressure standard. Russka precision dead-weight pressure testers with weights meeting National Bureau of Standards specifications, operated under environmentally-controlled conditions, were used as primary standards. The transfer standard was used to check the CTD pressure transducers at six-month intervals. The 1995 results of these tests showed a bias of less than 1.4 dbar in the 0 to 4500 dbar range between the CTD and transfer standard pressures. Therefore, the only correction applied to the CTD pressures was a constant offset determined at the time that the CTD first enters the water on each cast.

The transfer standard was a Paroscientific Model 760 pressure gauge equipped with a 10,000 PSI transducer. This instrument was purchased in March 1988, and the original calibration coefficients were obtained from a calibration at Paroscientific against a primary standard. Subsequent recalibrations of the instrument consisted of 11-point comparisons against a primary standard at 6 pressure levels between 0 and 7000 dbar, increasing and then decreasing the pressure. The first recalibration was performed by the Oceanographic Data Facility at Scripps Institution of Oceanography in May of 1991, followed by two more at the Northwest Regional Calibration Center (NWRCC) in September 1994 and March 1996. The latest of these calibrations shows that our transfer standard has an offset at 0 dbar of 0.07 dbar from its original calibration, and the offset increases by 1.2 dbar at 4500 dbar (our standard reading high). The calibration also reveals that the increase in the offset with increasing pressure is non-linear. The hysteresis is less than 0.3 dbar throughout the entire range. The offset at 0 dbar has decreased compared to the 0.3 dbar seen from the previous two calibrations, and the 4500 dbar offset is the same as the one on September 1994, but bigger than the one on May 1991, which was 0.6 dbar. An increase in the offset at 4500 dbar with time seems to be a characteristic of this type of sensor, as indicated also by the results of our CTD pressure transducer calibrations discussed below.

A correction to the transfer standard was obtained by comparing its nominally calibrated output against the primary standard values from the latest calibration data (March 1996). A cubic least squares fit to the difference between transfer standard and primary standard pressures as a function of pressure yielded a correction to the nominal pressures from the transfer standard. The RMS of the residuals from the least squares fit was 0.06 dbar, with a maximum residual of 0.12 dbar.

CTD pressure transducer bench tests were done using a dead-weight pressure tester and a manifold to apply pressure simultaneously to the CTD pressure transducer and to the transfer standard. All these tests had points at 6 pressure levels between 0 and 4500 dbar, increasing and decreasing pressures.

CTD pressure transducers are the same type as the transfer standard. Pressure transducer #26448 was used during all cruises in 1995. Calibrations against the transfer standard in 1995 are given in Table 2.1. The 16 December 1994 and 16 August 1995 offsets were used for the cruises in 1995 (Note that this offset was only used for real-time data acquisition, as more accurate offset was later determined for the time that the CTD first enters the water on each cast). Our backup pressure transducer #51412 was also calibrated against the pressure standard in 1995. The results in Table 2.1 indicate a clear trend in the offset at 0 dbar toward higher values in time for sensor #26448. Sensor #51412, which has not being used as regularly as the primary, does not show a similar trend. On the other hand, the offset at 4500 dbar shows an increase with time in #51412, and an increase between the beginning and the end of the year calibrations in #26448. A similar time drift in the 4500 dbar offset observed in the transfer standard indicates that this behavior is characteristic for this type of sensors.

Table 2.1: CTD Pressure Calibrations (units are decibars)

Calibration Date	Offset @ 0 dbar	0-4500 dbar offset	Hysteresis
Sea-Bird SBE-911 Plus #91361 / Pressure Transducer #26448			
16 December 1994	-5.7	0.9	0.2
16 August 1995	-5.9	1.4	0.02
9 January 1996	-6.3	1.2	---
Sea-Bird SBE-911 Plus #92859 / Pressure Transducer #51412			
16 December 1994	-0.1	0.8	0.05
16 August 1995	-0.25	1.0	0.1
9 January 1996	-0.1	1.2	0.1

2.1.2.2. temperature

Two Sea-Bird SBE-3-02/F temperature transducers, #741 and #1416, were used in 1995 and were calibrated at Sea-Bird after every cruise (see Tupas et al., 1995). The history of the sensors, as well as the procedures followed to obtain the sensor drift from the Sea-Bird calibrations are well-documented in Tupas et al. (1993, 1994a, 1995). Calibration coefficients obtained at Sea-Bird and used in the drift estimates are presented in Table 2.2. These coefficients were used in the following formula that gives the temperature (in °C) as a function of the frequency signal (f):

$$\text{temperature} = 1/\{a+b[\ln(f_0/f)]+c[\ln^2(f_0/f)]+d[\ln^3(f_0/f)]\}-273.15$$

For each sensor, the final calibration consists of two parts: first, a single "baseline" calibration is chosen from among the ensemble of calibrations during the year. Second, for each cruise a temperature-independent offset is applied to remove the temporal trend due to sensor drift (Table 2.3). The offset, a linear function of time, is calculated by least squares fit to the 0-30°C average of each calibration during the year. The maximum drift correction in 1995 was less than 2×10^{-3}°C. The baseline calibration is selected as the one for which the trend-corrected average from 0-5°C is nearest to the ensemble mean of these averages.

Table 2.2: Calibration Coefficients for Sea-Bird Temperature Transducers. RMS Residuals from Calibration Give an Indication of Quality of the Calibration

SN	YYMMDD	f_0	a	b	c	d	RMS (m°C)
741	951130	5936.76	3.68165657E-03	6.01974876E-04	1.55675430E-05	2.09609068E-06	0.03
741	951109	5936.75	3.68165818E-03	6.01978038E-04	1.55720771E-05	2.10144369E-06	0.04
741	951010	5936.79	3.68165301E-03	6.01972584E-04	1.55610823E-05	2.09136837E-06	0.03
741	951005	5936.73	3.68166104E-03	6.01980832E-04	1.55690345E-05	2.09403037E-06	0.03
741	950909	5936.70	3.68166527E-03	6.01982205E-04	1.55748402E-05	2.10165805E-06	0.03
741	950808	5936.74	3.68166884E-03	6.01958789E-04	1.55375917E-05	2.08417847E-06	0.03
741	950629	5950.31	3.68029889E-03	6.01922880E-04	1.55848314E-05	2.12215823E-06	0.03
741	950426	5950.13	3.68032155E-03	6.01926352E-04	1.55846907E-05	2.12208066E-06	0.04
741	950323	5936.34	3.68171541E-03	6.01986884E-04	1.55724264E-05	2.09918882E-06	0.03
741	950216	5936.60	3.68169344E-03	6.01996237E-04	1.56013792E-05	2.12417251E-06	0.03
741	950215	5949.60	3.68037702E-03	6.01920202E-04	1.55497105E-05	2.08953933E-06	0.03
741	950126	5949.94	3.68034368E-03	6.01924226E-04	1.55642017E-05	2.10107671E-06	0.03
741	950121	6292.63	3.64668625E-03	6.00212133E-04	1.52476911E-05	2.13423284E-06	0.02
741	941222	5949.39	3.68003968E-03	6.01927801E-04	1.55652465E-05	2.10162800E-06	0.04
741	941215	5949.34	3.68040278E-03	6.01926759E-04	1.55582030E-05	2.09415851E-06	0.04
741	941208	5949.34	3.68040232E-03	6.01929328E-04	1.55657411E-05	2.10163122E-06	0.03
741	941203	5936.46	3.68171123E-03	6.02001328E-04	1.55825130E-05	2.10229797E-06	0.02
741	941111	5949.08	3.68042870E-03	6.01939138E-04	1.55953709E-05	2.12995390E-06	0.03
741	941108	5949.06	3.68042925E-03	6.01939106E-04	1.55955066E-05	2.12866401E-06	0.03
1416	951128	6230.71	3.68164555E-03	6.01838091E-04	1.51229297E-05	2.22774169E-06	0.11
1416	951107	6230.72	3.68164747E-03	6.01868566E-04	1.52209156E-05	2.30775457E-06	0.13
1416	951010	6230.71	3.68165430E-03	6.01862471E-04	1.51919005E-05	2.28088302E-06	0.12
1416	951005	6230.65	3.68166225E-03	6.01868789E-04	1.52001653E-05	2.28815621E-06	0.10
1416	950909	6230.66	3.68166627E-03	6.01850522E-04	1.51385467E-05	2.23880325E-06	0.07
1416	950808	6230.60	3.68166972E-03	6.01826839E-04	1.50854479E-05	2.20135113E-06	0.06
1416	950629	6244.88	3.68029900E-03	6.01782528E-04	1.51291120E-05	2.24419184E-06	0.04
1416	950426	6244.66	3.68032097E-03	6.01723202E-04	1.49695983E-05	2.12976704E-06	0.05
1416	950323	6230.19	3.68171386E-03	6.01747188E-04	1.48356092E-05	2.00273790E-06	0.11
1416	950216	6230.51	3.68169292E-03	6.01746979E-04	1.47979567E-05	1.95138530E-06	0.10
1416	950215	6244.15	3.68037741E-03	6.01762536E-04	1.50487658E-05	2.17350592E-06	0.04
1416	950126	6244.52	3.68034429E-03	6.01762980E-04	1.50565351E-05	2.17979832E-06	0.07
1416	950121	6604.29	3.64668597E-03	6.00127980E-04	1.47845402E-05	2.26485999E-06	0.05
1416	941222	6243.96	3.68039767E-03	6.01763025E-04	1.50286299E-05	2.14854816E-06	0.07
1416	941215	6243.91	3.68040347E-03	6.01766822E-04	1.50357450E-05	2.15120592E-06	0.07
1416	941208	6243.93	3.68040318E-03	6.01760183E-04	1.50137803E-05	2.13377720E-06	0.07
1416	941203	6230.42	3.68171174E-03	6.01831351E-04	1.50357279E-05	2.13826316E-06	0.03
1416	941111	6243.62	3.68042712E-03	6.01685406E-04	1.48250606E-05	1.99520905E-06	0.12
1416	941108	6243.61	3.68042771E-03	6.01682891E-04	1.48103792E-05	1.97962260E-06	0.12
1392	951013	2458.52	3.67486724E-03	5.87218944E-04	9.15090348E-06	-1.97663220E-06	0.28
1392	940929	2458.32	3.67487069E-03	5.87155511E-04	9.27931149E-06	-1.74690868E-06	0.89
1496	960118	5946.31	3.68167257E-03	5.89965822E-04	1.47447188E-05	2.95734250E-06	0.21
1496	931102	5952.17	3.68121200E-03	5.89938744E-04	1.49486143E-05	3.09294466E-06	0.22

Table 2.3: Temperature and Conductivity Sensor Corrections Including the Thermal Inertia (α) Parameter (see text). Dual temperature and conductivity sensors were used in all cruises. The last column shows the sensor pairs whose data are reported.

Cruise	Temp Sensor #	T Correction (°C)	Cond Sensor #	α	Data Collected Station:Casts	Data Reported Station:Casts
60	741	0.00003	679	0.020	All casts	
	1416	-0.0001	527	0.028	All casts	All casts
61	741	0.00005	679	0.020	All casts	
	1416	0.00011	527	0.020	All casts	All casts
62	741	0.00007	1336	0.012	All casts	All casts
	1416	0.00033	527	0.020	All casts	
63	741	0.00009	1336	0.012	All casts	All casts
	1416	0.00054	679	0.028	All casts	
64	741	0.00015	1336	0.020	All casts	1:1, 6:1-2, 2:1-7, 12-20
	1416	0.00110	527	0.028	All casts	2:8-11
65	741	0.0000	679	0.020	2:1-19	2:1-19
	741	0.0000	1336	0.020	1:1, 6:1	
	1416	0.00130	527	0.020	All casts	1:1, 6:1
66	741	0.0000	1336	0.028	All casts	All casts
	1416	0.00150	527	0.020	1:1, 2:1-4, 6:1	
	1416	0.00150	679	0.028	2:5-16	
67	741	0.0000	1336	0.012	All casts	All casts
	1416	0.00170	679	0.028	1:1, 2:1-16	
	1416	0.00170	527	0.020	2:17, 3:1	
68	741	0.00001	1336	0.028	All casts	All casts
	1416	0.00191	679	0.028	All casts	

Dual sensors were used in all the 1995 cruises. The temperature differences between sensor pairs were calculated for each cast to evaluate the quality of the data, and to identify possible problems with the sensors. Means and standard deviations of the differences in 2-dbar bins were calculated from the ensemble of all casts at Station ALOHA for each cruise. Both sensors performed correctly during the 1995 cruises, showing temperature differences within expected values. The mean temperature difference as a function of pressure was typically less than 1×10^{-3}°C, with a standard deviation of less than 0.5×10^{-3}°C below 500 dbar. The largest variability was observed in the thermocline, with standard deviation values of up to 5×10^{-3}°C.

Sensor #741

This sensor was used as part of the dual-sensor configuration in all cruises during 1995. On 4 November 1994 the sensor's turret joint was resoldered as recommended by Sea-Bird to prevent sensor drift due to possible micro-cracks in the solder. This procedure produced a change in the sensor drift rate. The sensor also suffered a jump in its calibration level sometime between 8 August and 9 September 1995. The cause was not identified. The sensor drift was slightly affected as we will see below.

The calibrations made on 8 November 1994 after the turret joint resoldering and on 8 August 1995 before the jump in the calibration level, were used to calculate the sensor drift and drift correction for cruises HOT-60 through HOT-64. A linear fit to the 0-30°C average offset from each calibration (Table 2.2) relative to 8 November 1994 gave an intercept of -2.3×10^{-4}°C with a slope of 6.699×10^{-7}°C day^{-1}. The RMS deviation of the offsets from this fit was 1.4×10^{-4}°C.

The 22 December 1994 calibration was used as a baseline for cruises HOT-60 through 64. When corrected for linear drift to 1 May 1995 (the midpoint of the cruise dates), this calibration gave the smallest deviation in the 0-5°C temperature range from the set of all calibrations used to determine the drift (also corrected for linear drift to 1 May 1995). The mean deviation of this calibration was -2.3×10^{-6}°C with a range of variation of less than 2×10^{-5}°C. The deviation from this and the other calibrations in the same temperature range was $\pm 5 \times 10^{-4}$°C.

Calibrations between 9 September and 30 November 1995 were used to determine the sensor drift on cruises HOT-65 through HOT-68. The 28 November 1995 calibration was not used in this determination given its anomalous 0-30°C trace relative to the other calibrations. A linear drift rate of 4.053×10^{-7}°C day^{-1} was obtained with an intercept of 5.22×10^{-5}°C, and 3.66×10^{-5}°C RMS from the residuals of the fit. The 9 November 1995 calibration was used as baseline for cruises HOT-65 through HOT-68. The mean deviation of this calibration from the others in the 0-5°C range corrected for the drift on 7 October 1995 (the midpoint of the cruises dates), was -1.3×10^{-6}°C, with less than 2×10^{-5}°C range of variation. The deviation from this and the other calibrations was $\pm 1 \times 10^{-4}$°C.

Given the small drift in this sensor, the resulting drift corrections for each cruise were very small and inconsequential (Table 2.3) and, therefore, were not applied to the cruises.

Sensor #1416

This was the second sensor used in a dual-sensor configuration during the 1995 cruises. The turret joint of this sensor was also resoldered on 4 November 1994 to prevent possible sensor drift. The calibrations after this date were used to determine a sensor drift of 6.687×10^{-6}°C day^{-1} with a 1.64×10^{-4}°C intercept and 1.92×10^{-4}°C RMS residual. The 15 February 1995 calibration was used as baseline for cruises HOT-60 through HOT-68. This calibration yielded the smallest 0-5°C mean deviation from the others, all drift-corrected to 15 May 1995 (midpoint date between the cruises). The deviation was -3.7×10^{-6}°C with less than 2×10^{-5}°C range of variation. The deviation from this and all the other calibrations was $\pm 5 \times 10^{-4}$°C.

2.1.2.3. conductivity

Three sensors were used during the 1995 cruises: #1336, #679 and #527. The dual sensor configurations are shown in Table 2.3. In recent cruises, on board comparisons between the sensor pair measurements after each cast have helped to identify possible problems with the sensors, thus allowing us to correct them by replacing faulty sensors during the cruise. As mentioned earlier, only the data from the most reliable sensor (and its corresponding temperature sensor pair, as shown in Table 2.3) are reported here.

During HOT-61, sensor #679 differed from #527 by up to 2 x 10^{-3} Siemens m^{-1} near the surface, decreasing to 6 x 10^{-4} Siemens m^{-1} below 500 dbar. A Sea-Bird evaluation revealed that the cell of #679 had been shorted by water penetrating its epoxy jacket. This problem affected all measurements obtained with this sensor during the cruise. The sensor #679 conductivity cell was replaced on 12 April 1995.

The sensor #527 conductivity cell was replaced at Sea-Bird on 17 August 1995, also because of water in the epoxy jacket. This problem affected the measurements during HOT-62 and HOT-64. During four casts of HOT-64 (station 2, casts 8-11), the plumbing of the alternate sensor (#1336) became clogged, yielding unreliable data in the upper 20 dbar. Therefore, conductivities from sensor #527 were used for these casts, despite the leakage problem. The quality of these data was evaluated by comparing the salinities from both sensors after calibrating each against the bottle data (see below). The salinity differences for casts before and after the clogging problem were within ±0.002 in the whole pressure range; this is an estimate of the maximum error of sensor #527 salinities for HOT-64, casts 8 through 11.

Sensor #1336 performed correctly during cruises HOT-62 through HOT-64. Anomalous differences were detected between sensors #1336 and #527 in the first two casts of cruise HOT-65. Differences of up to 3 x 10^{-3} Siemens m^{-1} were observed near the surface, decreasing to a constant value of 1 x 10^{-3} Siemens m^{-1} below 500 dbar. The problem was solved by replacing sensor #1336 by #679 for the rest of the cruise. Sensor #1336 was sent to Sea-Bird where it was opened, evaluated and calibrated on 13 September 1995. No problems were found with the sensor.

Anomalous differences similar to those during HOT-65 were observed between sensors #1336 and #527 in the first six casts of HOT-66. The replacement of sensor #527 by #679 reduced the differences to acceptable values for the rest of the cruise. Sensor #527 was sent to Sea-Bird for evaluation where it was opened and calibrated on 10 October 1995. There were no problems found with the sensor.

Given the large differences between sensors #527 and #1336 in previous cruises, a test was performed during HOT-67 to see if the problem persisted. Sensor #679 was replaced by #527 on the last two casts of the cruise. Anomalous differences were observed again between sensors #1336 and #527. Both sensors were sent back to Sea-Bird for an extensive evaluation after HOT-68. Sea-Bird tests indicated that the anomalous sensor behavior was due to the slow stabilization or "aging" of the sensors after being opened and serviced. The sensors had been serviced between cruises and used immediately, without allowing enough time for them to stabilize. Sea-Bird now recommends budgeting several weeks for conductivity sensor service, with extra calibrations to check for sensor stability after the sensor has been opened.

Conductivity differences between sensor pairs were calculated the same way as for the temperature sensors (section 2.1.2.2). The range of variability as a function of pressure was about ± 1 x 10^{-4} Siemens m^{-1}, with a standard deviation of less than 0.5 x 10^{-4} Siemens m^{-1} below 500 dbar, from the ensemble of all the cruise casts. The largest variability was in the halocline, with standard deviations reaching up to 5 x 10^{-4} Siemens m^{-1} between 50 and 300 dbar.

Conductivity calibration procedures at the North West Regional Calibration Center are described in Winn et al. (1991). The nominal calibrations were used for data acquisition. Final calibration was determined empirically from salinities of discrete water samples acquired during each cast. Prior to empirical calibration, conductivity was corrected for thermal inertia (α) of the glass conductivity cell as described in Chiswell et al. (1990). Table 2.3 lists the value of α used for each cruise.

Preliminary screening of bottle samples and empirical calibration of the conductivity cell are described in Tupas et al. (1993, 1994a). For cruises HOT-60 through HOT-68, the standard deviation cutoff values for screening of bottle samples were: 0.0038 (0-150 dbar), 0.0053 (151-500 dbar), 0.0023 (501-1050 dbar) and 0.0012 (1051-5000 dbar).

The conductivity calibration coefficients (b_0, b_1, b_2) resulting from the least squares fit ($\Delta C = b_0 + b_1 C + b_2 C^2$) to the CTD-bottle conductivity difference (ΔC) as a function of conductivity (C) are given in Table 2.4. The quality of the CTD calibration is illustrated in Figure 2.1, which shows the differences between the corrected CTD salinities and the bottle salinities as a function of pressure for each cruise. The calibrations are best below 500 dbar because the weaker vertical salinity gradients at depth lead to less error when the bottle and CTD pressures are slightly mismatched.

The final step of conductivity calibration was a cast-dependent bias correction as described in Tupas et al. (1993) to allow for drift during each cruise or for sudden offsets due to fouling (Table 2.5). Note that a change of 1×10^{-4} Siemens m^{-1} in conductivity was approximately equivalent to 0.001 in salinity. Table 2.6 gives the mean and standard deviations for the final calibrated CTD minus water sample values.

Table 2.4: Conductivity Calibration Coefficients

Cruise	Sensor #	b_0	b_1	b_2
60	679	0.001434	-0.000713	
	527	0.001140	-0.000727	
61	679	0.001546	-0.000798	
	527	0.000019	-0.000125	
62	1336	0.006684	-0.003673	0.000440
	527	0.008519	-0.004438	0.000521
63	1336	-0.000783	-0.000015	
	679	-0.000525	0.000010	
64	1336	-0.000941	-0.000035	
	527	-0.000485	-0.000097	
65	679	-0.000824	-0.000003	
	1336	-0.000656	-0.000116	
	527	0.006744	-0.003793	0.000481
66	1336	-0.000648	0.000128	
	527	-0.001454	-0.000025	
	679	0.004461	-0.002557	0.000296
67	1336	0.000040	-0.000108	
	679	-0.000462	-0.000182	
	527	-0.003863	0.001771	-0.000322
68	1336	-0.000130	-0.000112	
	679	-0.000462	-0.000241	

Table 2.5: Individual Cast Conductivity Corrections (units are Siemens m^{-1}).

Cruise	Station	Cast	C correction
60	2	1	0.00017884
	2	6	-0.00014654
	2	7	-0.00027234
61	2	1	0.00011322
63	2	1	0.00011062
	2	17	0.00008645
64	2	17	0.00010578
	6	2	0.00019067
65	2	1	0.00008780
	2	2	0.00030810
	2	18	0.00017438
67	2	1	0.00012483
	2	16	0.00013679
	3	1	0.00014816
68	2	1	0.00011534
	2	16	0.00012490

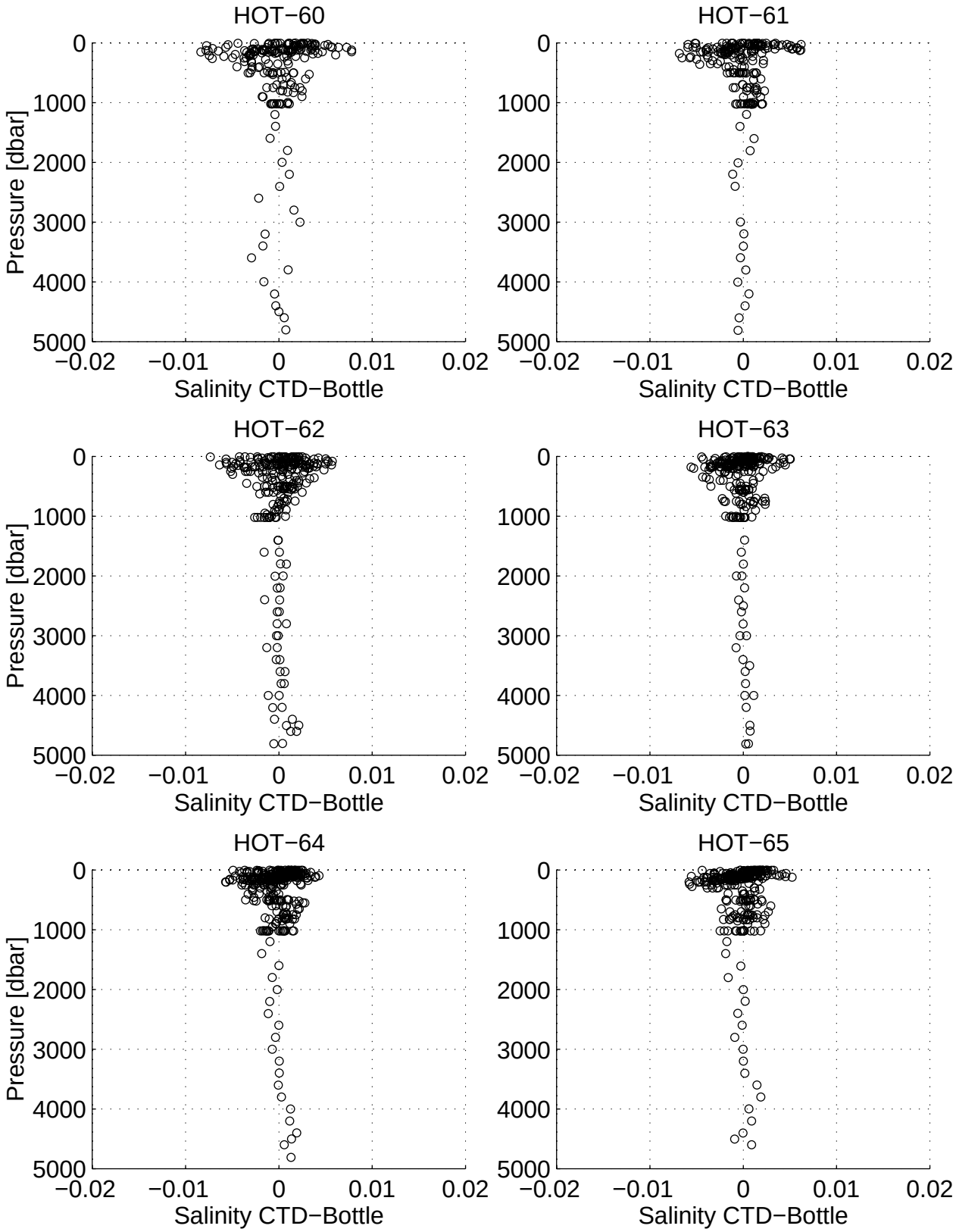

Figure 2.1: Differences between calibrated CTD salinities and bottle salinities for Station ALOHA

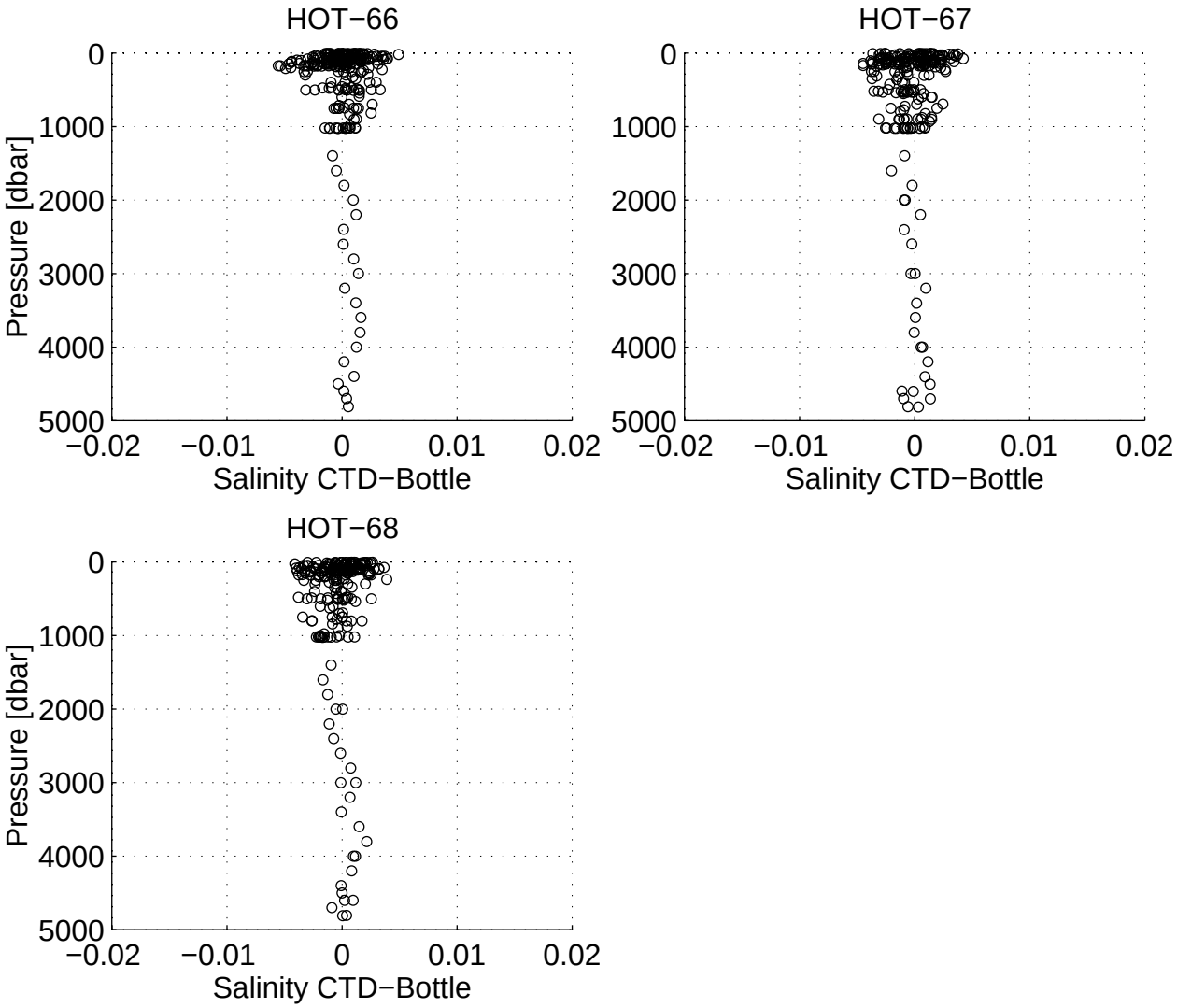

Figure 2.1 continued

Table 2.6: CTD-Bottle Salinity Comparison for Each Cruise

		0 to 4700 db		500 to 4700 db	
Cruise	**Sensor #**	**Mean**	**SD**	**Mean**	**SD**
60	679	0.0000	0.0029	0.0002	0.0014
	527	0.0000	0.0029	0.0002	0.0014
61	679	-0.0001	0.0020	0.0000	0.0009
	527	-0.0001	0.0025	0.0004	0.0009
62	1336	0.0000	0.0023	0.0000	0.0011
	527	0.0000	0.0028	0.0000	0.0015
63	1336	-0.0001	0.0017	-0.0001	0.0010
	679	-0.0001	0.0018	0.0000	0.0009
64	1336	-0.0001	0.0018	0.0002	0.0012
	527	-0.0001	0.0022	0.0005	0.0013
65	679	-0.0002	0.0019	0.0001	0.0012
	1336	0.0000	0.0014	0.0004	0.0014
	527	0.0000	0.0020	0.0002	0.0012
66	1336	0.0000	0.0019	0.0004	0.0010
	527	0.0000	0.0022	0.0006	0.0015
	679	0.0000	0.0018	0.0000	0.0009
67	1336	-0.0003	0.0017	-0.0004	0.0012
	679	0.0000	0.0022	0.0003	0.0013
	527	0.0000	0.0009	0.0000	0.0010
68	1336	-0.0002	0.0017	-0.0004	0.0013
	679	-0.0001	0.0019	0.0001	0.0012

2.1.2.4. oxygen

Two YSI Inc. probes (#13341 and #13251) were used in a dual-sensor configuration during the 1995 cruises. Water bottle oxygen data were screened and the sensors were empirically calibrated following procedures described previously (Winn et al., 1991; Tupas et al., 1993). Analysis of water bottle samples is described in section 2.2.2. The calibration procedure follows Owens and Millard (1985), and consists of fitting a non-linear equation to the CTD oxygen current and oxygen temperature. The bottle values of dissolved oxygen and the downcast CTD observations at the potential density of each bottle trip were grouped together for each cruise to find the best set of parameters with a non-linear least squares algorithm. Two sets of parameters were usually obtained per cruise, corresponding to the casts at Stations 1 (Kahe) and 2 (ALOHA). In some of the 1995 cruises there was an obvious drift in the CTD oxygen sensors throughout Station 2 casts, apparently due to sensor electrolyte depletion. These cruises required more than one set of calibration parameters at Station 2.

During some of the 1995 cruises, additional bottle oxygen measurements were obtained by scientists from the University of Washington (see section 2.2.2). These data were also used in the calibrations of the CTD sensors.

The history of the sensors is documented in Tupas et al. (1995). A new procedure has been implemented to check for possible sensor problems. The data from the sensor pair is plotted after each cast. In addition, before each cruise the sensor's membrane is inspected closely for wrinkles or tears, and for air bubbles in the electrolyte reservoir. Replacement of the membrane and electrolyte was performed on both sensors before cruises HOT-64 and HOT-66; on sensor #13251 before HOT-60, and on sensor #13341 before HOT-62.

Only the data from sensor #13341 are reported here for all cruises. This sensor showed less drift during cruises than sensor #13251. Table 2.7 gives the means and standard deviations for the final calibrated CTD oxygen values minus the water sample values.

Table 2.7: CTD-bottle Dissolved Oxygen per Cruise.
Mean and standard deviation (µmol kg^{-1})

		Station 1, Kahe Point		Station 2, ALOHA			
		0 to 1500 dbar		0 to 4700 dbar		500 to 4700 dbar	
Cruise	Sensor #	Mean	SD	Mean	SD	Mean	SD
60	13341	0.03	1.38	0.17	1.87	0.32	1.53
61	13341	-0.35	1.41	-0.06	1.53	0.02	1.51
62	13341	-0.29	2.42	-0.23	2.18	0.00	1.90
63	13341	-0.41	1.71	-0.01	2.23	0.32	2.52
64	13341	0.11	2.26	-0.35	2.18	-0.37	2.18
65	13341	0.01	1.98	0.45	2.24	0.51	1.73
66	13341	0.01	1.83	-0.41	2.07	0.02	1.32
67	13341	0.01	2.58	0.41	2.20	0.82	1.76
68	13341	0.01	1.57	-0.01	1.84	0.24	2.13

2.1.2.5. flash fluorescence

Flash fluorescence was measured with a Sea Tech Model ST0250 flash fluorometer and the data collected with the Sea-Bird CTD system. Flash fluorescence traces were collected on as many casts as possible. Because an absolute radiometric standard is not available for flash fluorometers, instrument drift was corrected by checking the relative response of the instrument between cruises using fluorescent plastic sheeting as described in Tupas et al. (1993). A linear relationship of the form, Vn = b Vo + a, was used to convert all fluorescence data to a common voltage scale, where Vn is the normalized voltage, Vo is the output voltage and a and b are constants derived from the two deep water intervals. The constants used during 1995 are given in Table 2.8.

2.1.2.6. beam transmission

Beam transmission was measured with a Sea Tech 25 cm path length transmissometer. Transmission data were collected using the Sea-Bird CTD system in a fashion analogous to that described for flash fluorescence. The transmissometer was calibrated as described by the manufacturer before each cruise to correct for instrument drift. To calculate percent transmission the following relationship was used: %T = 20 [(V-offset) (a/b)] where V is the measured

voltage, and a and b are the empirically derived calibration factors. The calibration parameters used during 1995 are given in Table 2.8.

Table 2.8: Fluorescence and Transmission Calibration Factors

	Fluorescence		Transmission		
Cruise	**a**	**b**	**a**	**b**	**offset**
60	1.6669	0.6503	0.25	20.318	0.0203
61	1.6669	0.6503	0.25	20.318	0.0203
62	1.6669	0.6503	0.25	20.318	0.0203
65	1.6669	0.6503	0.25	20.318	0.0203
64	1.6669	0.6503	0.25	20.318	0.0203
65	1.6669	0.6503	0.25	21.690	0.000
66	1.6669	0.6503	0.25	21.690	0.000
67	1.6669	0.6503	0.25	19.770	0.000
68	1.6669	0.6503	0.25	19.770	0.000

2.2. Discrete Water Column Measurements

Water samples for chemical analyses were collected at Station Kahe and ALOHA as well as other stations. Sampling strategies and procedures are well documented in the previous data reports (Tupas et al., 1993; Winn et al., 1993) and in the HOT Program Field and Laboratory Protocols manual. This data report contains only a subset of the total data base which can be extracted from the accompanying diskette or via anonymous ftp over Internet (see Chapter 8). To assist in the interpretation of these data and to save users the time to estimate the precision of individual chemical analysis, we have summarized precision estimates from replicate determinations for each constituent on each HOT cruise in 1995.

2.2.1. Salinity

Salinity samples were collected, stored and analyzed as described in Tupas et al. (1993). Samples from a large batch of "secondary standard" seawater are measured after every 24-48 HOT samples to detect drift in the salinometer. The typical standard deviation of the secondary standard salinity determination is less than ±0.001 (Table 2.9). The slightly larger standard deviation on HOT-65 coincides with a small drift observed in the secondary standard readings during the measurement of the deep cast bottles. Therefore, duplicate salinity samples were used for this cast. There was no drift observed during the measurement of the duplicate samples. Duplicate salinity samples were also used for the HOT-66 deep cast because they showed less variation relative to the CTD than the original salinity samples.

Secondary standard batches were prepared on the following dates: batch #9 was made on 28 November 1994, batch #10 was made on 30 September 1995 and batch #11 was made in November 1995.

Table 2.9: Precision of Salinity Measurements Using Lab Standards

Cruise	Mean Salinity ± SD	# Samples*	Substandard Batch #	IAPSO Batch #
60	34.49268 ± 0.00021	11	9	p123
61	34.49214 ± 0.00014	11	9	p123
62	34.49181 ± 0.00033	12	9	p123
63	34.49230 ± 0.00026	12	9	p123
64	34.49256 ± 0.00039	12	9	p123
65	34.49272 ± 0.00161	18	9	p123
66	34.49055 ± 0.00068	29	10	p123
67	34.49123 ± 0.00035	19	10	p123
68	34.42216 ± 0.00128	20	11	p123

*Number of samples of secondary standard salinity measurement taken during each run.

2.2.2. Oxygen

Oxygen samples were collected and analyzed using a computer-controlled potentiometric end-point titration procedure as described in Tupas et al. (1993). As in previous years we measured, using a calibrated digital thermistor, the temperature of the seawater sample within the individual Niskin bottles at the time the iodine flask was filled. This was done to evaluate the magnitude of oxygen sample temperature error which affects the calculation of oxygen concentrations in units of µmol kg^{-1}. Figure 2.2 (upper panel) shows a plot of the difference between on-deck sample temperature and potential temperature, computed from the *in situ* temperature measured at the time of bottle trip, versus pressure. The lower panel of the same figure shows a plot of the difference between oxygen concentration using on-deck and potential temperatures versus pressure. The depth dependent variability in Δ oxygen is a result of the absolute magnitude of the oxygen concentration and the standard procedures we employ for sampling the water column. For work of the highest accuracy, this error should be considered.

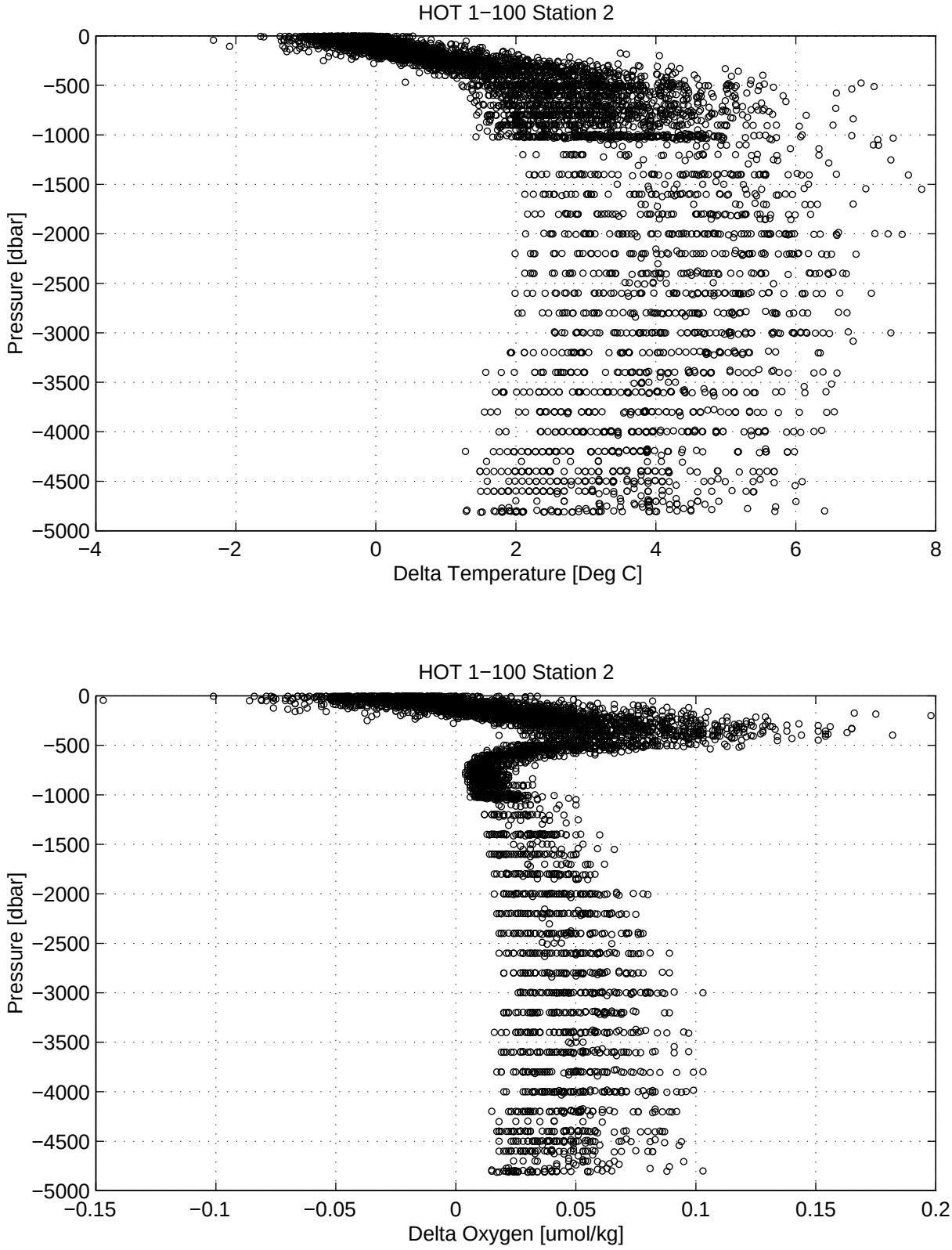

Figure 2.2: [Upper panel] Difference between sample temperature at the time of sample collection and potential temperature calculated from *in situ* temperature at the time of bottle trip. [Lower panel] Difference in oxygen concentration (µmol kg^{-1}) using temperatures measured at the time of sample collection and potential temperature computed from *in situ* temperature.

The precision of our oxygen analyses was assessed from both an analytical and field perspective and is presented in Table 2.10. The mean analytical and field precision of our oxygen analyses in 1995 was 0.16% and 0.09%, respectively. Oxygen concentrations measured over the 7 years of the program are plotted at three constant potential density horizons in the deep ocean along with their mean and 95% confidence intervals (Figure 2.3). The deviations ranged (maximum - minium values) from a low of 2.5 µmol kg^{-1} at σ_θ = 22.758 to 2.7 µmol kg^{-1} at σ_θ = 27.675. These results indicate that analytical consistency has been maintained over the first 7 yrs of the HOT program.

For selected cruises in 1995, oxygen determinations provided by S. Emerson (University of Washington) were also used for the CTD-oxygen sensor calibration (see section 2.1.2.4). Sampling, subsampling and fixation procedures are identical to those routinely used in the HOT program. The major difference is with the detection systems used, visual starch endpoint (U.W.) versus potentiometric endpoint (HOT).

Table 2.10: Precision of Winkler Titration Method

	Analytical			Field		
HOT	CV (%)	SD (µmol l^{-1})	n	CV (%)	SD (µmol l^{-1})	n
60	0.23	0.37	5	0.12	0.22	11
61	0.15	0.24	8	0.10	0.17	10
62	0.27	0.50	5	0.12	0.23	12
63	0.11	0.22	8	0.08	0.13	10
64	0.12	0.20	7	0.06	0.12	12
65	0.14	0.29	4	0.07	0.14	11
66	0.17	0.30	6	0.08	0.14	12
67	0.08	0.14	5	0.06	0.10	11
68	0.19	0.41	3	0.12	0.22	16

2.2.3. Dissolved inorganic carbon and titration alkalinity

Samples for dissolved inorganic carbon (DIC) were measured using a Single Operator Multi-parameter Metabolic Analyzer (SOMMA) which was manufactured at the University of Rhode Island and standardized at the Brookhaven National Laboratory. Analyses of primary DIC standards (Tupas et al., 1993) indicated that the precision of replicate samples is approximately 1 µmol kg^{-1}. Titration alkalinity was determined using the Gran titration method as described in Tupas et al. (1993). The precision of the titration procedure was approximately 5 µequiv kg^{-1}. Accuracy was established with certified reference standards obtained from Andrew Dickson, Scripps Institution of Oceanography.

Figure 2.3: Oxygen versus time at three potential density horizons at Station ALOHA. [Upper panel] Oxygen concentration at potential densities of 27.782, 27.758 and 27.675 during 1995. [Lower panel] Oxygen at these same three density horizons including all 7 years of program.

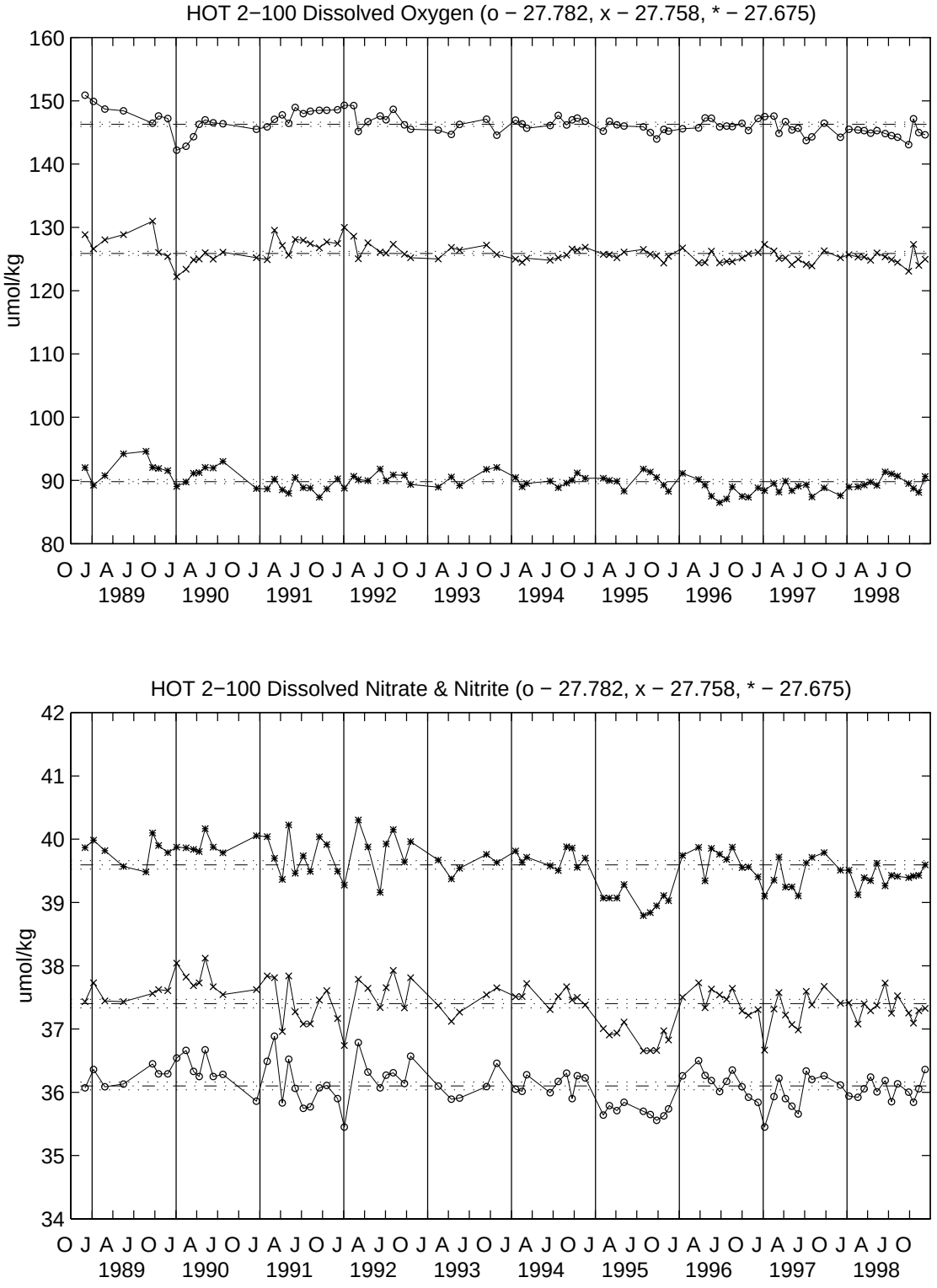

Figure 2.4: As in Figure 2.3, except for concentrations of dissolved [nitrate+nitrite].

2.2.4. pH

Beginning in 1995, pH was determined spectrophotometrically using the indicator m-cresol purple following the methods described in Tupas et al. (1993). The absorbance of the mixture was measured at 578 and 434 nm on a Perkin Elmer Model 3 dual-beam spectrophotometer and converted to pH on the seawater scale according to Clayton and Byrne (1993).

2.2.5. Dissolved inorganic nutrients

Samples for the determination of dissolved inorganic nutrients (soluble reactive phosphorus, [nitrate+nitrite] and silicate concentrations) were collected as described in Tupas et al. (1993). Analyses were conducted at room temperature on a four-channel Technicon Autoanalyzer II continuous flow system (Winn et al., 1991). A summary of the precision of analyses for 1995 is shown in Table 2.11. Figures 2.4-2.6 show the mean and 95% confidence limits of nutrient concentrations measured at three potential density horizons for the 7 years of the program. In addition to standard automated nutrient analyses, specialized chemical methods (section 2.2.7) were used to determine concentration of nutrients that are normally below the detection limits of autoanalyzer methods.

Table 2.11: Precision of Dissolved Inorganic Nutrient Analyses

	Soluble Reactive Phosphorus				[Nitrate+Nitrite]				Silicate			
	Analytical		Field		Analytical		Field		Analytical		Field	
HOT	mean CV (%)	mean SD (µM)	mean CV (%)	mean SD (µM)	mean CV (%)	Mean SD (µM)	mean CV (%)	mean SD (µM)	mean CV (%)	mean SD (µM)	mean CV (%)	mean SD (µM)
60	0.2	0.007	0.4	0.006	0.3	0.127	0.2	0.031	0.5	0.608	0.4	0.372
61	0.4	0.012	1.1	0.019	0.4	0.169	0.8	0.119	0.5	0.569	1.0	0.561
62	0.4	0.011	1.1	0.019	0.3	0.134	0.2	0.058	0.3	0.306	0.2	0.183
63	0.4	0.010	0.3	0.007	0.2	0.092	0.3	0.055	0.1	0.108	2.0	0.342
64	0.3	0.010	0.8	0.015	0.3	0.119	0.4	0.131	0.1	0.144	0.4	0.235
65	0.3	0.008	0.4	0.008	0.6	0.258	0.3	0.082	0.3	0.356	0.3	0.270
66	0.3	0.009	0.4	0.007	0.2	0.096	0.2	0.044	0.1	0.111	0.4	0.101
67	0.4	0.012	0.2	0.004	0.5	0.186	0.2	0.073	0.4	0.362	1.2	0.362
68	0.2	0.006	0.4	0.006	0.3	0.045	0.2	0.036	0.8	0.143	0.3	0.327

2.2.6. Dissolved organic nutrients

Dissolved organic carbon (DOC) was determined by the high temperature catalytic oxidation method described in Tupas et al. (1994b). Water samples were collected in acid-washed polyethylene tubes and were stored frozen until analyzed. The oxidation method used a

Figure 2.5: As in Figure 2.3, except for concentrations of soluble reactive phosphorus.

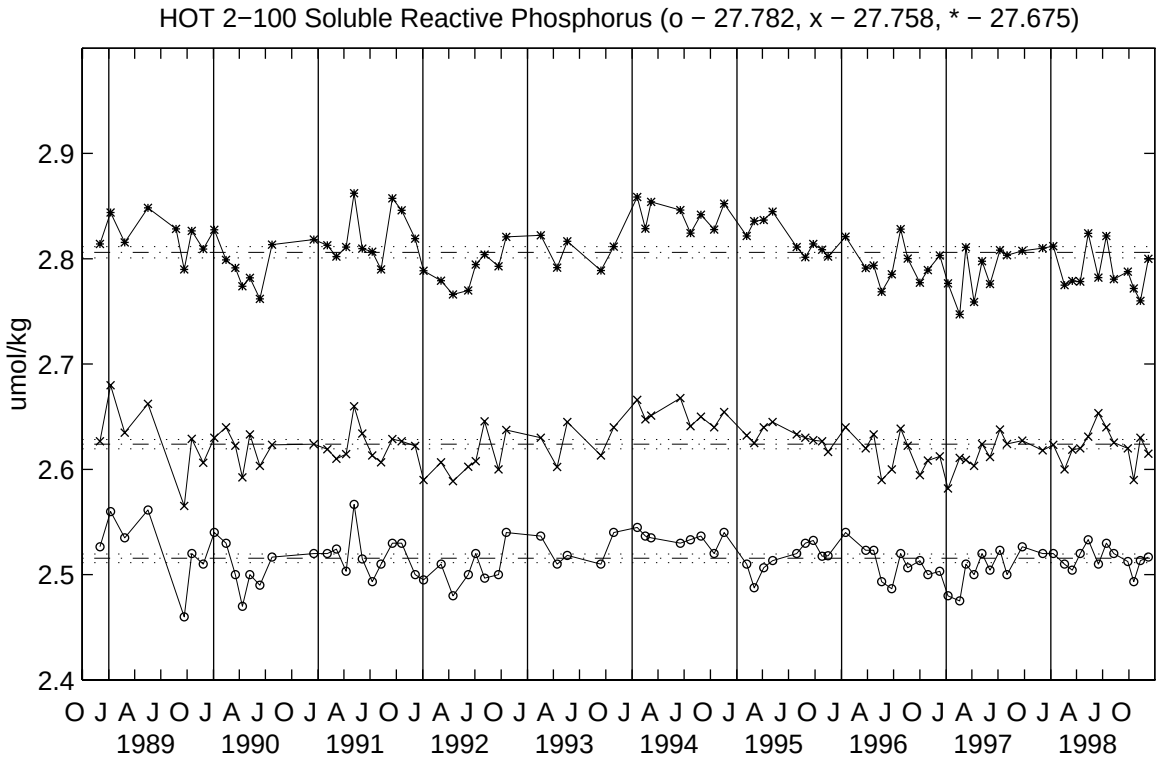

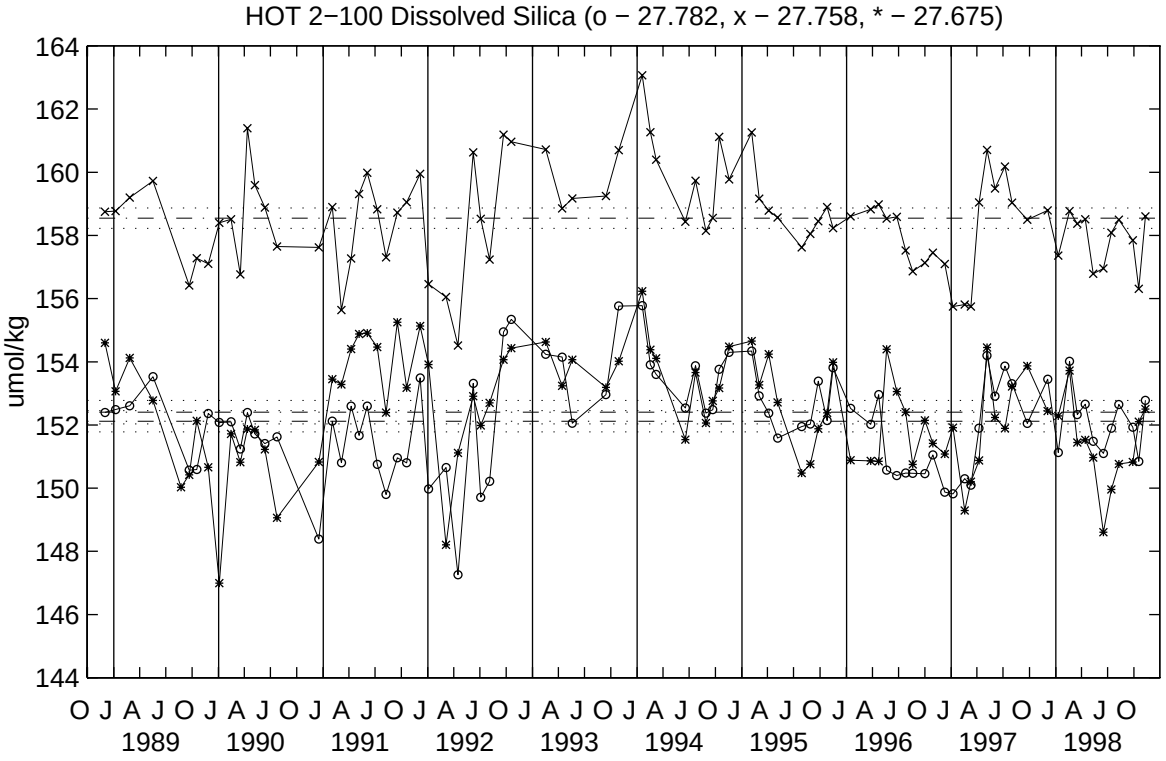

Figure 2.6: As in Figure 2.3, except for concentrations of dissolved silica.

pure platinum catalyst with infrared detection on a LI-COR 6252 carbon dioxide analyzer. Dissolved organic nitrogen (DON) was calculated as the difference between total dissolved nitrogen (TDN) and [nitrate+nitrite] concentrations determined by the autoanalyzer (section 2.2.5.). TDN and [nitrate+nitrite] were determined as described in Tupas et al. (1993). Dissolved organic phosphorus (DOP) was calculated as the difference between total dissolved phosphorus (TDP) and SRP concentrations. TDP and SRP were determined as described in Tupas et al. (1993). A summary of the precision of these analyses is given in Table 2.12. DOC, DON and DOP concentrations over the 7 years of the program at the 500 and 1000 dbar horizons are plotted with their mean and 95% confidence intervals (Figures 2.7-2.9).

Table 2.12: Precision of Dissolved Organic Nutrient Analyses

	DON		DOP		DOC	
Cruise	mean CV (%)	mean SD (µmol kg^{-1})	mean CV (%)	mean SD (µmol kg^{-1})	mean CV (%)	mean SD (µmol kg^{-1})
60	8.7	0.41	12.6	0.03	---	---
61	9.4	0.33	12.8	0.02	---	---
62	10.1	0.21	13.1	0.01	---	---
63	8.9	0.30	4.7	0.01	---	---
64	4.8	0.19	17.2	0.02	2.1	1.90
65	14.5	0.32	6.7	0.01	1.7	1.20
66	7.7	0.17	2.3	0.01	2.1	1.52
67	2.5	0.12	8.2	0.01	---	---
68	5.6	0.19	21.5	0.02	1.4	0.60

2.2.7. Low-level nutrients

The chemiluminescent method of Cox (1980) as modified for seawater by Garside (1982) was used to determine the [nitrate+nitrite] content of near surface (0-100 m interval) water samples (Tupas et al., 1993). The limit of detection for [nitrate+nitrite] was approximately 2 nM with a precision and accuracy of ±1 nM.

Low level SRP concentrations in the euphotic zone were determined according to the magnesium induced coprecipitation (MAGIC) method of Karl and Tien (1992). Typical precision estimates for triplicate determinations of SRP are from 1-3% with a limit of detection of 10 nmol l^{-1}.

2.2.8. Particulate matter

Samples for analysis of particulate matter were prefiltered through 202 µm Nitex mesh to remove large zooplankton and collected onto combusted GF/F glass fiber filters. Particulate carbon (PC) and nitrogen (PN) on the filters were analyzed using a Europa automated nitrogen

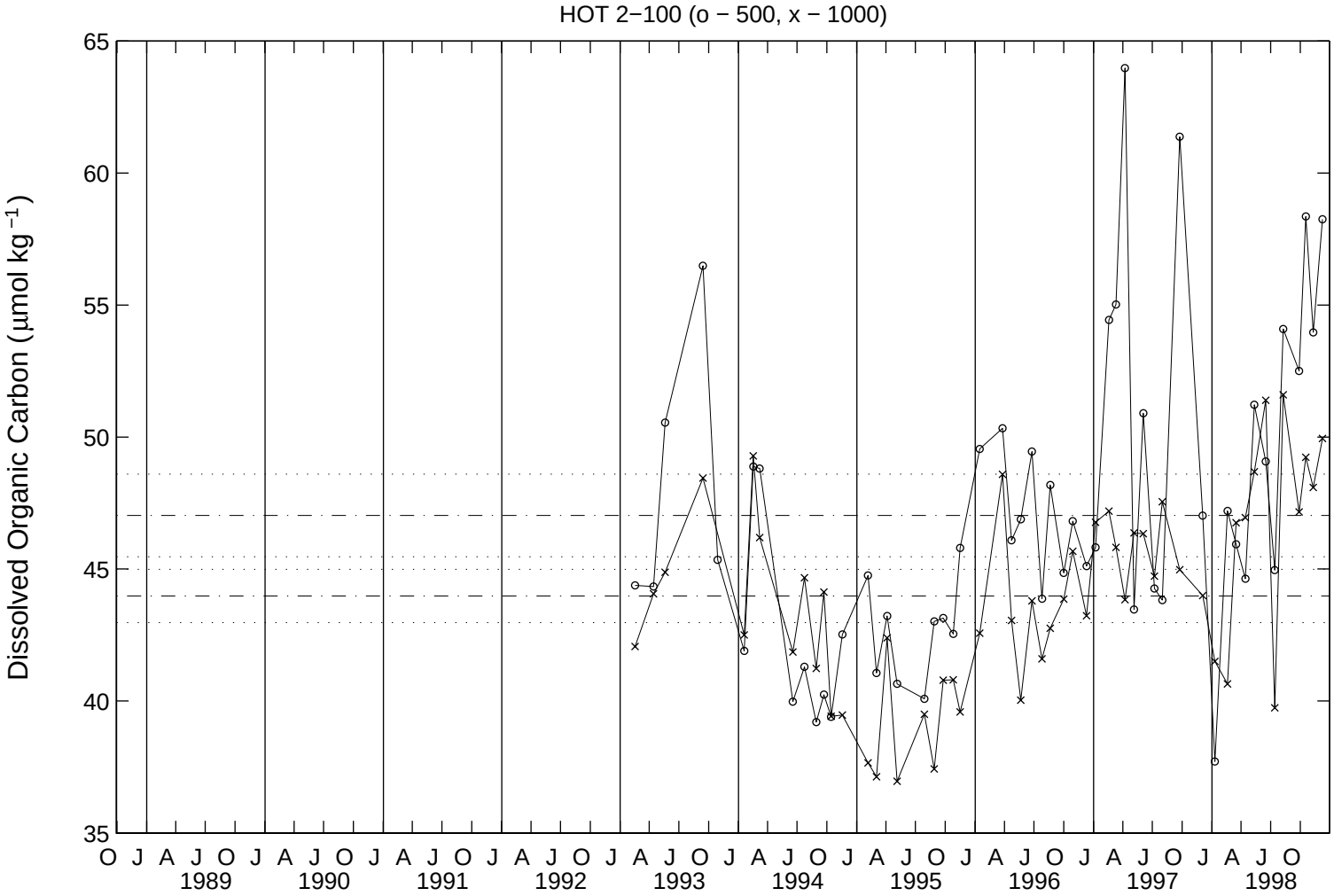

Figure 2.7: DOC versus time at 500 and 1000 dbar horizons at Station ALOHA. [Upper panel] DOC concentrations during 1995. [Lower panel] DOC concentrations from 1993-1995.

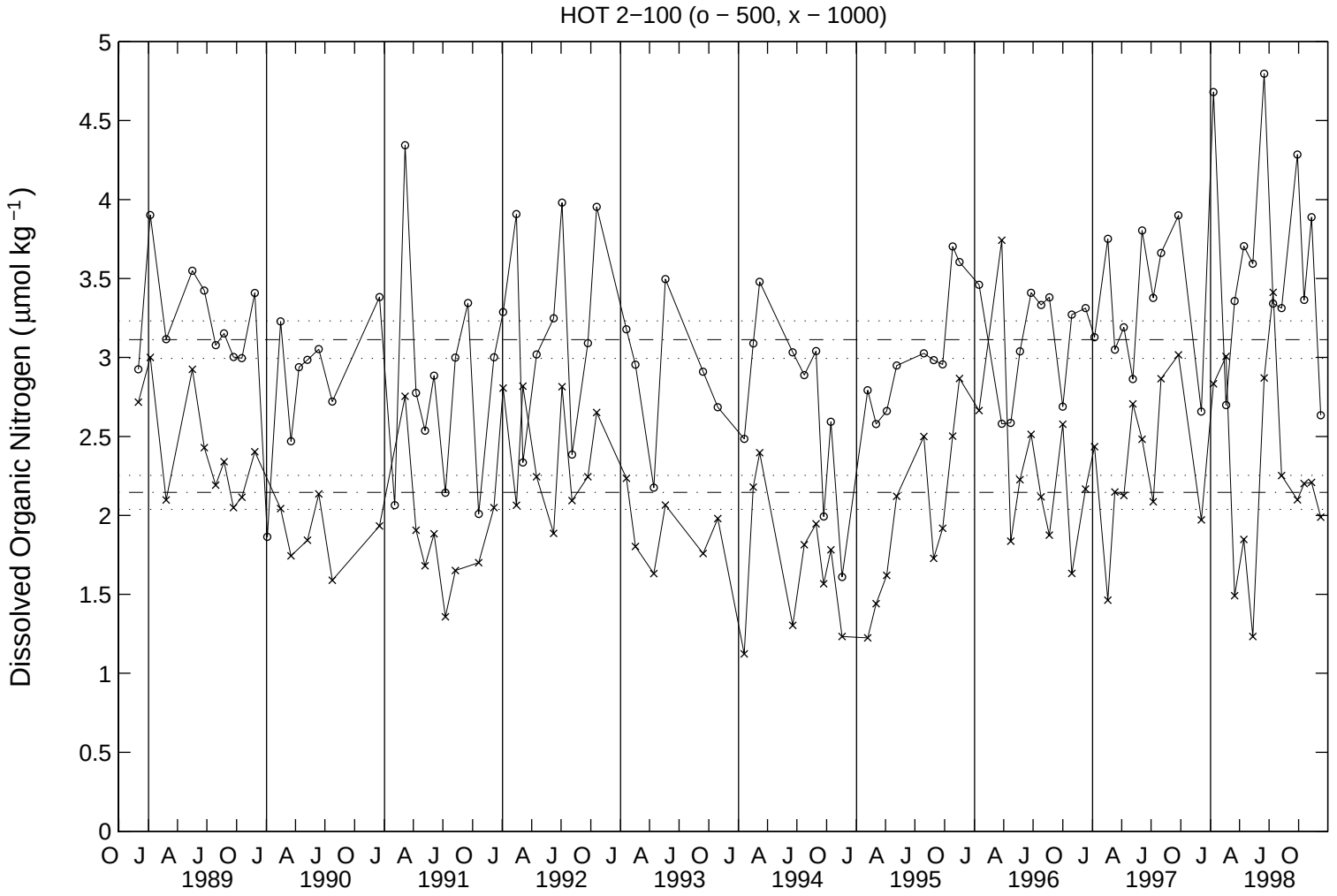

Figure 2.8: Same as Figure 2.7, but for dissolved organic nitrogen for 1988-1995.

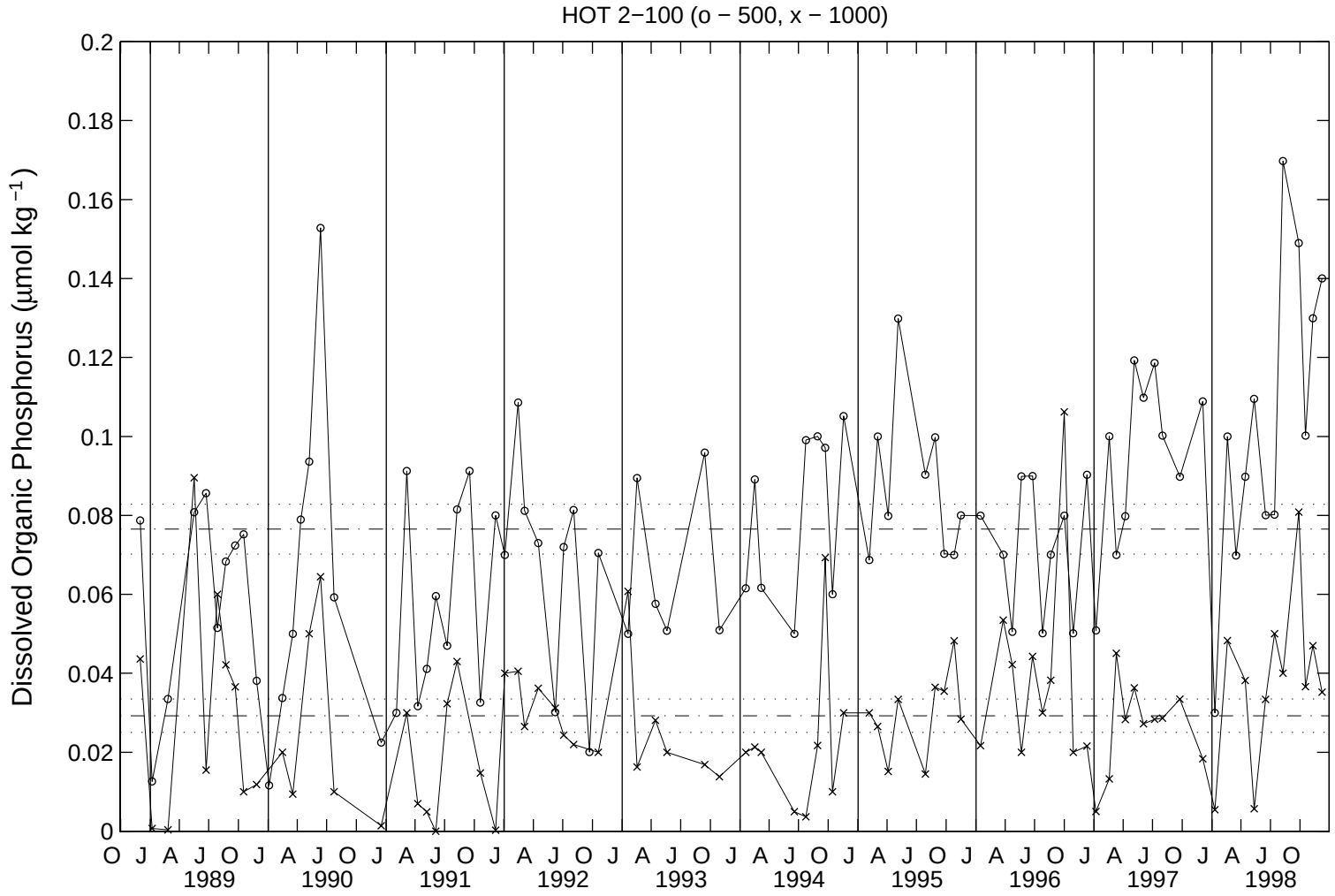

Figure 2.9: Same as Figure 2.7, but for dissolved organic phosphorus for 1988-1995.

and carbon analyzer. Particulate phosphorus (PP) was analyzed by converting the material to orthophosphate by high temperature ashing followed by acid hydrolysis and determining the orthophosphate content by colorimetry.

2.2.9. Pigments

Chlorophyll a (chl *a*) and phaeopigments were measured fluorometrically using 100% acetone as the extractant and standard techniques (Strickland and Parsons, 1972). Analytical precision for this analysis is presented in Table 2.13. Integrated values for pigment concentrations were calculated using the trapezoid rule.

We also measured chl *a* and accessory photosynthetic pigments (Table 2.14) by high performance liquid chromatography (HPLC) according to Bidigare et al. (1990). A new HPLC method following SCOR recommendation was adopted in 1994. This method is a modification of the method developed by Wright et al. (1991). The new method allows for a better separation of lutein and zeaxanthin as well as monovinyl and divinyl chlorophyll *a*. Figure 2.10 shows the relationship between chlorophyll *a* measured by fluorometry and chlorophyll *a* measured by HPLC for the first 7 years of the HOT program.

Table 2.13: Precision of Fluorometric Chlorophyll *a* and Phaeopigment Analyses

	Chl *a*		Phaeo	
Cruise	Mean CV (%)	SD (µg l^{-1})	Mean CV (%)	SD (µg l^{-1})
60	3.5	0.007	4.0	0.013
61	2.8	0.006	5.3	0.014
62	2.3	0.004	3.5	0.008
63	2.0	0.003	3.9	0.006
64	3.4	0.005	5.3	0.008
65	3.9	0.004	10.0	0.015
66	2.8	0.004	11.7	0.007
67	4.2	0.005	11.0	0.011
68	4.8	0.007	4.2	0.010

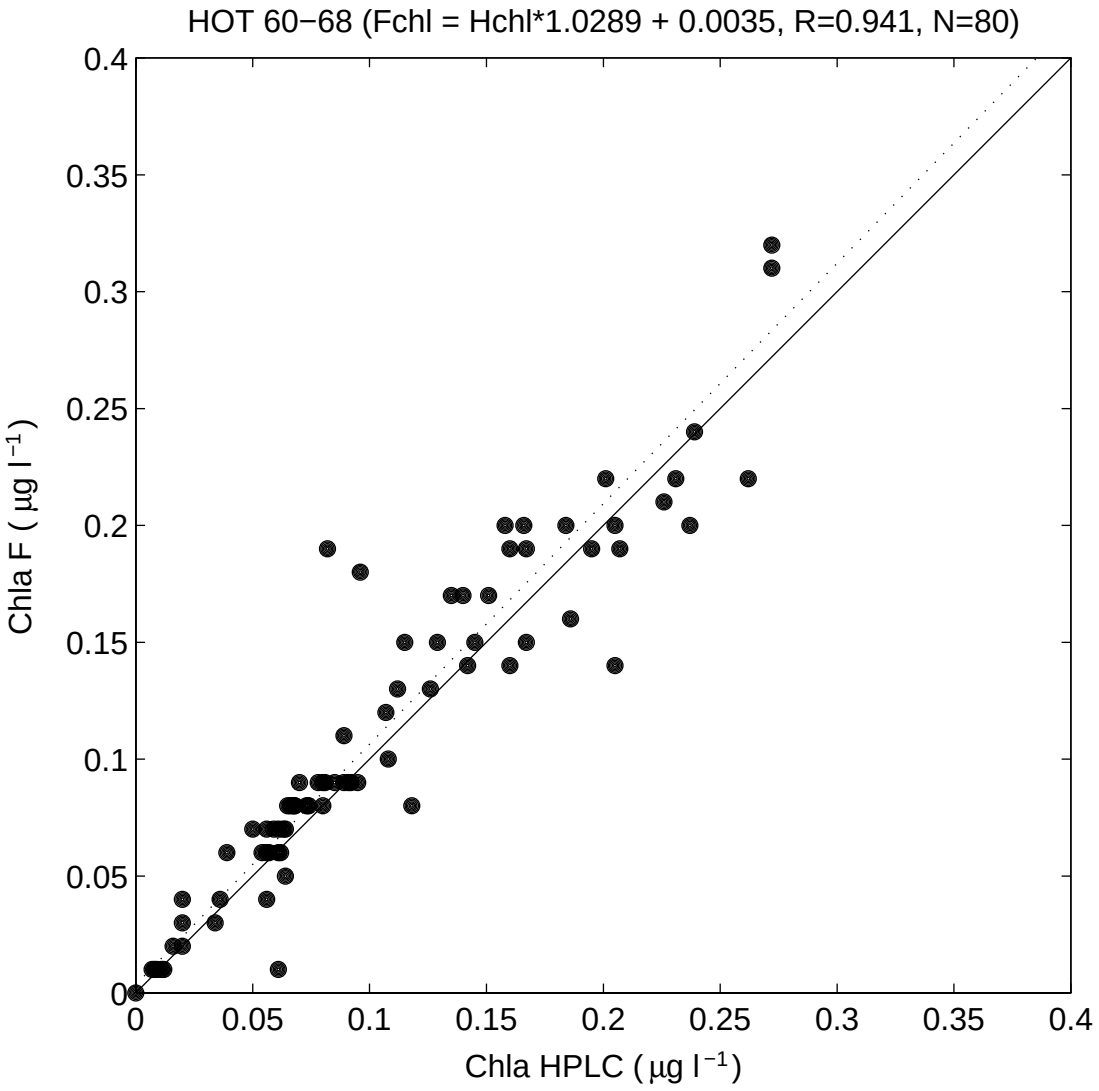

Figure 2.10: Chlorophyll *a* measured by fluorometry (Chla F) versus chlorophyll *a* measured by HPLC (Chla HPLC) for HOT-1 to HOT-68. The solid line shows the y = x relationship. The dashed line is a model II linear regression analysis for the data set. The regression equation is shown at the top of the figure.

Table 2.14: HPLC Pigment Analysis

Pigment	RF*	RT**
Chlorophyll c & Mg 2,4D***	0.000236	
Peridinin	0.000498	0.519
19'-Butanoyloxyfucoxanthin	0.000375	0.541
Fucoxanthin	0.000372	0.578
19'-Hexanoyloxyfucoxanthin	0.000364	0.601
Prasinoxanthin	0.000364	0.666
Diadinoxanthin	0.000251	0.758
Alloxanthin	0.000268	0.816
Lutein	0.000344	0.873
Zeaxanthin	0.000273	0.888
Chlorophyll *b* (monovinyl+divinyl)	0.000932	0.953
Chlorophyll *a* (monovinyl)	0.000436	1.000
Chlorophyll *a* (divinyl)	0.000697	1.000
α-carotene	0.000276	1.131
β-carotene	0.000285	1.137

* RF - Response Factor (mg pigment per unit absorbance peak area at 436 nm).
** RT - Retention Time in min (relative to chlorophyll *a*)
*** Chlorophyll c = (c_1+c_2+c_3),
Mg 2,4,D = Mg 2,4, divinyl pheoporphyrin a_5 monomethyl ester

2.2.10. Adenosine 5'-triphosphate

Water column adenosine 5'-triphosphate (ATP) concentrations were determined using the firefly bioluminesence technique as described by Karl and Holm-Hansen (1978). The precision of ATP determinations in 1995 are given in Table 2.15.

Table 2.15: Precision of ATP Analyses

Cruise	Mean CV (%)	Mean SD (μg m^{-3})
60	11.0	5.7
61	12.2	2.7
62	12.3	2.7
63	11.5	1.4
64	14.9	7.2
65	13.5	2.4
66	14.7	2.2
67	10.6	2.5
68	12.2	1.9

2.3. Biogeochemical Rate Measurements

2.3.1. Primary productivity

Photosynthetic production of organic matter was measured by a trace-metal clean, ^{14}C method. Incubations were conducted *in situ* at eight depths for at least 12 hours using a free-drifting array as described by Winn et al. (1991). Integrated carbon assimilation rates were calculated using the trapezoid rule with the shallowest value extended to 0 m and the deepest extrapolated to a value of zero at 200 m.

2.3.2. Particle flux

Particle flux was measured at reference depths of 150, 200, 300 and 500 m for HOT-60 through HOT-63 and at reference depths of 150 and 200 m for HOT-64 through HOT-68 using sediment traps deployed on a free-floating array for approximately 60-70 hrs during each cruise. Sediment trap design and collection methods are described in Winn et al. (1991). Samples were analyzed for particulate C, N and P using methods described in section 2.2.8. The drifts of the sediment trap arrays are shown in Figures 6.1.1. to 6.1.5.

2.4. ADCP Measurements

Shipboard ADCP data were obtained on eight HOT cruises with the RDI model VM-150 mounted on the R/V *Moana Wave*. There was no ADCP data collected on HOT-64, as the instrument aboard the R/V *Maurice Ewing* was not functioning. Major ADCP recording gaps occurred only on HOT-68 Leg I: a 1-hour gap at the start of the on-station period. No major GPS gaps, besides the time mentioned above, occurred. ASHTECH 3DF GPS heading and attitude were recorded on all cruises except HOT-64. Gaps of up to 20 hours occurred on HOT-62 and HOT-68; 2 to 5-hour gaps were common. These gaps were filled by linear interpolation, with the exception of the 20-hour gap on HOT-66. This was filled with heading corrections computed from a numerical model of gyro compass behavior developed by C. Huhta, T. Le and E. Firing. Giving ship's heading and velocity as functions of time, and the compass correction system used by the ship's officers, the model calculates the error of an idealized Sperry compass.

2.5. Optical Measurements

Incident irradiance at the sea surface was measured on each HOT cruise with a LI-COR LI-200 data logger and cosine collector. Vertical profiles of Photosynthetically Available Radiation (PAR) were also obtained using a Biospherical Instruments model PNF-300 optical profiler, until the instrument was lost on HOT-64. The entire data set is available via Internet, as described in Section 8.

2.6. Meteorology

Wind speed and direction, atmospheric pressure, wet- and dry-bulb air temperature, sea surface temperature (SST), cloud cover and sea state were recorded at four-hour intervals while on Station ALOHA by the science personnel. Meteorological observations were also obtained every 4 hours by the ship's officers on the bridge of the R/V *Moana Wave* throughout each cruise. Additionally, hourly wind speed and direction were obtained from NDBC buoys #51001 (23.4°

N, 162.3°W) and #51026 (21.4°N, 156.96°W). The time series of shipboard observations obtained by the science group was plotted and obvious outliers were identified and flagged. The SST-dry air temperature and wet-dry air temperature plots also helped to identify outliers. Bad data points were often replaced with the bridge data. Outliers in the shipboard wind observations were detected by comparison with the buoy winds. Data from buoy #51026 were not available during HOT-62.

2.7. Inverted Echo Sounder Network

Two inverted echo sounders (IESs) recorded data during 1995. The IESs located at Station Kaena and in the center of Station ALOHA (C) were deployed on 18 June 1994 and recovered on 25 and 28 October 1995. Another IES was deployed at Station ALOHA on 28 October. The history of the IESs in the HOT site is well documented in Tupas et al. (1994a, 1995).

2.8. Bottom-Moored Sediment Traps

A bottom-moored sediment trap experiment has been in place since June 1992 at a site near Station ALOHA (Figure 1.1). The first set of traps (ALOHA-I) was deployed in June 1992 and retrieved in September 1993. The second set (ALOHA-II) was deployed in September 1993 and retrieved in October 1994. The third set (ALOHA-III) was deployed in May 1995 and recovered in October 1995. The fourth set (ALOHA-IV) was deployed in November 1995 and recovered in October 1996. The ALOHA-V mooring was deployed in October 1996 and is currently on the seafloor. Each experiment consisted of from 1-4 Parflux MK7-21 sequencing sediment collectors located at depths ranging from 800-4000 m. A separate sampling cup is rotated into the collector position on an approximately 15-20 day cycle, depending on the experiment. Samples from each cup are initially divided into four 60-ml volumes (also referred to as splits). Each split is further divided into the volumes required for the various analyses (Table 2.16).

Table 2.16: Distribution of Sample Materials From Bottom-Moored Sediment Traps

Investigators	Analyses
D.Karl, L. Tupas, D. Hebel. U. Magaard, T. Houlihan (University of Hawaii)	Total mass, dissolved N, P, Si, total and biogenic particulate C, N, P, Si, fluorometric chlorophyll a, phaeopigments, stable C,N isotopes, bacterial abundance
R. Bidigare, M. Latasa, M. Ondrusek, R. Scharek (University of Hawaii)	Plant pigments by HPLC, diatom abundance and composition
D. Bird (University of Quebec at Montreal)	Virus abundance
S. Honjo, S. Manganini (Woods Hole Oceanographic Institution)	Lithogenic analysis
L. Sautter (College of Charleston)	Foraminiferan abundance
F. Prahl (Oregon State University)	Alkenone concentrations
J. Dymond (Oregon State University)	Barite
D. DeMaster (North Carolina State University)	Radioisotopes

2.9. Thermosalinograph

2.9.1. Data acquisition

A SBE-21 Seacat thermosalinograph (Serial Number 1392) was used during HOT-63, HOT-66, HOT-67 and HOT-68. The thermosalinograph was installed in a pumped intake line in the hull of the R/V *Moana Wave*. A Sea-Bird remote temperature sensor (Serial Number 1496), installed in a sea chest in the bow of the ship, recorded temperature data from about 3 m depth. This location allows for relatively undisturbed water to enter the thermosalinograph. The SBE-21 calculates salinity using an internal temperature and conductivity sensor. Data were obtained every 10 seconds. In order to calibrate the conductivity sensor, bottle salinity samples were periodically taken from the thermosalinograph intake line. To calculate salinity, a pressure of 20 dbar was assumed to compensate for the pressure caused by the pump for the intake line (30 psi). Salinity readings from the thermosalinograph for HOT-66 and HOT-67 were suspiciously low when compared with both bottle and CTD readings. It was thought that there could be a leak in the thermosalinograph system allowing fresh water to enter the system. After thorough investigations, a leak or a cause for the suspicious HOT-66 and HOT-67 salinities could not be determined. In subsequent cruises, we have made sure to closely monitor the thermosalinograph salinity and to compare it with the CTD on a near real-time basis during the cruise to make sure the thermosalinograph is recording accurate salinities. The salinity data from HOT-66 and HOT-67 have been labeled as suspect and are not included in this data report.

2.9.2. Data processing and sensor calibration

2.9.2.1. nominal calibration

The internal temperature sensor (#1392) and external temperature sensor (#1496) were calibrated at Sea-Bird. The calibration coefficients obtained at Sea-Bird are given in Table 2.2. Since these sensors are the same type as used for the CTD measurements, the same procedure for drift estimation were followed. For sensor #1392, a drift rate of -3.766×10^{-6}°C day^{-1} was determined using the 29 September 1994 and 13 October 1995 calibrations. The 29 September 1994 calibration was performed after the sensor's electronics had been reworked. This sort of work usually causes a change in the drift of a sensor so the calibrations prior to this date were not used for drift calculation purposes. HOT-63 and HOT-66 internal temperatures (sensor #1392) were calculated using the 29 September 1994 calibration as a baseline, with drift corrections of -0.8×10^{-3}°C and -1.4×10^{-3}°C respectively. HOT-67 and HOT-68 internal temperatures were calculated with the 13 October 1995 baseline calibration with drift corrections of 0.045×10^{-3}°C and 0.1×10^{-3}°C. However, these corrections are inconsequential and were not applied to the HOT-67 or HOT-68 data.

The external temperature sensor (#1496) was calibrated on 2 November 1993 and 18 January 1996. From these calibrations a drift rate of 1.51×10^{-5}°C day^{-1} was determined. The 2 November 1993 calibration was used to process the data. Drift corrections of 8.3×10^{-3}°C, 10.4×10^{-3}°C, 10.9×10^{-3}°C and 11.2×10^{-3}°C were used for HOT-63, HOT-66, HOT-67 and HOT-68 respectively, for the external temperature data.

Sea-Bird sensor #1392 was used to collect the thermosalinograph conductivity data. The HOT-63 and HOT-66 cruises were nominally calibrated with coefficients obtained at Sea-Bird on 29 September 1994 and the conductivity data from HOT-67 and HOT-68 were nominally calibrated using coefficients obtained at Sea-Bird on 13 October 1995.

2.9.2.2. processing

The thermosalinograph data were screened for gross errors, setting upper and lower bounds of 35°C and 18°C for temperature and 6 Siemens m^{-1} and 3 Siemens m^{-1} for conductivity. No gross errors were detected in any of the cruises.

A 5-point running median filter was used to detect temperature and conductivity glitches. Glitches in temperature and conductivity were immediately replaced by the median. Threshold values of 0.3°C for temperature and 0.1 Siemens m^{-1} for conductivity were used for the median filter. Three conductivity points were replaced with median values for HOT-63. A 3-point triangular running mean filter was used to smooth the temperature and conductivity data from all the cruises after they had gone through glitch detection.

2.9.2.3. empirical calibration

The thermosalinograph salinity was calibrated empirically by comparing it to bottle salinity samples drawn from the plumbing near the thermosalinograph. Bottle salinity samples were analyzed as described in section 2.2.1.

For HOT-63 and HOT-68, the time delay between the water passing through the thermosalinograph and it reaching the bottle sampling area was determined to be about 50 seconds using autocorrelation between bottle and thermosalinograph samples. The

thermosalinograph data were extracted within ±15 seconds around the sample time minus the 50 second delay for the comparison with the bottle data.

A cubic spline was fit to the time-series of the differences between the bottle conductivity and the thermosalinograph conductivity separately for HOT-63 and HOT-68 (Figure 2.11). The correction of the thermosalinograph conductivities was obtained from the cubic spline fit. Salinity was calculated using these corrected conductivities, thermosalinograph temperatures and pressure of 20 dbar. The bottle samples taken at the end of HOT-68 (November 18-20) appear to show more variation with the thermosalinograph than the other bottles. The ship was in transit for most of this time period and this may have induced some greater variation between the thermosalinograph and the bottle samples. Most of the bottle samples taken before November 18 were taken while the ship was on station.

2.9.2.4. comparison with CTD data

The corrected thermosalinograph salinity data were compared with the downcast CTD salinity at 4 dbar for the purpose of checking the calibration.

The thermosalinograph data for HOT-63 and HOT-68 were averaged using data sampled one minute after the acquisition time of the CTD sample. The linear fit of the time-series of the CTD-thermosalinograph salinity differences showed that the CTD salinity was higher than the thermosalinograph salinity most of the time, and the average offset was 0.019 for HOT-63 and 0.0057 for HOT-68 (Figure 2.12).

2.10. Endeco Towfish

At the end and during the returning transit of each cruise in 1995, scientists from Scripps Institution of Oceanography (M. Huntley and M. Lopez, P.I.s) obtained data from a towed instrument package consisting of an Endeco Instruments 1.5 m fin, a Sea-Bird (SBE-19) CTD and a Focal Instruments Optical Plankton Counter (OPC). A WetLabs SeaStar fluorometer was added to the package in June 1996. The package is deployed on a 3-conductor cable and towed at a constant depth at a speed of 8-10 kts. The package collects data on physical (T and C) and biological (zooplankton biomass and size spectrum, chl *a*) variability in the mixed-layer of the water column. The sampling pattern typically consists of zigzags within a square extending from 22.65°N to 22.85°N, 157.9°W to 158.1°W, and a transect along the regular ship track into Honolulu. The target towing depth was 45 m, with variations of approximately ±5 m due to changes in ship speed and heading. The CTD worked only intermittently, even after repeated repairs by Sea-Bird. After HOT-68, a SBE-19 with temperature, conductivity and pressure sensors was purchased and has worked satisfactorily in subsequent cruises.

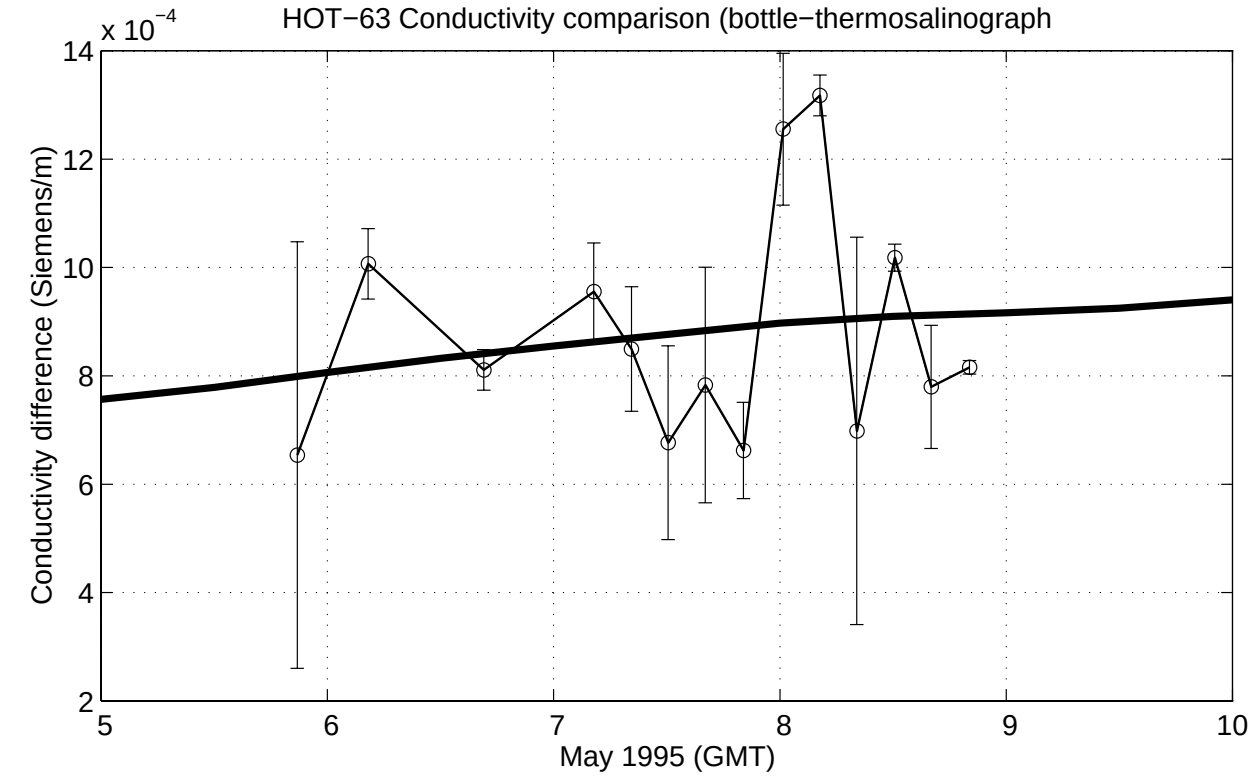

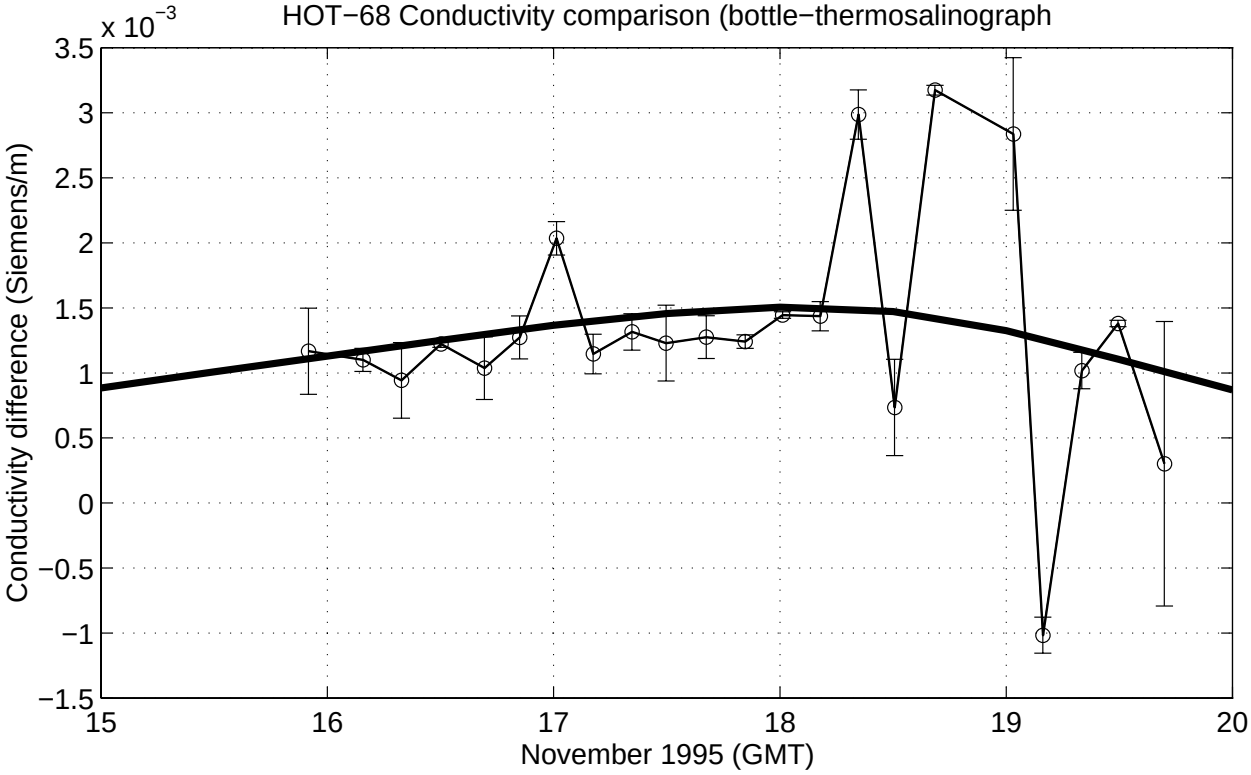

Figure 2.11: Differences between conductivities from bottle samples and thermosalinograph for HOT-63 [Upper panel], and HOT-68 [Lower panel]. Thick lines show the cubic spline fit. Circles indicate average values around the sampling time, and the bars indicate standard deviation within the averaging interval. See text for the details of the averaging procedures.

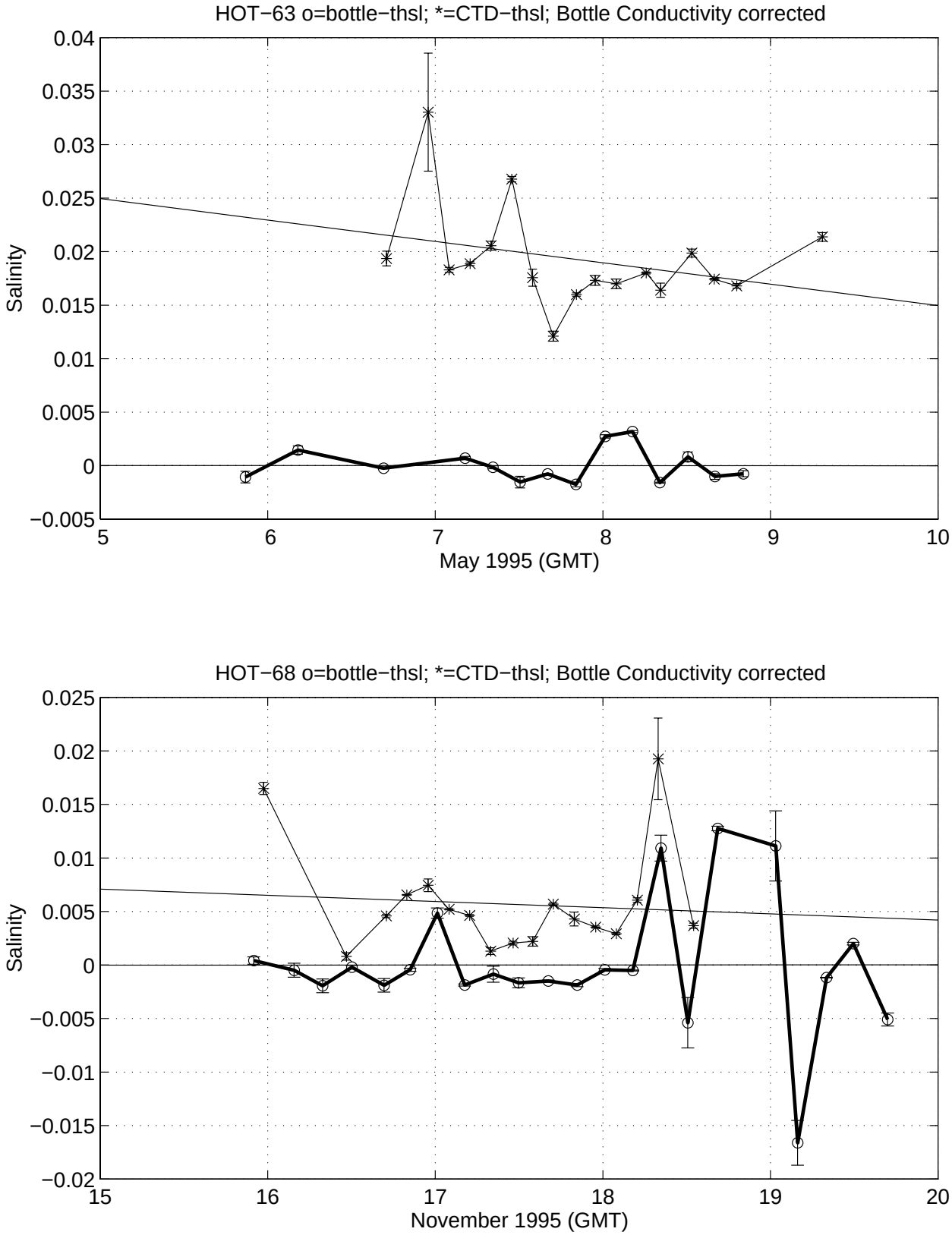

Figure 2.12: Differences between bottle salinities and thermosalinograph salinities (thick line), and differences between CTD salinities and thermosalinograph salinities (thin line) for HOT-63 [Upper panel], and HOT-68 [Lower panel]. Thin straight lines show the linear fit. Circles indicate average values around the bottle sampling time, and asterisks indicate average values around the acquisition time of the CTD data. The bars indicate the standard deviation. See text for the details of the averaging procedures.

3. CRUISE SUMMARIES

3.1. HOT-60: Luis Tupas, Chief Scientist

The R/V *Moana Wave* departed Snug Harbor at 0900 hr on 4 February 1995 with 17 scientists aboard. All objectives of the JGOFS and WOCE programs were accomplished despite losing one day of work due to CTD winch problems and inclement weather. Only Stations Kahe, Kaena and ALOHA were occupied. All core samples were taken but the 36-hour CTD burst sampling period was disrupted for 24 hours after the first 12 hours of sampling. All samples for ancillary projects were taken. Floating sediment trap and primary production arrays were successfully deployed and recovered. Aside from the CTD winch, there were no other equipment failures. The optical plankton counter (OPC) was towed from Stations Kahe to Kaena without any problem. The moored sediment trap array was deployed as the last scientific activity of the cruise. Deployment went smoothly until it was time to release the anchor. The bridge informed the science group that we were near a submarine telephone line and wanted the ship to move a little before releasing the anchor. The ship was moving at about 1.5 knots for approximately 10 minutes before the Chief Scientist decided to drop the anchor. While obtaining the slant ranges for the mooring, it was noticed that the surface VHF transmitter was still transmitting a signal. After locating the source of the signal it was discovered that 3/4 of the array was on the surface. The science group then proceeded to retrieve the array and plans to recover the remaining 1/4, now on the seabed, on another cruise. The ship arrived back at Snug Harbor at 1130 hr on 9 February 1995.

3.2. HOT-61: Luis Tupas, Chief Scientist

The R/V *Moana Wave* departed Snug Harbor at 0900 hr on 2 March 1995 with 16 scientists aboard. All objectives of the JGOFS and WOCE programs were accomplished. Only Stations Kahe, Kaena and ALOHA were occupied. All core samples were taken but the 36-hour CTD burst sampling period was disrupted at 2 instances (approximately 3 hours each) when the cable was twisted and needed to be reterminated. All samples for ancillary projects were taken. During the floating sediment trap deployment, the spar buoy broke and the whole array had to be retrieved. The experiment was terminated. The primary production array was successfully deployed and recovered. Aside from the reterminations of CTD cable, there were no other equipment failures. The optical plankton counter was towed from Stations Kaena to ALOHA without any problem. After all work at Station ALOHA was accomplished (5 March, 1830 hr), the ship was preparing to move to the location of the sediment trap site when it received a distress call from a sinking fishing vessel. The *Moana Wave* arrived on the scene at 2300 hr and the Coast Guard cutter *Washington* arrived at 2330 hr. The *Moana Wave* was instructed to stand by as the Coast Guard took over the rescue. The *Moana Wave* was released at 0300 hr on 6 March. The ship proceeded to the mooring site where it did survey work for the remains of the sediment trap mooring. After the survey, the ship proceeded to Station ALOHA to conduct an areal study of the station with the OPC/v-fin. After the transect, the ship proceeded to Honolulu still towing the v-fin which was retrieved just before the ship entered Honolulu harbor. The ship arrived back at Snug Harbor at 0730 on 7 March 1995.

3.3. HOT-62: Dale Hebel, Chief Scientist

The R/V *Moana Wave* departed Snug Harbor at 0900 hr on 4 April 1995 with 16 scientists aboard. All over-the-side operations were completed and all samples collected although the nutrient samples collected at Kahe and Kaena were most likely compromised because of laboratory freezer malfunction. Ricardo Letelier (OSU) deployed a moored optical buoy (MOB), followed by a dragging attempt to recover our lost equipment. The optical plankton counter (OPC) was deployed on the return leg. The ship arrived back at Snug Harbor at 0730 hr on 9 April 1995.

3.4. HOT-63: Dale Hebel, Chief Scientist

The R/V *Moana Wave* departed Snug Harbor at 0900 hr on 5 May 1995 with 17 scientists aboard. All over-the-side operations were completed and all samples collected. Jim Richman (OSU) recovered the moored optical buoy (MOB) deployed on HOT-62, while Dave Karl and company deployed a single moored sediment trap. Bob Miller completed all plankton net tows and the optical plankton counter (OPC) was deployed on the Kaena-ALOHA, ALOHA-sediment trap, and sediment trap-Snug Harbor transits. In addition, testing was conducted on the continuous water sampler and AC-3 instruments. The OPC was deployed during the return transit. The ship arrived back at Snug Harbor at 0740 hr on 10 May 1995.

3.5. HOT-64: Luis Tupas, Chief Scientist

The R/V *Maurice Ewing* departed Snug Harbor at 0900 hr on 28 July 1995 with 23 scientists aboard. All objectives of the JGOFS and WOCE programs were accomplished. Stations Kahe, Kaena and ALOHA were occupied. All core samples were taken within the 36-hour CTD burst sampling period but several sampling intervals were delayed because of on-going operations on deck. All samples for ancillary projects were taken. The floating sediment trap and the primary production arrays were successfully deployed and recovered. Problems were encountered with the CTD winch which did not brake properly during descent. This was a major safety concern because during the retrieval the package would slam onto the deck. A crane was used to lift the package and retrieve the package once it was out of the water. Additionally, the new rosette frame was spinning during deployement which twisted the wire badly and required retermination of the CTD cable after the first cast. The profiling natural fluorescence instrument was lost during its initial deployment. The instrument was apparently dragged under the ship and the cable was cut by the ship's propellers. There were no other equipment failures. The optical plankton counter (OPC) was towed on a series of transects through Station ALOHA. After the transect, the ship proceeded to Honolulu still towing the v-fin which was retrieved just before the ship entered Honolulu harbor. The ship arrived back at Snug Harbor at 0800 hr on 2 August 1995.

3.6. HOT-65: Luis Tupas, Chief Scientist

The R/V *Moana Wave* departed Snug Harbor at 0900 hr on 27 August 1995 with 16 scientists aboard. All objectives of the JGOFS and WOCE programs were accomplished. All planned stations were occupied. All core samples were taken within the 36-hour CTD burst sampling period. All samples for ancillary projects were taken. Floating sediment trap array and primary production array were deployed and recovered successfully. There were no major equipment failures. The optical plankton counter (OPC) was towed from Station ALOHA to Honolulu without any problem. The inverted echo sounder (IES) mooring was successfully deployed. All samples for ancillary investigators were collected. On-board experiments were also conducted. The ship arrived back at Snug Harbor at 0730 hr on 1 September 1995.

3.7. HOT-66: Dale Hebel, Chief Scientist

The R/V *Moana Wave* departed Snug Harbor at 0900 hr on 25 September 1995 with 14 scientists aboard. All over-the-side operations were completed and all samples collected. This was the first cruise to use a 4-day cruise schedule. Steve Emerson and Peter Kolman deployed a gas tension device (GTD) on the sediment trap line at approximately 20 m which was used to measure total gas pressures. Since oxygen and nitrogen contribute ~99% of the total, the independent measurement of oxygen allows quantification of nitrogen. During the deployment period gas calibration samples were collected in close proximity to the array. This was one of the few cruises where the trap array remained within the confines of the station boundary for most of the deployment period. It was also unusual with the drift track almost due north. The optical plankton counter (OPC) was deployed on the Kaena-ALOHA and sediment-trap-ALOHA-Snug Harbor legs. We experienced two accidents which were relatively minor. One was an injury to Molly Lucas and the other a small electrical fire in the JGOFS laboratory van. The ship arrived back at Snug Harbor at 0730 hr on 29 September 1995.

3.8. HOT-67: Fernando Santiago-Mandujano, Chief Scientist

The R/V *Moana Wave* departed Snug Harbor at 0800 hr on 25 October 1995 with 15 scientists aboard. All the primary JGOFS and WOCE objectives were accomplished. All samples for ancillary projects were taken, and the ADCP and thermosalinograph were running without interruption throughout the cruise. Weather conditions were very favorable during the first three and a half days, allowing for the safe recovery of the Kaena Station inverted echo sounder (IES), the deployment of the sediment trap array, the deployment and recovery of the primary production array, the completion of the 36-hour CTD burst sampling and two near-bottom CTD casts, and the recovery and deployment of the Station ALOHA IESs. Chuck Stump attached his gas tension device-Seacat package on the sediment trap line, at about 15 m. Mike Mulroney suffered a minor accident after the IES deployment while retrieving the transducer from the side of the ship. He was pulling the cable a little fast, when the transducer came over the rail and onto his head, resulting in a small cut on his forehead that was quickly treated on board. The Captain was notified and an incident report was filled.

With the weather deteriorating on the fourth day, the conditions became less favorable for the recovery of the sediment trap array. The spar buoy broke in half during recovery and the bottom half, with the lead weight, went to the sea floor. The rest of the array, including all samples, was safely retrieved. The moored sediment trap was successfully recovered on the fifth

day. Station 3 was also visited, and a near-bottom CTD cast was conducted. The optical plankton counter-CTD fish was towed from Staion ALOHA to Station Kahe without any problem, although its CTD did not work correctly. Station Kahe was occupied near the end of the cruise, and a CTD cast was obtained. The carousel failed to fire 8 of the 16 intended bottles during this cast. The ship arrived back at Snug Harbor at 0730 hr on 30 October 1995.

3.9. HOT ST-4: David Karl, Chief Scientist

The R/V *Moana Wave* departed Snug Harbor at 0900 hr on 12 November 1995 with 9 scientists aboard. The cruise objectives were to recover a bottom-moored sediment trap at 22° 50.158'N, 157°55.881'W that was deployed on HOT-63 (May 1995), to service the components and to redeploy a three-trap array for a scheduled 1-yr period. A secondary objective was to pressure test an instrument case for colleagues in the DUMAND project. All objectives were successfully accomplished. The ship arrived back at Snug Harbor at 0730 hr on 14 November 1995.

3.10. HOT-68: Luis Tupas, Chief Scientist

The R/V *Moana Wave* departed Snug Harbor at 0930 hr on 15 November 1995 with 12 scientists aboard. All objectives of the JGOFS and WOCE programs were accomplished. All planned stations were occupied. All core samples were taken and the 36-hour CTD burst sampling period was not interrupted. All samples for ancillary projects were taken. Both the floating sediment trap array and primary production array were deployed and recovered successfully. There were no major equipment failures. The optical plankton counter was towed from Station ALOHA to Honolulu without any problem. Extra Go-Flo casts to accommodate the sampling requirements of Charles Stump were conducted. The ship arrived back at Snug Harbor at 0730 hr on 19 November 1995.

4. RESULTS

4.1. Hydrography

Calendar year 1995 was particularly active with regards to the variability of the hydrographic parameters in the water column at Station ALOHA. Very low salinities were observed in the upper 100 dbar for about 5 months early in the year. These extreme low values had not been observed since 1989. At about 300 dbar, an oxygen minimum developed in late 1994 and lasted about half a year, this minimum seemed to be accompanied by a decrease in salinity and an increase in nutrient concentration. Similar features had been observed previously in 1990 and 1992. In the bottom water, a cold water anomaly of up to 0.024°C developed in a 200-m layer above the bottom between cruises HOT-64 and HOT-68 (Lukas et al., in prep.). This anomaly was accompanied by an increase in salinity and oxygen concentrations. Similar cold events were also observed in 1991 and 1993.

4.1.1. 1995 CTD profiling data

Profiles of temperature, salinity, oxygen and potential density (σ_θ) were collected at both Station Kahe and Station ALOHA. The profiles from Station ALOHA during 1995 are presented in Figure 6.2.1. The results of bottle determinations of oxygen, salinity and inorganic nutrients are also shown. In addition, stack plots of CTD temperature and salinity profiles for all 1000 m casts conducted at Station ALOHA are presented (Figure 6.2.2). The data collected for Station Kahe during 1995 are presented in Figures 6.2.3. The temperature, salinity and oxygen profiles obtained from the deep casts at Station ALOHA during 1995 are presented in Figures 6.2.4-6. The development of a cold water anomaly near the bottom between cruises HOT-64 and 68 is apparent in the potential temperature profiles of Figure 6.2.4. In the same figure, a single temperature profile obtained during HOT-64 shows higher temperatures than those from the other profiles between 1000 and 4500 dbar. These temperatures were confirmed by the measurements obtained during the up-cast and by those from the second temperature sensor. This anomaly seems to be related to events preceding the bottom cold anomaly (Lukas et al., in prep.).

4.1.2. Time-series hydrography (1988-1995)

The hydrographic data collected during the first 7 years of HOT are presented in a series of contour plots (Figures 6.3.1-14). These figures show the data collected in 1995 within the context of the longer time-series database. The CTD data used in these plots are obtained by averaging the data collected during the 36-hour period of burst sampling. Therefore, much of the variability which would otherwise be introduced by internal tides in the upper ocean has been removed. Figures 6.3.1 and 6.3.2 show the contoured time-series record for potential temperature and density in the upper 1000 dbar for all HOT cruises through 1995. Seasonal variations in temperature for the upper ocean are apparent in the maximum of near-surface temperature of about 26°C and the minimum of approximately 23°C. Oscillations in the depth of the 5°C isotherm below 500 dbar appear to be relatively large with displacements up to 100 dbar. The main pycnocline is observed between 100 and 600 dbar, with a seasonal pycnocline developing between June and December in the 50-100 dbar range (Figure 6.3.2). The cruise-to-cruise changes between February and July 1989 in the upper pycnocline illustrate that variability in density is not always resolved by our quasi-monthly sampling.

Figures 6.3.3-6 show the contoured time-series record for salinity in the upper 1000 dbar for all HOT cruises through 1995. The plots show both the CTD and bottle results plotted against pressure and potential density. Most of the differences between the contoured sections of bottle salinity and CTD salinity are due to the coarse distribution of bottle data in the vertical as compared to the CTD observations. Some of the bottles in Figure 6.3.6 are plotted at density values lower than the indicated sea surface density. This is due to surface density changing from cast to cast within each cruise, and even between the downcast and the upcast during a single cast.

Surface salinity is variable from cruise-to-cruise, with no obvious seasonal cycle and some substantial interannual variability. The surface salinity is low in late 1989, increases to a maximum in late 1990, decreases again during 1991 and 1992, rises to an extreme high in late 1993 and decreases again in 1994. For about five months in early 1995 it reached extreme low values only comparable to those in 1989. The salinity maximum is generally found between 50 and 150 dbar, and within the potential density range 24-25 kg m^{-3}. A salinity maximum region extends to the sea surface in the later part of 1990 and 1993, as indicated by the 35.2 contour reaching the surface. This contour nearly reaches the surface late in 1988 and 1989. The maximum shows salinities smaller than normal in early 1995, and throughout that year the values are below 35.2. The maximum value of salinity in this feature is subject to short-term variations of about 0.1 which is probably due to the proximity of Station ALOHA to the region where this water is formed at the sea surface (Tsuchiya, 1968). The variability of this feature is itself variable. Throughout 1989 there were extreme variations of a couple of months duration with 0.2 amplitude. The variability was much smaller and slower thereafter, except for a few months of rapid variation in earlier 1992. The salinity minimum is found between 400 and 600 dbar (26.35-26.85 kg m^{-3}). There is no obvious seasonal variation in this feature, but there are distinct periods of higher than normal minimum salinity in early 1989, in the fall of 1990 and early 1992. These variations are related to the episodic appearance at Station ALOHA of energetic fine structure and submesoscale water mass anomalies (Lukas and Chiswell, 1991).

Figures 6.3.7 and 6.3.8 show contoured time-series data for oxygen in the upper 1000 dbar at Station ALOHA. The oxygen data show a strong oxycline between 400 and 625 dbar (26.25-27.0 kg m^{-3}), and an oxygen minimum centered near 800 dbar (27.2 kg m^{-3}). During 1989, there was a persistent oxygen maximum near 300 dbar (25.75 kg m^{-3}), which appeared again during 1991 and shortly in early 1993 and mid 1994. At the same level, an oxygen minimum developed in early 1990 and late 1991, mid 1992, and late 1994. This minimum was accompanied by an increase in the concentration of nutrients (see below), and a decrease in salinity. The oxygen minimum exhibited some interannual variability as well, with values less than 30 mol kg^{-1} appearing in the last half of 1989 and the first half of 1990, reappearing, less intensely, in 1991 and 1992, again strongly in 1993 and 1994, and weakening in 1995. The surface layer shows a seasonality in oxygen concentrations, with highest values in the winter. This roughly corresponds to the minimum in surface layer temperature (Figure 6.3.1). An oxygen maximum at about 100 m appears in the latter half of 1991 and persists through 1992, reappears again in 1993 and persists through 1994.

Figures 6.3.9-14 show [nitrate+nitrite], phosphate and silica at Station ALOHA plotted against both pressure and potential density. The nitricline is located between about 200 and 600 dbar (25.75-27 kg m^{-3}; Figures 6.3.9-10). Most of the variations seen in these data are associated

with vertical displacements of the density structure, and when [nitrate+nitrite] is plotted versus potential density, most of the contours are level. The upper reaches of the water column show considerable variability in density space. The record is dominated by a few short events where nutrients appear to be brought up into the surface layers (Karl et al., 1996). These events occurred in March-April 1990, January 1992, February 1993 and February-March 1995, and were accompanied by a decrease in the oxygen concentration apparent between 200 and 400 dbar (Figure 6.3.7). Possible smaller events also occurred in September 1989, March 1991 and February 1994. These events are probably important in the upper ocean nutrient balance, but are of such short duration that it is difficult to capture them with quasi-monthly sampling. The phosphate and silica records are similar to the [nitrate+nitrite].

4.2. Flash Fluorescence and Beam Transmission

Stack plots of the flash fluorescence and beam transmission data from each HOT cruise in 1995 are presented in Figures 6.4.1 to 6.4.9. *In situ* flash fluorescence profiles show the fluorescence maximum at the base of the euphotic zone, characteristic of the North Pacific subtropical gyre. Percent transmission profiles consistently show increased attenuation due to increased particle load at depths shallower than 100 dbar. Both fluorescence and beam transmission profiles show the influence of internal waves when plotted against pressure, but remain relatively constant within a cruise when plotted in density space. However, both data sets show substantial cruise-to-cruise variability in these properties.

Representative fluorescence profiles for a period of 7 years are shown in Figures 6.4.10 and 6.4.11. In order to facilitate comparison, only night-time profiles are presented after normalization to the average density profile obtained from the CTD burst sampling for each cruise. Month-to-month variability in the average depth of the fluorescence maximum is apparent. This is particularly evident in year 3 where the depth of the fluorescence maximum appears to increase in mid to late summer and in year 4 from summer to winter (Figure 6.4.10). The depth of the fluorescence maximum decreased significantly from spring to fall in 1993. Beam transmission profiles for the 7-year observation period are shown in Figure 6.4.12 and 6.4.13. These profiles were collected at approximately midnight and were normalized to the average density profile obtained for each cruise. Beam transmission profiles also show considerable variability on monthly time scales (Figure 6.4.12 and 6.4.13).

4.3. Biogeochemistry

Biogeochemical data collected during 1995 are summarized in Figures 6.5.1 to 6.5.11. In some cases the results from the first 7 years of the program have been combined to produce these figures.

4.3.1. Dissolved inorganic carbon and titration alkalinity

Dissolved inorganic carbon (DIC) and titration alkalinity measured in the upper 1000 dbar of the water column over the first 7 years of the time-series program are presented in Figures 6.5.1 and 6.5.2. Time-series of titration alkalinity and DIC in the mixed layer are presented in Figure 6.5.3. Titration alkalinity normalized to 35 ppt salinity averages approximately 2305 µmol kg^{-1} and, within the precision of the analysis, appears to remain relatively constant at Station ALOHA. This observation is consistent with the results of Weiss et

al. (1982) who concluded that titration alkalinity normalized to salinity remains constant in both the North and South Pacific subtropical gyres. In contrast to titration alkalinity, the concentration of DIC varies annually. DIC in the mixed layer is highest in winter and lowest in summer. This oscillation is consistent with an exchange of carbon dioxide across the air-sea interface driven by temperature dependent changes in mixed layer pCO_2.

Titration alkalinity shows considerable time-dependent variability around the shallow salinity maximum, centered at about 125 dbar, and the salinity minimum, centered at about 400 dbar. These variations are largely associated with variability in salinity at these depths and disappear when alkalinity is normalized to 35 ppt. Titration alkalinity normalized to 35 ppt salinity is elevated in surface waters in spring of 1990 and winter of 1994. This corresponds to the appearance of mesoscale eddies at Station ALOHA at this time (Winn et al., 1991).

4.3.2. Low-level nutrient profiles

Euphotic zone nutrient concentrations at Station ALOHA are at or well below the detection limits of the autoanalyzer methods. Other analytical techniques and instrumentation are used to measure the nanomolar levels of [nitrate + nitrite] and SRP in these waters. Figures 6.5.4 and 6.5.5 show the profiles obtained from our low level nutrient analyses in 1995. At depths shallower than 100 dbar, SRP is typically less than 150 nmol kg^{-1} and on occasion, as low as 15 nmol kg^{-1}. SRP concentrations appear to vary by at least 3-fold in this region (Figure 6.5.4). Concentrations of [nitrate + nitrite] at depths less than 100 m are always less than 10 nmol kg^{-1} and are often less the 5 nmol kg^{-1} (Figure 6.5.5). Figures 6.5.6 and 6.5.7 show integrated upper water column (0-100 m) inventories for [nitrate+nitrite] and SRP. The trends observed are very different for these two important macronutrients. The [nitrate+nitrite] plot shows evidence of the, generally, late winter (February) nutrient injections into the euphotic zone that were discussed previously. SRP on the other hand displays a systematic and sustained decrease from about 10 mmol SRP m^{-2} in 1989 to less than 5 mmol SRP m^{-2} in 1995 (Karl and Tien, 1996). We believe that this drawdown in SRP is a result of bacterial nitrogen fixation, and a shift from a N-controlled to a P-controlled ecosystem (Karl et al., 1995). The reasons for this shift are not known for sure but an experimental investigation of several mechanisms is currently under investigation.

4.3.3. Pigments

A contour plot of chl a concentrations measured using standard fluorometric techniques from 0 to 200 dbar over the first seven years of the program is shown in Figure 6.5.8. As expected a chlorophyll maximum with concentrations up to 300 µg m^{-3} is observed at approximately 100 dbar. The chl a concentrations at depths shallower than 50 m display a clear annual cycle increasing in the fall and winter and decreasing through spring and summer which is approximately 4-6 months out of phase with the annual oscillation at the base of the euphotic zone (Winn et al., 1995).

4.3.4. Particulate carbon, nitrogen and phosphorus

Particulate carbon (PC), nitrogen (PN) and phosphorus (PP) in the surface ocean over the first seven years of the program are shown in Figures 6.5.9 to 6.5.11. PC varies between 1.3-3.0 µmol kg^{-1}, PN between 0.08-0.65 µmol kg^{-1} and PP between 8-35 nmol kg^{-1} in the upper 100 m

of the water column. PC and PN show a clear annual cycle with the greatest particulate concentrations in summer/fall and lowest in winter. A significantly larger PN concentration was observed in the late fall of 1993 with only a slight increase in PC and a decrease in PP. The temporal distribution and magnitude of PC, PN, and PP in 1995 were similar to previous years.

4.4. Primary Production and Particle Flux

4.4.1. Primary productivity

The results of the ^{14}C incubations and pigment determinations for samples collected from Go-Flo casts in 1995 are presented in Tables 4.4.1 and 4.4.2. Table 4.4.1 presents the primary production and fluorometric pigment measurements made at individual depths on all 1995 cruises. Table 4.4.2 presents integrated values for irradiance, pigment concentration and primary production rates. The pigment concentrations and ^{14}C incorporation rates reported are the average of triplicate determinations. Integrated primary production rates measured over all 7 years of the program are shown in Figure 6.6.1 in order to place the 1995 results within the context of the time-series data set.

Variability in rates of primary production, integrated over the euphotic zone during the first 7 years of the time-series program, appear to be stochastic with no obvious evidence of a seasonal cycle (but see Winn et al., 1995). Measured rates ranged from less than 200 to greater than 1000 mg C m^{-2} day^{-1} with the highest rate being observed in August 1989. This high rate of primary production coincided with a cyanobacterial bloom observed in surface waters near Station ALOHA on HOT-9 (Karl et al., 1992). This variability, with a range of a factor of 5, is surprisingly large. However, the majority of the primary production estimates were between 250 and 600 mg C m^{-2} d^{-1}, and the average rate of primary production was approximately 450 mg C m^{-2} d^{-1}. Although this value is higher than historical measurements for the central ocean basins (Ryther, 1969), it is consistent with more recent measurements using modern methodology (Martin et al., 1987; Laws et al., 1989; Knauer et al., 1990).

Table 4.1: Primary Production and Pigment Summary

Cruise	Depth (m)	Mean Chl *a* (mg m^{-3})	Std. Dev. Chl *a* (mg m^{-3})	Mean Phaeo (mg m^{-3})	Std. Dev. Phaeo (mg m^{-3})	Light (mg C m^{-3}) Rep #1	Light (mg C m^{-3}) Rep #2	Light (mg C m^{-3}) Rep #3	Dark (mg C m^{-3}) Rep #1	Dark (mg C m^{-3}) Rep #2	Dark (mg C m^{-3}) Rep #3
60	5	0.087	0.005	0.063	0.002	5.12	5.26	4.87	0.27	0.38	0.25
60	25	0.090	0.006	0.074	0.011	5.14	4.39	6.25	0.22	0.21	0.21
60	45	0.089	0.002	0.067	0.008	4.62	3.62	4.36	0.21	0.19	0.17
60	75	0.108	0.005	0.083	0.008	2.40	2.10	2.87	0.16	0.16	0.17
60	100	0.151	0.024	0.122	0.007	0.87	0.72	0.82	0.14	0.17	0.16
60	125	0.199	0.036	0.370	0.046	0.53	0.55	0.57	0.14	0.10	0.11
60	150	0.112	0.005	0.255	0.012	0.17	0.13	0.16	0.08	0.09	0.08
60	175*	0.093	0.004	0.081	0.019	0.12	0.11	0.13	0.16	0.15	0.13
61	5	0.083	0.005	0.041	0.002	7.66	6.88	7.86	0.33	0.31	0.21
61	25	0.086	0.002	0.043	0.003	7.33	5.43	6.44	0.26	0.24	0.23
61	45	0.075	0.002	0.046	0.007	4.55	3.93	5.73	0.28	0.23	0.26
61	75	0.118	0.004	0.148	0.008	2.42	1.56	2.00	0.20	0.20	0.21
61	100	0.187	0.014	0.350	0.018	1.20	ND	1.69	0.16	0.13	0.12
61	125	0.074	0.003	0.168	0.008	0.23	0.21	0.23	0.07	0.07	0.06
61	150*	0.031	0.002	0.060	0.014	0.06	0.06	0.08	0.06	0.06	0.06
61	175*	0.078	0.001	0.066	0.006	0.15	0.12	0.13	0.13	0.14	0.13
62	5	0.078	0.001	0.049	0.004	6.44	7.86	7.42	0.32	0.37	0.28
62	25	0.078	0.001	0.052	0.002	6.11	6.24	6.72	0.21	0.21	0.19
62	45	0.085	0.001	0.072	0.011	3.16	4.33	4.61	0.22	0.20	0.16
62	75	0.148	0.001	0.147	0.005	2.97	3.20	3.49	0.13	0.14	0.14
62	100	0.178	0.003	0.224	0.015	1.68	2.23	1.47	0.10	0.11	0.12
62	125	0.139	0.015	0.303	0.045	ND	0.67	0.61	0.11	0.06	0.10
62	150	0.078	0.002	0.193	0.029	0.12	0.11	0.12	0.06	0.06	0.07
62	175	0.035	0.002	0.084	0.002	0.05	0.05	0.04	0.05	0.05	0.04
63	5	0.090	0.001	0.067	0.001	15.66	17.12	12.23	0.41	0.44	0.30
63	25	0.084	0.001	0.067	0.004	13.43	11.83	12.88	0.28	0.31	0.29
63	45	0.117	0.003	0.092	0.002	4.76	4.97	9.45	0.29	0.36	0.35
63	75	0.199	0.005	0.173	0.008	5.05	5.79	6.55	0.21	0.20	0.18
63	100	0.206	0.007	0.384	0.020	2.49	3.84	4.88	0.16	0.18	0.22
63	125	0.133	0.004	0.247	0.011	1.14	1.25	1.08	0.14	0.12	0.12
63	150	0.051	0.003	0.066	0.003	0.19	0.16	0.19	0.14	0.11	0.16
63	175	0.014	0.000	0.024	0.001	0.05	0.05	0.04	0.06	0.06	0.06

Table 4.1: (continued)

Cruise	Depth (m)	Mean Chl *a* (mg m^{-3})	Std. Dev. Chl *a* (mg m^{-3})	Mean Phaeo (mg m^{-3})	Std. Dev. Phaeo (mg m^{-3})	Light (mg C m^{-3}) Rep #1	Light (mg C m^{-3}) Rep #2	Light (mg C m^{-3}) Rep #3	Dark (mg C m^{-3}) Rep #1	Dark (mg C m^{-3}) Rep #2	Dark (mg C m^{-3}) Rep #3
64	5	0.051	0.002	0.034	0.004	7.89	9.54	9.17	0.58	0.62	0.39
64	25	0.054	0.002	0.035	0.001	8.51	7.12	2.78	0.32	0.42	0.40
64	45	0.096	0.002	0.070	0.006	8.99	5.49	6.69	0.33	0.33	0.26
64	75	0.168	0.008	0.171	0.020	5.22	4.78	2.35	0.18	0.23	0.25
64	100	0.267	0.011	0.461	0.031	3.71	3.83	4.81	0.09	0.17	0.20
64	125	0.125	0.003	0.355	0.009	0.91	0.98	0.83	0.10	0.14	0.12
64	150	0.040	0.002	0.082	0.003	0.14	0.11	0.08	0.08	0.10	0.15
64	175**	0.066	0.001	0.153	0.004	0.10	0.11	0.11	0.10	0.08	0.10
65	5	0.066	0.002	0.035	0.001	10.59	8.27	7.85	0.29	0.30	0.22
65	25	0.064	0.004	0.039	0.005	5.68	6.11	7.96	0.21	0.23	0.19
65	45	0.067	0.004	0.038	0.001	3.34	3.43	3.30	0.40	0.32	0.39
65	75	ND	ND	ND	ND	ND	ND	ND	ND	ND	ND
65	100	0.222	0.006	0.304	0.030	1.57	1.88	1.62	0.05	0.12	0.05
65	125	0.114	0.005	0.212	0.006	0.39	0.58	0.52	0.04	0.04	0.04
65	150	0.019	0.000	0.022	0.003	0.04	0.05	0.05	0.04	0.04	0.03
65	175*	0.069	0.001	0.127	0.002	0.07	0.06	0.07	ND	ND	0.04
66	5	0.061	0.004	0.021	0.003	6.94	4.61	7.37	0.57	0.26	0.42
66	25	0.071	0.001	0.022	0.006	0.42***	4.37	6.81	0.37	0.29	0.30
66	45	0.119	0.005	0.058	0.001	0.79***	3.78	6.11	0.26	0.24	0.23
66	75	0.209	0.007	0.350	0.001	2.91	2.76	2.94	0.09	0.10	0.09
66	100	0.081	0.023	0.339	0.101	1.12	1.03	1.19	0.06	0.05	0.10
66	125	0.033	0.003	0.054	0.001	0.11	0.13	0.12	0.05	0.06	0.05
66	150	0.036	0.004	0.045	0.003	0.06	0.06	0.06	0.04	0.09	0.10
66	175	0.010	0.000	0.007	0.003	0.04	0.03	0.03	0.06	0.05	0.12
67	5	0.072	0.001	0.055	0.006	6.07	7.57	7.98	0.21	0.24	0.15
67	25	0.070	0.008	0.054	0.000	5.89	5.05	6.46	0.18	0.19	0.16
67	45	0.080	0.001	0.057	0.002	4.90	4.76	5.91	ND	ND	ND
67	75	0.091	0.000	0.076	0.004	1.70	1.46	1.79	0.19	0.18	0.20
67	100	0.179	0.011	0.374	0.003	1.03	1.32	0.79	0.13	0.08	0.09
67	125	0.099	0.008	0.246	0.018	0.27	0.26	0.31	0.11	0.07	0.16
67	150	0.051	0.001	0.145	0.005	0.11	0.09	0.10	0.08	0.06	0.09
67	175	0.028	0.002	0.068	0.006	0.02	0.05	0.04	ND	ND	ND

Table 4.1: (continued)

Cruise	Depth (m)	Mean Chl *a* (mg m^{-3})	Std. Dev. Chl *a* (mg m^{-3})	Mean Phaeo (mg m^{-3})	Std. Dev. Phaeo (mg m^{-3})	Light (mg C m^{-3}) Rep #1	Light (mg C m^{-3}) Rep #2	Light (mg C m^{-3}) Rep #3	Dark (mg C m^{-3}) Rep #1	Dark (mg C m^{-3}) Rep #2	Dark (mg C m^{-3}) Rep #3
68	5	0.091	0.005	0.059	0.003	7.76	6.86	6.63	0.24	0.27	0.22
68	25	0.085	0.005	0.069	0.003	5.57	4.61	5.83	0.22	0.20	0.21
68	45	0.100	0.012	0.054	0.004	4.86	4.37	4.28	0.43	0.71	0.30
68	75	0.175	0.000	0.167	0.014	2.29	2.36	0.89	0.16	0.15	0.16
68	100	0.222	0.011	0.426	0.009	0.78	1.03	1.14	ND	ND	ND
68	125	0.055	0.002	0.169	0.002	0.12	0.14	0.12	ND	ND	ND
68	150	0.016	0.001	0.039	0.001	0.01	0.04	0.03	0.06	0.05	0.08
68	175	ND	ND	ND	ND	ND	ND	ND	ND	ND	ND

* Salts and chlorophyll indicate mis-trip.
** Chlorophyll indicates mis-trip
*** outlier
ND = no data

Table 4.2: Primary Production and Pigment Summary Integrated Values (0-200 m)

Cruise	Incident Irradiance* (E m^{-2} d^{-1})	Pigments (mg m^{-2}) Chl a	Pigments (mg m^{-2}) Phaeo	Incubation Duration (hrs)	Assimilation Rates (mg C m^{-2} d^{-1}) light**	Assimilation Rates (mg C m^{-2} d^{-1}) Dark**
60	32.7	22.2	27.1	13.8	395	31
61	34.8	17.3	22.6	14.3	460	31
62	32.9	19.9	28.4	13.1	490	25
63	53.7	21.5	27.6	13.3	926	38
64	48.2	21.3	33.8	14.2	676	41
65	***	18.7	24.0	14.0	474	28
66	45.3	15.8	24.0	14.0	442	28
67	40.0	16.8	29.0	13.0	436	25
68	22.8	17.9	24.5	12.3	410	26

* cosine collector
** 12 hrs
*** no data

4.4.2. Particle flux

Particulate carbon (PC), nitrogen (PN), phosphorus (PP) and mass fluxes (150, 200, 300 and 500 m) are presented in Table 4.3 and Figures 6.6.2 to 6.6.9 for the first 7 years of the program. Carbon flux displays a clear annual cycle with peaks in both the early spring and in the late summer months. The magnitude of particle flux varies by a factor of approximately three. With the exception of anomalous PP fluxes measured on the first two HOT cruises, temporal variability in PN, PP and mass flux show similar temporal trends, and also vary between cruises by about a factor of three. Elemental ratios of carbon-to-nitrogen (atom:atom) at 150 m are typically between 6-10 and show no obvious temporal pattern. These particle flux measurements and elemental ratios are consistent with those measured in the central North Pacific Ocean by the VERTEX program (Martin et al., 1987; Kanuer et al., 1990). Nitrogen flux at 150 m, as a percent of photosynthetic nitrogen assimilation (calculated from ^{14}C primary production values assuming a C:N ratio [atom:atom] of 6.6) ranges between 2-10%. The average value (approximately 6.5%) is consistent with the estimate of new production for the oligotrophic central gyres made by Eppley and Peterson (1979) and with field data from the VERTEX program (Knauer et al., 1990). Average fluxes of PC, PN, PP and mass at 150 m from the first 6 years of the time-series observations are shown in Figures 6.6.2 to 6.6.5. Contour plots of concentration are shown in Figures 6.6.6 to 6.6.9. For carbon, nitrogen, phosphorus and total mass, the flux declines rapidly with depth, presumably due to the rapid dissolution and remineralization of organic particles sinking through the water column. The flux of carbon at 500 m is less than 50% of the flux at 150 m.

Table 4.3: Station ALOHA Sediment Trap Flux Data

Cruise	Depth (m)	Carbon Flux (mg m^{-2} d^{-1}) mean	SD	n	Nitrogen Flux (mg m^{-2} d^{-1}) mean	SD	n	Phosphorus Flux (mg m^{-2} d^{-1}) mean	SD	n	Mass Flux (mg m^{-2} d^{-1}) mean	SD	n
60	150	18.9	1.4	3	2.5	0.30	3	0.33	0.02	3	31.8	4.3	3
60	200	16.3	1.1	3	2.0	0.14	3	0.15	0.09	3	30.6	11.2	3
60	300	6.9	1.7	4	0.7	0.19	4	0.10	0.02	3	26.9	8.8	3
60	500	7.6	4.3	4	0.6	0.17	3	0.06	0.01	3	27.5	25.1	3
62	150	21.7	5.9	4	3.1	0.96	4	0.30	0.25	3	32.7	13.3	3
62	200	16.0	5.2	4	2.0	0.60	4	0.13	0.06	3	36.8	2.6	3
62	300	12.0	2.6	4	1.2	0.18	4	0.13	---	1	25.2	4.3	3
62	500	11.6	1.3	4	0.9	0.13	4	0.10	0.05	3	17.6	2.7	3
63	150	21.8	10.5	4	4.2	1.86	4	0.49	0.05	3	63.7	11.6	3
63	200	12.6	3.5	4	2.2	0.37	4	0.15	0.08	3	56.8	2.6	3
63	300	9.5	1.3	4	1.3	0.09	4	0.18	0.06	3	28.1	4.3	3
63	500	8.8	3.7	4	0.9	0.29	4	0.19	0.02	3	26.1	11.6	3
64	150	22.7	2.6	3	4.1	0.47	3	0.36	0.15	3	51.7	11.4	3
64	200	5.4	0.7	4	0.8	0.17	4	0.14	0.08	3	56.8	19.2	3
65	150	25.9	5.8	4	3.5	0.99	4	0.13	0.03	3	100.2	24.4	3
65	200	17.5	4.0	4	2.1	0.58	4	0.12	0.10	3	90.3	30.4	3
66	150	23.0	3.7	4	2.0	0.44	4	0.41	0.19	3	78.3	13.0	3
66	200	19.6	0.9	4	1.5	0.11	4	0.27	0.07	3	74.9	20.1	3
67	150	25.8	4.5	3	2.5	0.60	3	0.44	0.04	2	41.8	21.4	3
67	200	14.8	1.3	3	1.3	0.20	3	0.18	0.03	3	41.7	24.6	3
68	150	21.5	2.8	3	2.8	0.50	3	0.30	0.04	3	59.0	26.1	3
68	200	14.2	3.5	3	1.7	0.40	3	0.26	0.05	3	51.9	7.9	3

4.5. ADCP Measurements

An overview of the shipboard ADCP data is given by the plots of velocity as a function of time and depth while on station (Figures 6.7.1a to 6.7.1i) and velocity as a function of latitude and depth during transit to and from Station ALOHA and Station 3, combined (Figures 6.7.2a to 6.7.2i). As in previous years, currents were highly variable from cruise to cruise and within each cruise.

4.6. Meteorology

The meteorological data collected by HOT program scientists include atmospheric pressure, sea-surface temperature and wet and dry bulb air temperature. These data are presented

in Figures 6.8.1 to 6.8.13. As described by Winn et al. (1991), parameters show evidence of annual cycles, although the daily and weekly ranges are nearly as high as the annual range for some variables. In particular, during HOT-60 the dry and wet bulb air temperatures (Figure 6.8.2) show large variations due to a change in the weather pattern after the second day of the cruise. These measurements were confirmed by the observations collected by the ship's officers on the bridge. A low pressure system during HOT-61 is evident in the observations of atmospheric pressure (Figure 6.8.1), these low values were confirmed by the pressure observations from the NDBC buoy #51001 (section 4.8). Wind speed and direction are also collected on HOT cruises. These data are presented in Figures 6.8.4 to 6.8.12.

4.7. Light Measurements

Integrated irradiance measurements made with the on-deck cosine collector on days that primary production experiments were conducted are presented in Table 4.4.2.

4.8. Buoy and Shipboard Observations

Two National Data Buoy Center (NDBC) meteorological buoys are located in the vicinity of the ALOHA Station (Figure 1.1). Buoy #51001 is 400 km west of ALOHA at 23.4°N, 162.3° W and buoy #51026 is located north of Molokai at 21.4°N, 156.96°W. These buoys collect hourly observations of air temperature, sea surface temperature, atmospheric pressure, wind speed and direction and significant wave height. The coherence of the data from Buoy #51001 with the data collected on HOT cruises was examined and reported in Tupas et al. (1993). We concluded from these analyses, that the buoy data can be used to get useful estimates of air temperature, sea-surface temperature and atmospheric pressure at Station ALOHA.

The wind vectors from these two buoys are plotted together with the ship observations in Figures 6.8.4-6.8.12. Data from buoy #51026 were not available during the HOT-62 cruise period.

4.9. Inverted Echo Sounder Observations

Plots of dynamic height are presented in Figure 4.1. The IES records prior to 1994 were examined and reported in Tupas et al. (1994a). It was concluded that large events with time-scales from weeks to months dominate dynamic height to such an extent that there is no clearly defined annual cycle, for instance, the highest and lowest dynamic height in 1991 occurred within the space of about a month. These events are not well sampled with the monthly spacing of the HOT cruises.

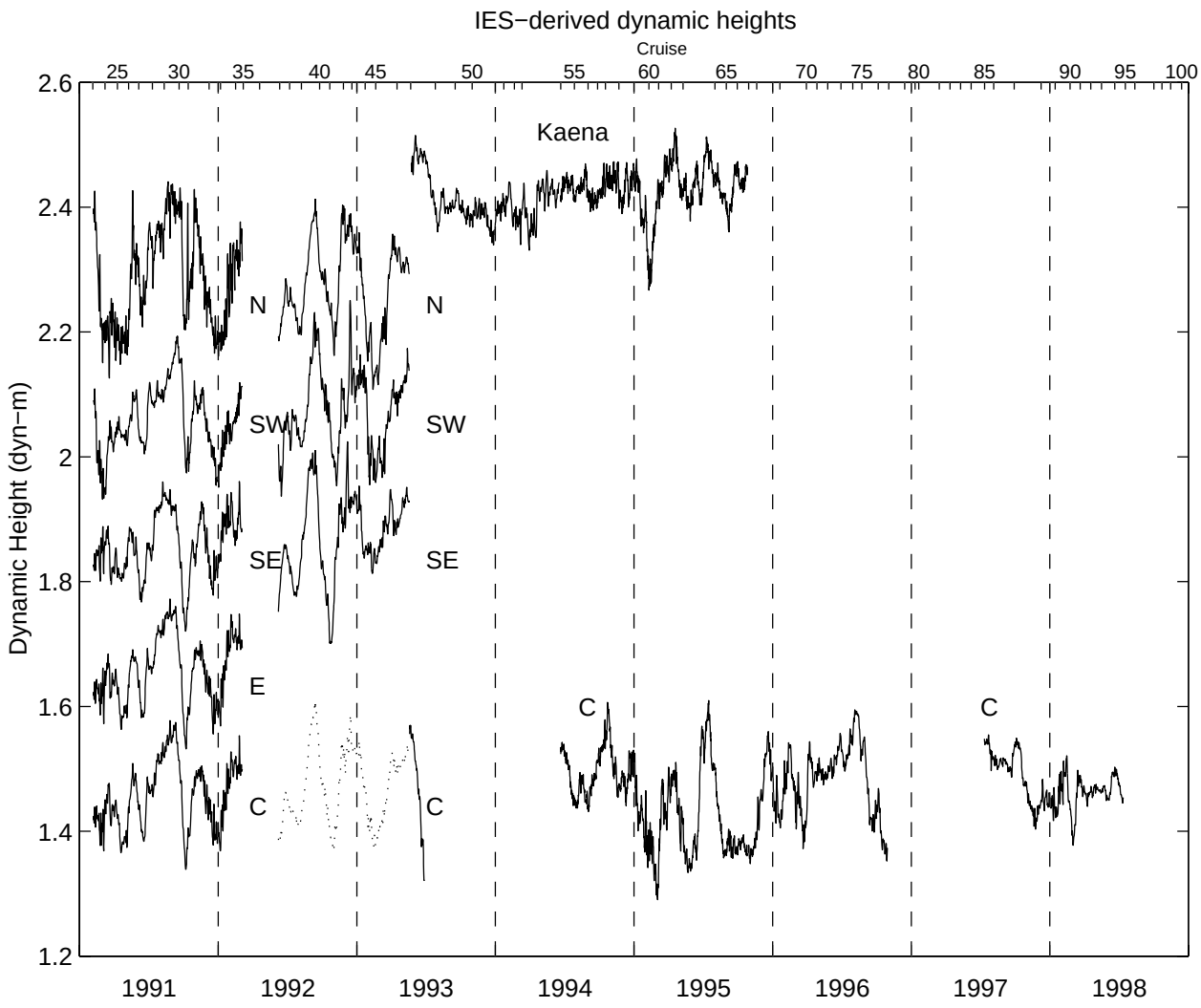

Figure 4.1: Dynamic height from the inverted echo sounders (IES) after removal of the semi-diurnal, diurnal tides and variability with time-scales less than one day. The plots are staggered at 0.2 dyn-m intervals (the curve labeled "C" corresponds to the y-scale). The dotted line is an average of the N, SW and SE records between June 1992 and May 1993. This and the 1991-1992 C-record have been calibrated from CTD casts at Station ALOHA made during 25 cruises. The horizontal axis above the plots shows the HOT cruise numbers. The deployed locations of the IESs are shown in Figure 1.1. The locations of the deployments were changed in May 1993 (one IES was deployed at Station Kaena) in order to span the Hawaiian Ridge Current.

4.10. Bottom-Moored Sediment Traps

Initial results have been obtained from analyses of samples from ALOHA-I were reported in HOT Data Report #6 and in Karl et al. (1996). The mass, particulate carbon, nitrogen and phosphorus time-series flux data all displayed an unexpected and major export pulse in July-August 1992, during a period of time when the upper water column is well stratified. A second peak was also observed in late winter-early spring but this feature appears to be very different from the summer peak. The major particulate matter export event was recorded in the same collector cups (#'s 3 to 5) regardless of the water depth, suggesting a sinking rate of at least 200 m d^{-1}. Analysis of chlorophyll a by fluorometry and phytoplankton pigments by HPLC reveal that the peak export event is coincident with the removal of pigmented cells. The summer event contained the full spectrum of plant pigments and most accessory pigments. Direct microscopic analyses show that this major export event was dominated by diatoms. This pattern of particle export was observed also in subsequent deployments of the ALOHA sediment trap mooring (Figure 4.2).

4.11. Thermosalinograph time-series

Time-series of near surface temperature (NST) and near surface salinity (NSS) measured by the thermosalinograph as well as potential density, navigation and ship speed during HOT-63, HOT-66, HOT-67 and HOT-68 are presented in Figures 6.9.1 to 6.9.4.

Time-series of NST and NSS measured by the thermosalinograph during HOT-63 are shown in Figure 6.9.1. Temperatures for HOT-63 ranged from 22.9 to 25.2°C and salinities ranged from 34.5 to 35.1. A large change in temperature and salinity can be seen as the ship travels to and from Station ALOHA. Salinity bottle samples were not taken near the end of the cruise (May 9-10). In subsequent cruises we have made sure to take bottle samples at regular time intervals throughout the entire cruise.

Figure 6.9.2 shows the time-series of NST during HOT-66. NSS is not available for this cruise as all salinity data from the thermosalinograph are considered suspect as both the thermosalinograph salinity as well as the bottle samples taken from the thermosalinograph are suspiciously low.

Figure 6.9.3 shows the time-series of NST during HOT-67. NSS is once again not available as all salinity data from the thermosalinograph are considered suspect as both the thermosalinograph salinity as well as the bottle samples taken from the thermosalinograph are suspiciously low for this cruise. Signals of strong daytime warming can be seen in the middle of this cruise.

Figure 6.9.4 shows the time-series of NST and NST during HOT-68. Temperatures range from 25.5 to 26.6°C and salinities range from 34.75 to 35. Instances of lowered salinity due to rainwater input can be seen during this cruise.

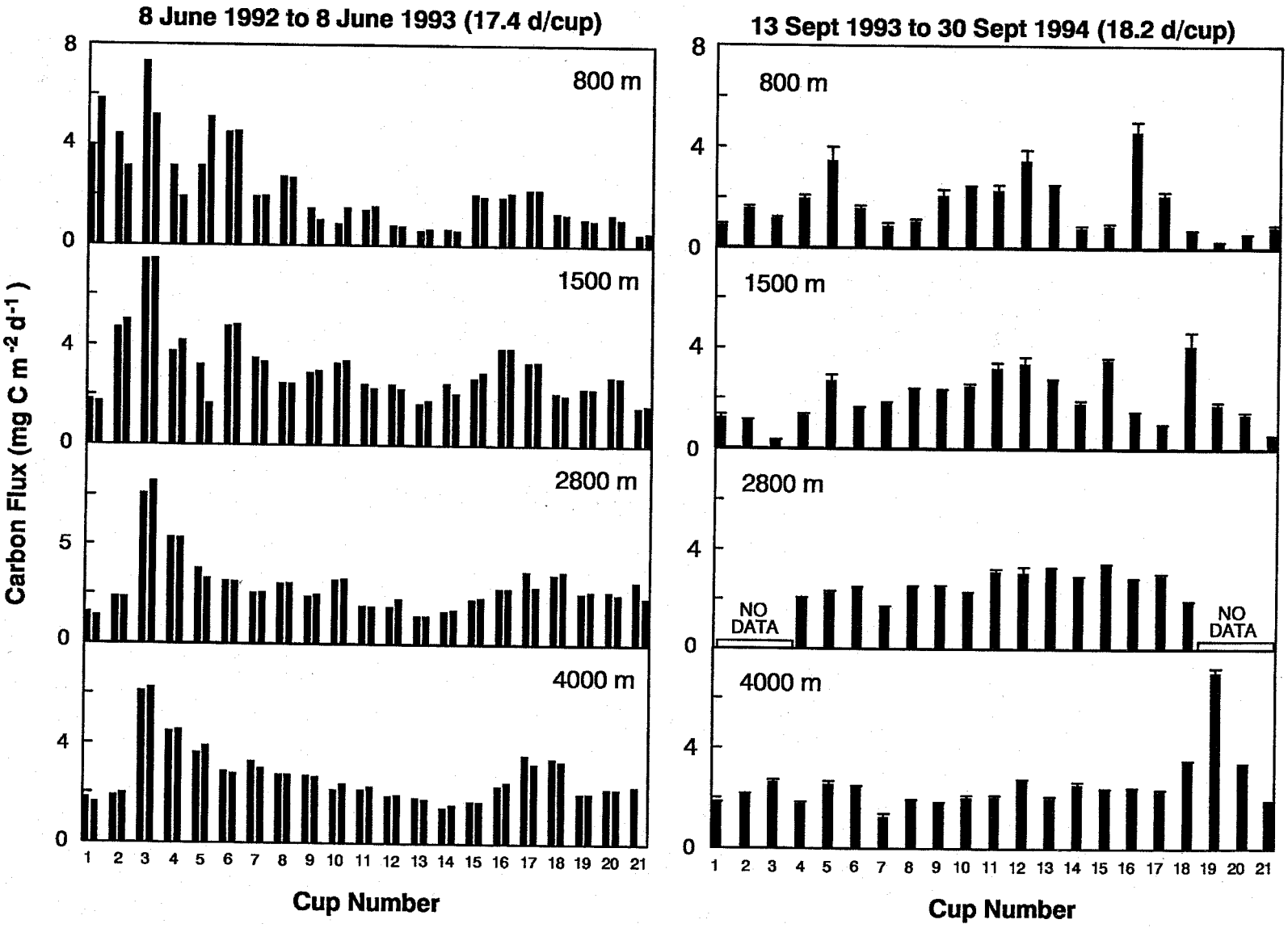

Figure 4.2: Time-series record of total carbon flux as a function of time at Station ALOHA (22°45'N, 158°W) at the reference depths indicated. [Left] ALOHA I; 1992-1993, [Right] ALOHA II, 1993-1994

5. REFERENCES

Atkinson, M.J., F.I.M. Thomas, N. Larson, E. Terrill, K. Morita and C.C. Liu. 1995. A micro-hole potentiostatic oxygen sensor for oceanic CTDs. *Deep-Sea Research*, 42, 761-771.

Barnett, T.P. 1978. The role of the oceans in the global climate system. In: *Climatic Change*, J. Gribben, editor, Cambridge University Press, pp. 157-179.

Bidigare, R.R., J. Marra, T.J. Dickey, R. Iturriaga, K.S. Baker, R.C. Smith and H. Pak. 1990. Evidence for phytoplankton succession and chromatic adaptation in the Sargasso Sea during Spring 1985. *Marine Ecology Progress Series*, 60, 113-122.

Brewer, P.G., K.W. Bruland, R.W. Eppley and J.J. McCarthy. 1986. The Global Ocean Flux Study (GOFS): Status of the U.S.GOFS program. *Eos, Transactions of the American Geophysical Union*, 67, 827-832.

Chiswell, S.M. 1996. Intra-annual oscillations at Station ALOHA, north of Oahu, Hawaii. *Deep-Sea Research II*, 43, 305-319.

Chiswell, S.M., E. Firing, D. Karl, R. Lukas, C. Winn. 1990. *Hawaii Ocean Time-series Program Data Report 1, 1988-1989*. School of Ocean and Earth Science and Technology, University of Hawaii, 269 pp.

Clayton, T.D. and R.H. Byrne. 1993. Spectrophotometric seawater pH measurements: total hydrogen ion concentration scale calibration of m-cresol purple and at-sea results. *Deep-Sea Research*, 40, 2115-2129.

Cox, R.D. 1980. Determination of nitrate at the parts per billion level by chemiluminescence. *Analytical Chemistry*, 52, 332-335.

Dickey, T. 1991. The emergence of concurrent high-resolution physical and bio-optical measurements in the upper ocean and their applications. *Reviews of Geophysics*, 29, 383-413.

Dore, J.E. and D.M. Karl. 1996. Nitrite distributions and dynamics at Station ALOHA. *Deep-Sea Research II*, 43, 385-402.

Doty, M.S. and M. Oguri. 1956. The island mass effect. *Journal du Conseil pour l'Internationale Exploration de la Mer*, 22, 33-37.

Dymond, J.D. and M. Lyle. 1985. Flux comparisons between sediments and sediment traps in the eastern tropical Pacific: implication for atmospheric CO_2 variations during the pleistocene. *Limnology and Oceanography*, 30, 699-712.

Eppley, R.W. and B.J. Peterson. 1979. Particulate organic matter flux and planktonic new production in the deep ocean. *Nature*, 282, 677-680.

Firing, E. 1996. Currents observed north of Oahu during the first 5 years of HOT. *Deep-Sea Research II*, 43, 281-303.

Firing, E. and R.L. Gordon. 1990. Deep ocean acoustic Doppler current profiling. In: *Proceedings of the Fourth IEEE Working Conference on Current Measurements*, G.F. Appell and T.B. Curtin, editors, IEEE, New York, pp. 192-201.

Garside, C. 1982. A chemiluminescent technique for the determination of nanomolar concentrations of nitrate and nitrite in seawater. *Marine Chemistry*, 11, 159-167.

Gordon, D.C., Jr. 1970. Chemical and biological observations at station Gollum, an oceanic station near Hawaii, January 1969 to June 1970. *Hawaii Institute of Geophysics Report*, HIG-70-22, 44 pages + 2 appendices.

Harrison, W.G., L.R. Harris, D.M. Karl, G.A. Knauer and D.G. Redalje. 1992. Nitrogen dynamics at the VERTEX time-series site. *Deep-Sea Research*, 39, 1535-1552.

Hayward, T.L. 1987. The nutrient distribution and primary production in the central North Pacific. *Deep-Sea Research*, 34, 1593-1627.

JSC/CCCO. 1981. *JSC/CCCO Meeting on Time Series of Ocean Measurements (Tokyo, May 11-15, 1981)*. World Climate Research Programme, Geneva, Switzerland.

Karl, D.M. 1994. HOT stuff: Surprises emerging from five years' worth of data. *U.S. JGOFS Newsletter*, July, 9-10.

Karl, D.M., J.R. Christian, J.E. Dore, D.V. Hebel, R.M Letelier, L.M. Tupas and C.D. Winn. 1996 Seasonal and interannual variability in primary production and particle flux at Station ALOHA. *Deep-Sea Research II*, 43, 539-568.

Karl, D.M. and O. Holm-Hansen. 1978. Methodology and measurement of adenylate energy charge ratios in environmental samples. *Marine Biology*, 48, 185-197.

Karl, D.M., R. Letelier, D.V. Hebel, D.F. Bird and C.D. Winn. 1992. *Trichodesmium* blooms and new nitrogen in the North Pacific gyre. In: *Marine Pelagic Cyanobacteria: Trichodesmium and Other Diazotrophs*, E.J. Carpenter et al., editors, Kluwer Academic Publishers, Netherlands, pp. 219-237.

Karl, D.M., R. Letelier, D. Hebel, L. Tupas, J. Dore, J. Christian and C. Winn. 1995 Ecosystem changes in the North Pacific subtropical gyre attributed to the 1991-92 El Niño. *Nature*, 373, 230-234.

Karl, D.M. and R. Lukas. 1996. The Hawaii Ocean Time-series (HOT) program: Background, rationale and field implementation. *Deep-Sea Research II*, 43, 129-156.

Karl, D.M. and G. Tien. 1992. MAGIC: A sensitive and precise method for measuring dissolved phosphorus in aquatic environments. *Limnology and Oceanography*, 37, 105-116.

Karl, D.M. and G.Tien. 1996. Temporal variability in dissolved phosphorus concentrations at Station ALOHA (22°45'N, 158°W). *Marine Chemistry*, in press.

Keeling, C.D., R.B. Bacastow, A.E. Bainbridge, C.A. Ekdahl, Jr., P.R. Guenther, L.S. Waterman and J.F.S. Chin. 1976. Atmospheric carbon dioxide variations at Mauna Loa Observatory, Hawaii. *Tellus*, 28, 538-551.

Keeling, R.F. and S.R. Shertz. 1992. Seasonal and interannual variations in atmospheric oxygen and implications for the global carbon cycle. *Nature*, 358, 723-727.

Knauer, G.A., J.H. Martin and K.W. Bruland. 1979. Fluxes of particulate carbon, nitrogen and phosphorus in the upper water column of the northeast Pacific. *Deep-Sea Research*, 26, 97-108.

Knauer, G.A., D.G. Redalje, W.G. Harrison and D.M. Karl. 1990. New production at the VERTEX time-series site. *Deep-Sea Research*, 37, 1121-1134.

Laws, E.A., G.R. DiTullio, P.R. Betzer, D.M. Karl and R.L. Carder. 1989. Autotrophic production and elemental fluxes at 26°N, 155°W in the North Pacific subtropical gyre. *Deep-Sea Research*, 36, 103-120.

Likens, G.E., F.H. Bormann, R.S. Pierce, J.S. Eaton and N.M. Johnson. 1977. *Biogeochemistry of a Forested Ecosystem*. Springer-Verlag, New York.

Longhurst, A.R. and W.G. Harrison. 1989. The biological pump: Profiles of plankton production and consumption in the upper ocean. *Progress in Oceanography*, 22, 47-123.

Lukas, R. and S. Chiswell. 1991. Submesoscale water mass variations in the salinity minimum of the north Pacific near Hawaii. *WOCE Notes*, 3(1), 1,6-8.

Lukas, R. and F. Santiago-Mandujano. 1996. Interannual variability of Pacific deep- and bottom-waters observed in the Hawaii Ocean Time-series. *Deep-Sea Research II*, 43, 243-255.

Lukas, R., F. Santiago-Mandujano, F. Bingham and A. Mantyla. In preparation. Cold bottom water events observed in the Hawaii Ocean Time-series: Implications for vertical mixing.

Martin, J.H., G.A. Knauer, D.M. Karl and W.W. Broenkow. 1987. VERTEX: Carbon cycling in the northeast Pacific. *Deep-Sea Research*, 34, 267-285.

Michaels, A. and A. Knap. 1996. Overview of the U.S.-JGOFS Bermuda Atlantic Time-series Study and Hydrostation S program. *Deep-Sea Research II*, 43, 157-198.

National Research Council. 1984a. *Global Observations and Understanding of the General Circulation of the Oceans: Proceedings of a Workshop*, National Academy Press, Washington, D.C., 418 pp.

National Research Council. 1984b. *Global Ocean Flux Study: Proceedings of a Workshop*, National Academy Press, Washington, D.C., 360 pp.

Owens, W.B. and R.C. Millard. 1985. A new algorithm for CTD oxygen calibration. *Journal of Physical Oceanography*, 15, 621-631.

Quay, P.D., B. Tilbrook and C.S. Wong. 1992. Oceanic uptake of fossil fuel CO_2: Carbon-13 evidence. *Science*, 256, 74-79.

Ryther, J.H.. 1969 Photosynthesis and fish production in the sea. The production of organic matter and its conversion to higher forms of life vary throughout the world ocean. *Science* 166, 72-76.

Sarmiento, J.L. and J.R. Toggweiler. 1984. New model for the role of the oceans in determining atmospheric pCO_2. *Nature*, 308, 621-624.

Scientific Committee on Oceanic Research. 1990. *The Joint Global Ocean Flux Study (JGOFS) Science Plan.* JGOFS Report No. 5. International Council of Scientific Unions, 61 pp.

Strickland, J.D.H. and T.R. Parsons. 1972 *A Practical Handbook of Seawater Analysis*. Fisheries Research Board of Canada, 167 pp.

Tabata, S. 1965. Variability of oceanographic conditions at ocean station "P" in the Northeast Pacific Ocean. *Transactions of the Royal Society of Canada*, 3, 367-418.

Tans, P.P., I.Y. Fung and T. Takahashi. 1990. Observational constraints on the global atmospheric carbon budget. *Science*, 247, 1431-1438.

Thomson, C.W. 1877. *The Atlantic, a Preliminary Account of the General Results of the Exploring Voyage of H.M.W. "Challenger,"* vol. 2, Macmillan and Company, London, p. 291.

Troup, A.J. 1965. The "southern oscillation." *Quarterly Journal of the Royal Meteorological Society*, 91, 490-506.

Tsuchiya, M. 1968. *Upper Waters of the Intertropical Pacific Ocean*. Johns Hopkins Oceanographic Studies, 4, 49 pp.

Tupas, L.M., B.N. Popp and D.M. Karl. 1994b. Dissolved organic carbon in oligotrophic waters: experiments on sample preservation, storage and analysis. *Marine Chemistry*, 48, 207-216.

Tupas, L., F. Santiago-Mandujano, D. Hebel, E. Firing, F. Bingham, R. Lukas and D. Karl. 1994a. *Hawaii Ocean Time-series Program Data Report 5, 1993.* School of Ocean and Earth Science and Technology, University of Hawaii, 156 pp.

Tupas, L., F. Santiago-Mandujano, D. Hebel, E. Firing, R. Lukas and D. Karl. 1995. *Hawaii Ocean Time-series Data Report 6: 1994*. School of Ocean and Earth Science and Technology, University of Hawaii, 199 pp.

Tupas, L., F. Santiago-Mandujano, D. Hebel, R. Lukas, D. Karl and E. Firing. 1993. *Hawaii Ocean Time-series Program Data Report 4, 1992*. School of Ocean and Earth Science and Technology, University of Hawaii, 248 pp.

UNESCO. 1981. *Tenth Report of the Joint Panel on Oceanographic Tables and Standards*. UNESCO Technical Papers in Marine Science, No. 36. UNESCO, Paris.

Volk, T. and M.I. Hoffert. 1985. Ocean carbon pumps: Analysis of relative strengths and efficiencies in ocean-driven atmospheric CO_2 changes. In: *The Carbon Cycle and Atmospheric CO_2: Natural Variations Archean to Present*, E.T. Sundquist and W.S. Broecker, editors, American Geophysical Union, Washington, D.C., pp. 99-110.

Weiss, R.F., R.A. Jahnke and C.D. Keeling. 1982. Seasonal effects of temperature and salinity on the partial pressure of CO_2 in seawater. *Nature*, 300, 511-513.

Wiebe, P.H., C.B. Miller, J.A. McGowan and R.A. Knox. 1987. Long time series study of oceanic ecosystems. *EOS, Transactions of the American Geophysical Union*, 68, 1178-1190.

Wiggert, J., T. Dickey and T. Granata. 1994. The effect of temporal undersampling on primary production estimates. *Journal of Geophysical Research*, 99, 3361-3371.

Winn, C.D., L. Campbell, J.R. Christian, R.M. Letelier, D.V. Hebel, J.E. Dore, L. Fujieki and D.M. Karl. 1995. Seasonal variability in the phytoplankton community of the North Pacific subtropical gyre. *Global Biogeochemical Cycles*, in press.

Winn, C., S.M. Chiswell, E. Firing, D. Karl, R. Lukas. 1991. *Hawaii Ocean Time-series Program Data Report 2, 1990.* School of Ocean and Earth Science and Technology, University of Hawaii, 175 pp.

Winn, C., R. Lukas, D. Karl, E. Firing. 1993. *Hawaii Ocean Time-series Program Data Report 3, 1991*. School of Ocean and Earth Science and Technology, University of Hawaii, 228 pp.

Wright, S.W., S.W. Jeffrey, R.F.C. Mantoura, C.A. Llewellyn, T. Bjornland, D. Repeta and N. Welschmeyer. 1991. Improved HPLC method for the analysis of chlorophylls and carotenoids from marine phytoplankton. *Marine Ecology Progress Series*, 77, 183-196.

Wyrtki, K., E. Firing, D. Halpern, R. Knox, G.J. McNally, W.C. Patzert, E.D. Stroup, B.A. Taft and R. Williams. 1981. The Hawaii to Tahiti shuttle experiment. *Science*, 211, 22-28.

6. FIGURES

6.1. CTD Station Locations and Sediment Trap Drift Tracks

Figure 6.1.1: CTD station locations on HOT-60 and 61. CTD stations represented by open circles relative to Station ALOHA. Solid lines connect casts taken in sequence and numbers show location of casts. Dashed line shows area nominally defined as Station ALOHA. Drift track for the sediment trap array during the 72-hour deployment period is indicated by a solid line with the start point indicated by an S.

Figure 6.1.2: As in Figure 6.1.1, except for HOT-62 and 63.

Figure 6.1.3: As in Figure 6.1.1, except for HOT-64 and 65.

Figure 6.1.4: As in Figure 6.1.1, except for HOT-66 and 67.

Figure 6.1.5: As in Figure 6.1.1, except for HOT-68.

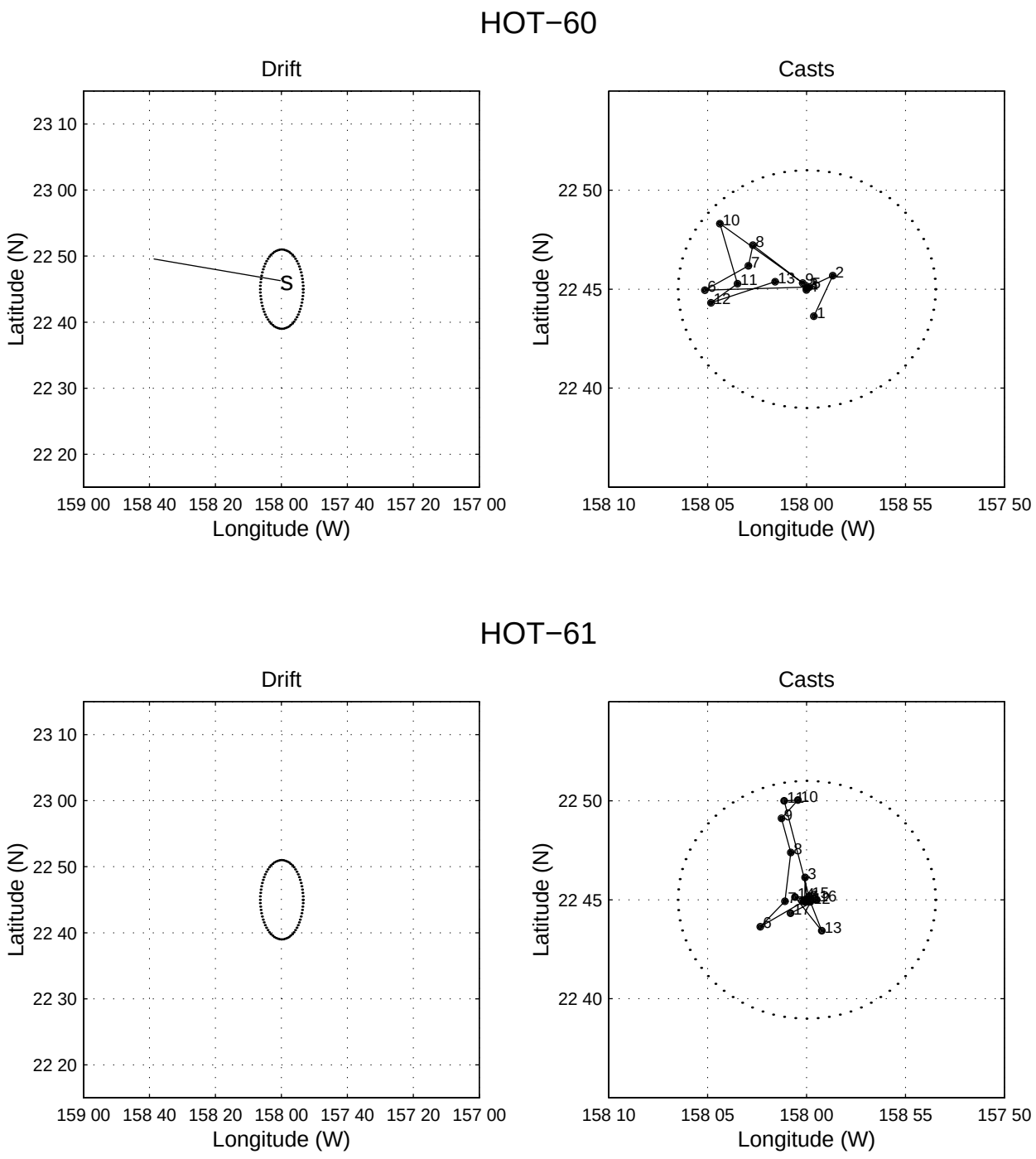
HOT−60
Drift
Casts
Latitude (N)
Longitude (W)
23 10
23 00
22 50
22 40
22 30
22 20
159 00
158 40
158 20
158 00
157 40
157 20
157 00
S
22 45
158 10
158 05
158 55
157 50
HOT−61

Figure 6.1.1

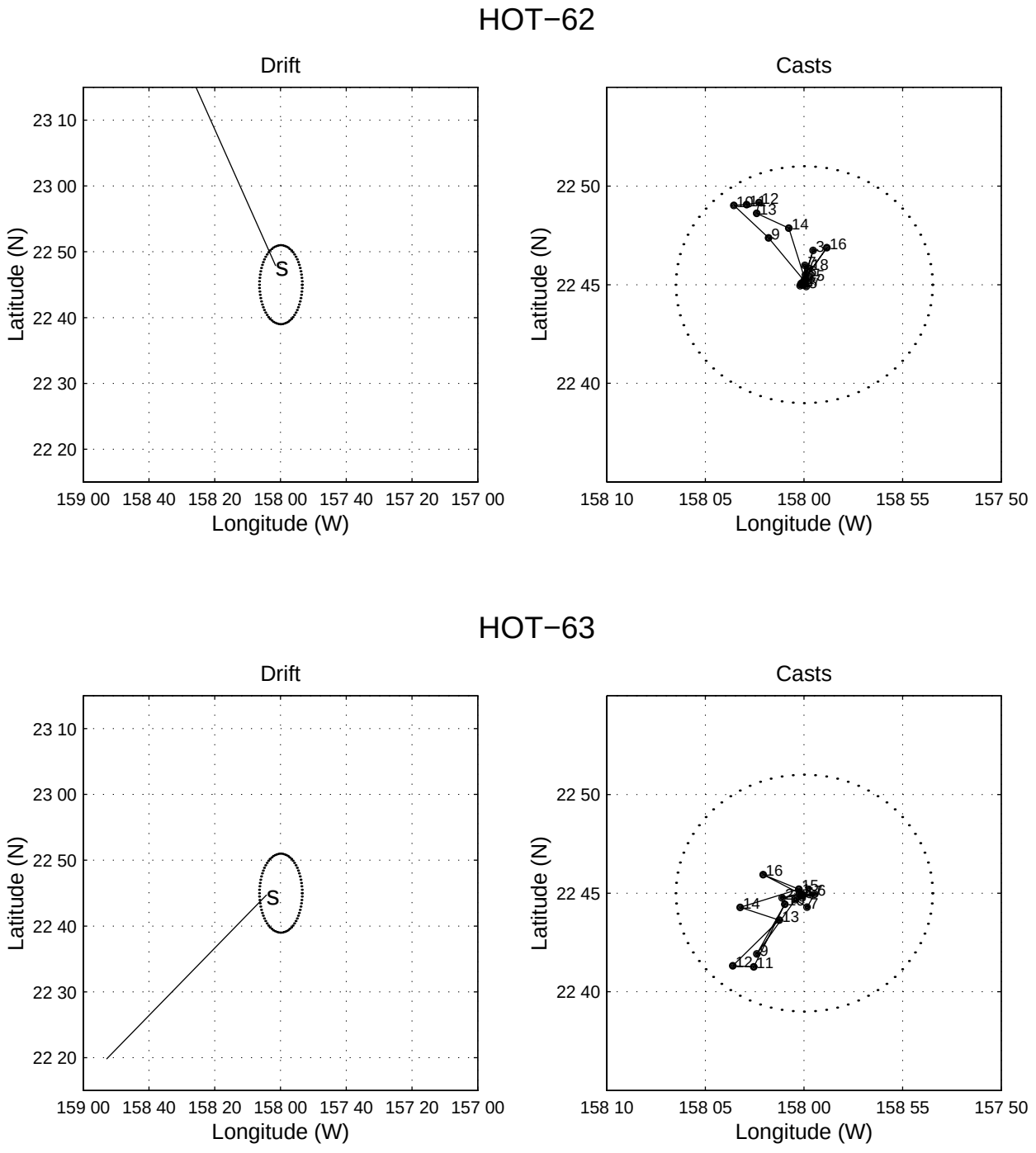
HOT−62
Drift
Casts
23 10
23 00
22 50
22 40
22 30
22 20
Latitude (N)
159 00 158 40 158 20 158 00 157 40 157 20 157 00
Longitude (W)
S
22 50
22 45
22 40
158 10 158 05 158 00 158 55 157 50
HOT−63
Drift
Casts
23 10
23 00
22 50
22 40
22 30
22 20
Latitude (N)
159 00 158 40 158 20 158 00 157 40 157 20 157 00
Longitude (W)
S
22 50
22 45
22 40
158 10 158 05 158 00 158 55 157 50

Figure 6.1.2

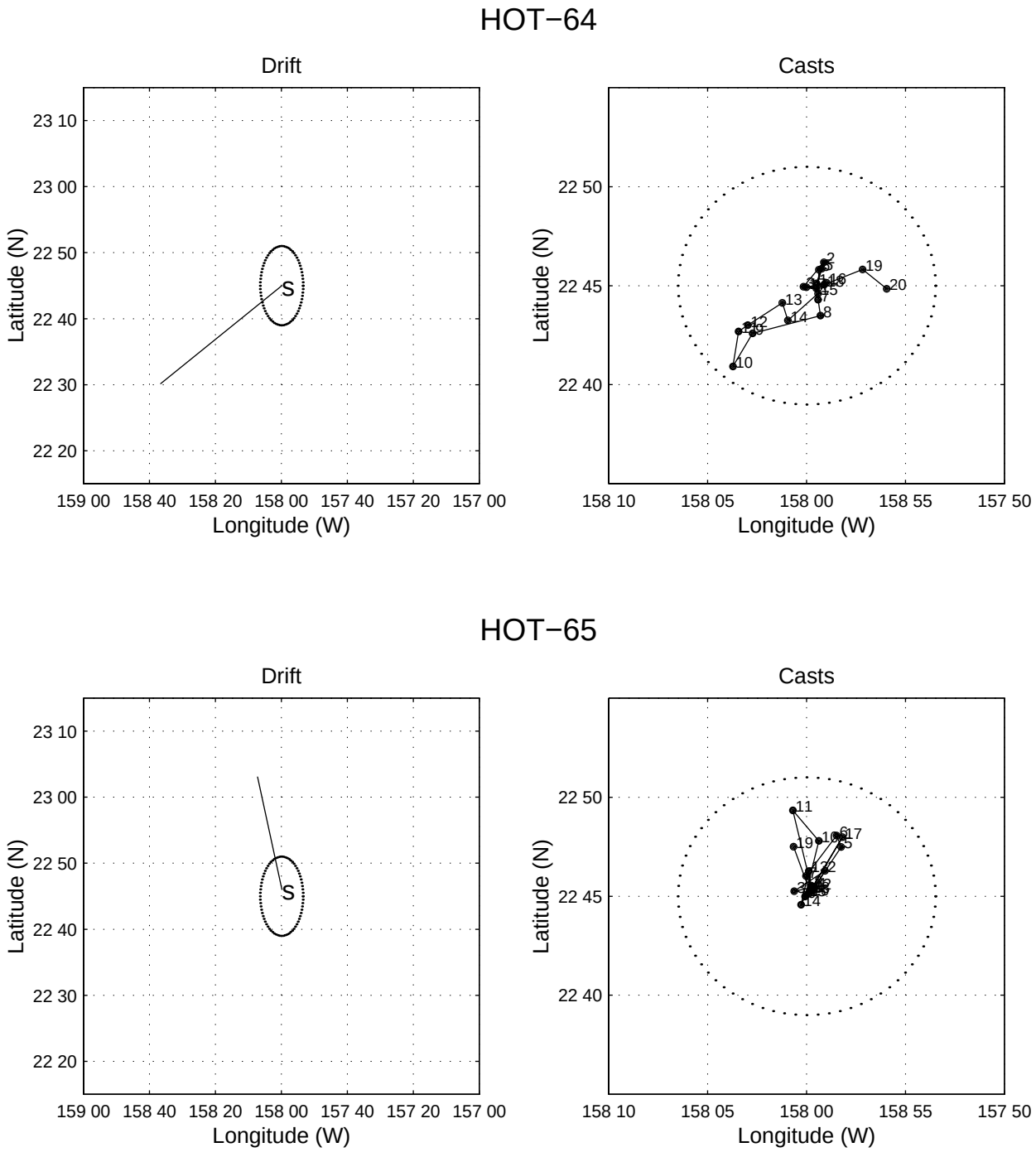
HOT−64
Drift
Casts
Latitude (N)
Longitude (W)
23 10
23 00
22 50
22 40
22 30
22 20
159 00
158 40
158 20
158 00
157 40
157 20
157 00
S
22 50
22 45
22 40
158 10
158 05
158 00
158 55
157 50
HOT−65
Drift
Casts
Latitude (N)
Longitude (W)
23 10
23 00
22 50
22 40
22 30
22 20
159 00
158 40
158 20
158 00
157 40
157 20
157 00
S
22 50
22 45
22 40
158 10
158 05
158 00
158 55
157 50

Figure 6.1.3

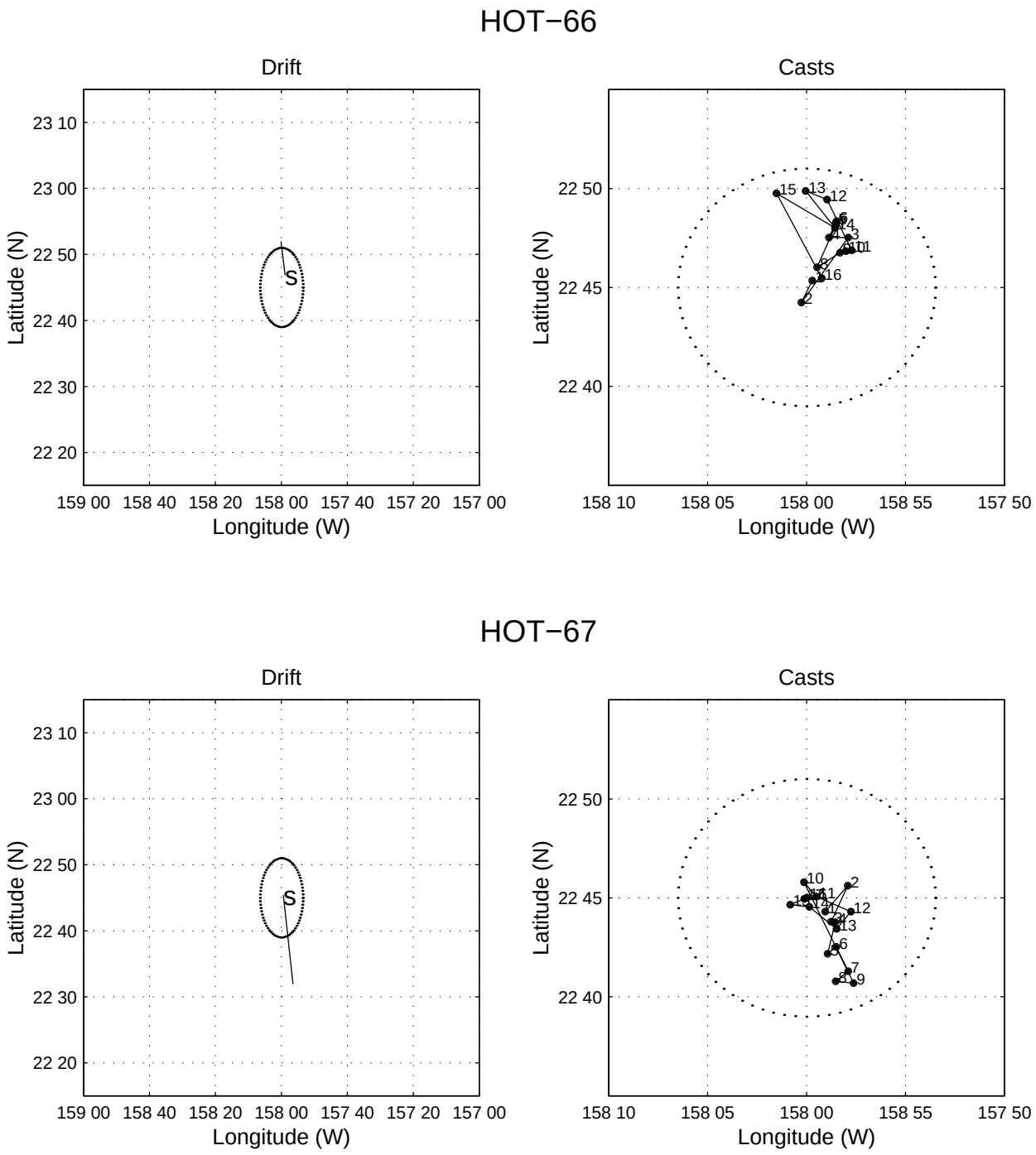
HOT−66
Drift
Casts
Latitude (N)
Longitude (W)
23 10
23 00
22 50
22 40
22 30
22 20
159 00
158 40
158 20
158 00
157 40
157 20
157 00
S
22 45
158 10
158 05
158 55
157 50
HOT−67

Figure 6.1.4

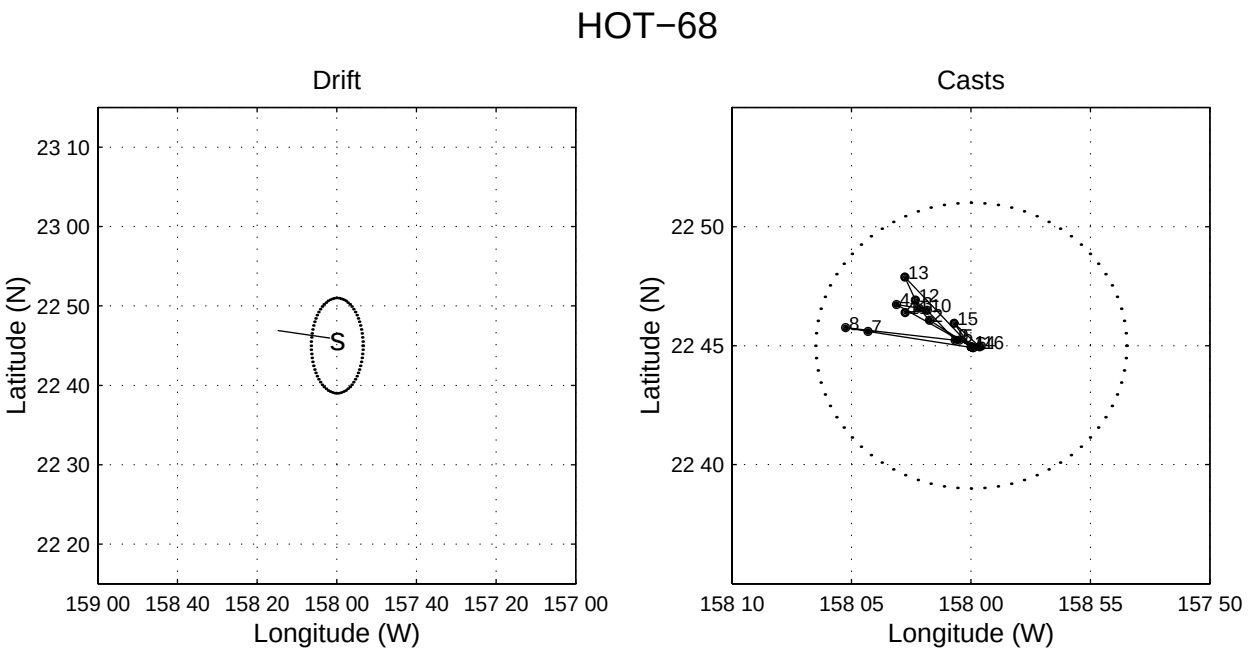
HOT−68
Drift
Casts
23 10
23 00
22 50
22 40
22 30
22 20
Latitude (N)
159 00
158 40
158 20
158 00
157 40
157 20
157 00
Longitude (W)
S
22 50
22 45
22 40
158 10
158 05
158 00
158 55
157 50
13
12
15
8
7

Figure 6.1.5

6.2. CTD Profiles

Figures 6.2.1a-i: [Upper left panel] Temperature, salinity, oxygen and potential density ($\sigma\theta$) as a function of pressure for WOCE deep cast. Salinity and oxygen water bottle data are also plotted. [Upper right panel] Nutrients [nitrate+nitrite], soluble reactive phosphorus and silicate and oxygen as a function of potential temperature for all water samples. [Lower left panel] CTD temperature and salinity profiles plotted as a function of pressure to 1000 dbar. [Lower right panel] Salinity and oxygen from CTD and water samples plotted as a function of potential temperature.

Figures 6.2.2a-i: [Upper panel] Stack plots of temperature versus pressure to 1000 dbar. Offset is 2ºC. [Lower panel] Stack plots of salinity versus pressure to 1000 dbar. Offset is 0.1.

Figures 6.2.3a-i: As in 6.2.1 but for Station Kahe.

Figure 6.2.4: [Upper panel] Potential temperature versus pressure for all deep casts in 1995. [Lower panel] Potential temperature for all deep casts in 1995 plotted from 2500 dbar.

Figure 6.2.5: [Upper panel] Salinity versus potential temperature for all deep casts collected during 1995. [Lower panel] Salinity versus potential temperature on same casts in the 1-5°C range.

Figure 6.2.6: [Upper panel] Oxygen values derived from calibrated CTD sensor data versus potential temperature for all deep casts collected during 1995. [Lower panel] Oxygen versus potential temperature for 1995 deep casts within the 1-5°C range.

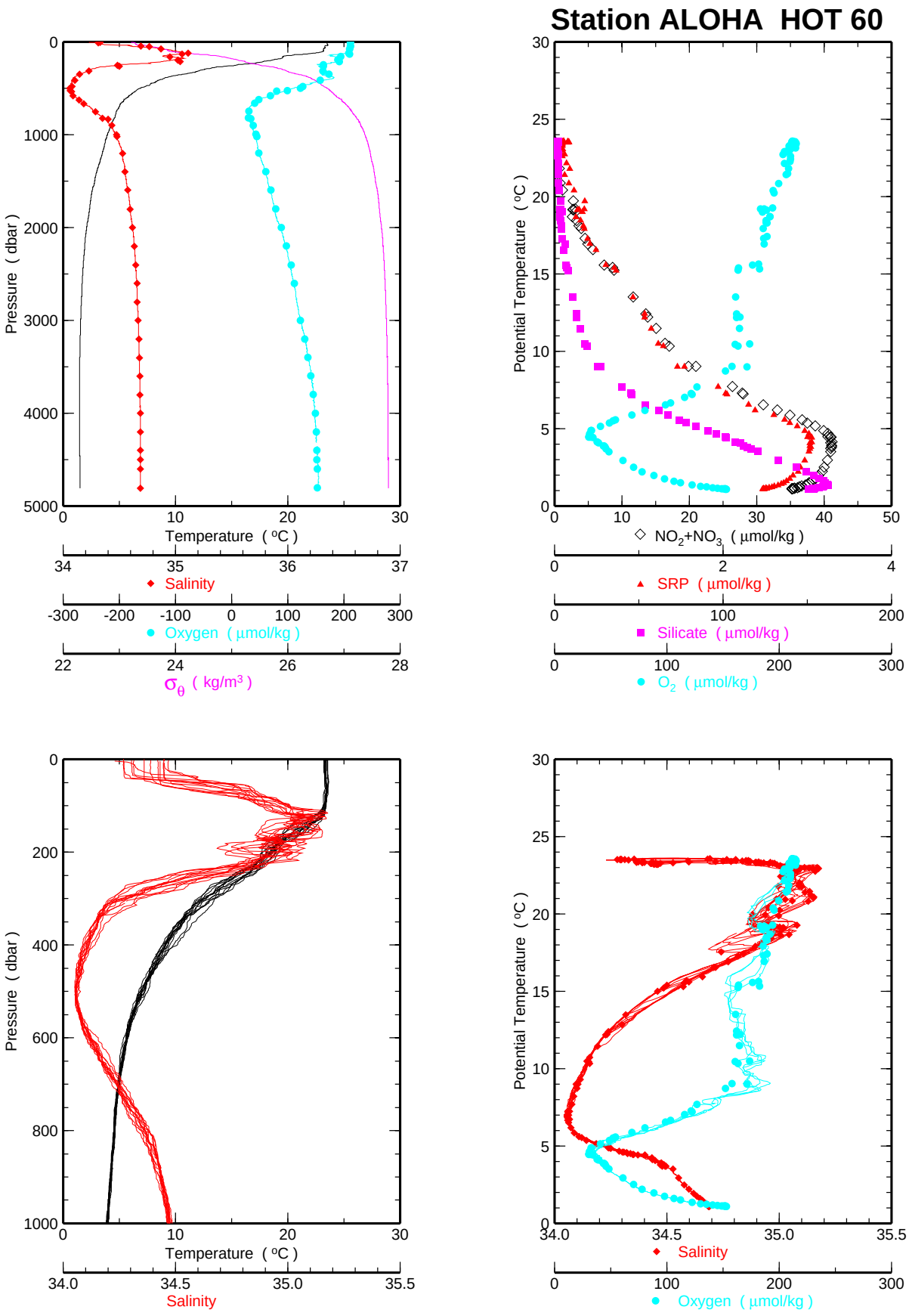
Station ALOHA HOT 60
Pressure (dbar)
Temperature (°C)
Salinity
Oxygen (µmol/kg)
σθ (kg/m³)
Potential Temperature (°C)
NO2+NO3 (µmol/kg)
SRP (µmol/kg)
Silicate (µmol/kg)
O2 (µmol/kg)

Figure 6.2.1a

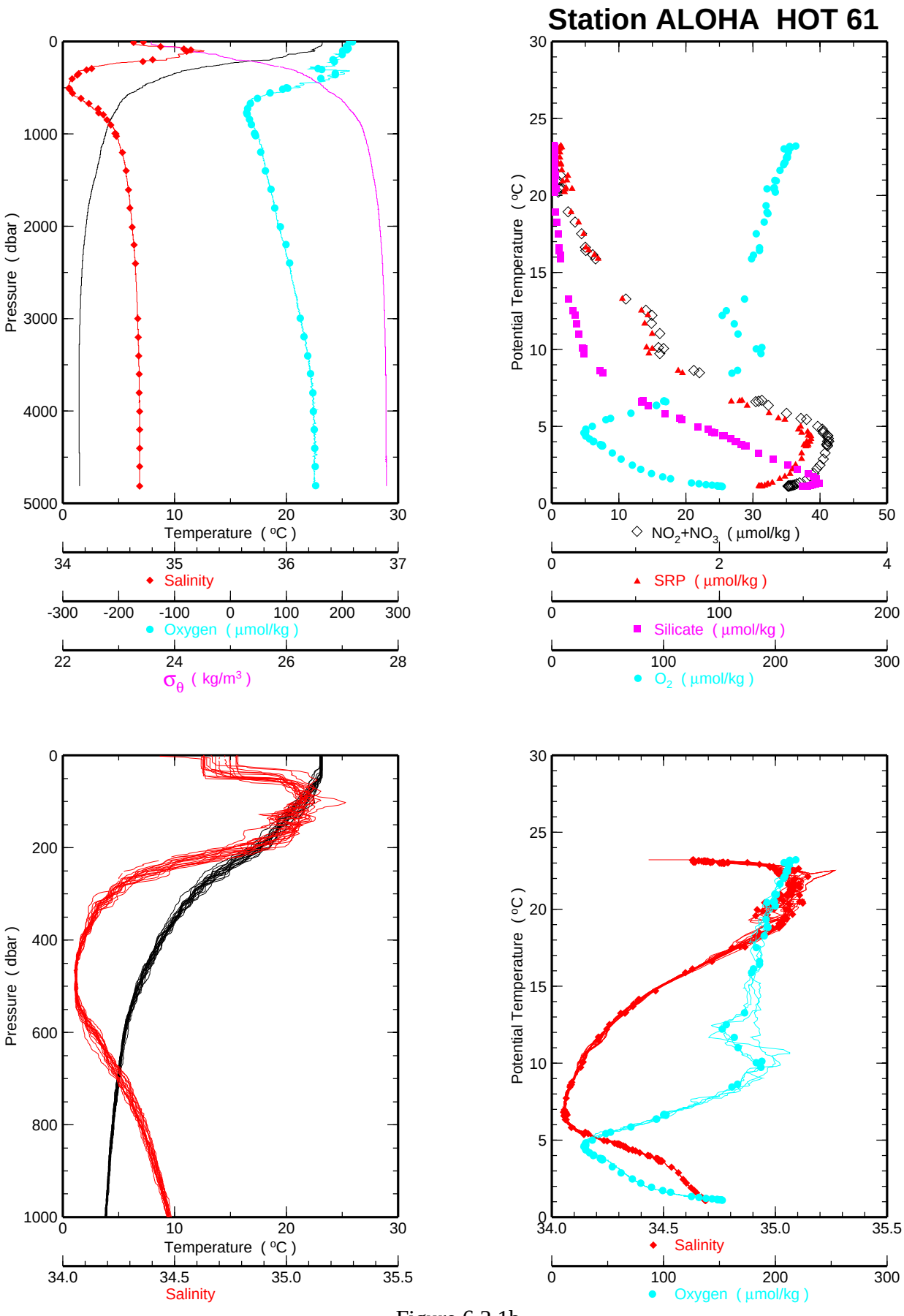
Station ALOHA HOT 61
Pressure (dbar)
Temperature (ºC)
Salinity
Oxygen (µmol/kg)
σθ (kg/m³)
Potential Temperature (ºC)
NO2+NO3 (µmol/kg)
SRP (µmol/kg)
Silicate (µmol/kg)
O2 (µmol/kg)

Figure 6.2.1b

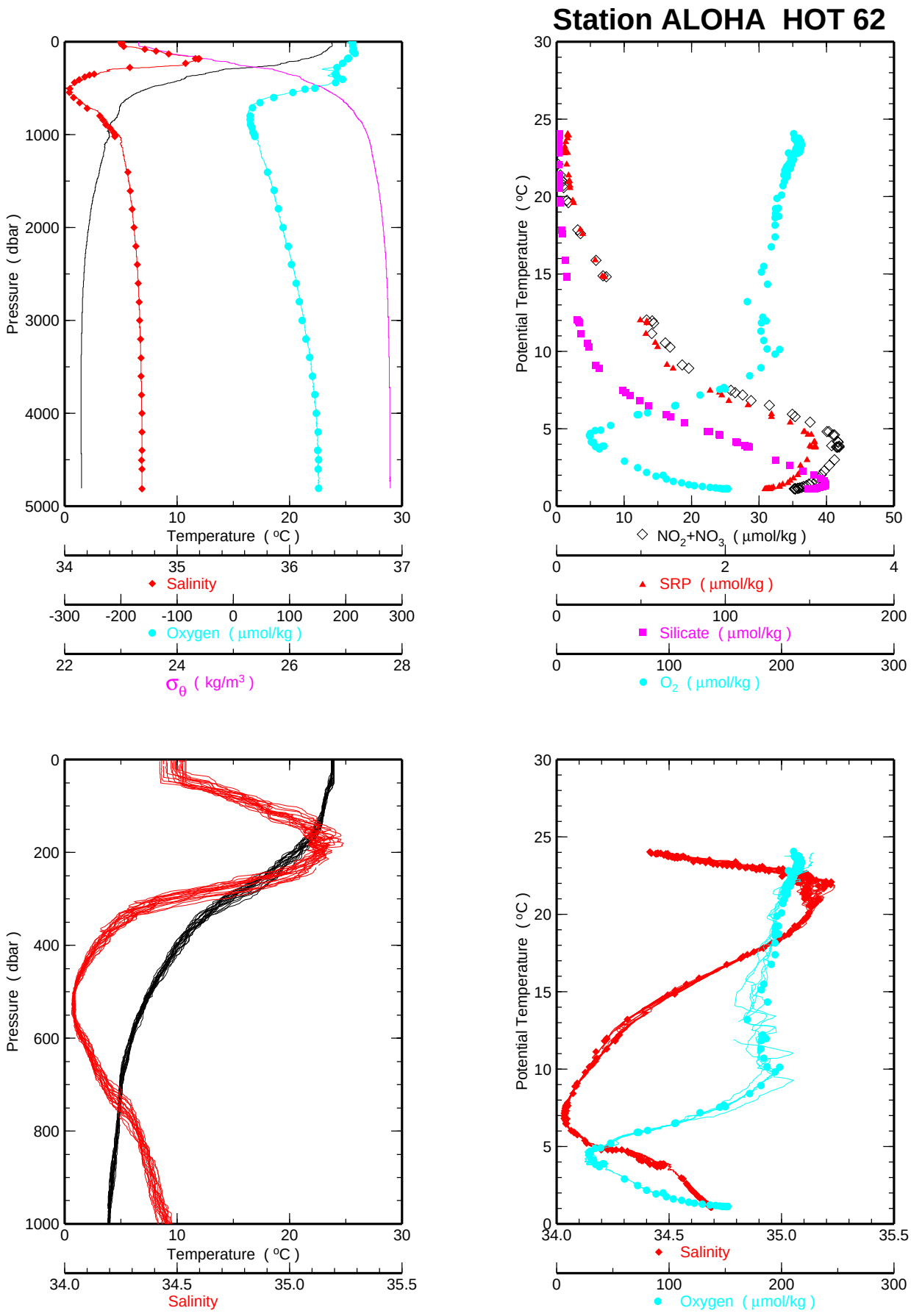
Station ALOHA HOT 62
Pressure (dbar)
Temperature (ºC)
Salinity
Oxygen (µmol/kg)
σθ (kg/m3)
Potential Temperature (ºC)
NO2+NO3 (µmol/kg)
SRP (µmol/kg)
Silicate (µmol/kg)
O2 (µmol/kg)

Figure 6.2.1c

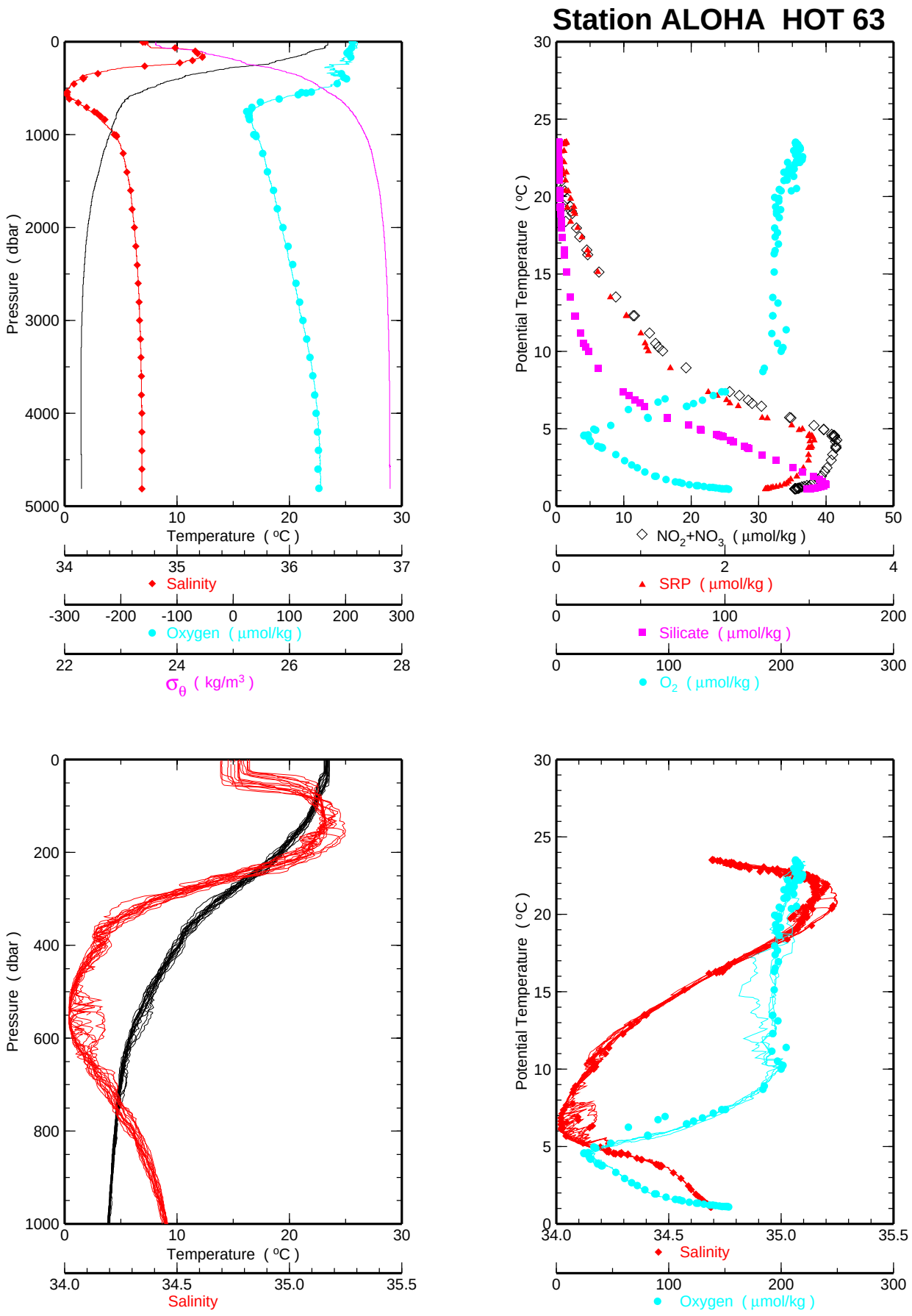
Station ALOHA HOT 63
Pressure (dbar)
Temperature (ºC)
Salinity
Oxygen (µmol/kg)
σθ (kg/m3)
Potential Temperature (ºC)
NO2+NO3 (µmol/kg)
SRP (µmol/kg)
Silicate (µmol/kg)
O2 (µmol/kg)

Figure 6.2.1d

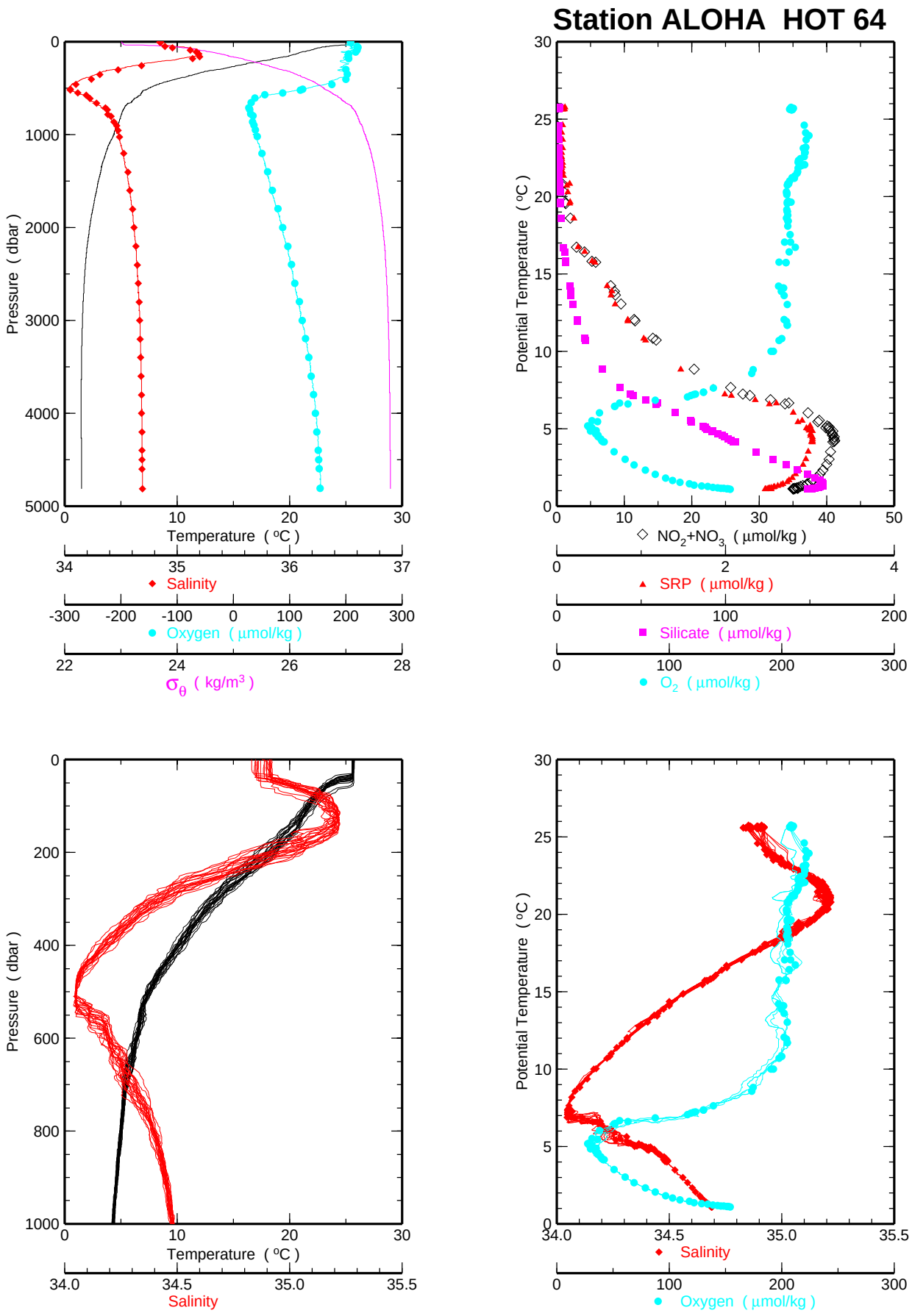
Station ALOHA HOT 64
Pressure (dbar)
Temperature (ºC)
Salinity
Oxygen (µmol/kg)
σθ (kg/m3)
Potential Temperature (ºC)
NO2+NO3 (µmol/kg)
SRP (µmol/kg)
Silicate (µmol/kg)
O2 (µmol/kg)

Figure 6.2.1e

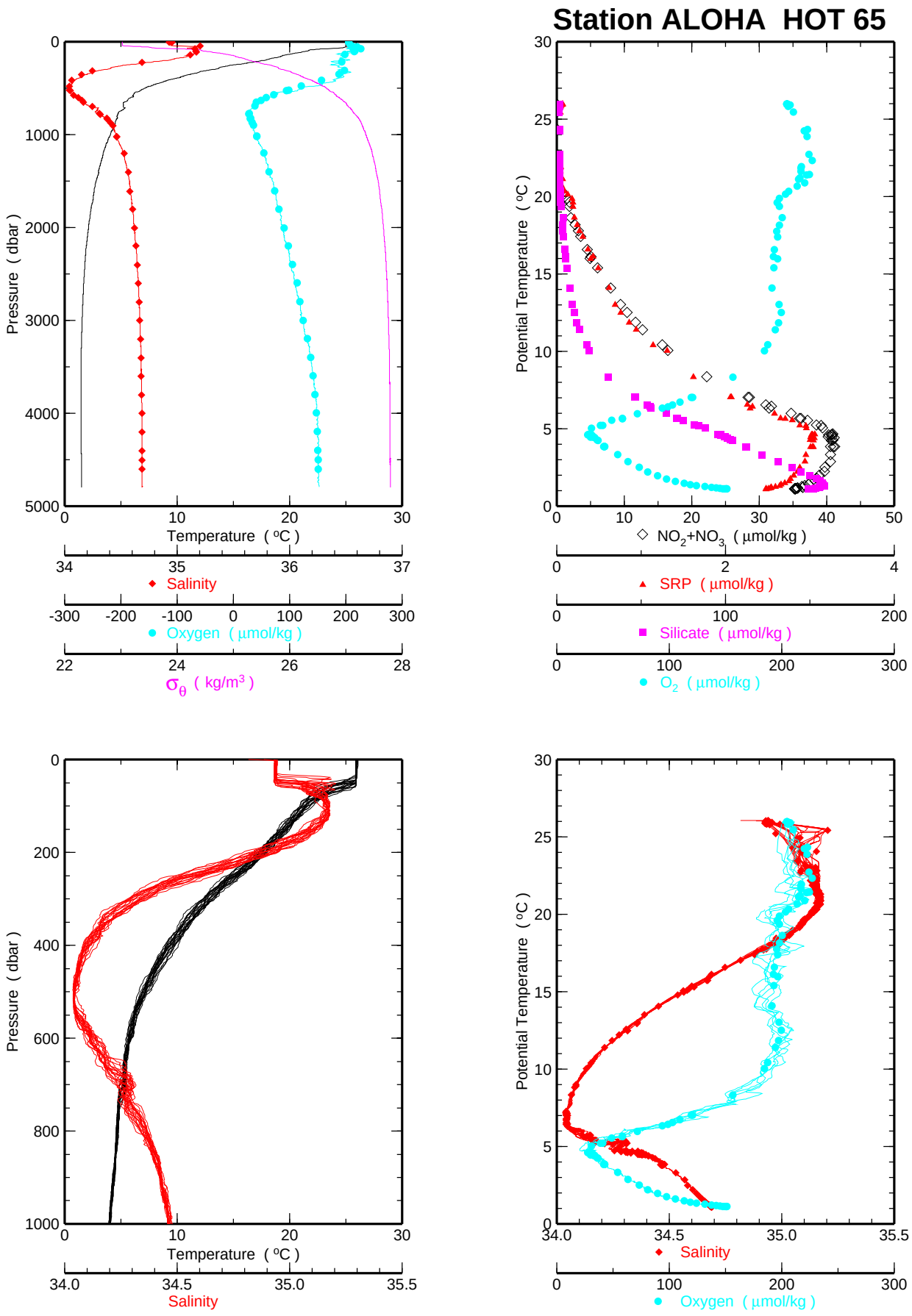
Station ALOHA HOT 65
Pressure (dbar)
Temperature (ºC)
Salinity
Oxygen (µmol/kg)
σθ (kg/m3)
Potential Temperature (ºC)
NO2+NO3 (µmol/kg)
SRP (µmol/kg)
Silicate (µmol/kg)
O2 (µmol/kg)

Figure 6.2.1f

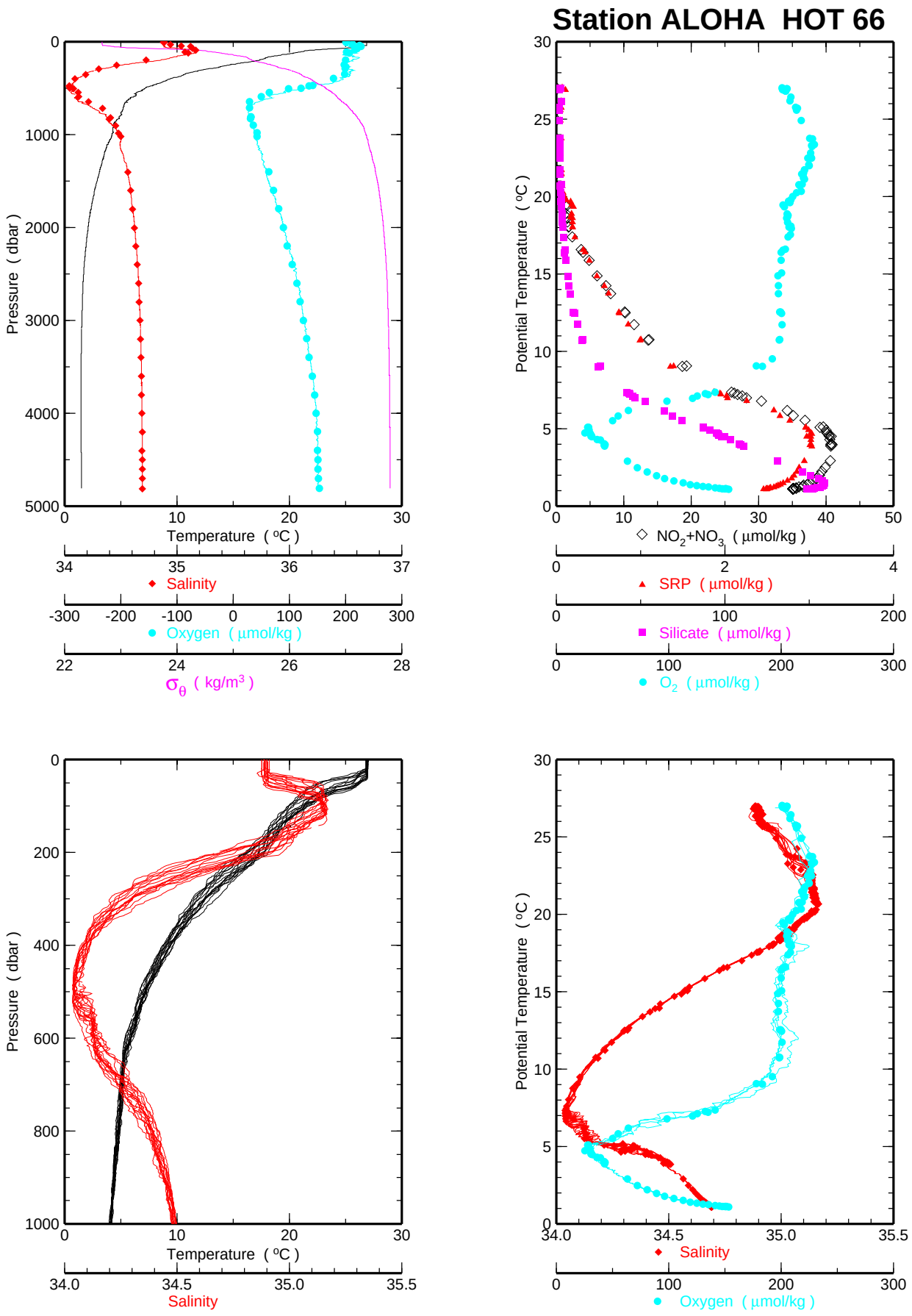
Station ALOHA HOT 66
Pressure (dbar)
Temperature (ºC)
Salinity
Oxygen (µmol/kg)
σθ (kg/m3)
Potential Temperature (ºC)
NO2+NO3 (µmol/kg)
SRP (µmol/kg)
Silicate (µmol/kg)
O2 (µmol/kg)

Figure 6.2.1g

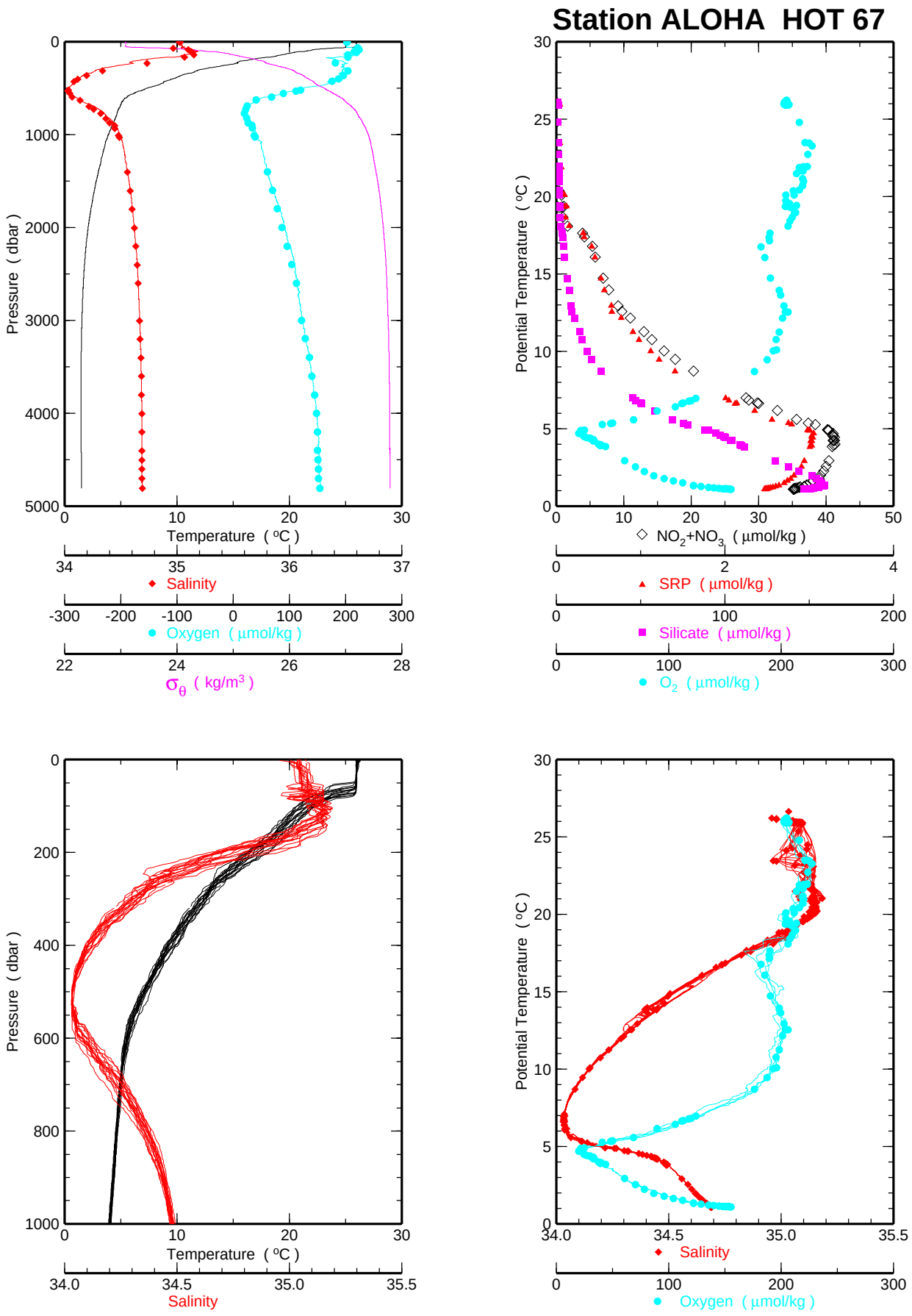
Station ALOHA HOT 67
Pressure (dbar)
Temperature (ºC)
Salinity
Oxygen (µmol/kg)
σθ (kg/m3)
Potential Temperature (ºC)
NO2+NO3 (µmol/kg)
SRP (µmol/kg)
Silicate (µmol/kg)
O2 (µmol/kg)

Figure 6.2.1h

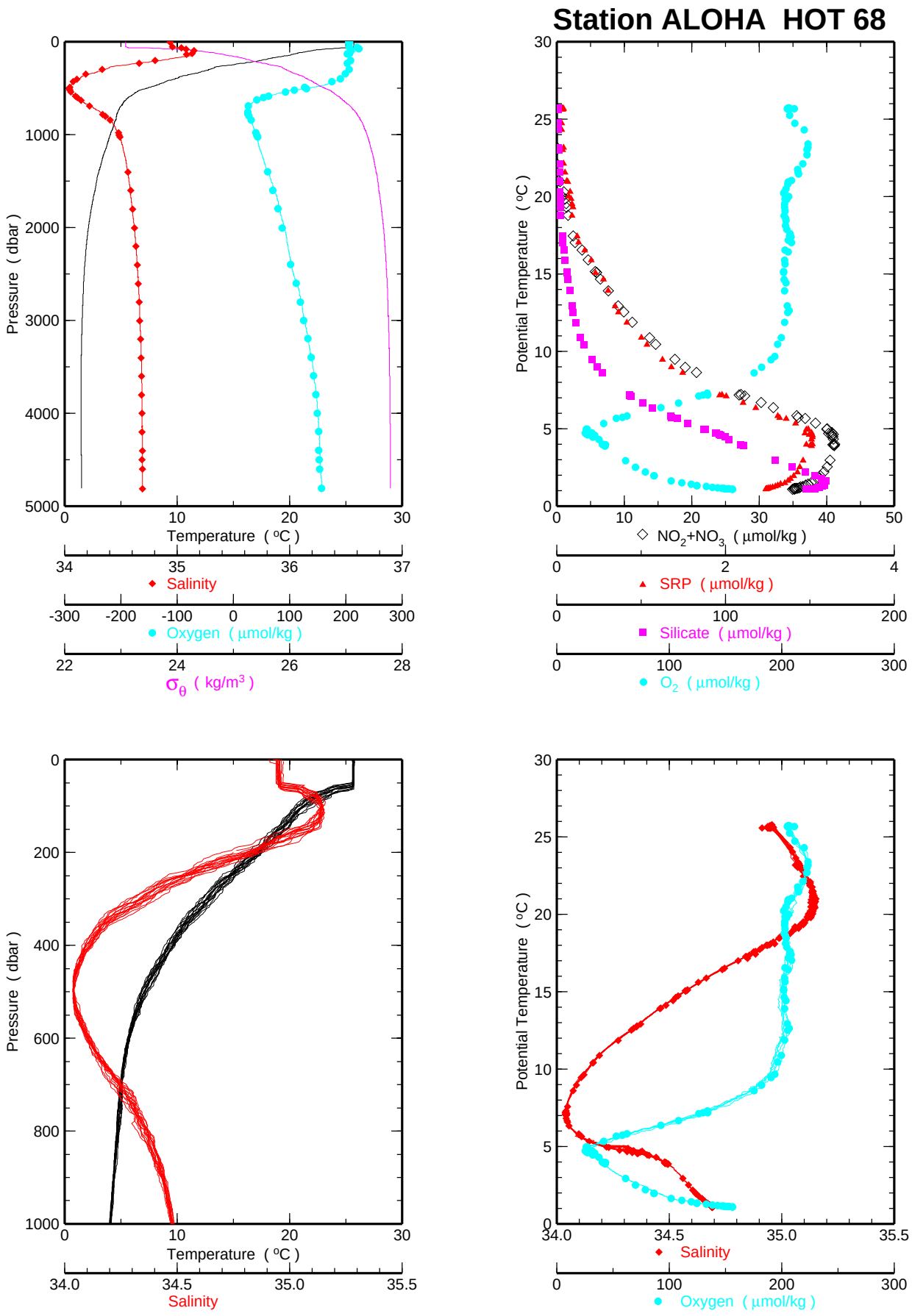
Station ALOHA HOT 68
Pressure (dbar)
Temperature (ºC)
Salinity
Oxygen (µmol/kg)
σθ (kg/m3)
Potential Temperature (ºC)
NO2+NO3 (µmol/kg)
SRP (µmol/kg)
Silicate (µmol/kg)
O2 (µmol/kg)

Figure 6.2.1i

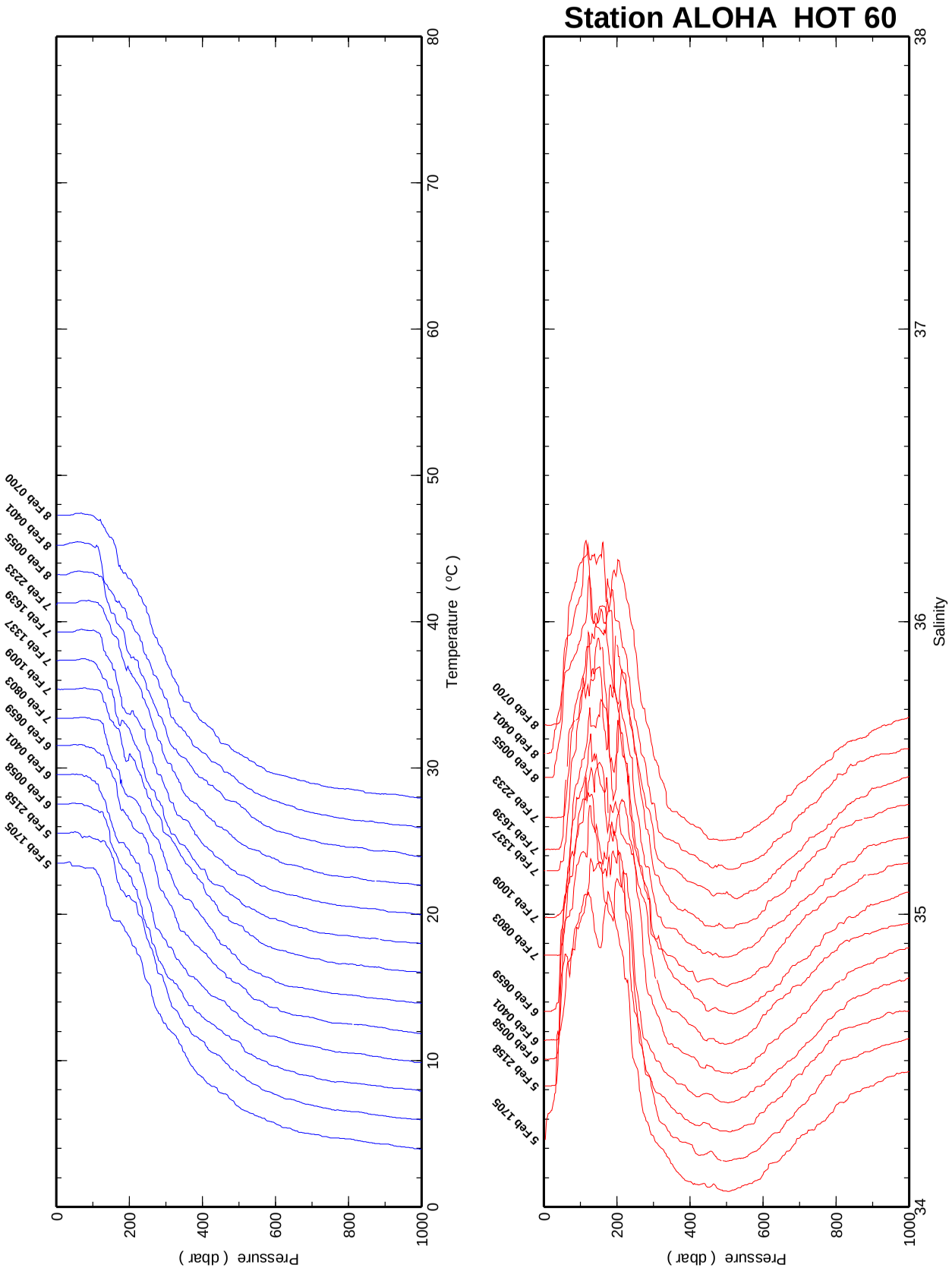
Station ALOHA HOT 60
Temperature (°C)
Salinity
Pressure (dbar)
Pressure (dbar)
0
200
400
600
800
1000
0
10
20
30
40
50
60
70
80
34
35
36
37
38
8 Feb 0700
8 Feb 0401
8 Feb 0055
7 Feb 2233
7 Feb 1639
7 Feb 1337
7 Feb 1009
7 Feb 0803
6 Feb 0659
6 Feb 0401
6 Feb 0058
5 Feb 2158
5 Feb 1705

Figure 6.2.2a

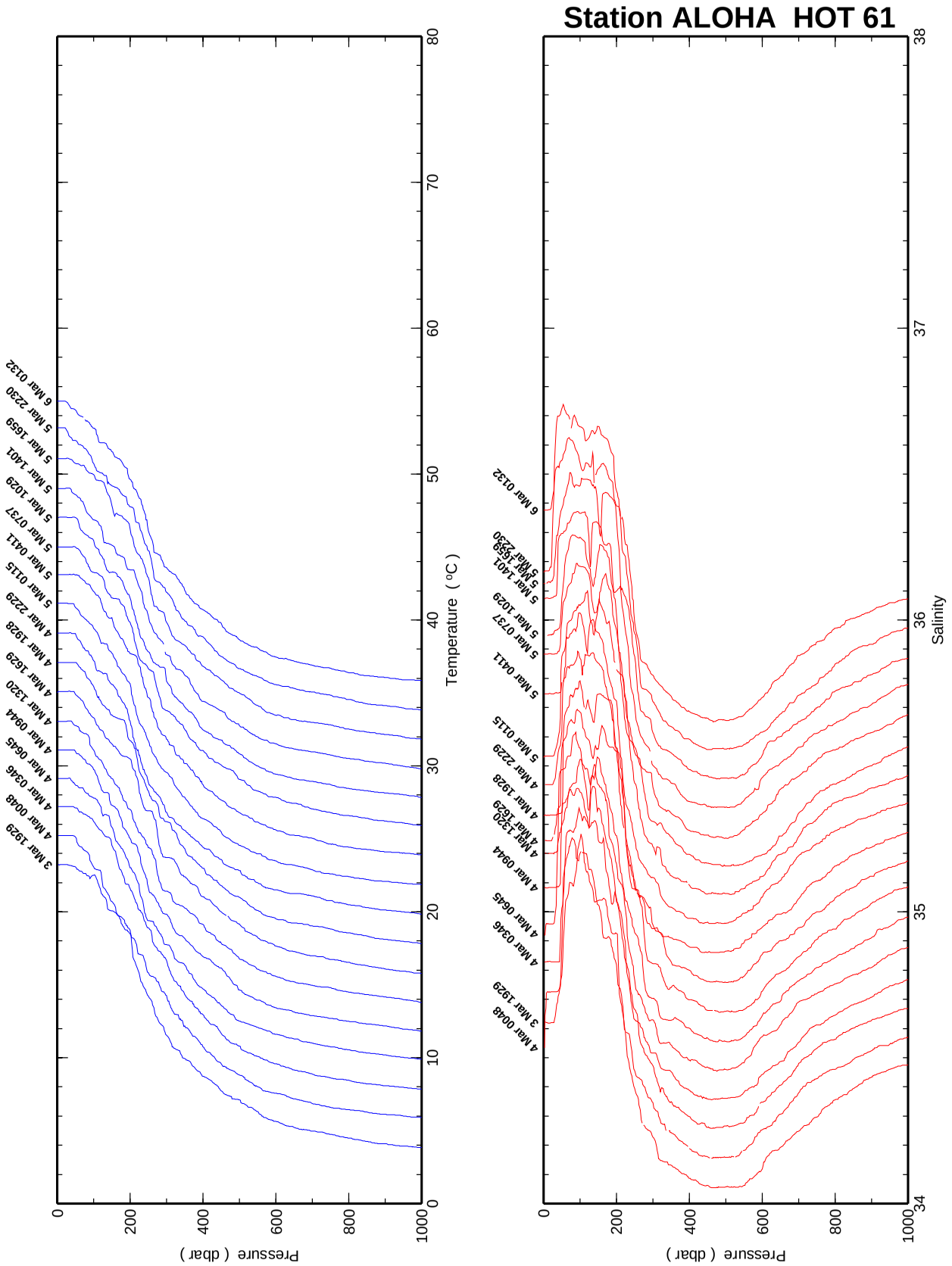
Station ALOHA HOT 61
Temperature (°C)
Salinity
Pressure (dbar)
Pressure (dbar)
6 Mar 0132
5 Mar 2230
5 Mar 1659
5 Mar 1401
5 Mar 1029
5 Mar 0737
5 Mar 0411
5 Mar 0115
4 Mar 2229
4 Mar 1928
4 Mar 1629
4 Mar 1320
4 Mar 0944
4 Mar 0645
4 Mar 0346
4 Mar 0048
3 Mar 1929

Figure 6.2.2b

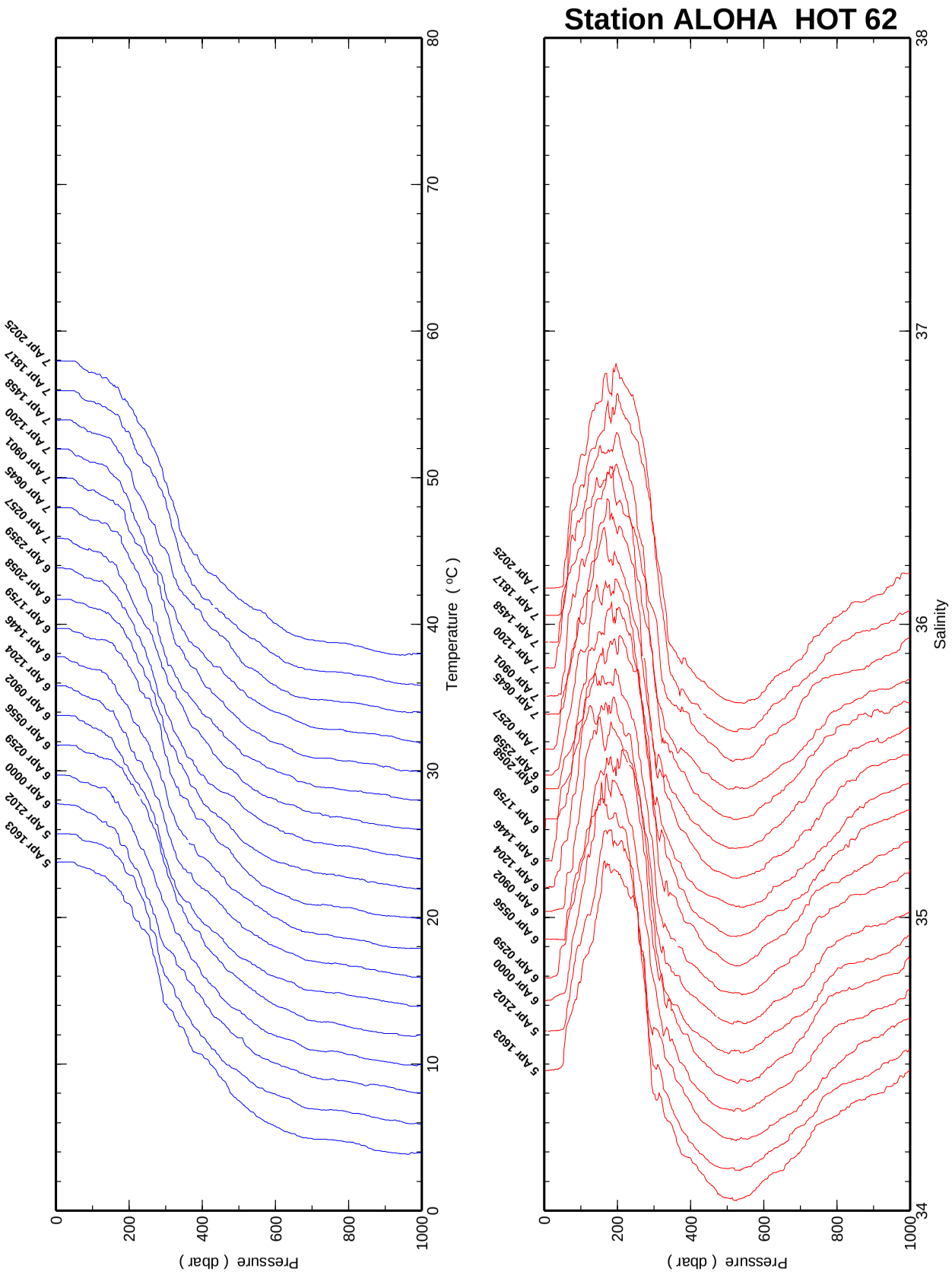
Station ALOHA HOT 62
Temperature (°C)
Salinity
Pressure (dbar)
Pressure (dbar)
5 Apr 1603
5 Apr 2102
6 Apr 0000
6 Apr 0259
6 Apr 0556
6 Apr 0902
6 Apr 1204
6 Apr 1446
6 Apr 1759
6 Apr 2058
6 Apr 2359
7 Apr 0257
7 Apr 0645
7 Apr 0901
7 Apr 1200
7 Apr 1458
7 Apr 1817
7 Apr 2025

Figure 6.2.2c

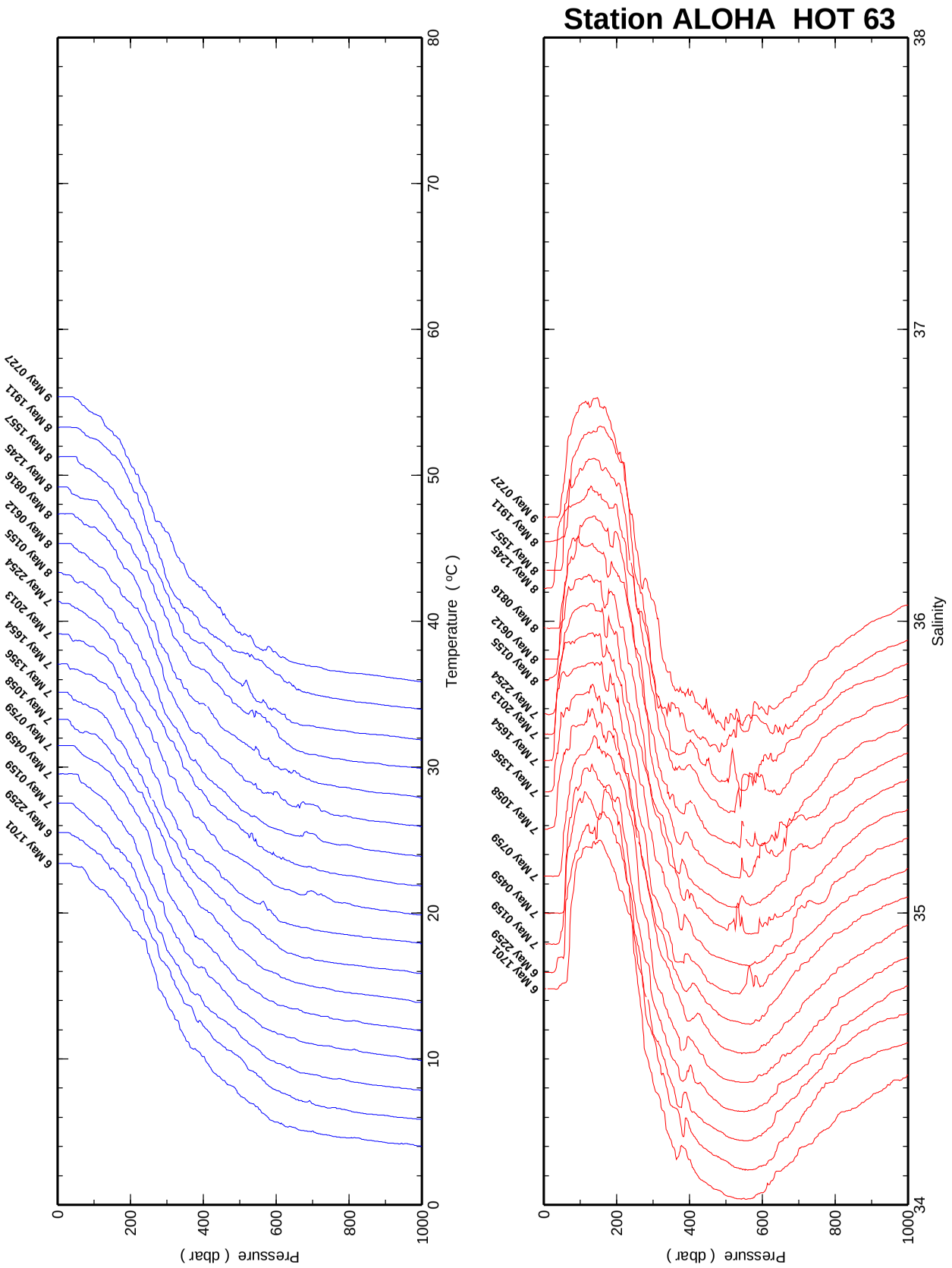
Station ALOHA HOT 63
Temperature (°C)
Salinity
Pressure (dbar)
Pressure (dbar)
6 May 1701
6 May 2259
7 May 0159
7 May 0459
7 May 0759
7 May 1058
7 May 1356
7 May 1654
7 May 2013
7 May 2254
8 May 0155
8 May 0612
8 May 0816
8 May 1245
8 May 1557
8 May 1911
9 May 0727

Figure 6.2.2d

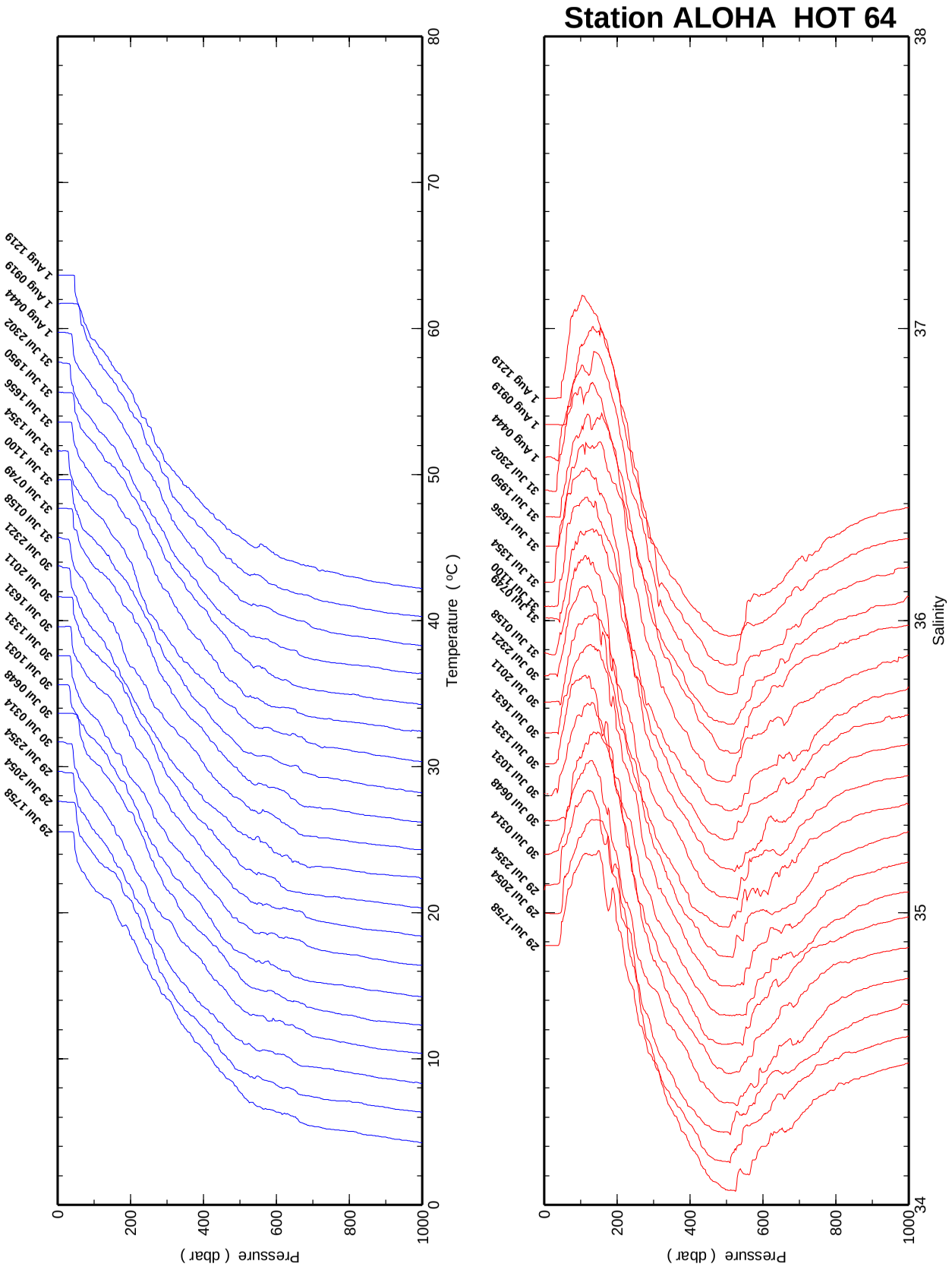
Station ALOHA HOT 64
Temperature (°C)
Salinity
Pressure (dbar)
Pressure (dbar)
29 Jul 1758
29 Jul 2054
29 Jul 2354
30 Jul 0314
30 Jul 0648
30 Jul 1031
30 Jul 1331
30 Jul 1631
30 Jul 2011
30 Jul 2321
31 Jul 0158
31 Jul 0749
31 Jul 1100
31 Jul 1354
31 Jul 1656
31 Jul 1950
31 Jul 2302
1 Aug 0444
1 Aug 0919
1 Aug 1219

Figure 6.2.2e

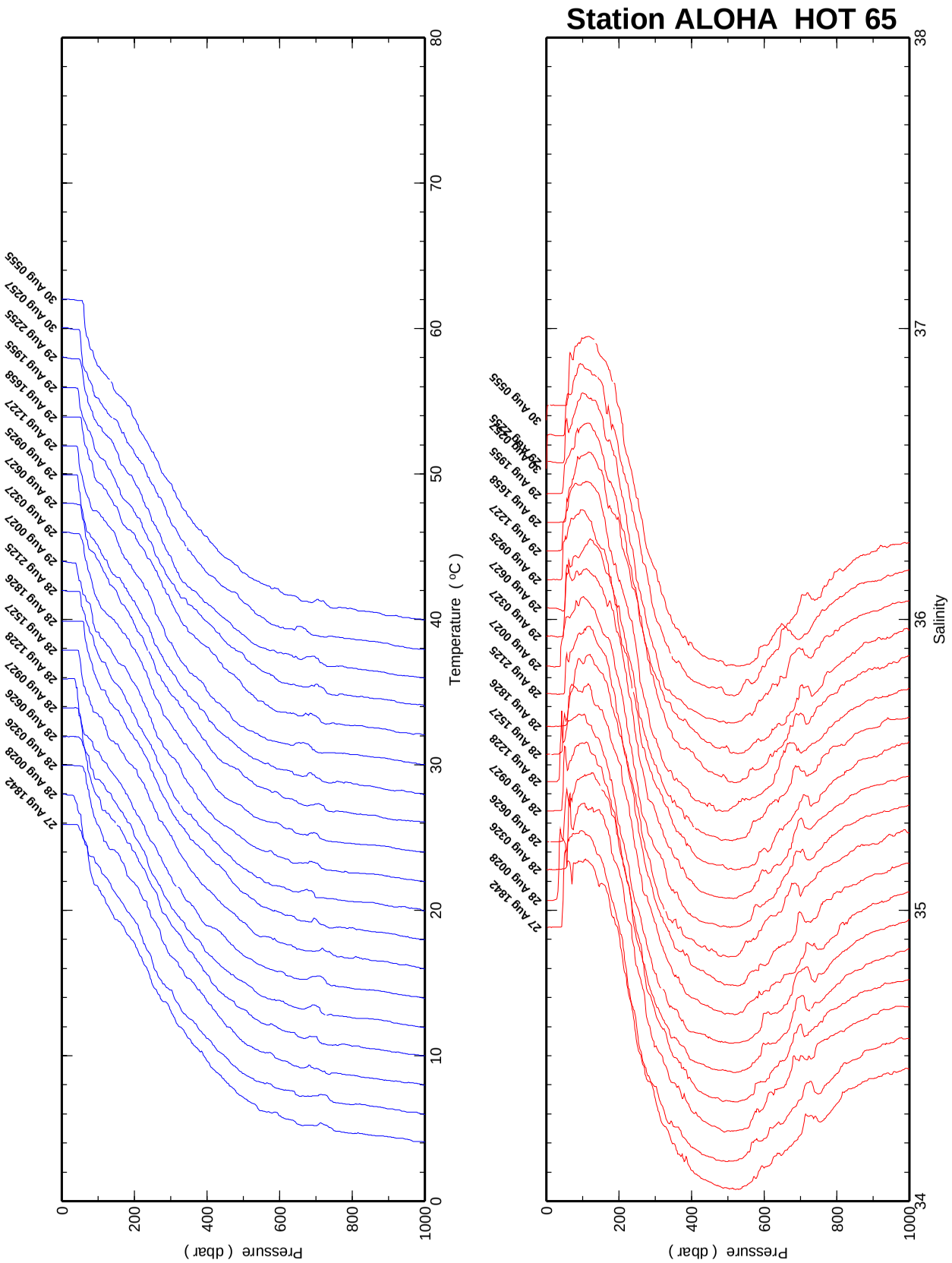
Station ALOHA HOT 65
Temperature (°C)
Salinity
Pressure (dbar)
Pressure (dbar)
0
200
400
600
800
1000
0
10
20
30
40
50
60
70
80
34
35
36
37
38
30 Aug 0555
30 Aug 0257
30 Aug 2255
29 Aug 1955
29 Aug 1658
29 Aug 1227
29 Aug 0925
29 Aug 0627
29 Aug 0327
29 Aug 0027
29 Aug 2125
28 Aug 1826
28 Aug 1527
28 Aug 1228
28 Aug 0927
28 Aug 0626
28 Aug 0326
28 Aug 0028
27 Aug 1842

Figure 6.2.2f

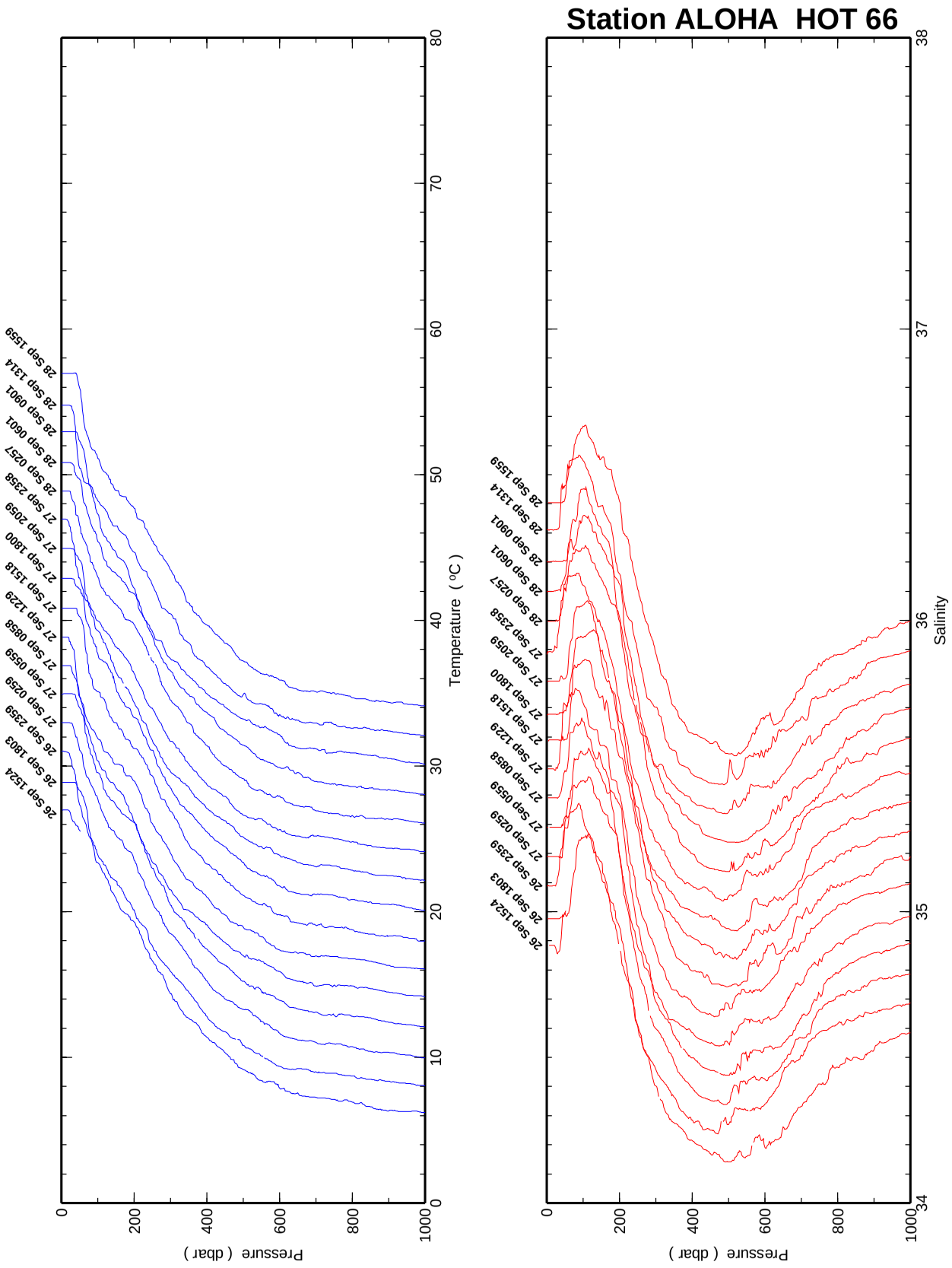
Station ALOHA HOT 66
Temperature (°C)
Salinity
Pressure (dbar)
Pressure (dbar)
28 Sep 1559
28 Sep 1314
28 Sep 0901
28 Sep 0601
28 Sep 0257
28 Sep 2358
27 Sep 2059
27 Sep 1800
27 Sep 1518
27 Sep 1229
27 Sep 0858
27 Sep 0559
27 Sep 0259
26 Sep 2359
26 Sep 1803
26 Sep 1524

Figure 6.2.2g

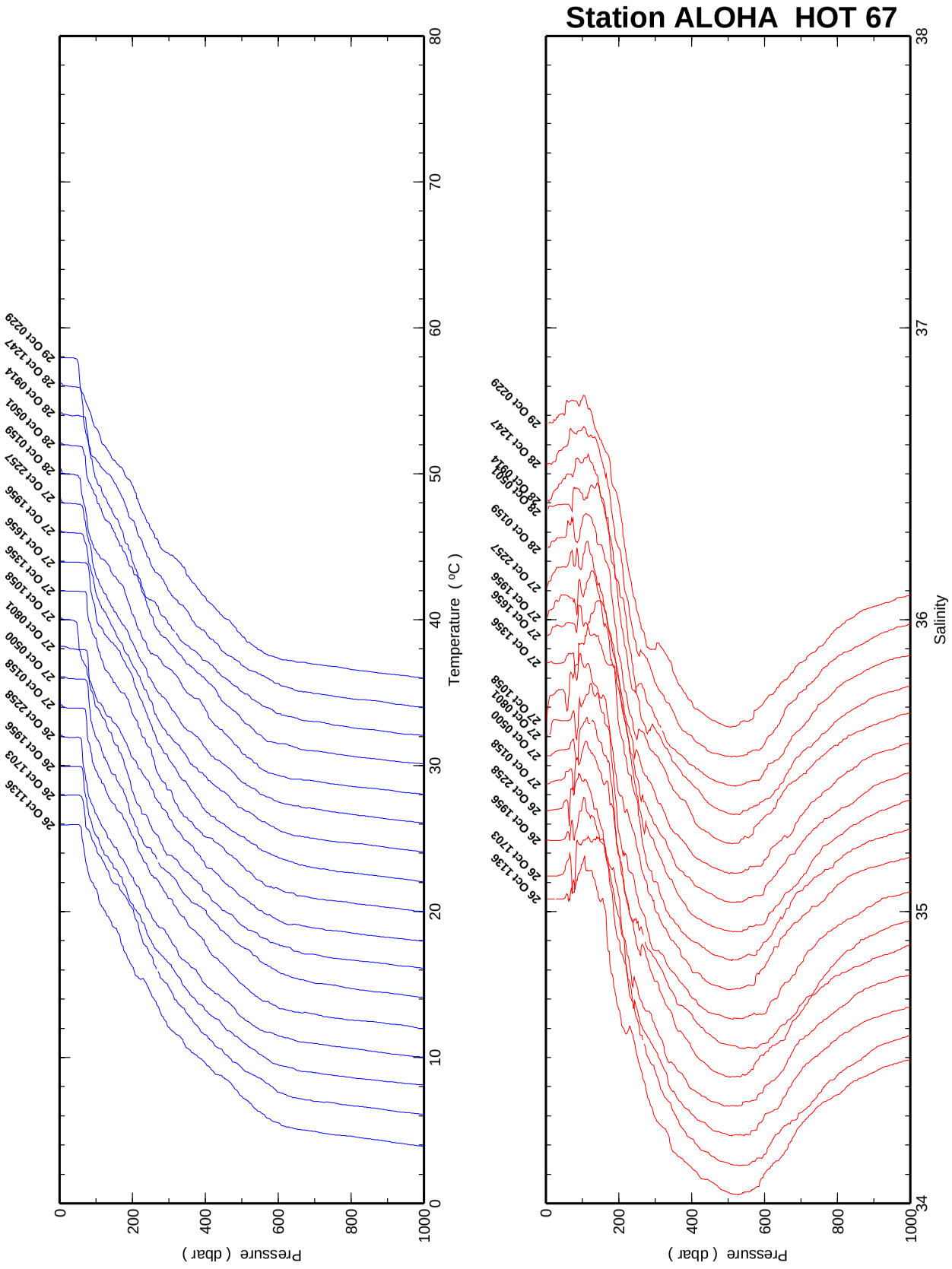
Station ALOHA HOT 67
Temperature (°C)
Salinity
Pressure (dbar)
Pressure (dbar)
29 Oct 0229
28 Oct 1247
28 Oct 0914
28 Oct 0501
28 Oct 0159
27 Oct 2257
27 Oct 1956
27 Oct 1656
27 Oct 1356
27 Oct 1058
27 Oct 0801
27 Oct 0500
27 Oct 0158
26 Oct 2258
26 Oct 1956
26 Oct 1703
26 Oct 1136

Figure 6.2.2h

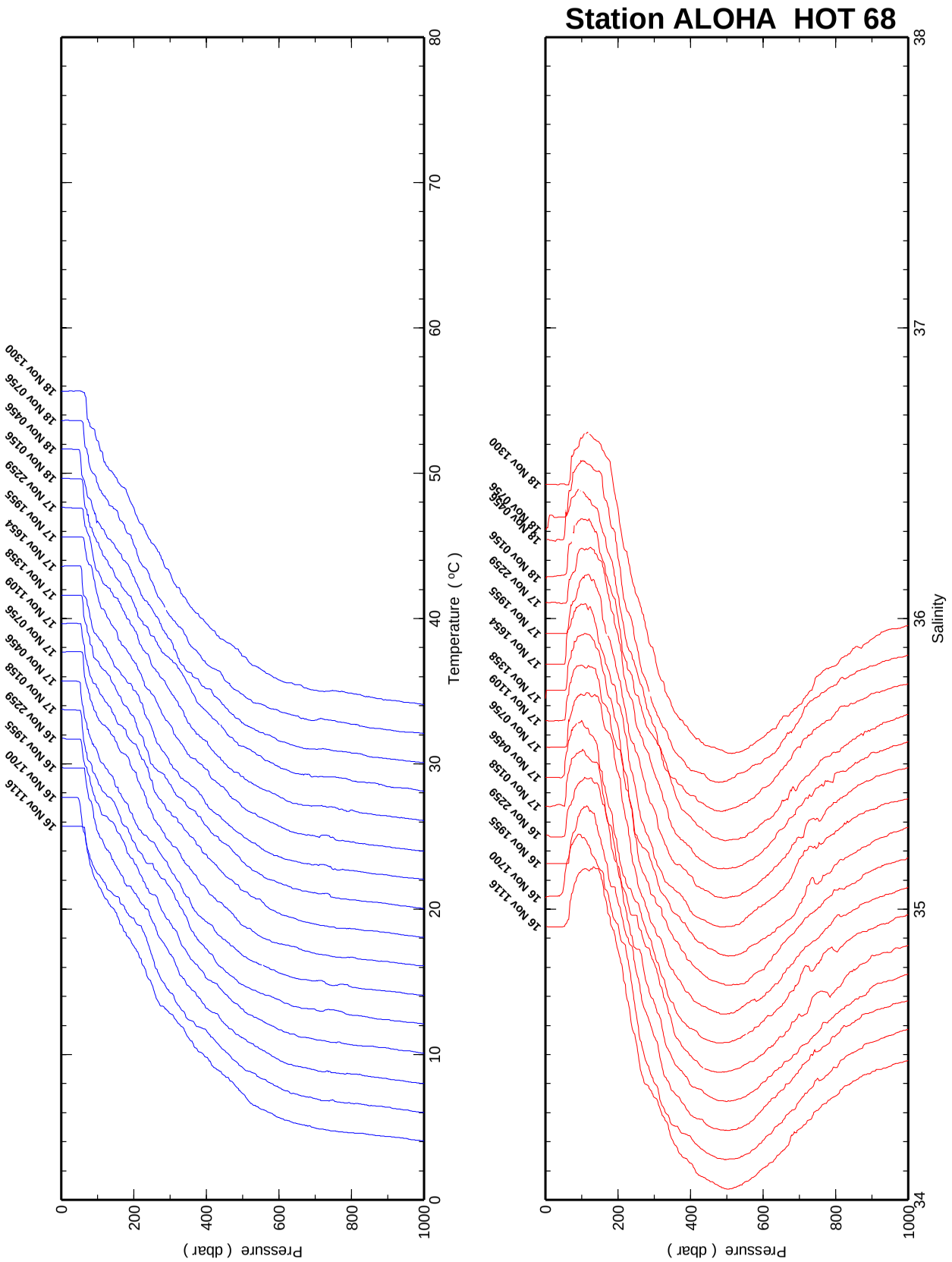
Station ALOHA HOT 68
Temperature (°C)
Salinity
Pressure (dbar)
Pressure (dbar)
16 NOV 1116
16 NOV 1700
16 NOV 1955
16 NOV 2259
17 NOV 0158
17 NOV 0456
17 NOV 0756
17 NOV 1109
17 NOV 1358
17 NOV 1654
17 NOV 1955
17 NOV 2259
18 NOV 0156
18 NOV 0456
18 NOV 0756
18 NOV 1300

Figure 6.2.2i

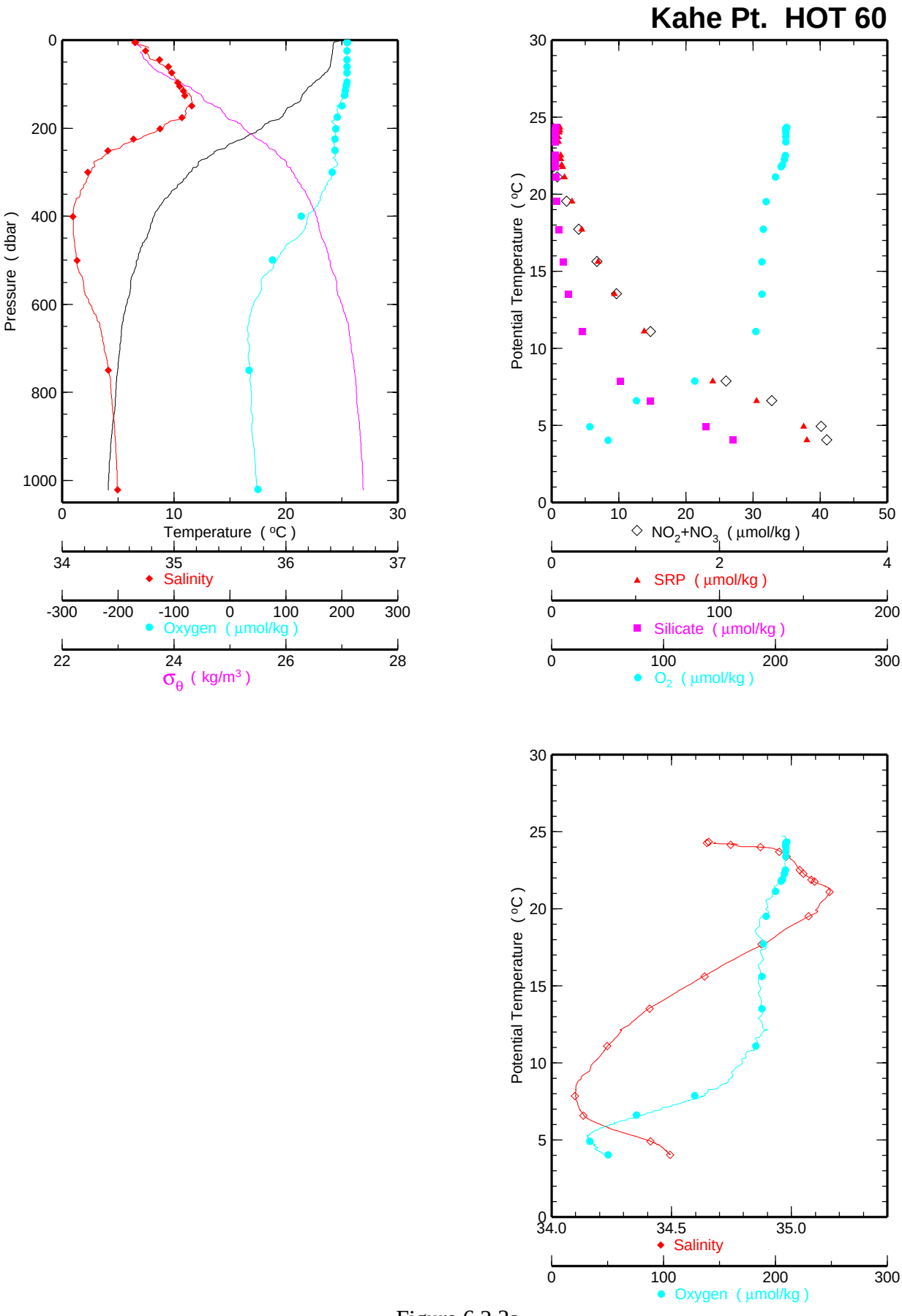
Kahe Pt. HOT 60
Pressure (dbar)
Temperature (ºC)
Salinity
Oxygen (µmol/kg)
σθ (kg/m³)
Potential Temperature (ºC)
NO2+NO3 (µmol/kg)
SRP (µmol/kg)
Silicate (µmol/kg)
O2 (µmol/kg)
Potential Temperature (ºC)
Salinity
Oxygen (µmol/kg)

Figure 6.2.3a

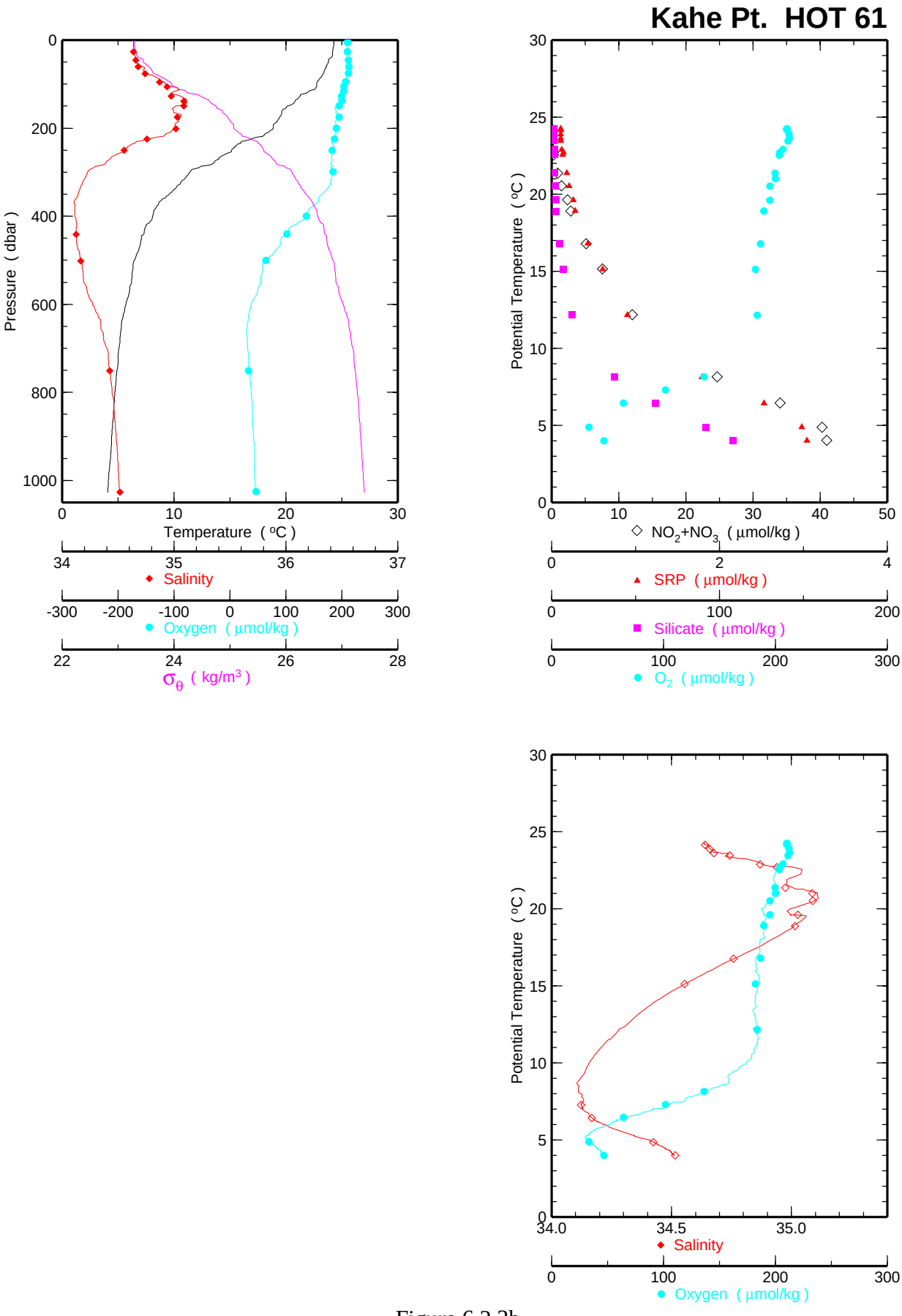
Kahe Pt. HOT 61
Pressure (dbar)
Temperature (ºC)
Salinity
Oxygen (µmol/kg)
σθ (kg/m³)
Potential Temperature (ºC)
NO2+NO3 (µmol/kg)
SRP (µmol/kg)
Silicate (µmol/kg)
O2 (µmol/kg)
Potential Temperature (ºC)
Salinity
Oxygen (µmol/kg)

Figure 6.2.3b

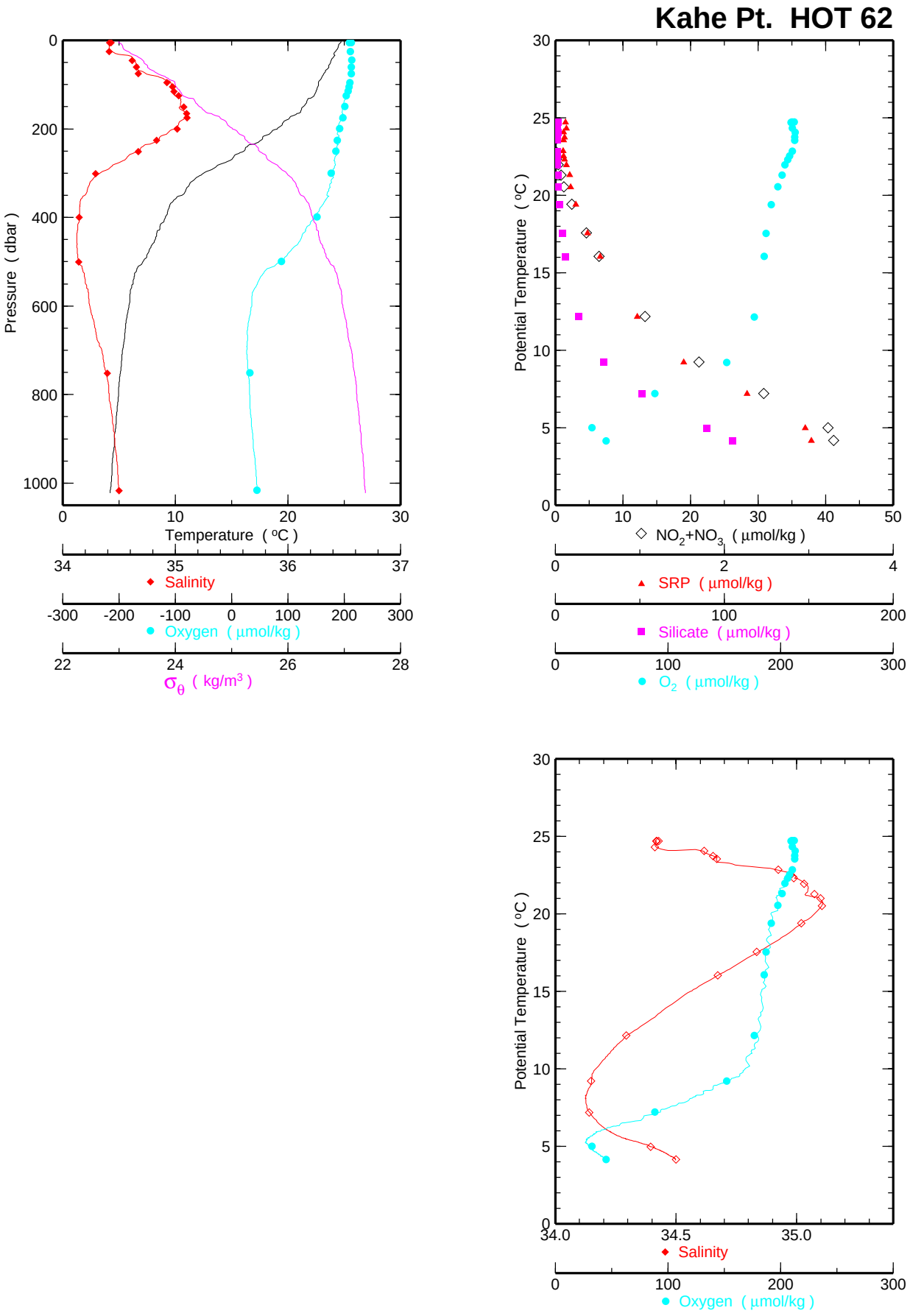
Kahe Pt. HOT 62
Pressure (dbar)
Temperature (ºC)
Salinity
Oxygen (µmol/kg)
σθ (kg/m3)
Potential Temperature (ºC)
NO2+NO3 (µmol/kg)
SRP (µmol/kg)
Silicate (µmol/kg)
O2 (µmol/kg)
Potential Temperature (ºC)
Salinity
Oxygen (µmol/kg)

Figure 6.2.3c

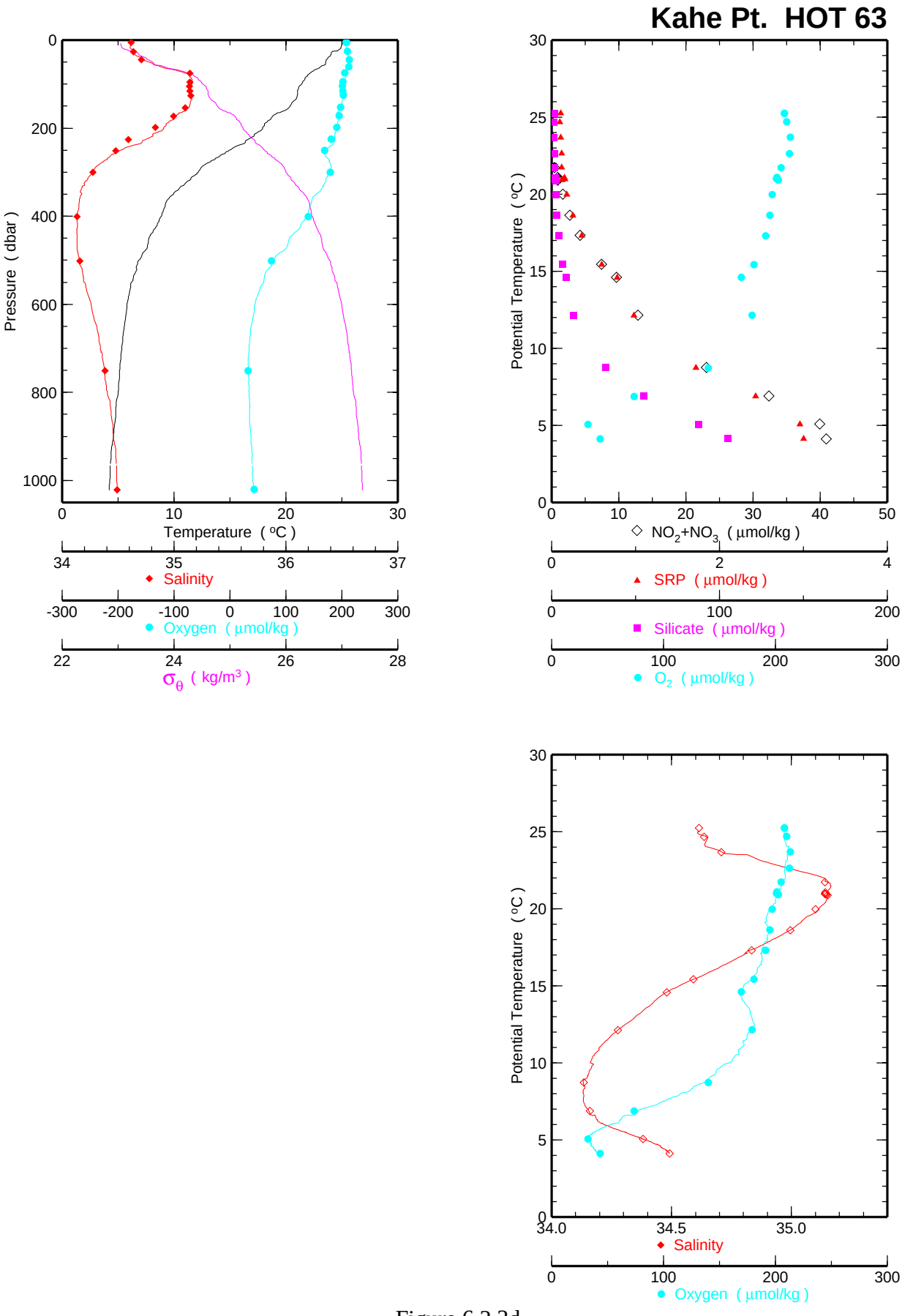
Kahe Pt. HOT 63
Pressure (dbar)
Temperature (ºC)
Salinity
Oxygen (µmol/kg)
σθ (kg/m³)
Potential Temperature (ºC)
NO2+NO3 (µmol/kg)
SRP (µmol/kg)
Silicate (µmol/kg)
O2 (µmol/kg)
Potential Temperature (ºC)
Salinity
Oxygen (µmol/kg)

Figure 6.2.3d

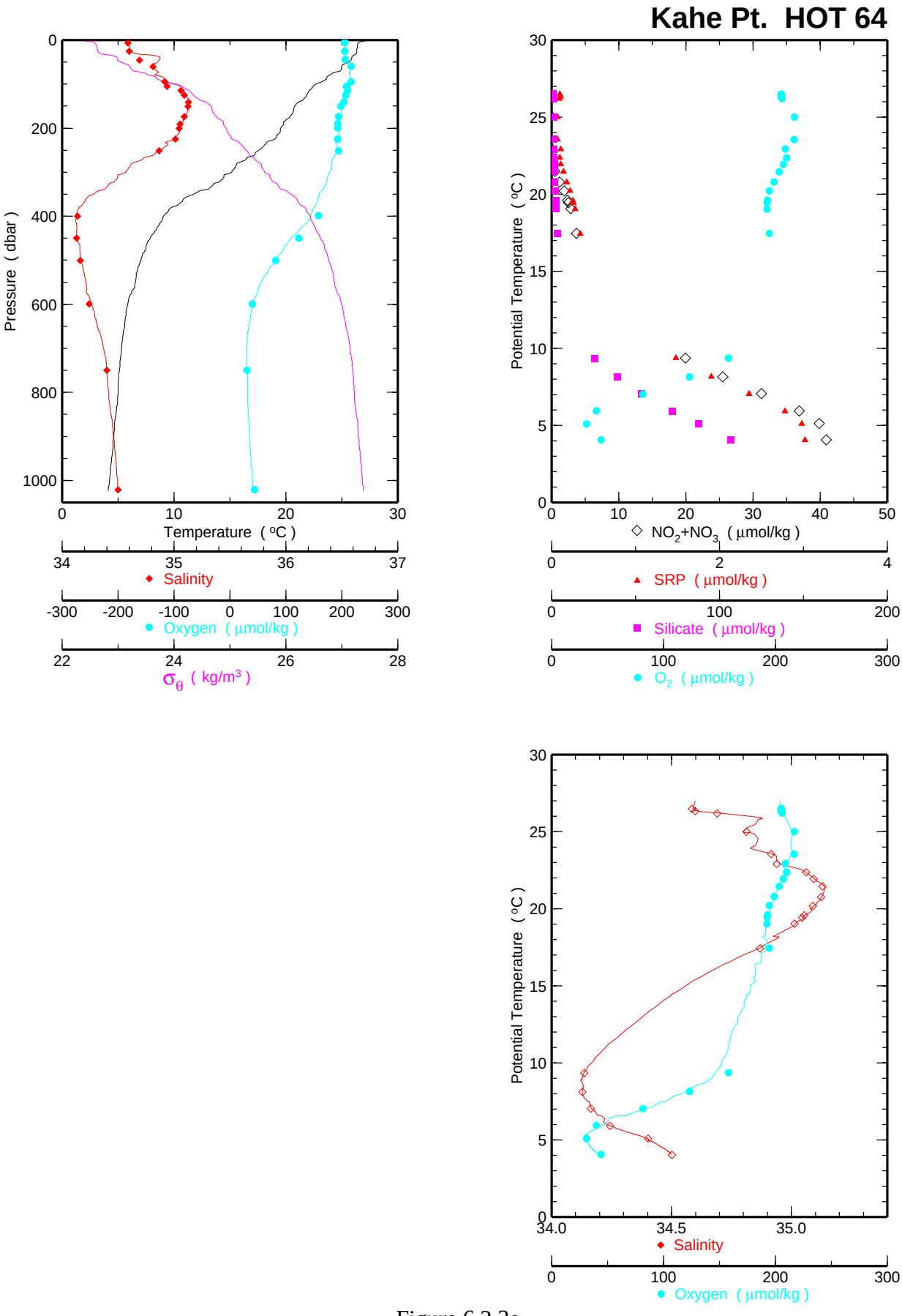
Kahe Pt. HOT 64
Pressure (dbar)
Temperature (ºC)
Salinity
Oxygen (µmol/kg)
σθ (kg/m³)
Potential Temperature (ºC)
NO2+NO3 (µmol/kg)
SRP (µmol/kg)
Silicate (µmol/kg)
O2 (µmol/kg)
Potential Temperature (ºC)
Salinity
Oxygen (µmol/kg)

Figure 6.2.3e

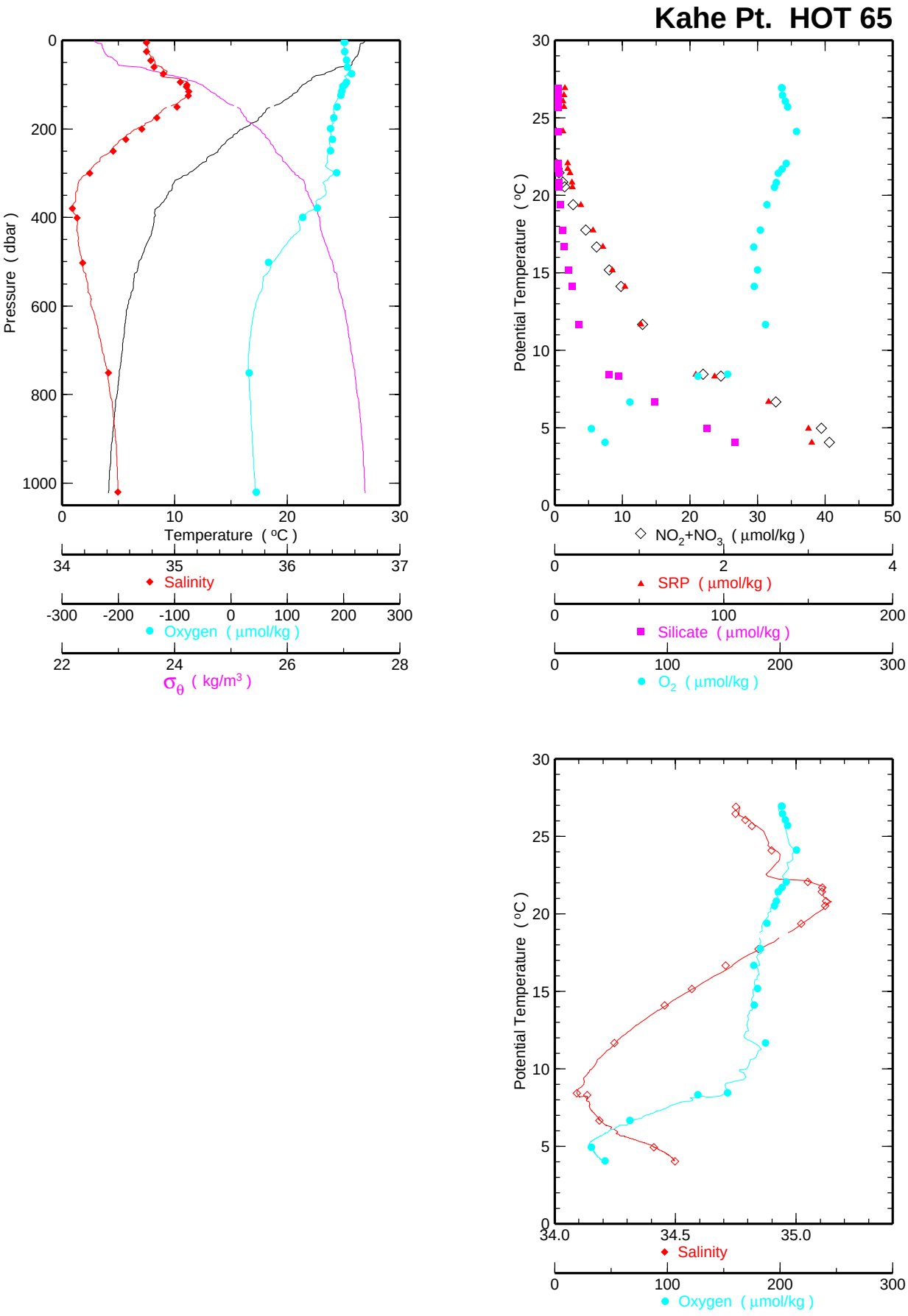
Kahe Pt. HOT 65
Pressure (dbar)
Temperature (ºC)
Salinity
Oxygen (µmol/kg)
σθ (kg/m3)
Potential Temperature (ºC)
NO2+NO3 (µmol/kg)
SRP (µmol/kg)
Silicate (µmol/kg)
O2 (µmol/kg)
Potential Temperature (ºC)
Salinity
Oxygen (µmol/kg)

Figure 6.2.3f

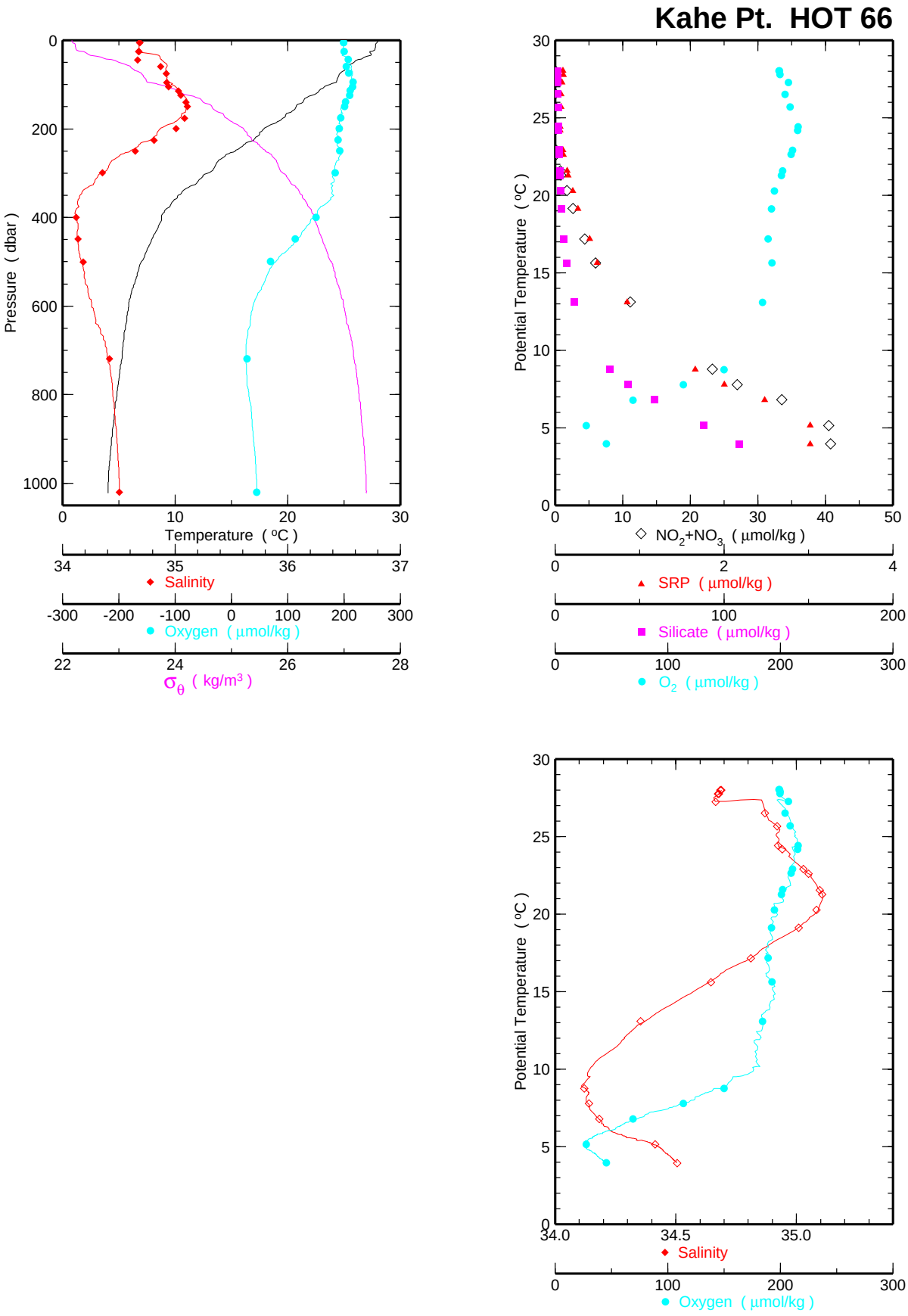
Kahe Pt. HOT 66
Pressure (dbar)
Temperature (°C)
Salinity
Oxygen (µmol/kg)
σθ (kg/m³)
Potential Temperature (°C)
NO2+NO3 (µmol/kg)
SRP (µmol/kg)
Silicate (µmol/kg)
O2 (µmol/kg)
Potential Temperature (°C)
Salinity
Oxygen (µmol/kg)

Figure 6.2.3g

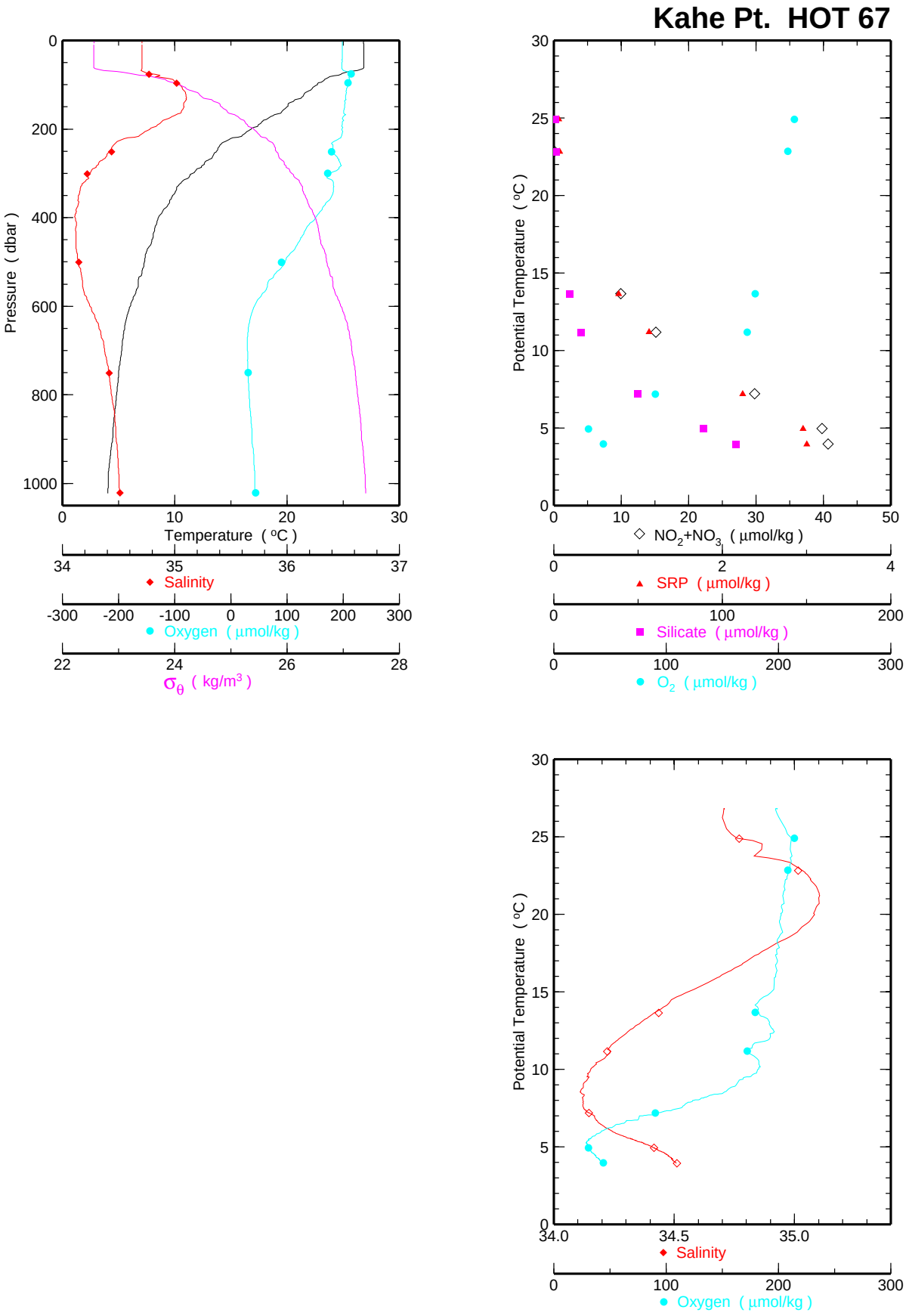
Kahe Pt. HOT 67
Pressure (dbar)
Temperature (°C)
Salinity
Oxygen (µmol/kg)
σθ (kg/m3)
Potential Temperature (°C)
NO2+NO3 (µmol/kg)
SRP (µmol/kg)
Silicate (µmol/kg)
O2 (µmol/kg)
Potential Temperature (°C)
Salinity
Oxygen (µmol/kg)

Figure 6.2.3h

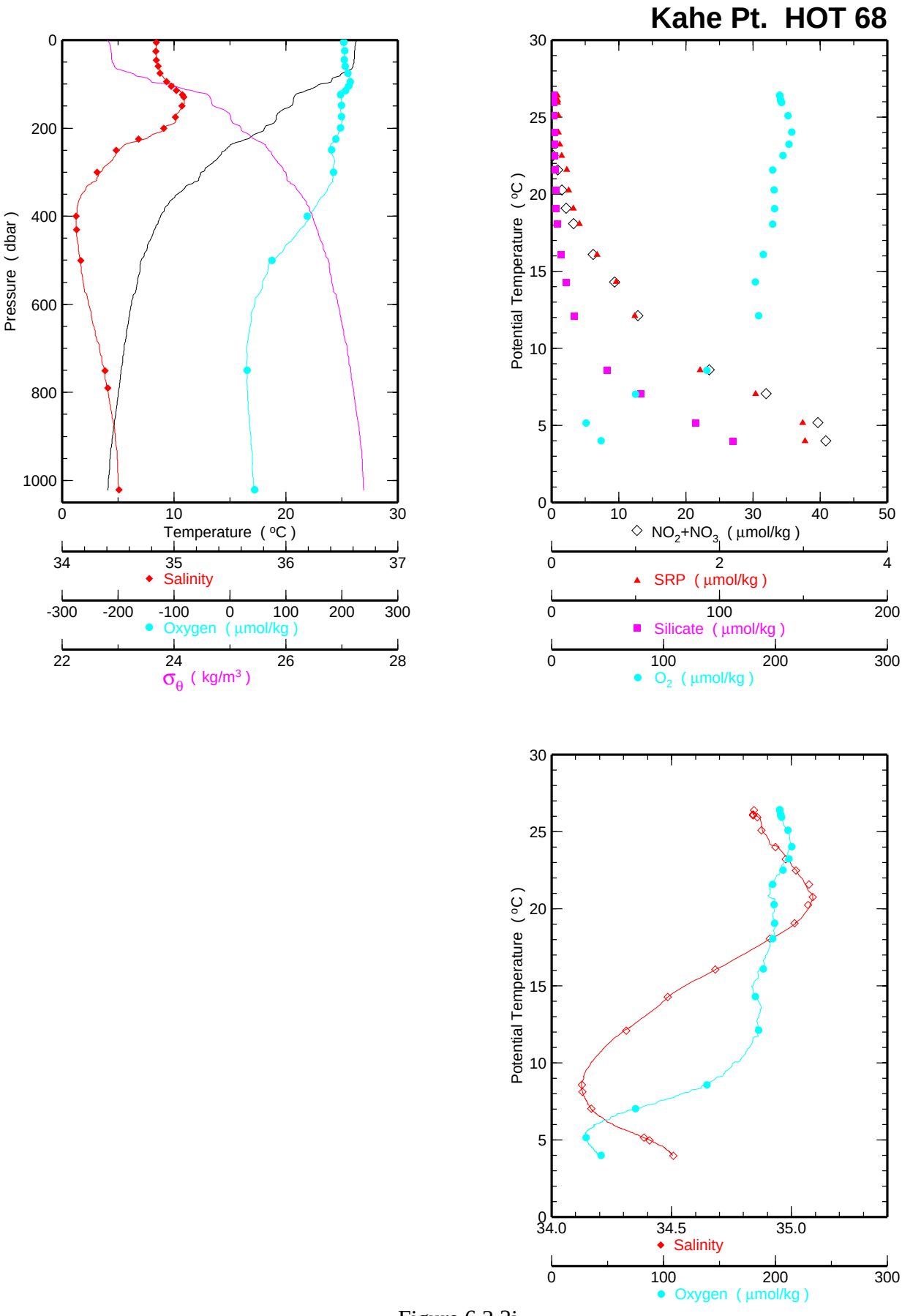
Kahe Pt. HOT 68
Pressure (dbar)
Temperature (ºC)
Salinity
Oxygen (µmol/kg)
σθ (kg/m³)
Potential Temperature (ºC)
NO2+NO3 (µmol/kg)
SRP (µmol/kg)
Silicate (µmol/kg)
O2 (µmol/kg)
Potential Temperature (ºC)
Salinity
Oxygen (µmol/kg)

Figure 6.2.3i

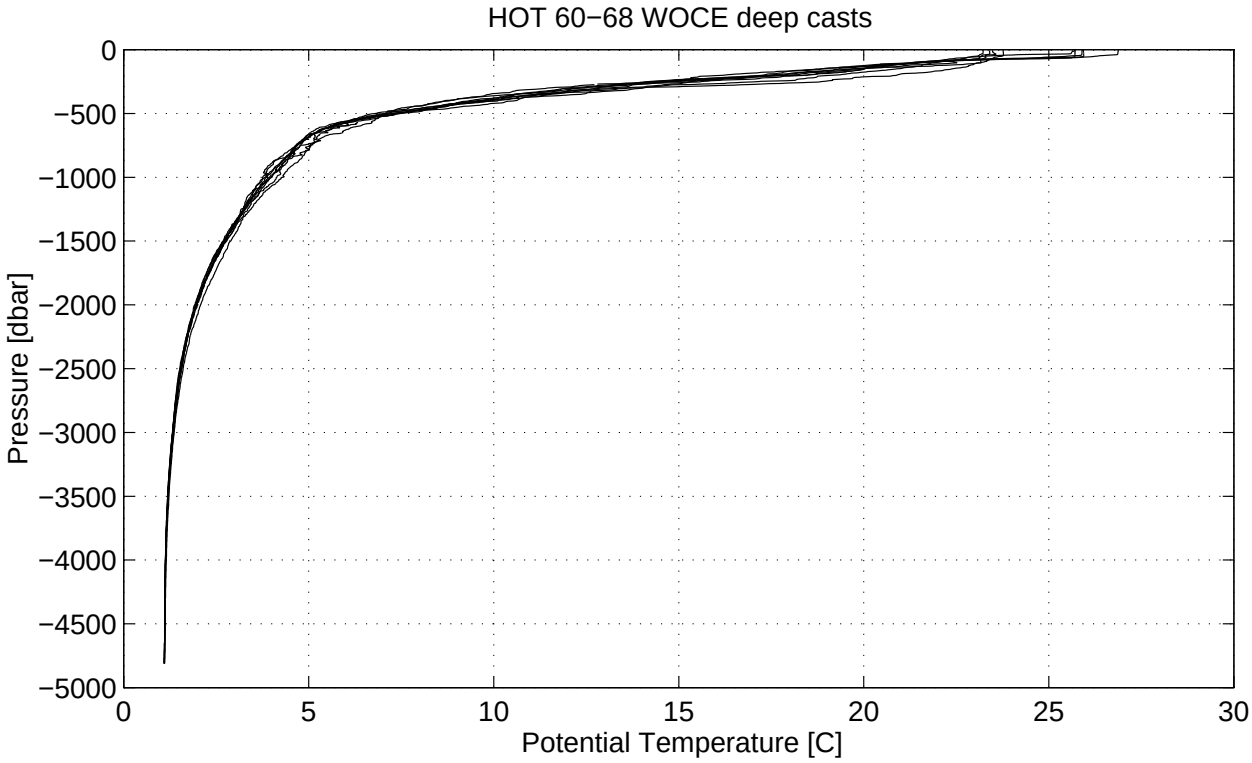
HOT 60−68 WOCE deep casts
Pressure [dbar]
Potential Temperature [C]
0
−500
−1000
−1500
−2000
−2500
−3000
−3500
−4000
−4500
−5000
0
5
10
15
20
25
30

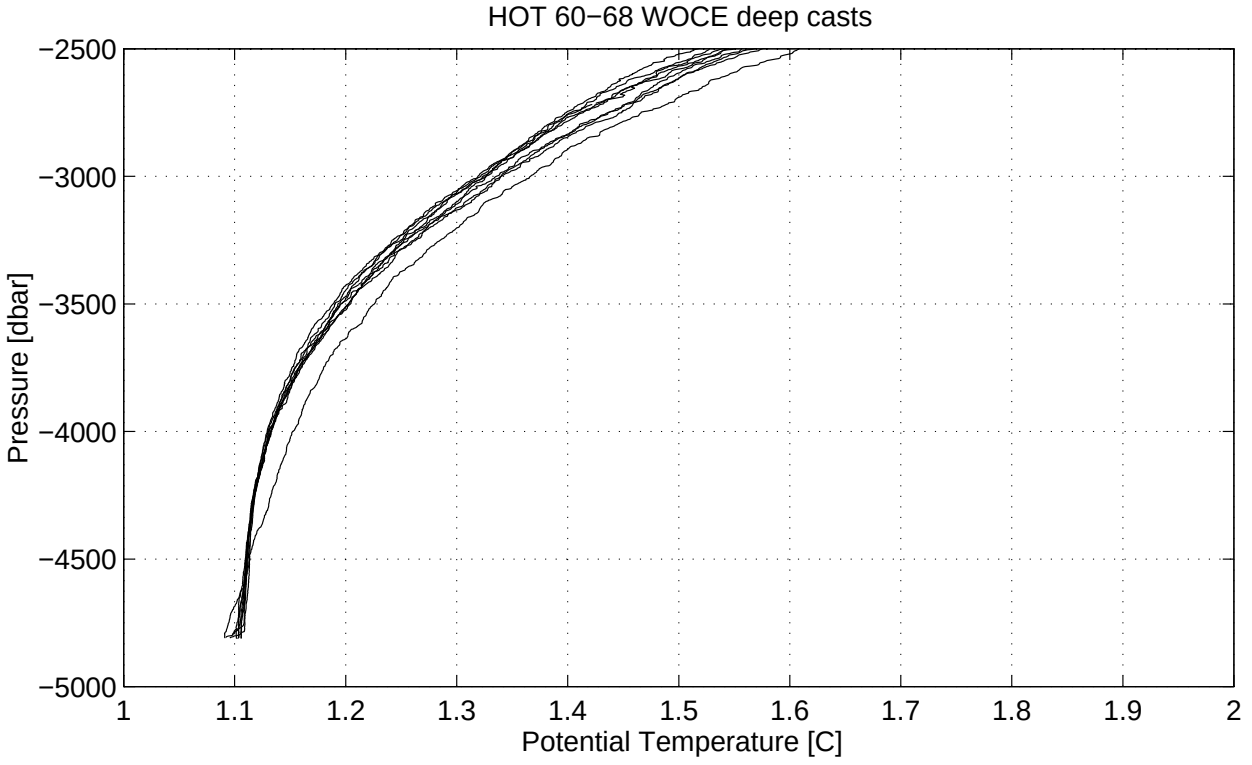
HOT 60−68 WOCE deep casts
Pressure [dbar]
Potential Temperature [C]
−2500
−3000
−3500
−4000
−4500
−5000
1
1.1
1.2
1.3
1.4
1.5
1.6
1.7
1.8
1.9
2

Figure 6.2.4

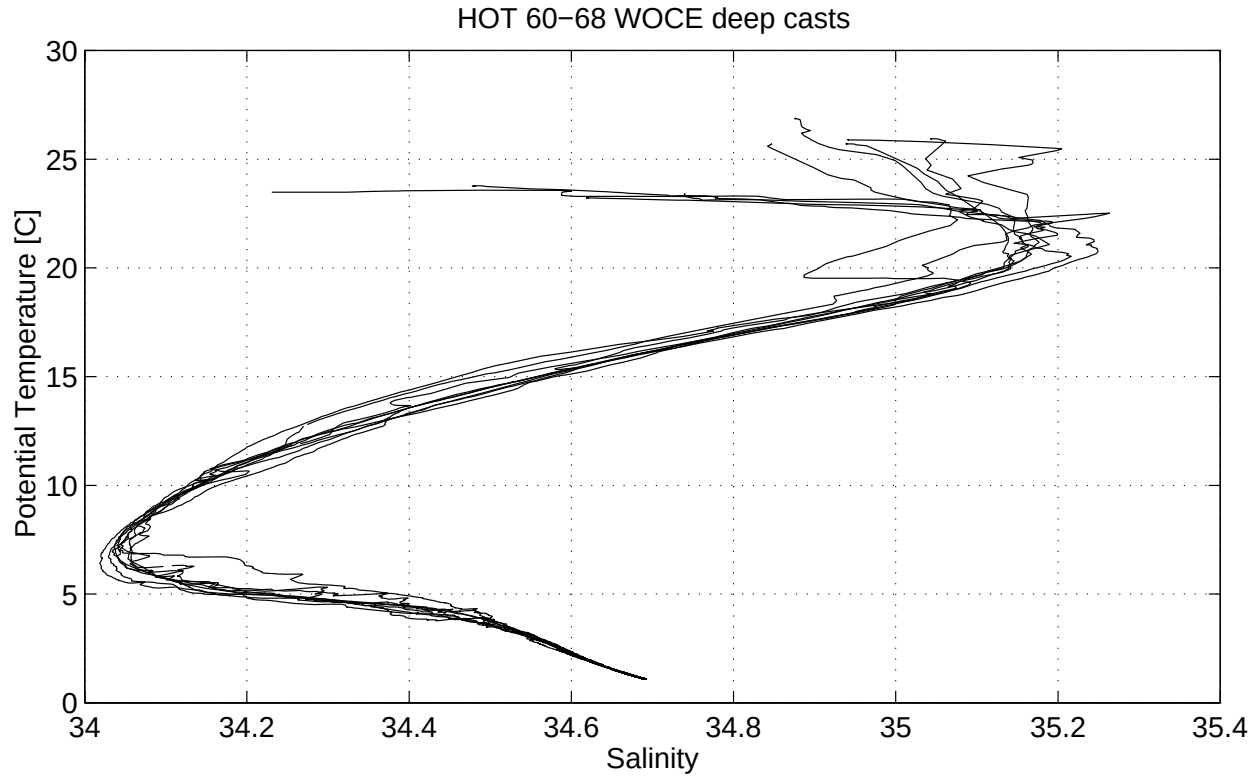
HOT 60−68 WOCE deep casts
Potential Temperature [C]
Salinity
30
25
20
15
10
5
0
34
34.2
34.4
34.6
34.8
35
35.2
35.4

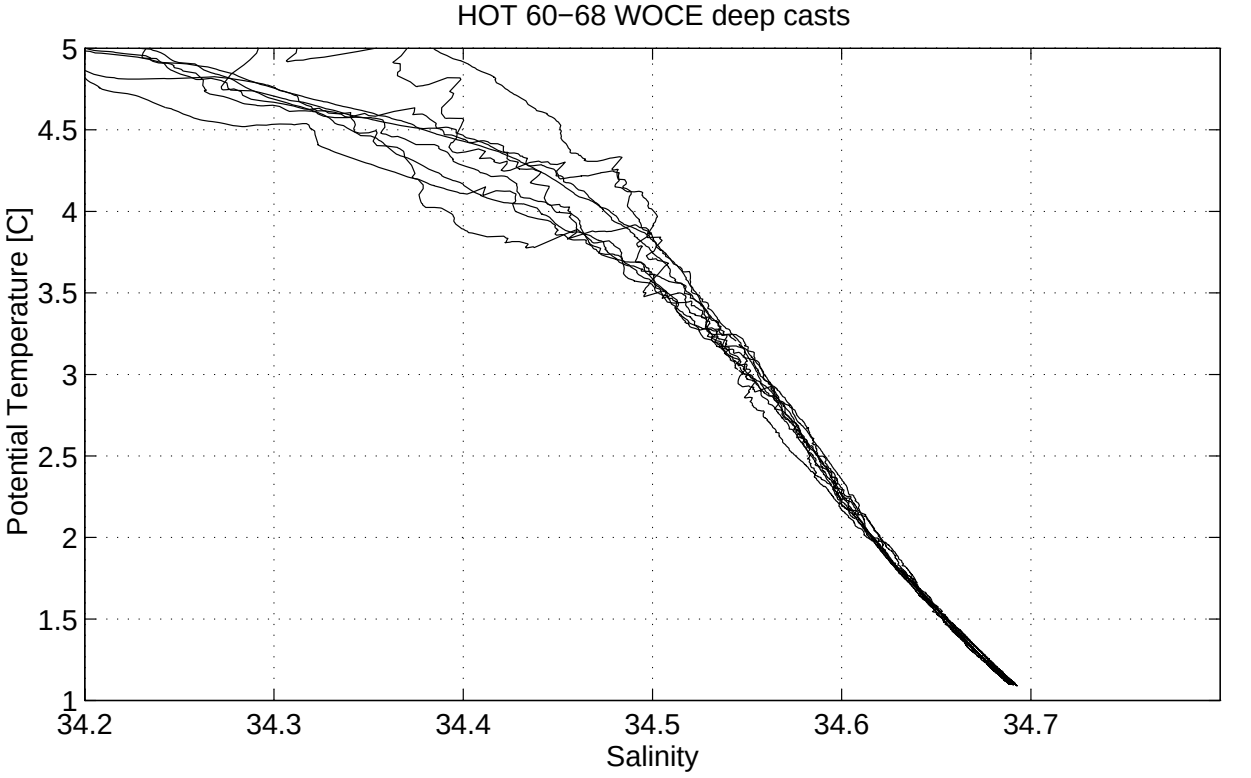
HOT 60−68 WOCE deep casts
Potential Temperature [C]
Salinity
5
4.5
4
3.5
3
2.5
2
1.5
1
34.2
34.3
34.4
34.5
34.6
34.7

Figure 6.2.5

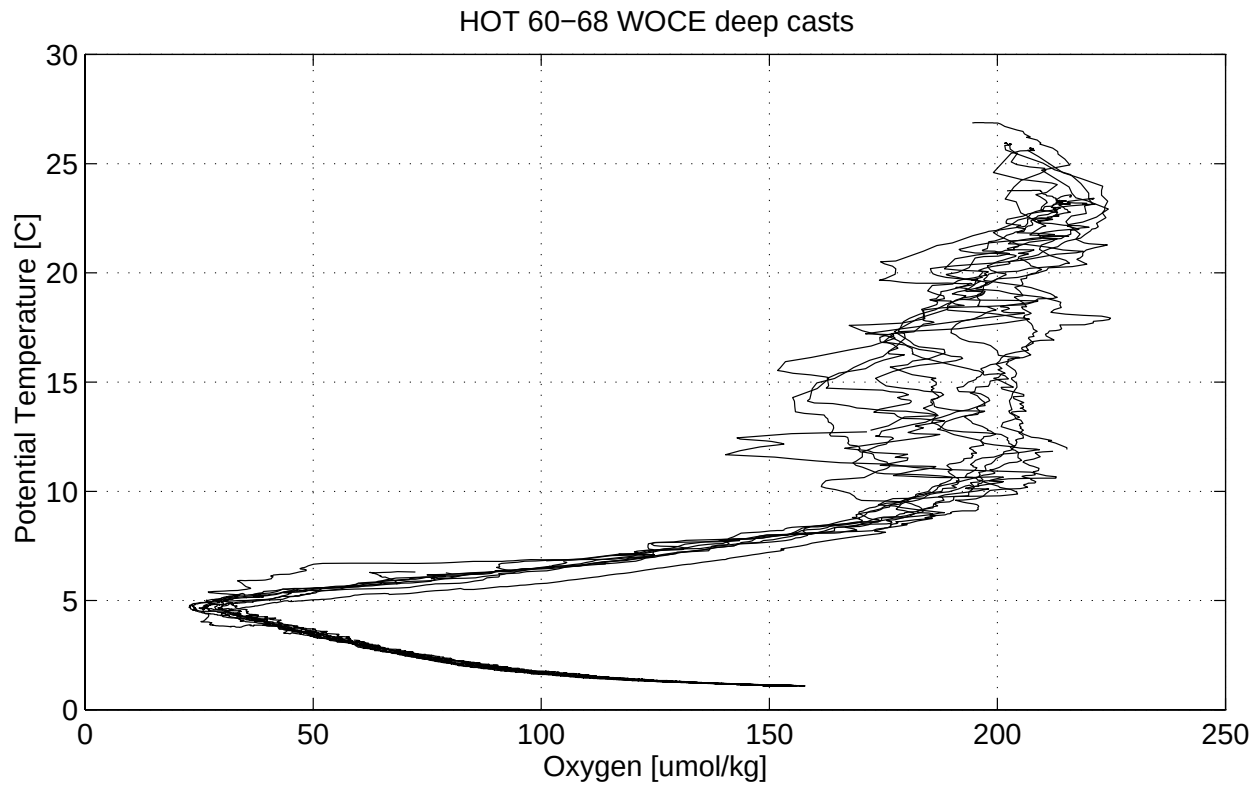
HOT 60−68 WOCE deep casts
Potential Temperature [C]
Oxygen [umol/kg]
0
5
10
15
20
25
30
0
50
100
150
200
250

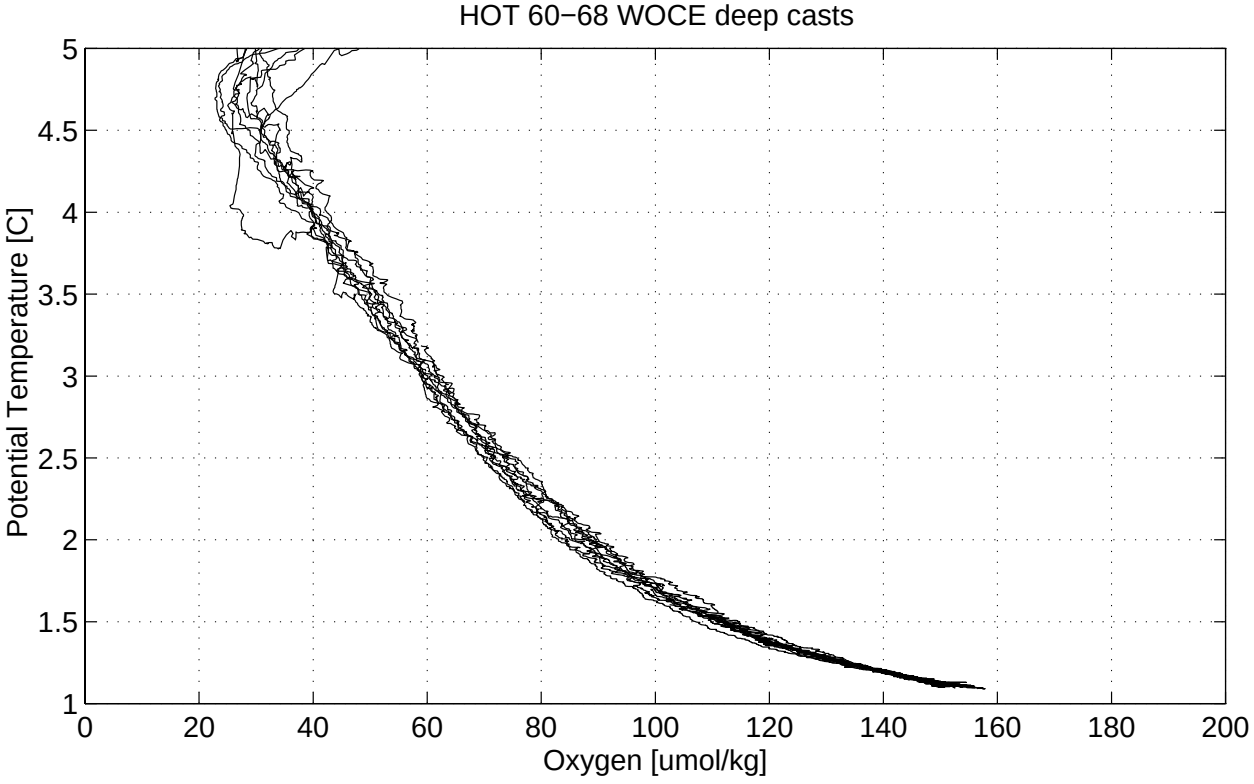
HOT 60−68 WOCE deep casts
Potential Temperature [C]
Oxygen [umol/kg]
1
1.5
2
2.5
3
3.5
4
4.5
5
0
20
40
60
80
100
120
140
160
180
200

Figure 6.2.6

6.3. Contour Plots

Figures 6.3.1 to 14 show data from HOT-1 to 68. Cruise is indicated by a diamond symbol along the time axis. Data are the average of all casts for each cruise.

Figure 6.3.1: Potential temperature measured by CTD versus pressure.

Figure 6.3.2: Potential density (σ_θ), calculated from CTD measurements of pressure, temperature and salinity versus pressure.

Figure 6.3.3: Salinity measured by CTD plotted versus pressure.

Figure 6.3.4: Salinity measured by CTD versus potential density (σ_θ). The average density of the sea surface for each cruise is connected by a heavy line.

Figure 6.3.5: Salinity from discrete water samples plotted versus pressure. Locations of bottle closures are indicated by solid circles.

Figure 6.3.6: Salinity from discrete water samples plotted versus potential density (σ_θ). The average density of the sea surface for each cruise is connected by a heavy line. Locations of bottle closures are indicated by solid circles.

Figure 6.3.7: Oxygen from discrete water samples plotted versus pressure. Locations of bottle closures are indicated by solid circles.

Figure 6.3.8: Oxygen from discrete water samples plotted versus potential density (σ_θ). The average density of the sea surface for each cruise is connected by a heavy line. Locations of bottle closures are indicated by solid circles.

Figure 6.3.9: [Nitrate+nitrite] from discrete water samples plotted versus pressure. Locations of bottle closures are indicated by solid circles.

Figure 6.3.10: [Nitrate+nitrite] from discrete water samples plotted versus potential density (σ_θ). The average density of the sea surface for each cruise is connected by a heavy line. Locations of bottle closures are indicated by solid circles.

Figure 6.3.11: Soluble reactive phosphorus from discrete water samples plotted versus pressure. Locations of bottle closures are indicated by solid circles.

Figure 6.3.12: Soluble reactive phosphorus from discrete water samples plotted versus potential density (σ_θ). The average density of the sea surface for each cruise is connected by a heavy line. Locations of bottle closures are indicated by solid circles.

Figure 6.3.13: Silica from discrete water samples plotted versus pressure. Locations of bottle closures are indicated by solid circles.

Figure 6.3.14: Silica from discrete water samples plotted versus potential density (σ_θ). The average density of the sea surface for each cruise is connected by a heavy line. Locations of bottle closures are indicated by solid circles.

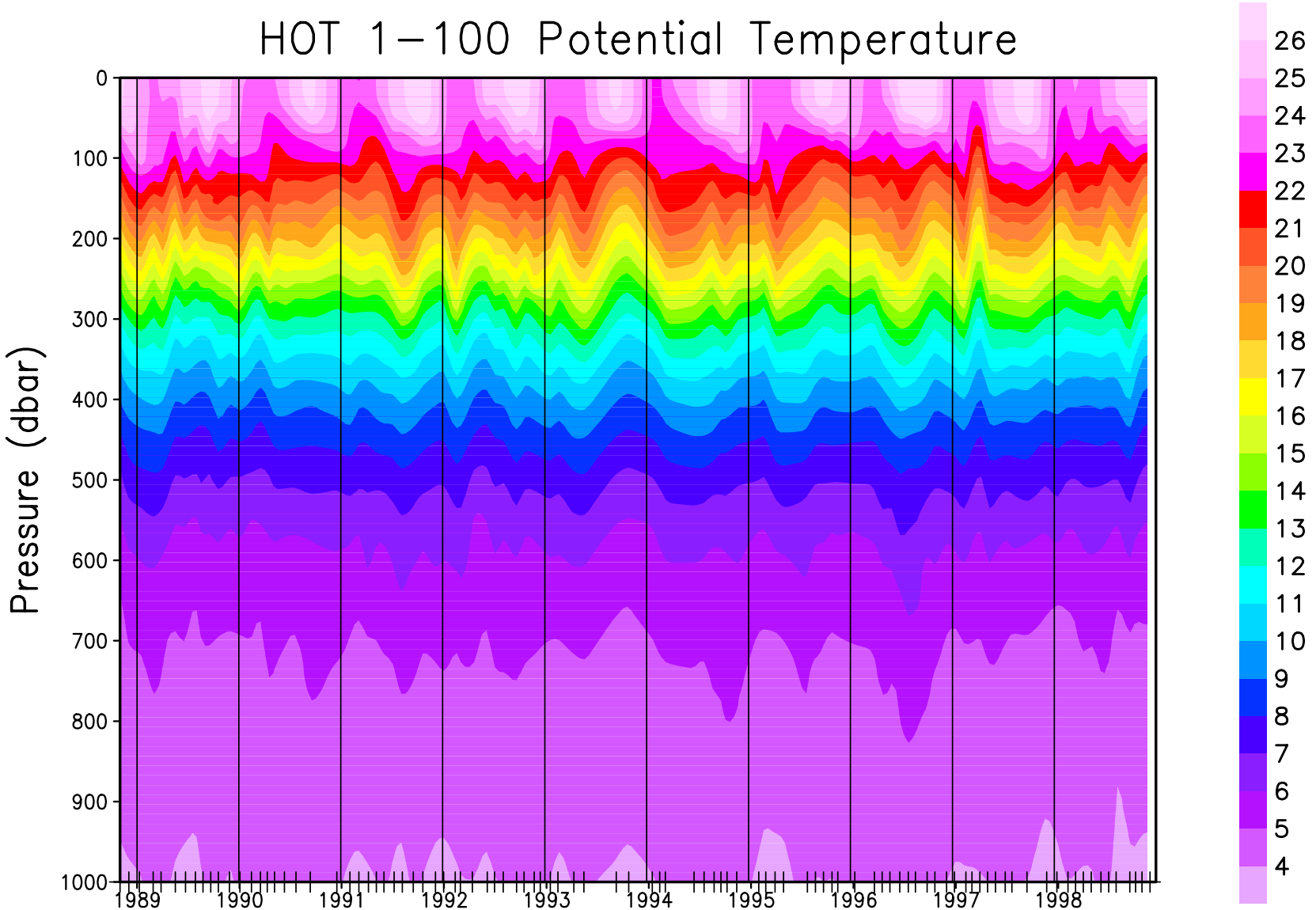

Figure 6.3.1: Contour plot of CTD potential temperature versus pressure

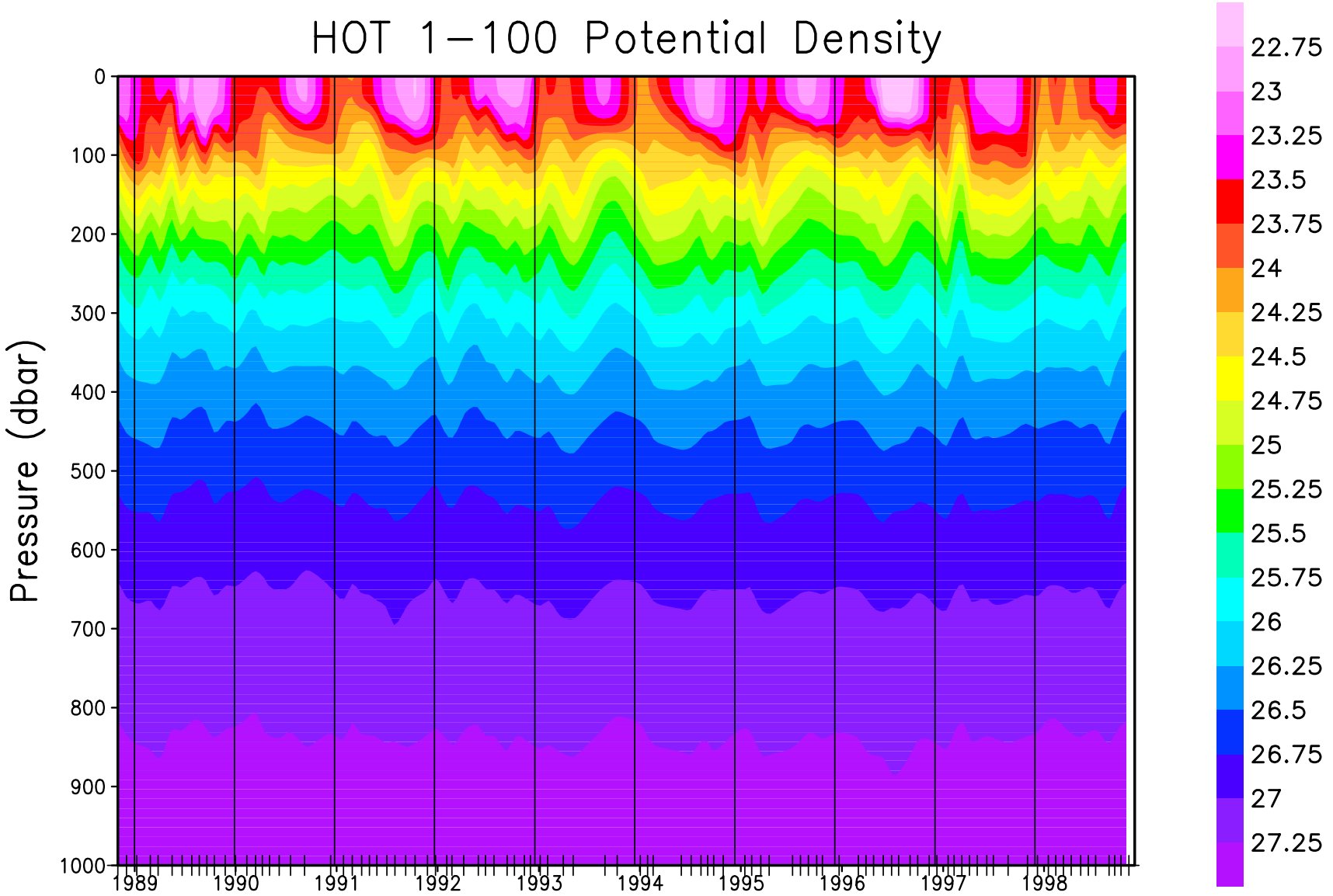

Figure 6.3.2: Contour plot of potential density (σ_θ), calculated from CTD pressure, temperature and salinity, versus pressure for HOT cruises 1-100.

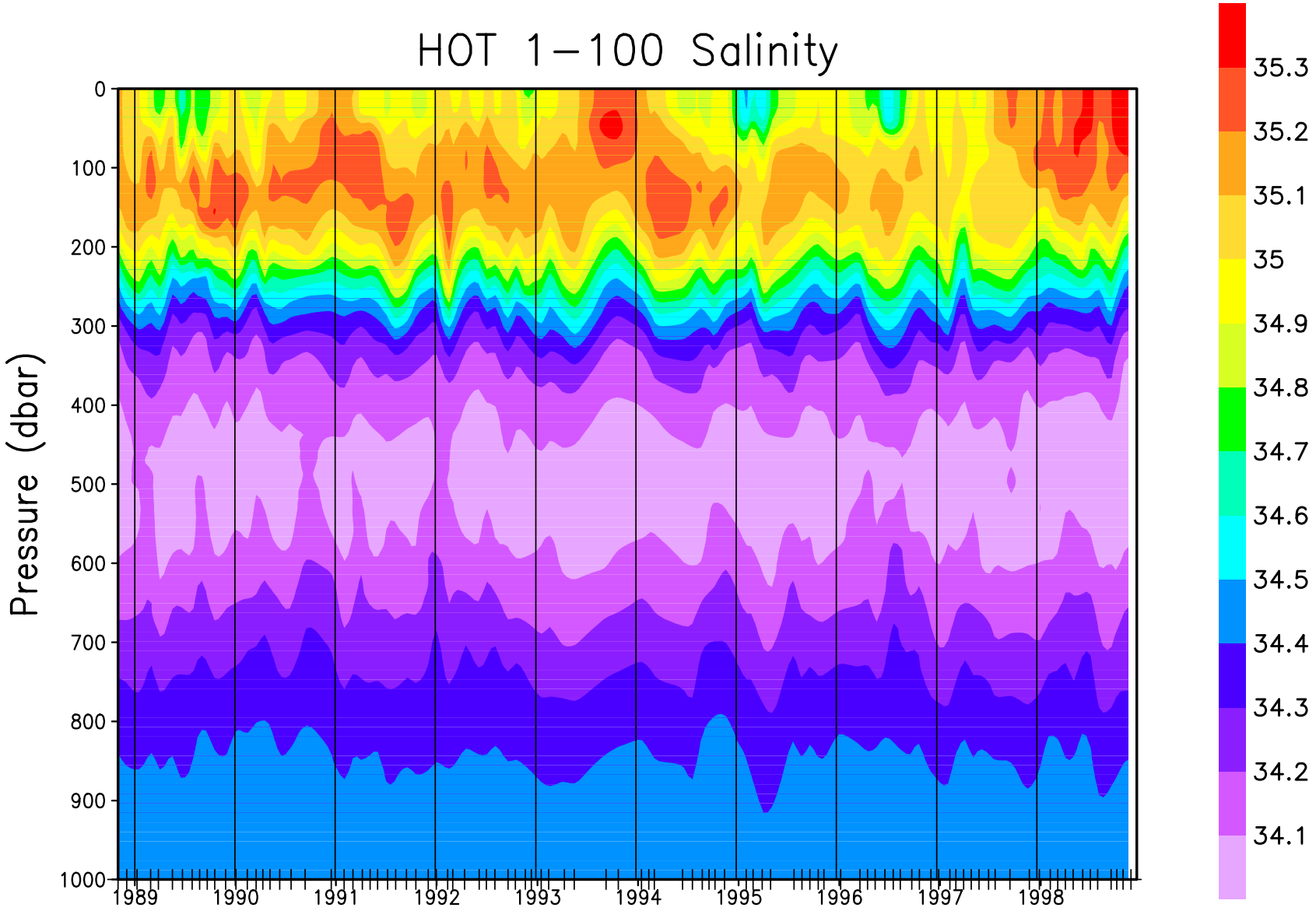

Figure 6.3.3: Contour plot of CTD salinity versus pressure for HOT cruises 1-

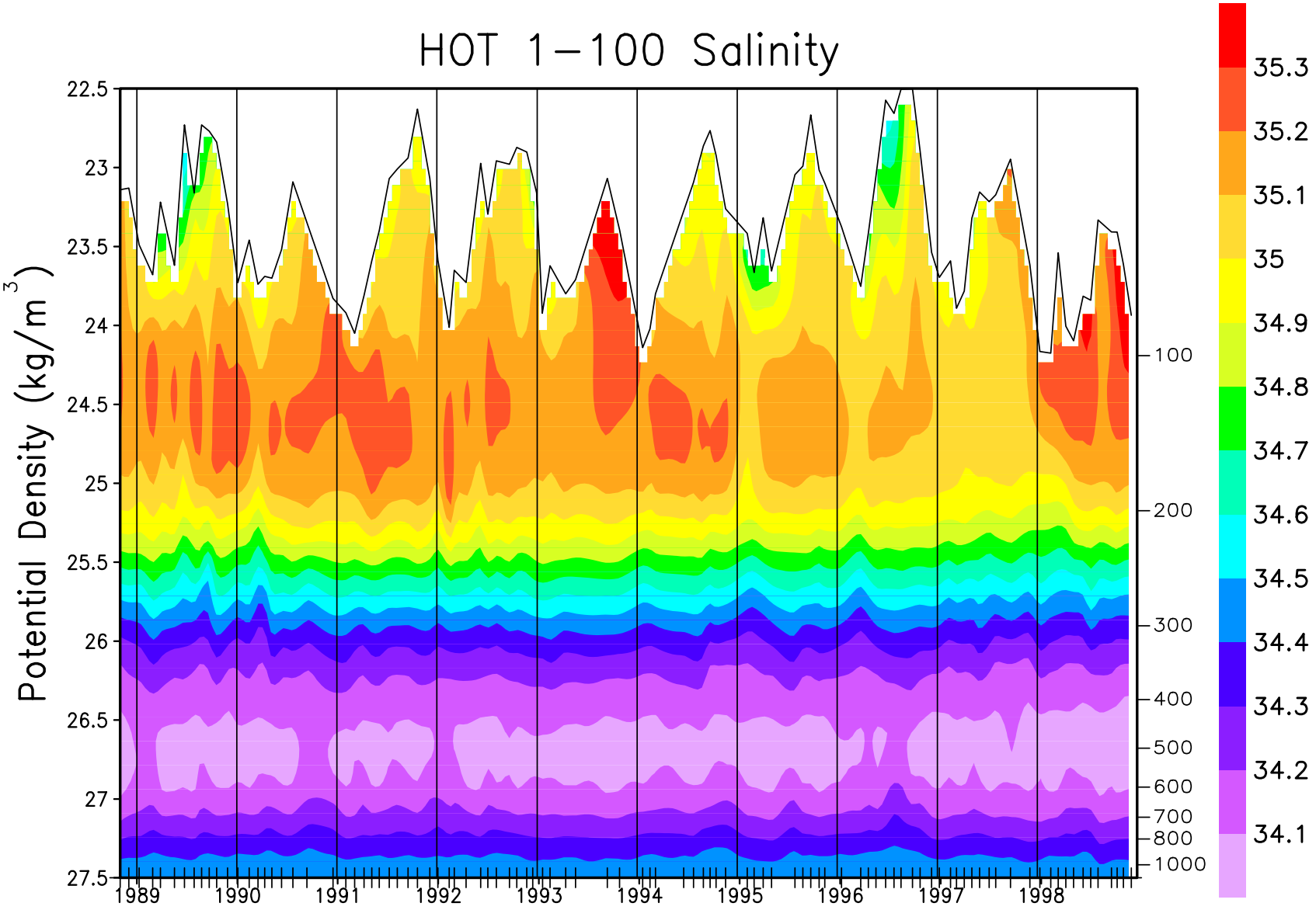

Figure 6.3.4: Contour plot of CTD salinity versus potential density (σ_θ) to 27.5 kg m^{-3} for HOT cruises 1-100. The average density of the sea surface is connected by the heavy line.

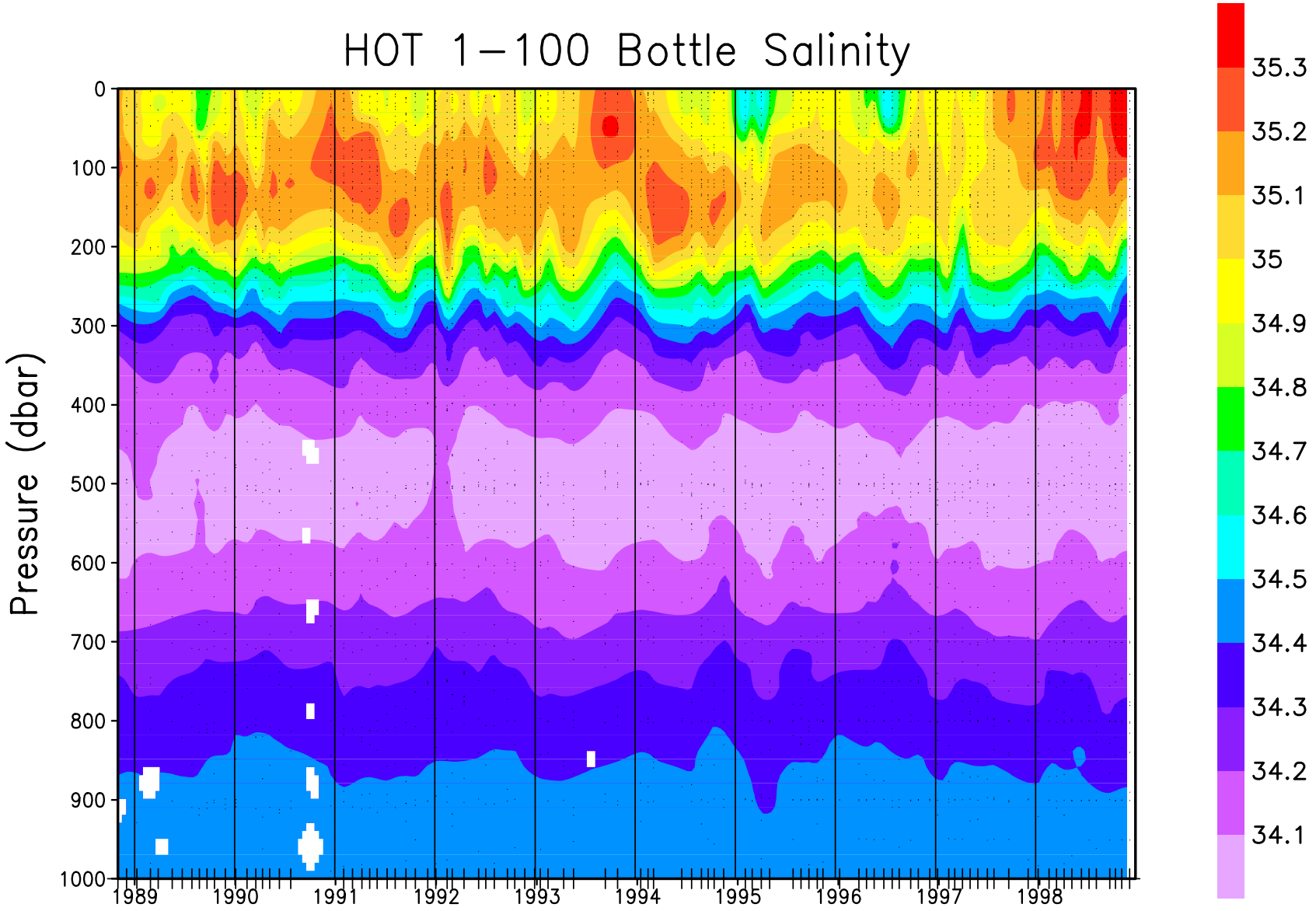

Figure 6.3.5: Contour plot of bottle salinity versus pressure for HOT cruises 1-100. Location of samples in the water column are indicated by the solid circles.

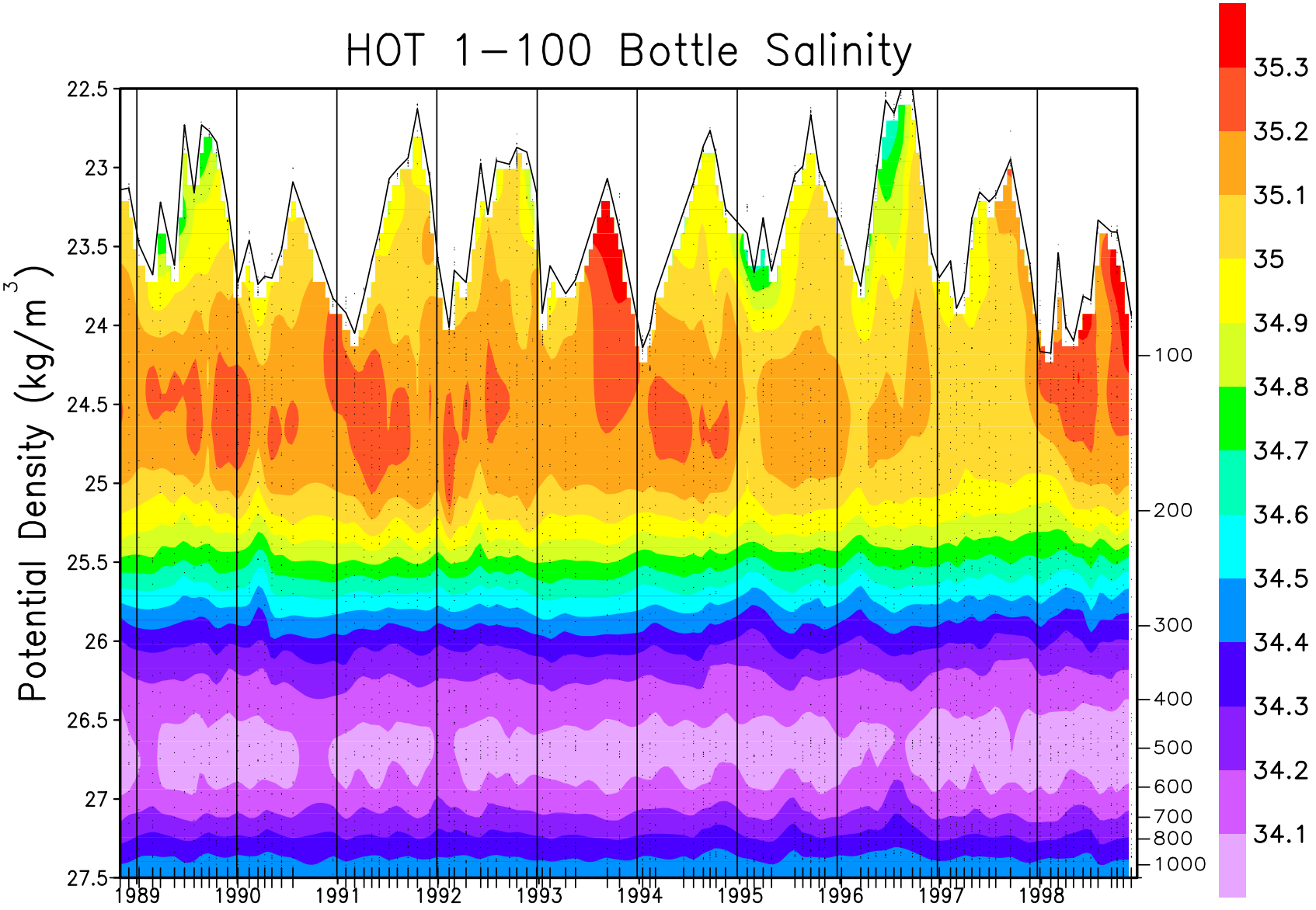

Figure 6.3.6: Contour plot of bottle salinity versus potential density (σ_θ)to 27.5 kg m^{-3} for HOT cruises 1-100. The average density of the sea surface is connected by the heavy line.

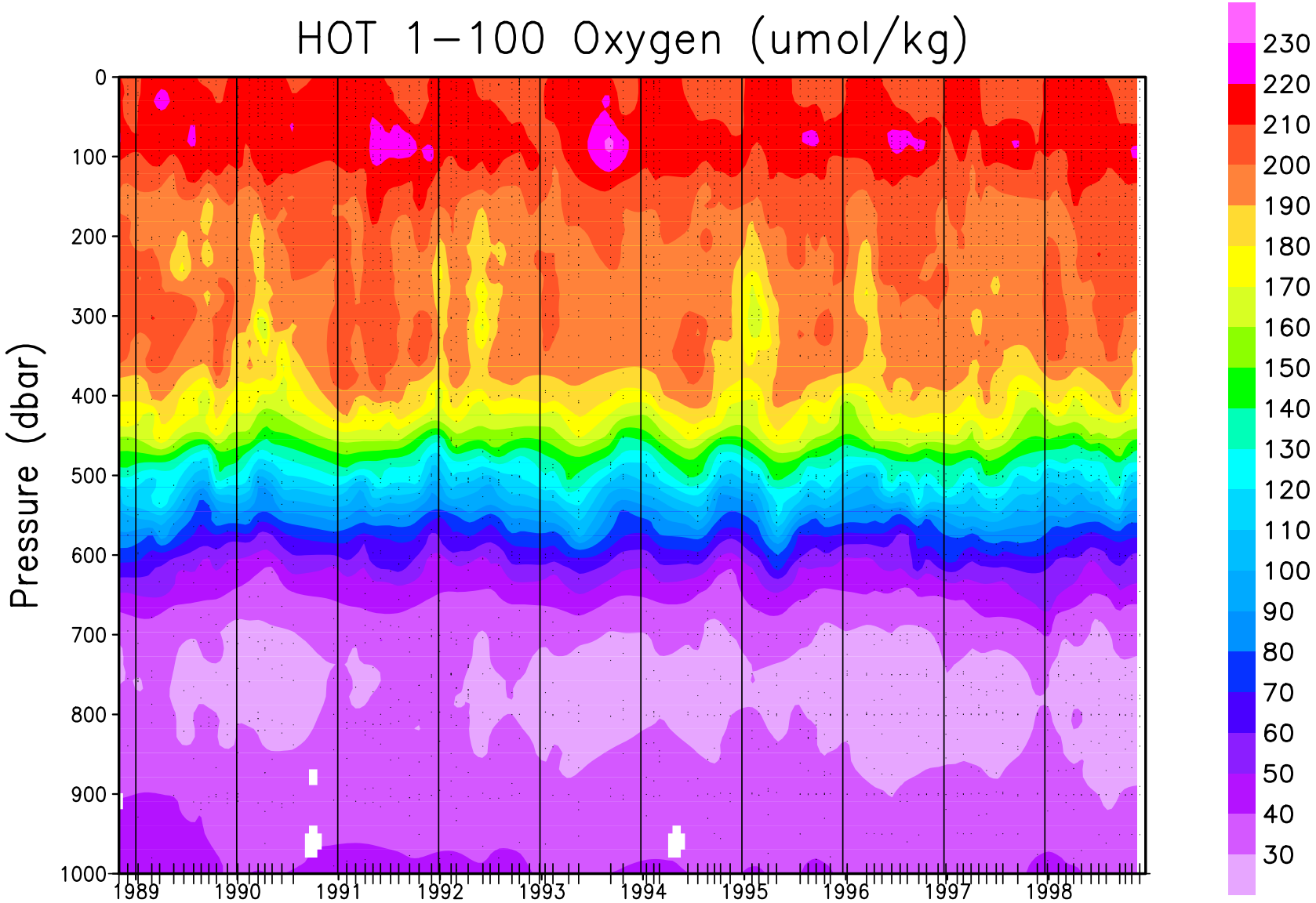

Figure 6.3.7: Contour plot of bottle oxygen versus pressure for HOT cruises 1-100. Location of samples in the water column are indicated by the solid circles.

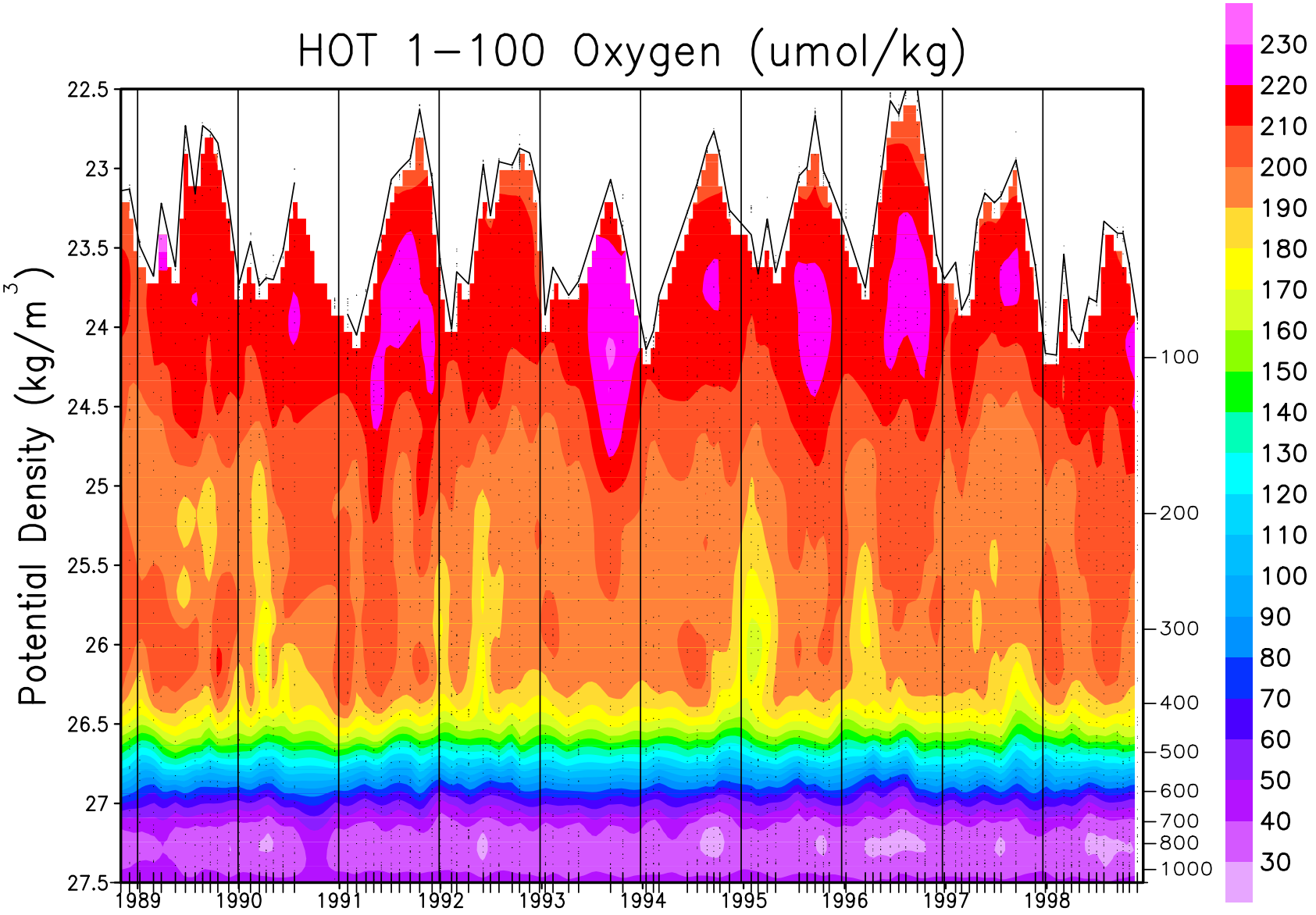

Figure 6.3.8: Contour plot of bottle oxygen versus potential density (σ_θ) to 27.5 kg m^{-3} for HOT cruises 1-100. The average density of the sea surface is connected by the heavy line.

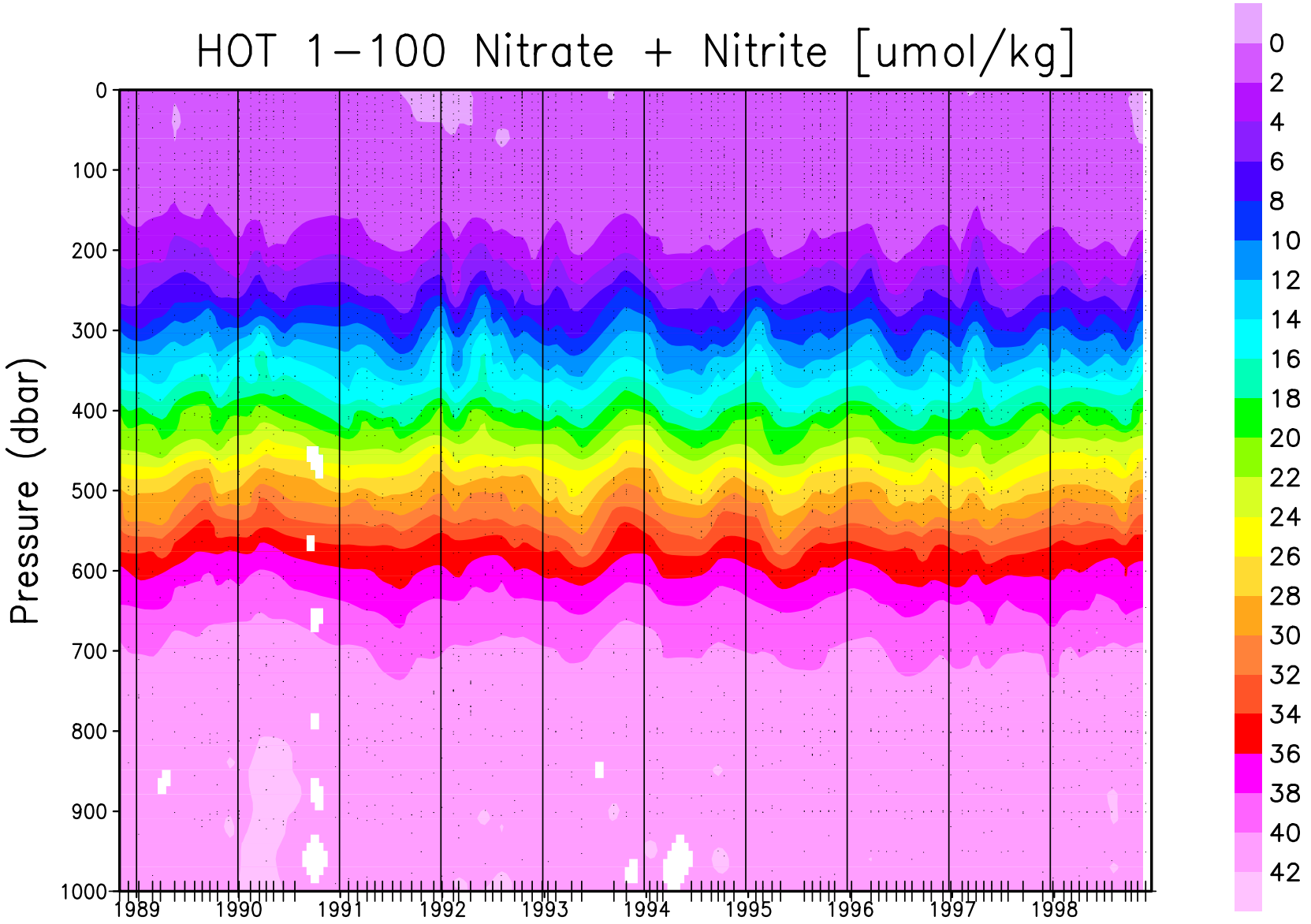

Figure 6.3.9: Contour plot of [nitrate + nitrite] versus pressure for HOT cruises 1-100. Location of samples in the water column are indicated by the solid circles.

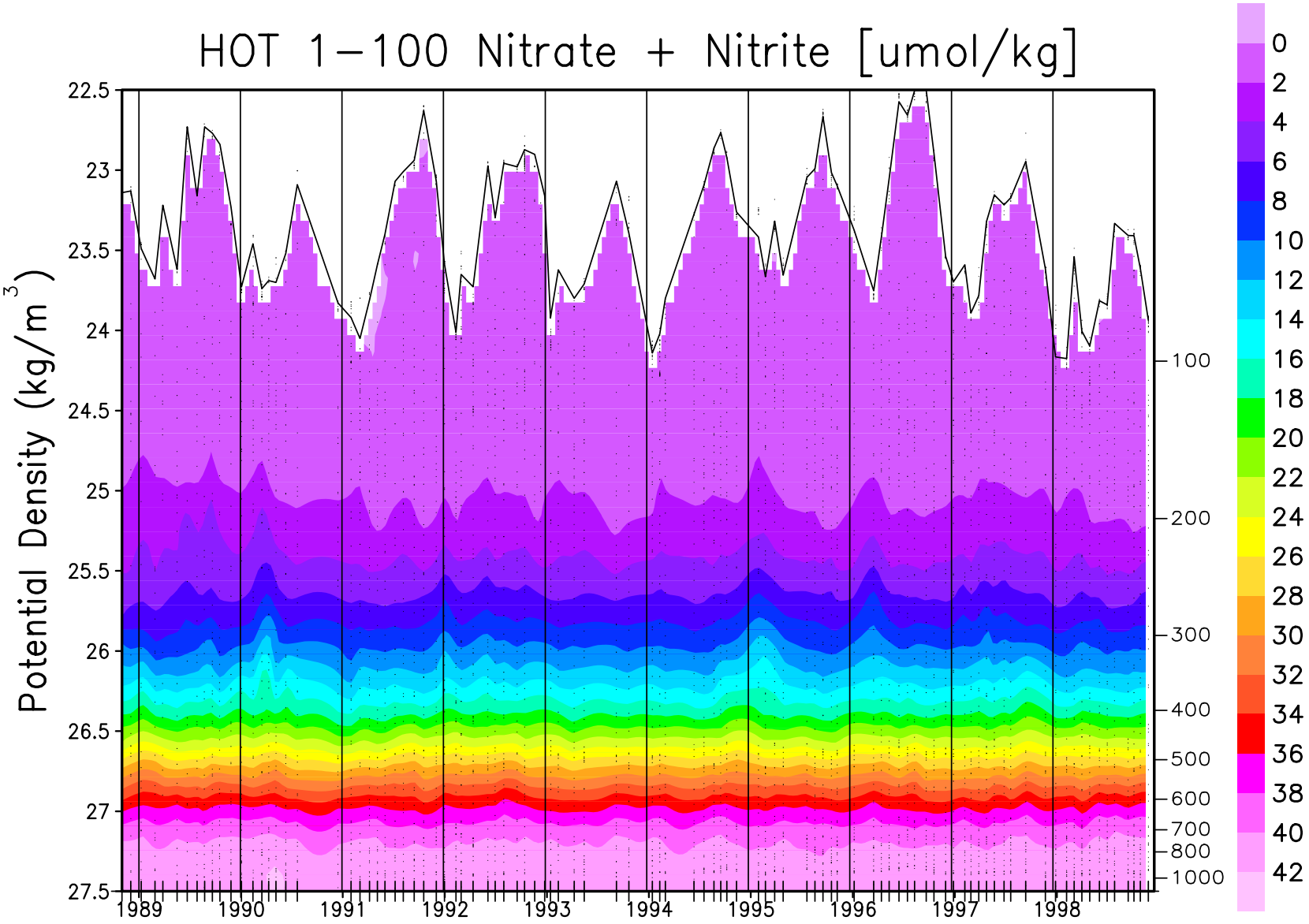

Figure 6.3.10: Contour plot of [nitrate + nitrite] versus potential density (σ_θ) to 27.5 kg m^{-3} for HOT cruises 1-100. The average density of the sea surface is connected by the heavy line.

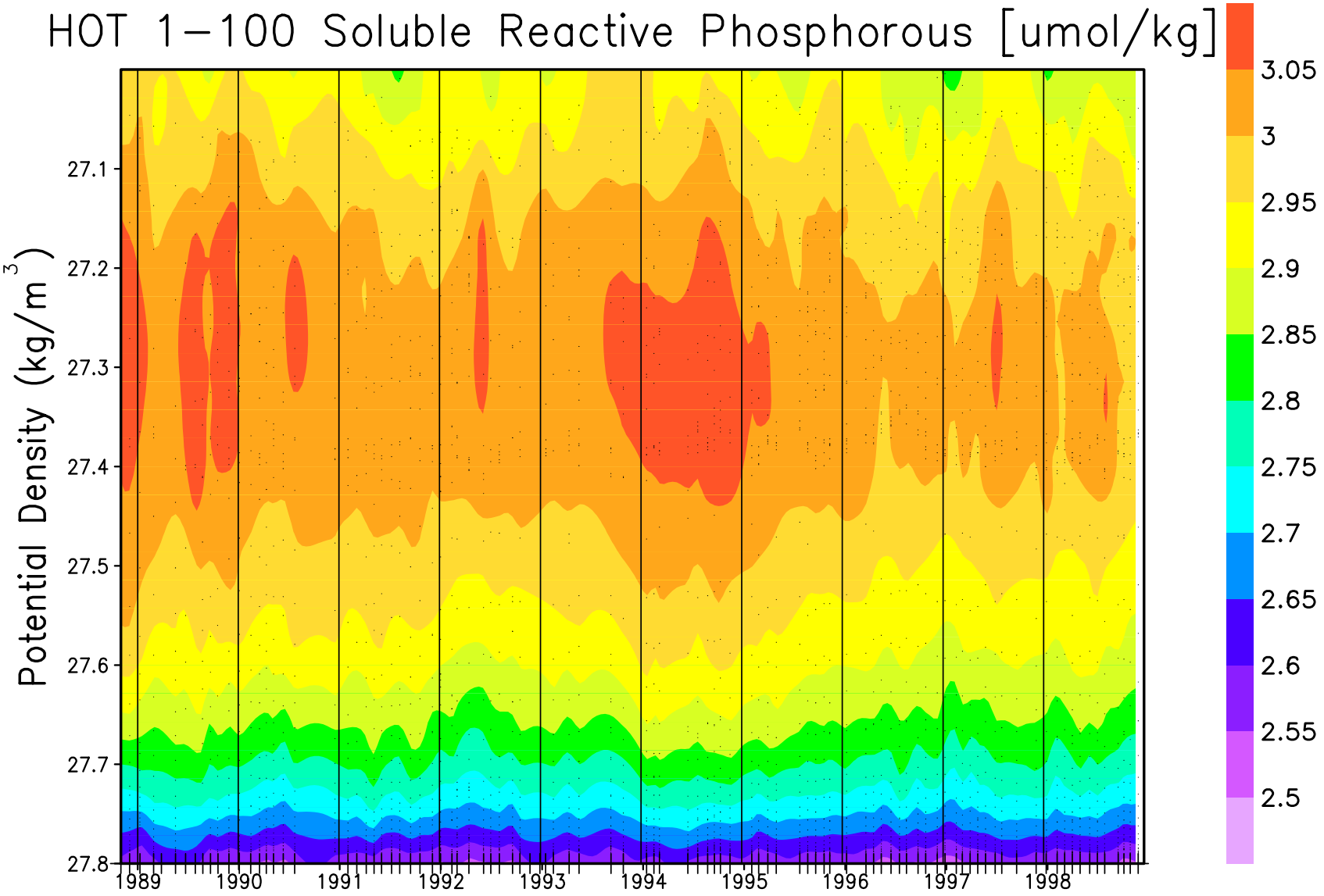

Figure 6.3.11: Contour plot of soluble reactive phosphate versus pressure for HOT cruises 1-100. Location of samples in the water column are indicated by the solid circles.

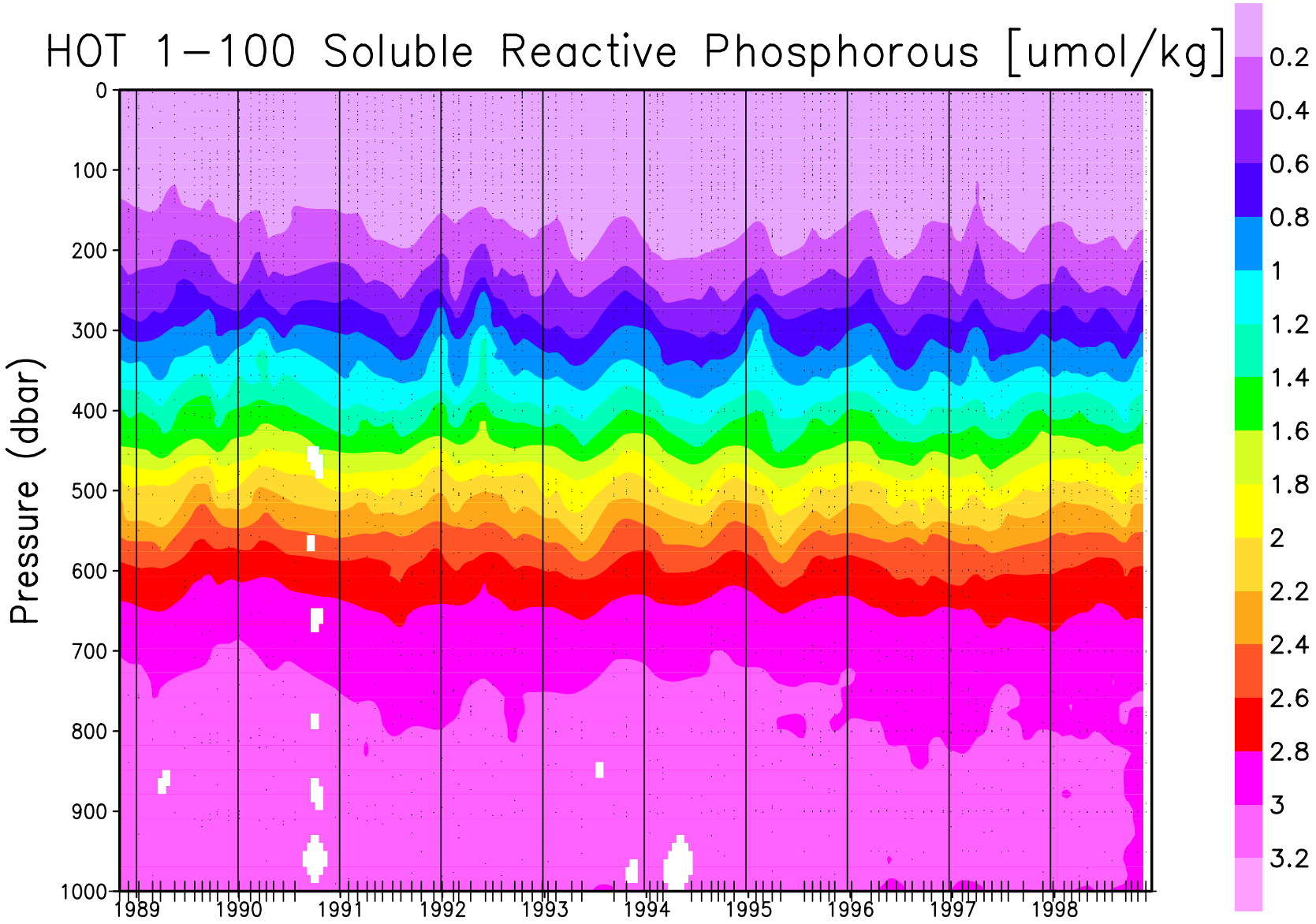

Figure 6.3.12: Contour plot of soluble reactive phosphate versus potential density (σ_θ) to 27.5 kg m^{-3} for HOT cruises 1-100. The average density of the sea surface is connected by the heavy line.

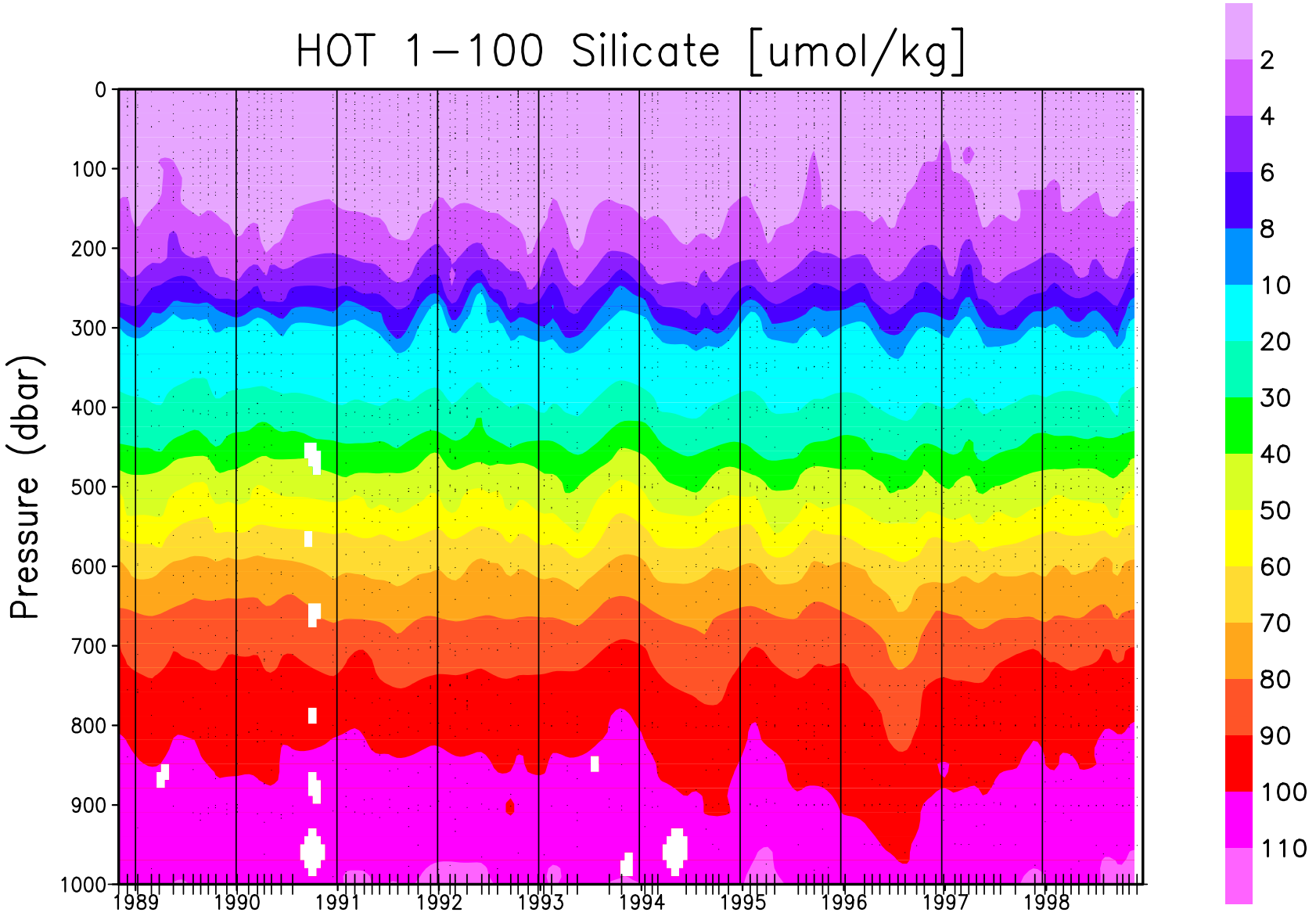

Figure 6.3.13: Contour plot of silicate versus pressure for HOT cruises 1-100. Location of samples in the water column are indicated by the solid circles.

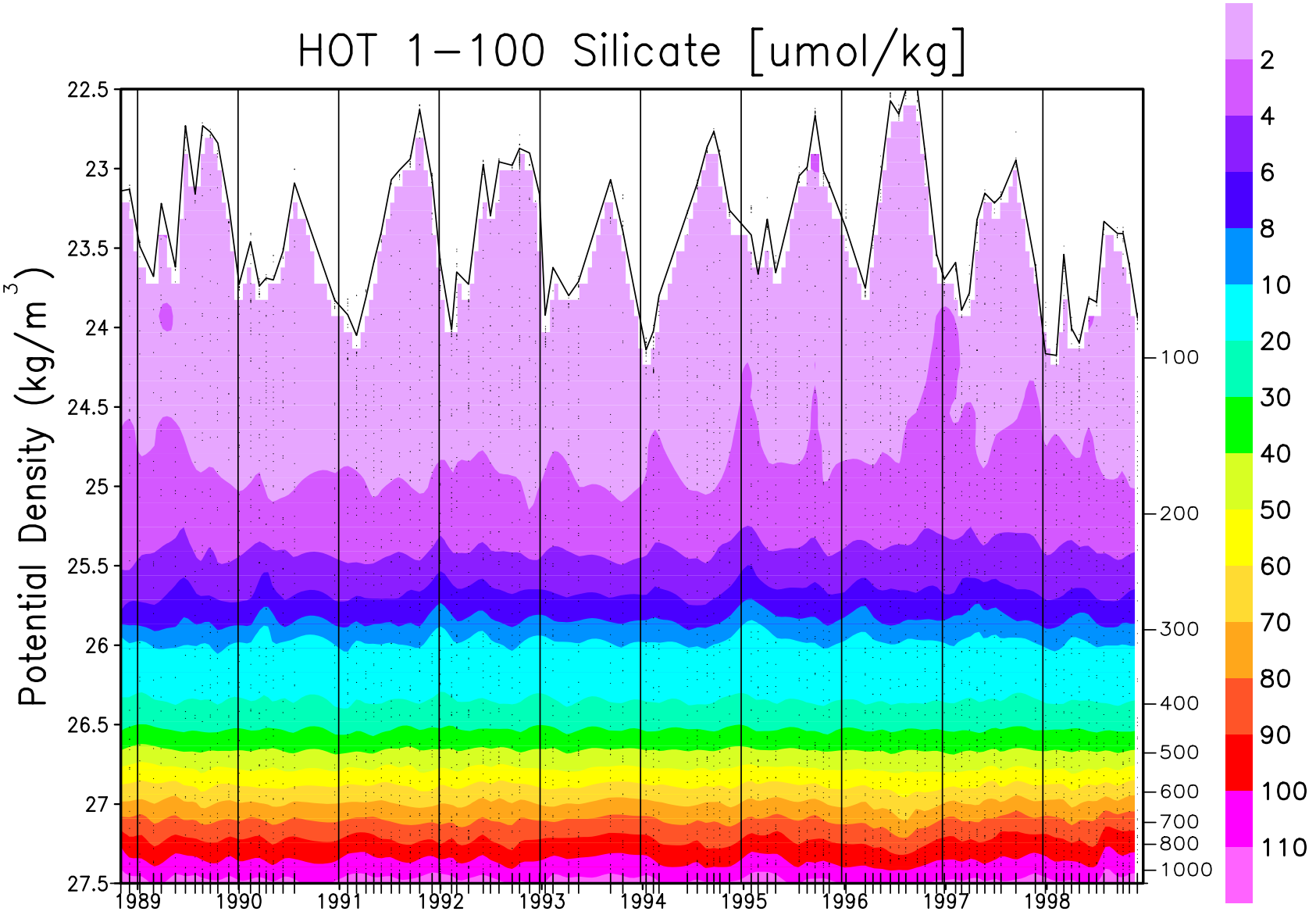

Figure 6.3.14: Contour plot of silicate versus potential density (σ_θ) to 27.5 kg m^{-3} for HOT cruises 1-100. The average density of the sea surface is connected by the heavy line.

6.4. Flash Fluorescence and Beam Transmission

Figures 6.4.1 to 6.4.9: Stack plots of flash fluorescence and beam transmission (when available) collected at Station ALOHA on HOT-60 to HOT-68. Upper two panels show flash fluorescence data collected on each cruise plotted versus pressure to 250 dbar and potential density at 26 σ_θ. Offset is 20 mvolts. Lower two panels show % transmittance data collected on each cruise plotted versus pressure to 250 dbar and potential density at 26 σ_θ. Offset is 33%.

Figure 6.4.10: Stack plots of averaged night-time fluorescence profiles plotted versus pressure to 250 dbar collected on each HOT cruise from 1988 through 1995. The HOT cruise number is shown at the top of each panel.

Figure 6.4.11: As in 6.4.10, except profiles are plotted versus potential density at 26 σ_θ.

Figure 6.4.12: Stack plots of averaged beam transmission profiles collected in 1991-1995 plotted versus pressure to 250 dbar. The HOT cruise number is shown at the top of each panel.

Figure 6.4.13: As in 6.4.12, except profiles are plotted versus potential density at 26 σ_θ.

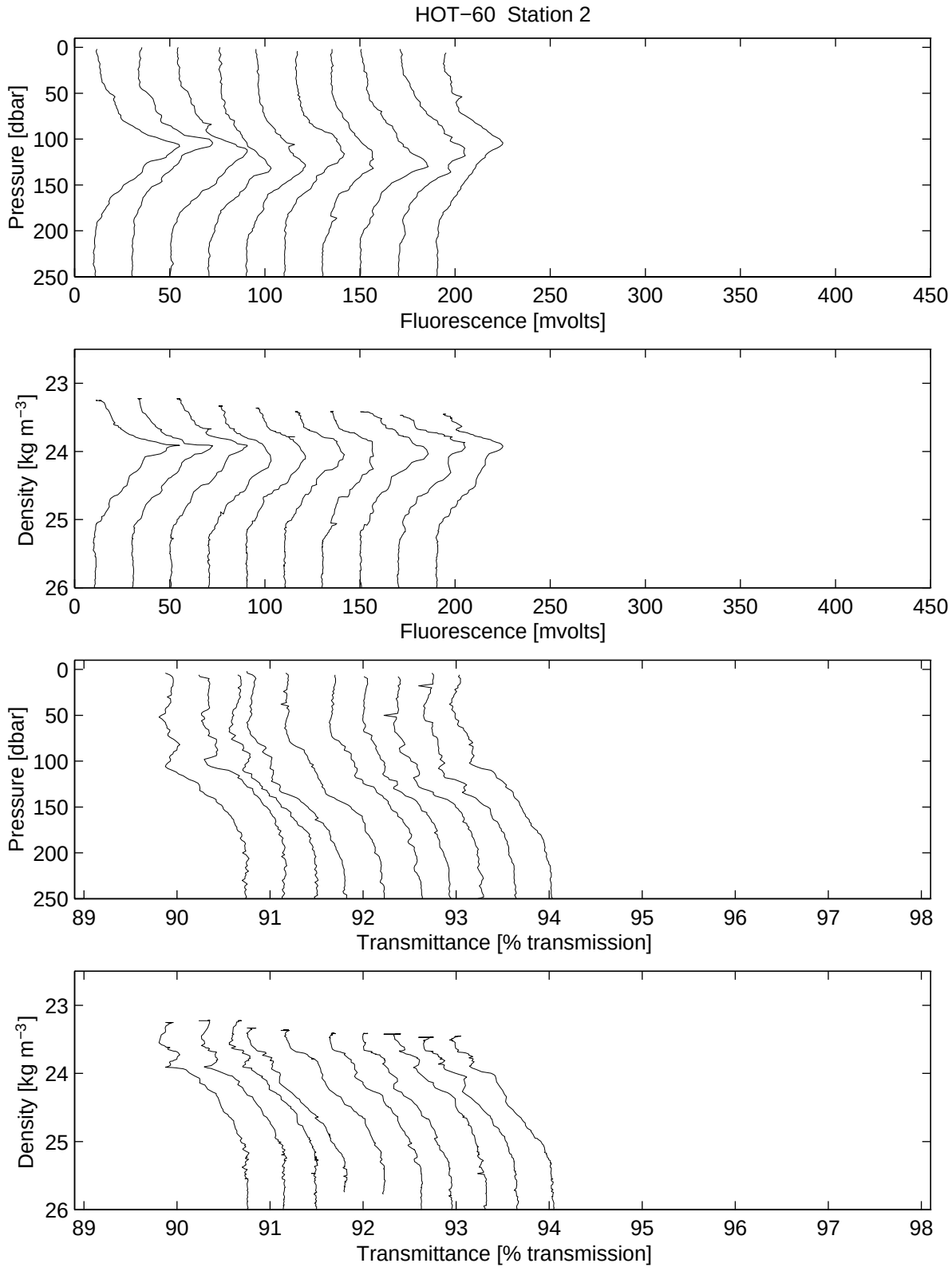
HOT−60 Station 2
Pressure [dbar]
Fluorescence [mvolts]
Density [kg m^{-3}]
Fluorescence [mvolts]
Pressure [dbar]
Transmittance [% transmission]
Density [kg m^{-3}]
Transmittance [% transmission]

Figure 6.4.1

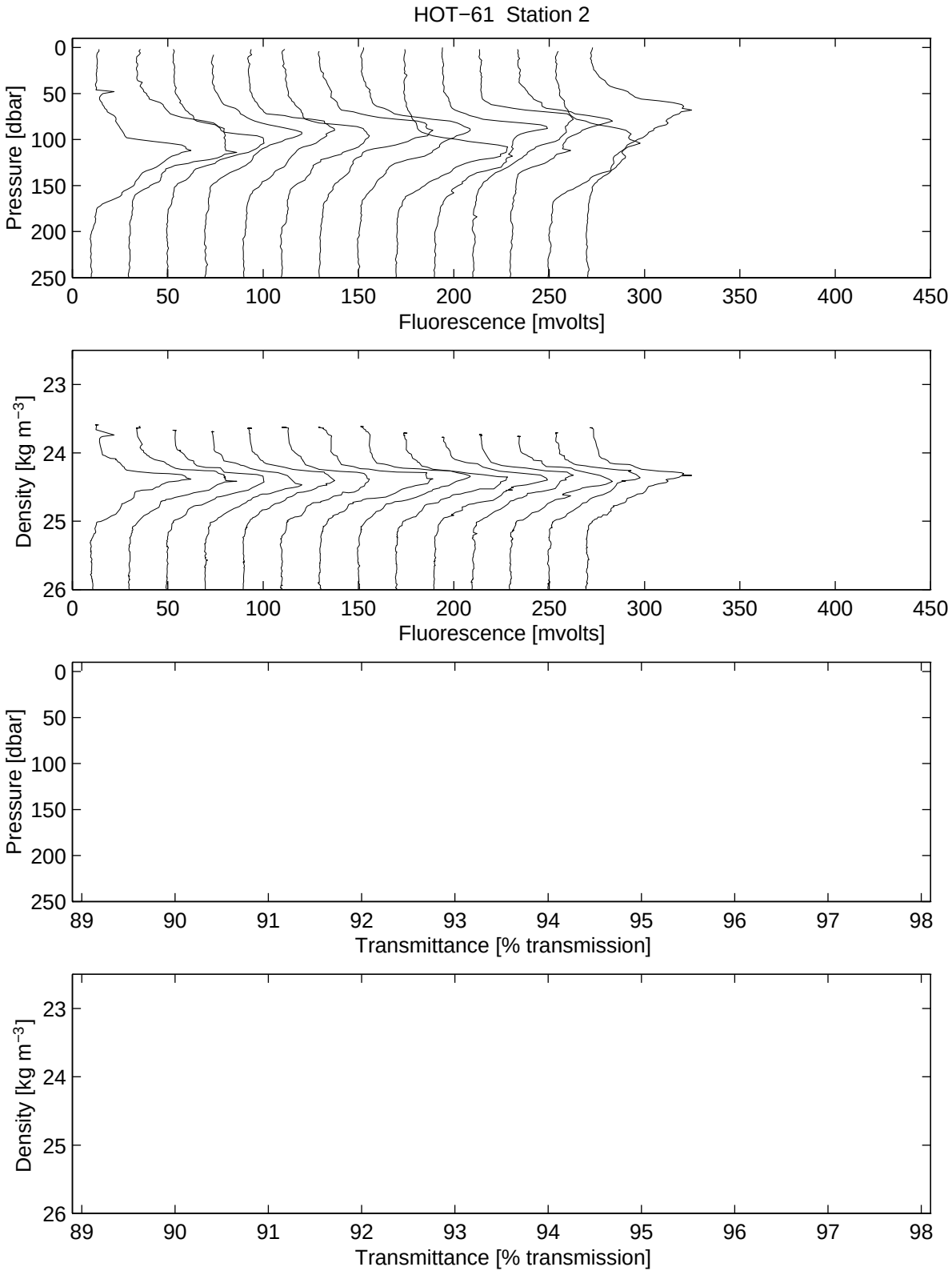
HOT−61 Station 2
Pressure [dbar]
Fluorescence [mvolts]
Density [kg m^{-3}]
Fluorescence [mvolts]
Pressure [dbar]
Transmittance [% transmission]
Density [kg m^{-3}]
Transmittance [% transmission]

Figure 6.4.2

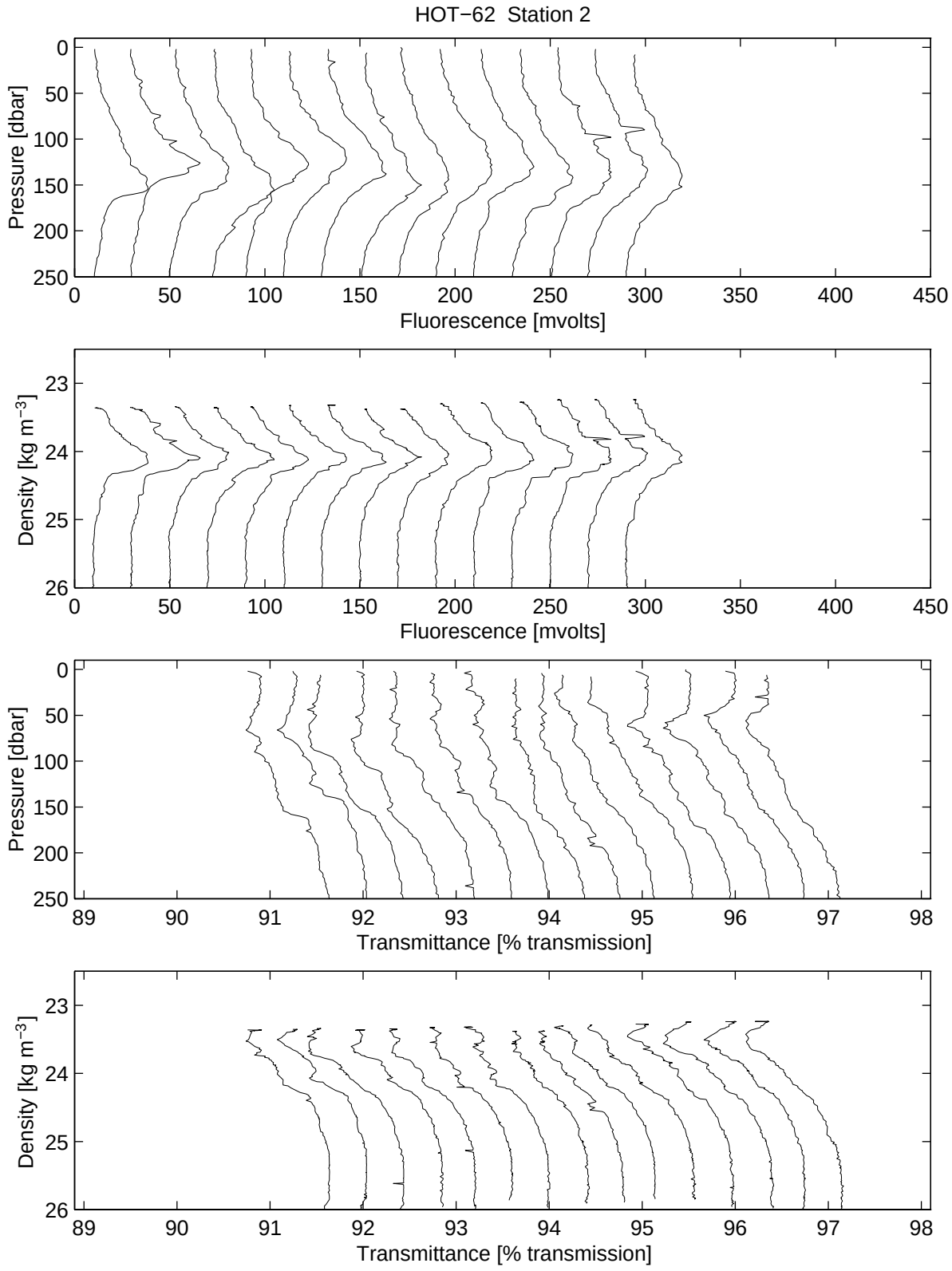
HOT−62 Station 2
Pressure [dbar]
Fluorescence [mvolts]
Density [kg m−3]
Fluorescence [mvolts]
Pressure [dbar]
Transmittance [% transmission]
Density [kg m−3]
Transmittance [% transmission]

Figure 6.4.3

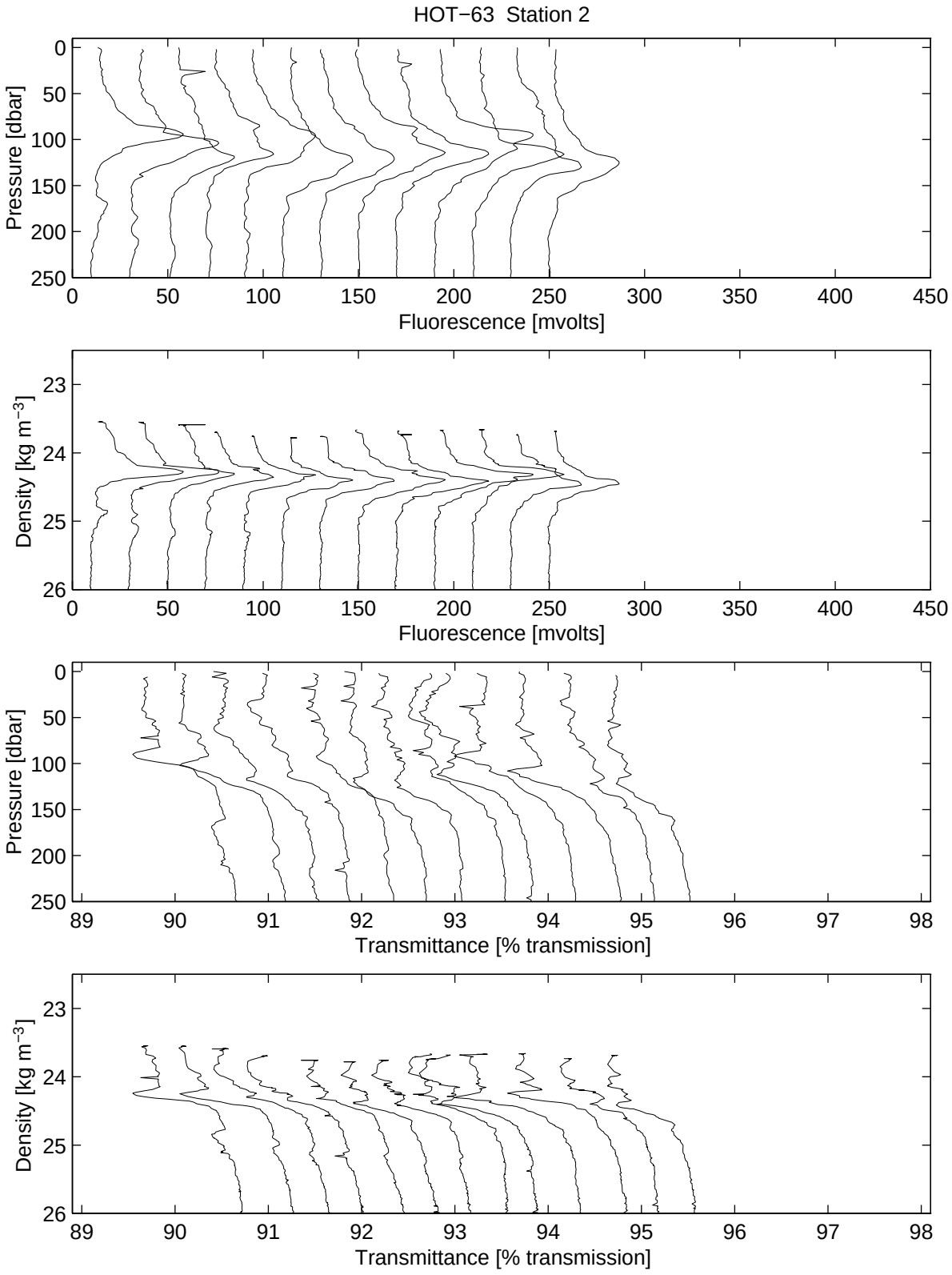
HOT−63 Station 2
Pressure [dbar]
Fluorescence [mvolts]
Density [kg m^{-3}]
Fluorescence [mvolts]
Pressure [dbar]
Transmittance [% transmission]
Density [kg m^{-3}]
Transmittance [% transmission]

Figure 6.4.4

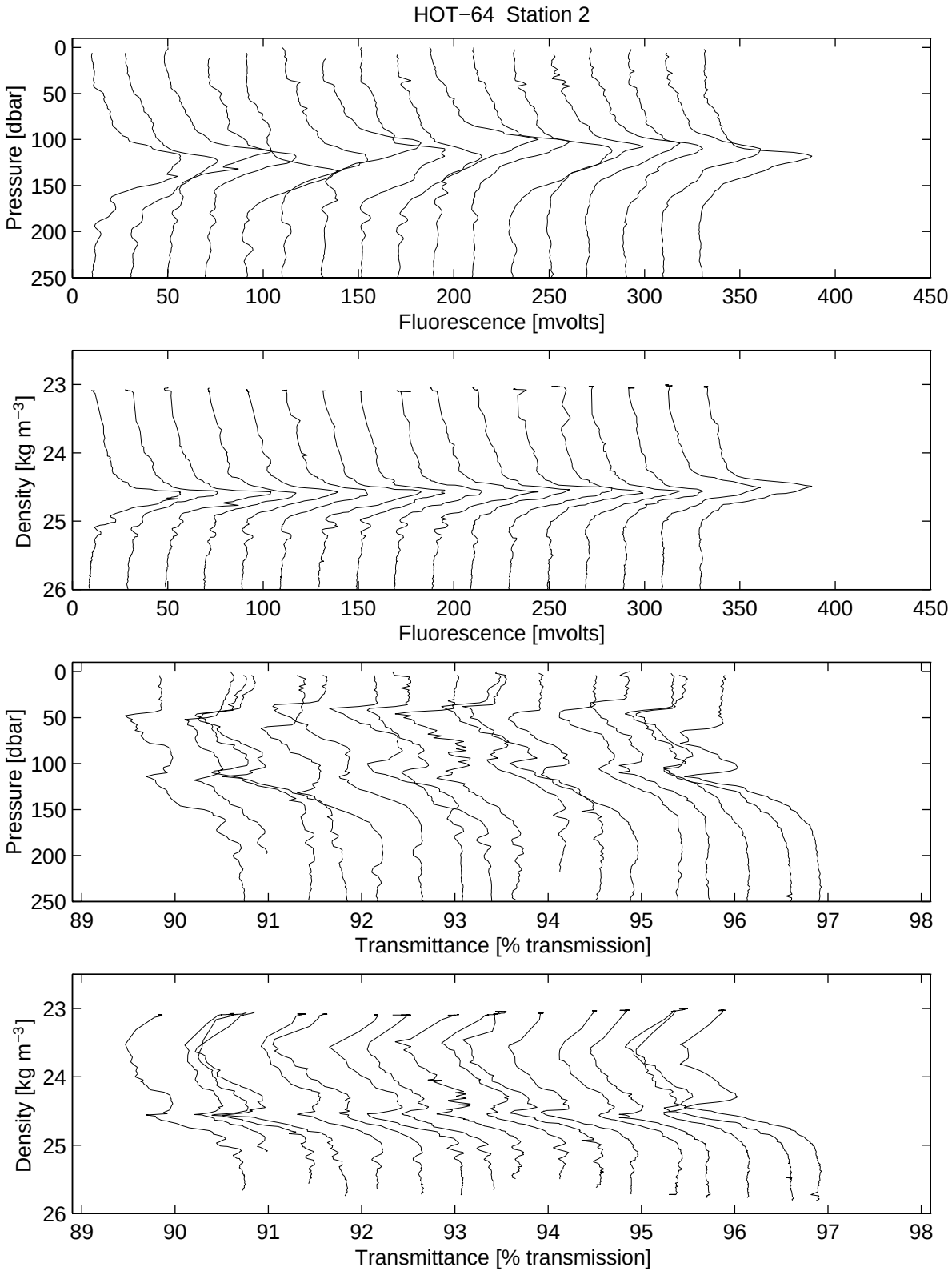
HOT−64 Station 2
Pressure [dbar]
Fluorescence [mvolts]
Density [kg m^{-3}]
Fluorescence [mvolts]
Pressure [dbar]
Transmittance [% transmission]
Density [kg m^{-3}]
Transmittance [% transmission]

Figure 6.4.5

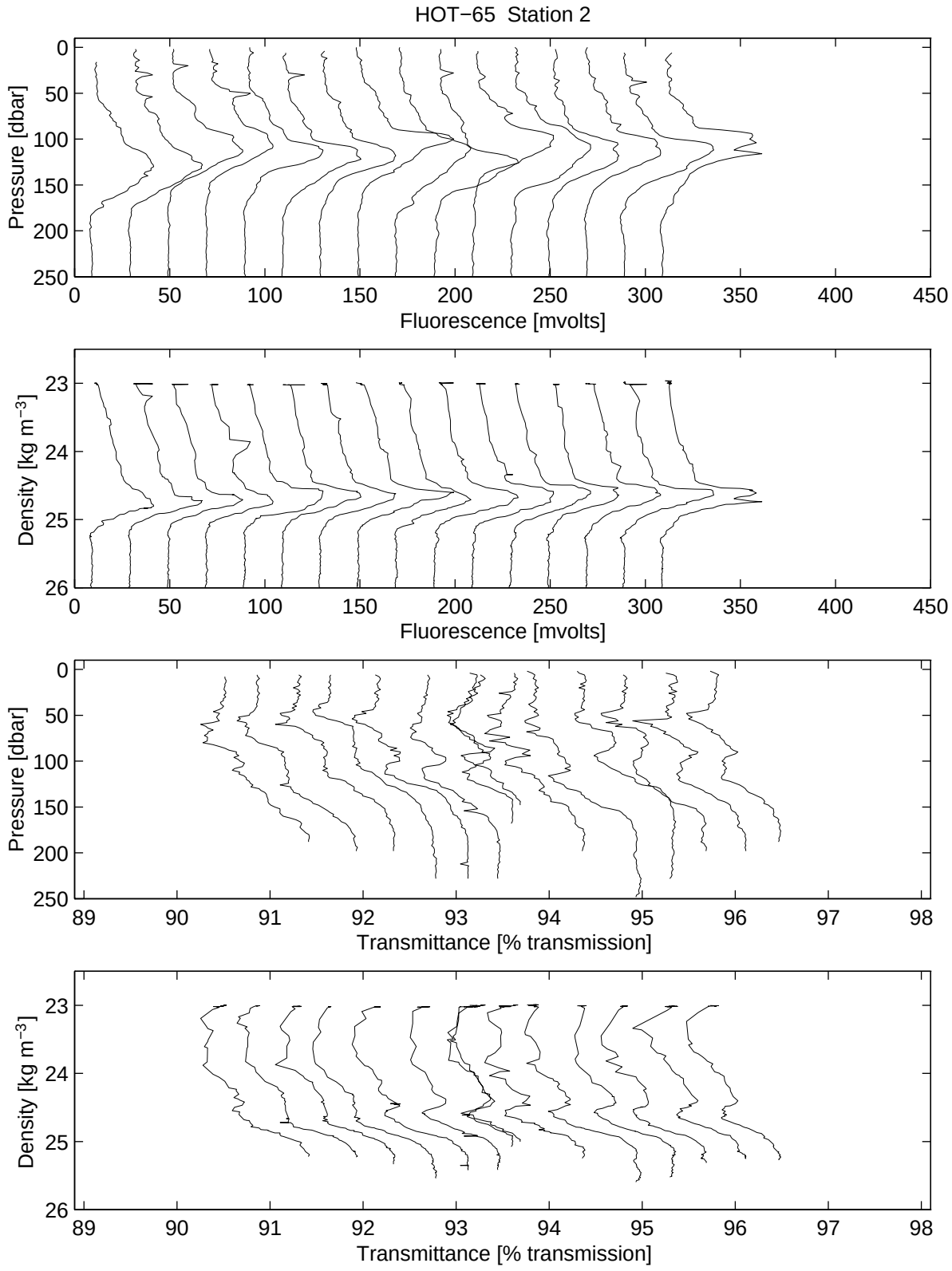
HOT−65 Station 2
Pressure [dbar]
Fluorescence [mvolts]
Density [kg m^{-3}]
Fluorescence [mvolts]
Pressure [dbar]
Transmittance [% transmission]
Density [kg m^{-3}]
Transmittance [% transmission]

Figure 6.4.6

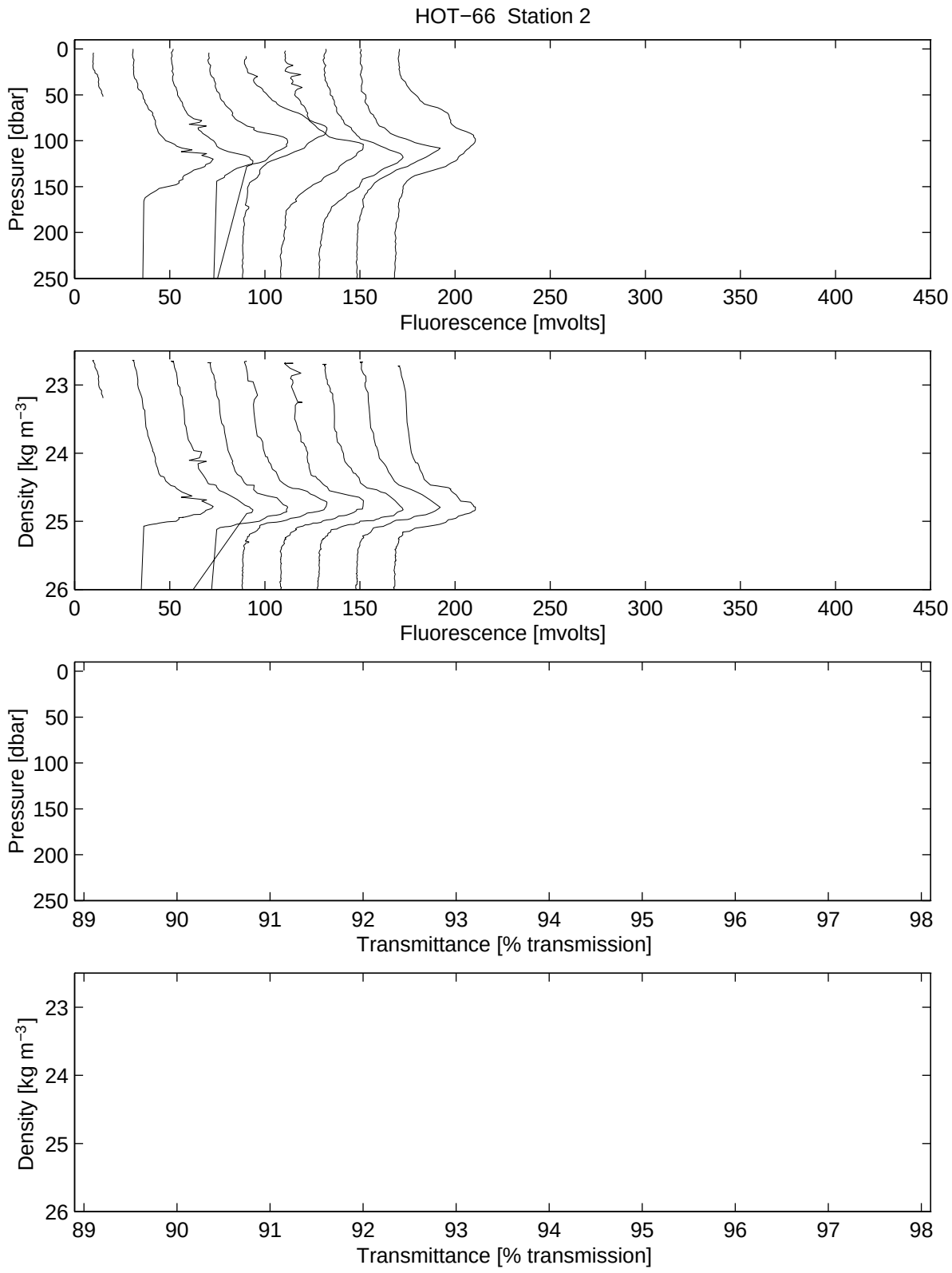
HOT−66 Station 2
Pressure [dbar]
Fluorescence [mvolts]
Density [kg m^{-3}]
Fluorescence [mvolts]
Pressure [dbar]
Transmittance [% transmission]
Density [kg m^{-3}]
Transmittance [% transmission]

Figure 6.4.7

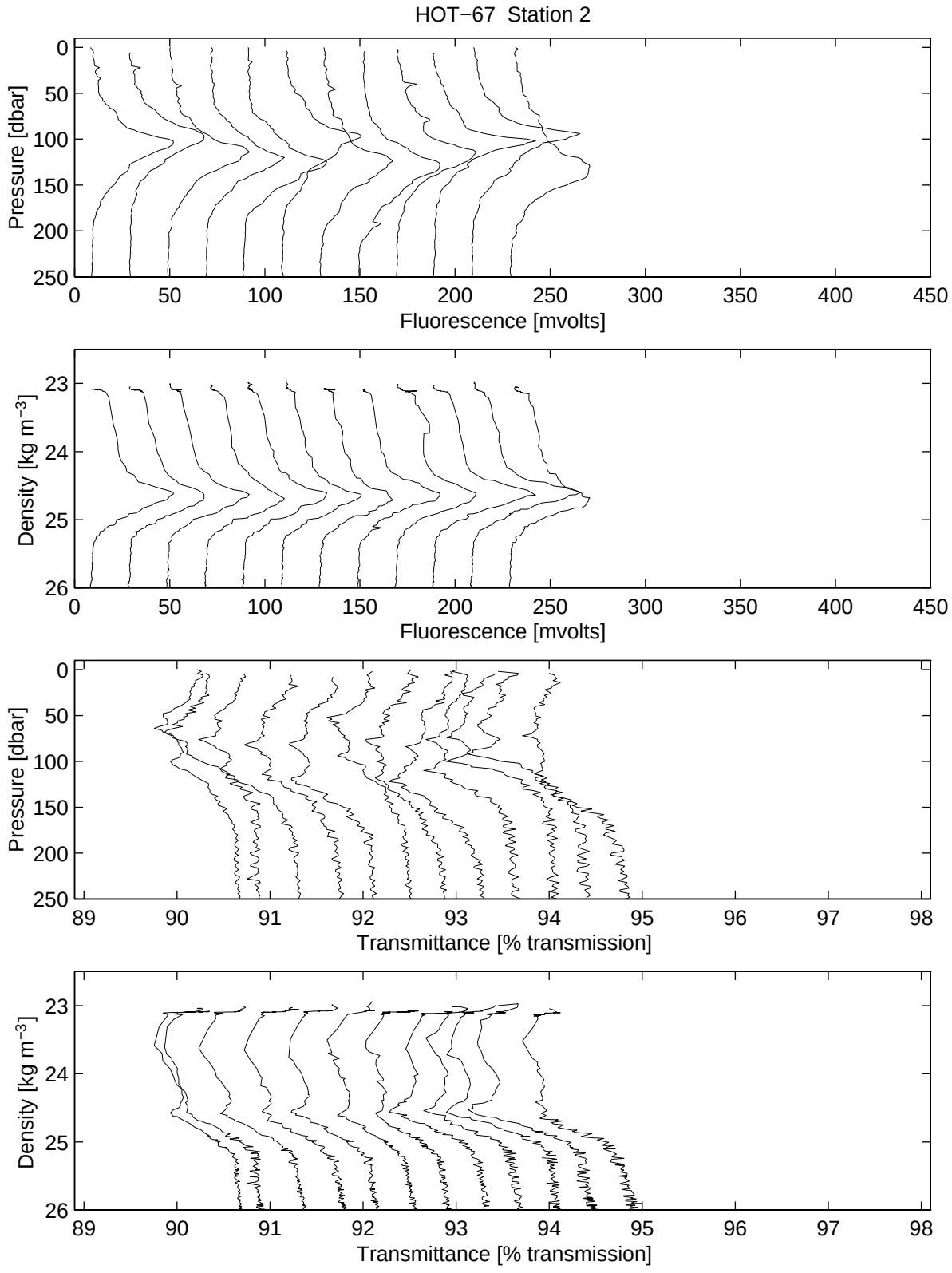
HOT−67 Station 2
Pressure [dbar]
Fluorescence [mvolts]
Density [kg m^{-3}]
Fluorescence [mvolts]
Pressure [dbar]
Transmittance [% transmission]
Density [kg m^{-3}]
Transmittance [% transmission]

Figure 6.4.8

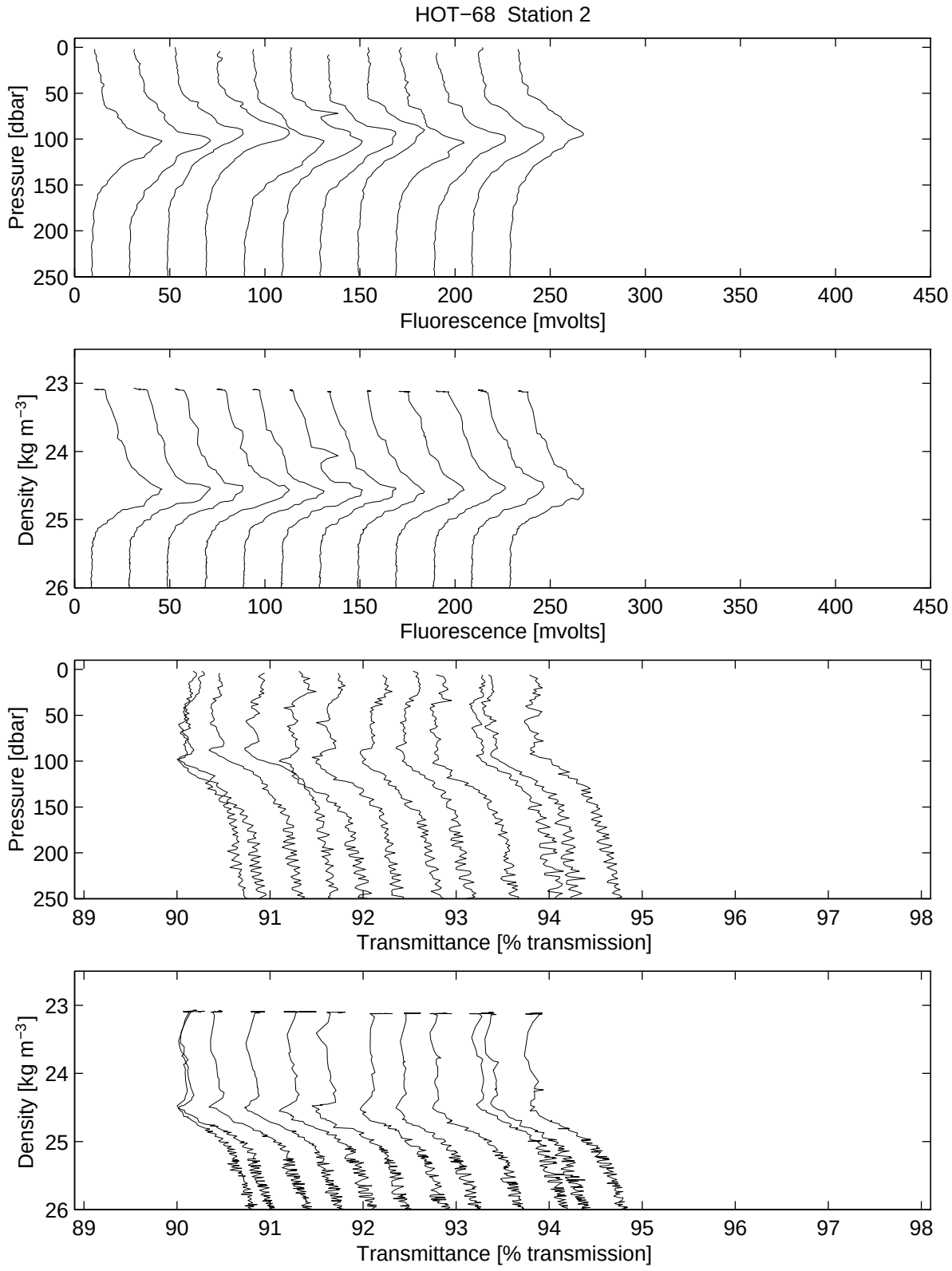
HOT−68 Station 2
Pressure [dbar]
Fluorescence [mvolts]
Density [kg m^{-3}]
Fluorescence [mvolts]
Pressure [dbar]
Transmittance [% transmission]
Density [kg m^{-3}]
Transmittance [% transmission]

Figure 6.4.9

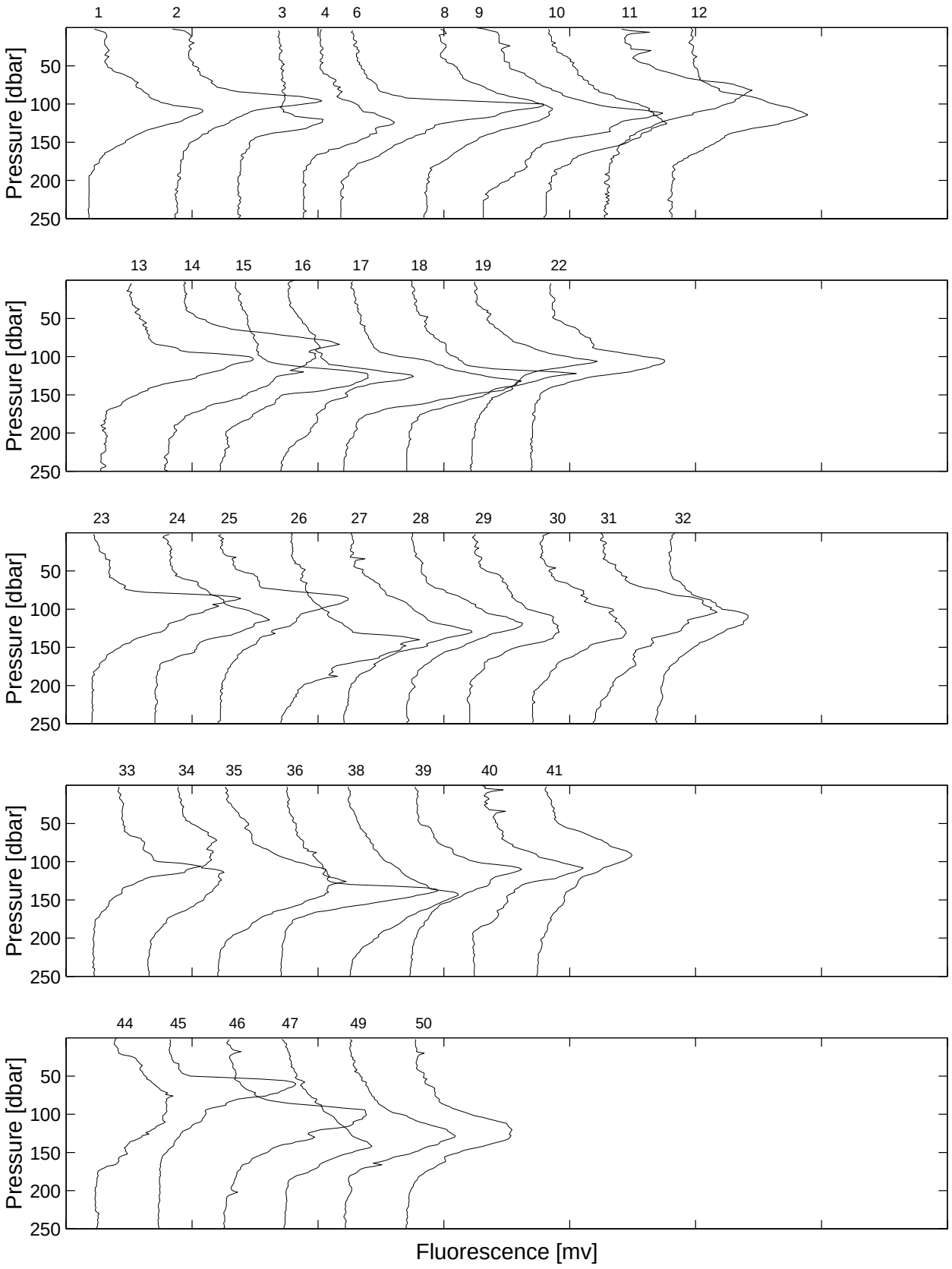
1 2 3 4 6 8 9 10 11 12
13 14 15 16 17 18 19 22
23 24 25 26 27 28 29 30 31 32
33 34 35 36 38 39 40 41
44 45 46 47 49 50
Pressure [dbar]
50
100
150
200
250
Fluorescence [mv]

Figure 6.4.10

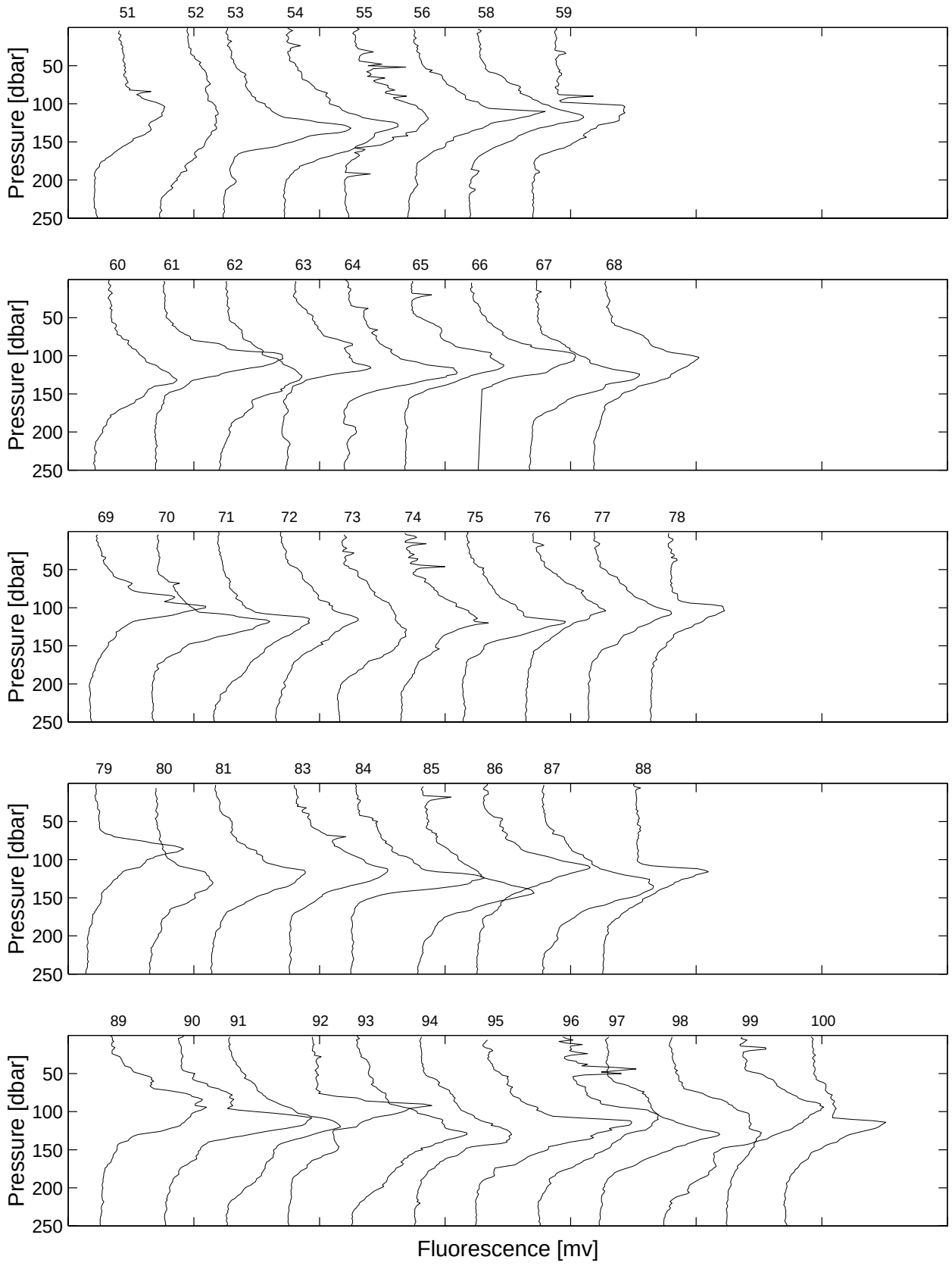

Figure 6.4.10 continue

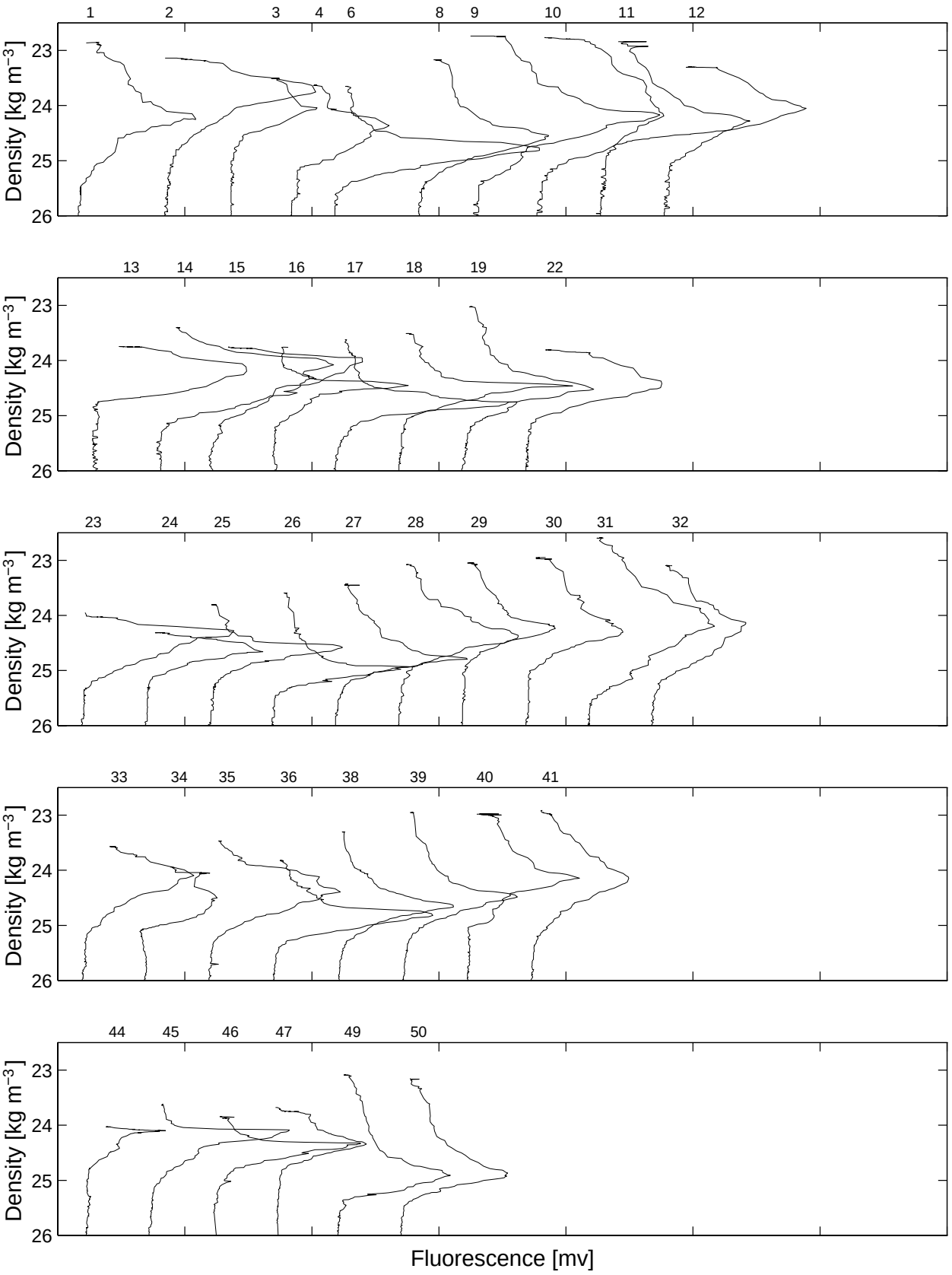
1 2 3 4 6 8 9 10 11 12
13 14 15 16 17 18 19 22
23 24 25 26 27 28 29 30 31 32
33 34 35 36 38 39 40 41
44 45 46 47 49 50
Density [kg m−3]
23
24
25
26
Fluorescence [mv]

Figure 6.4.11

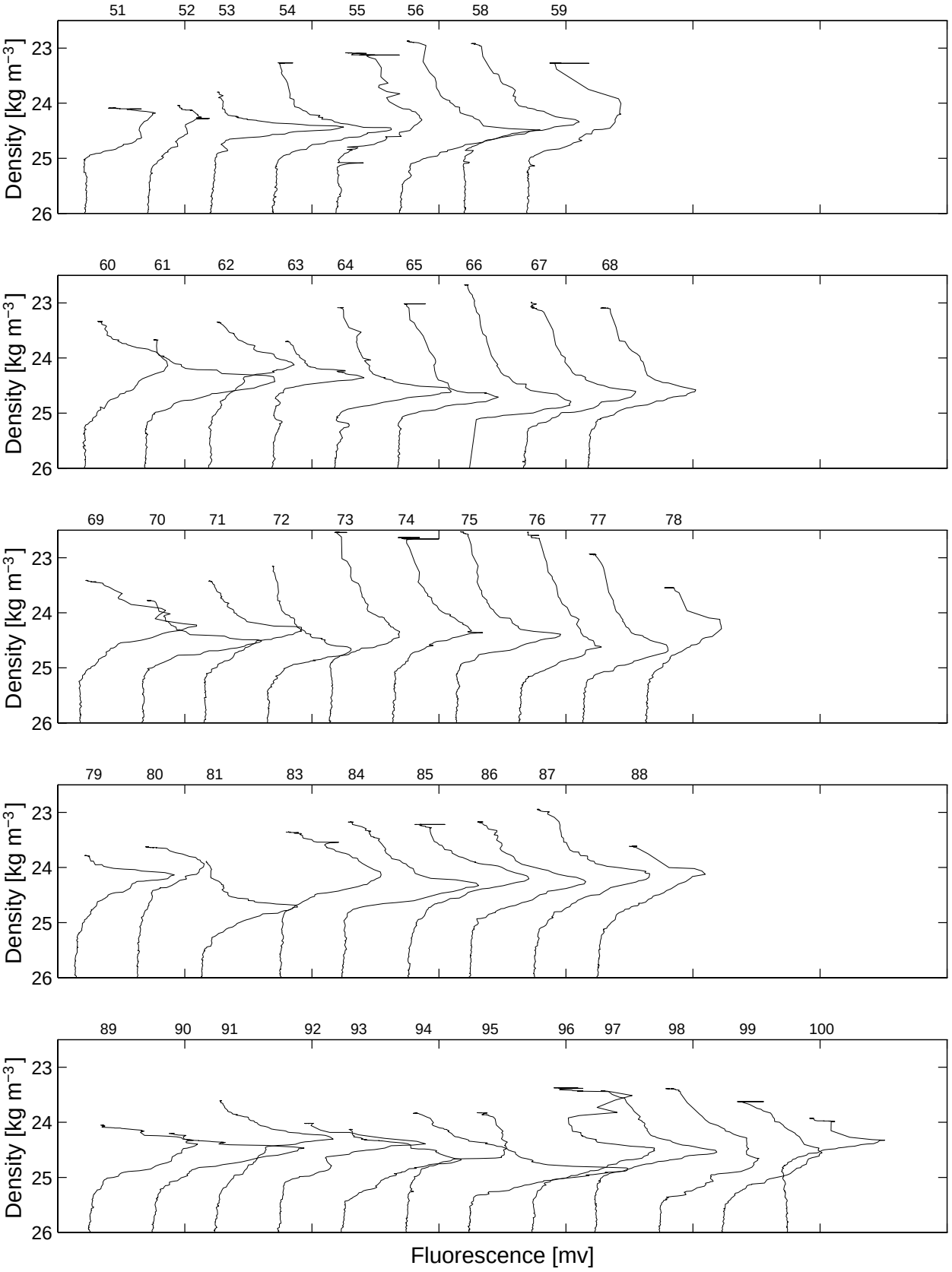

Figure 6.4.11 continue

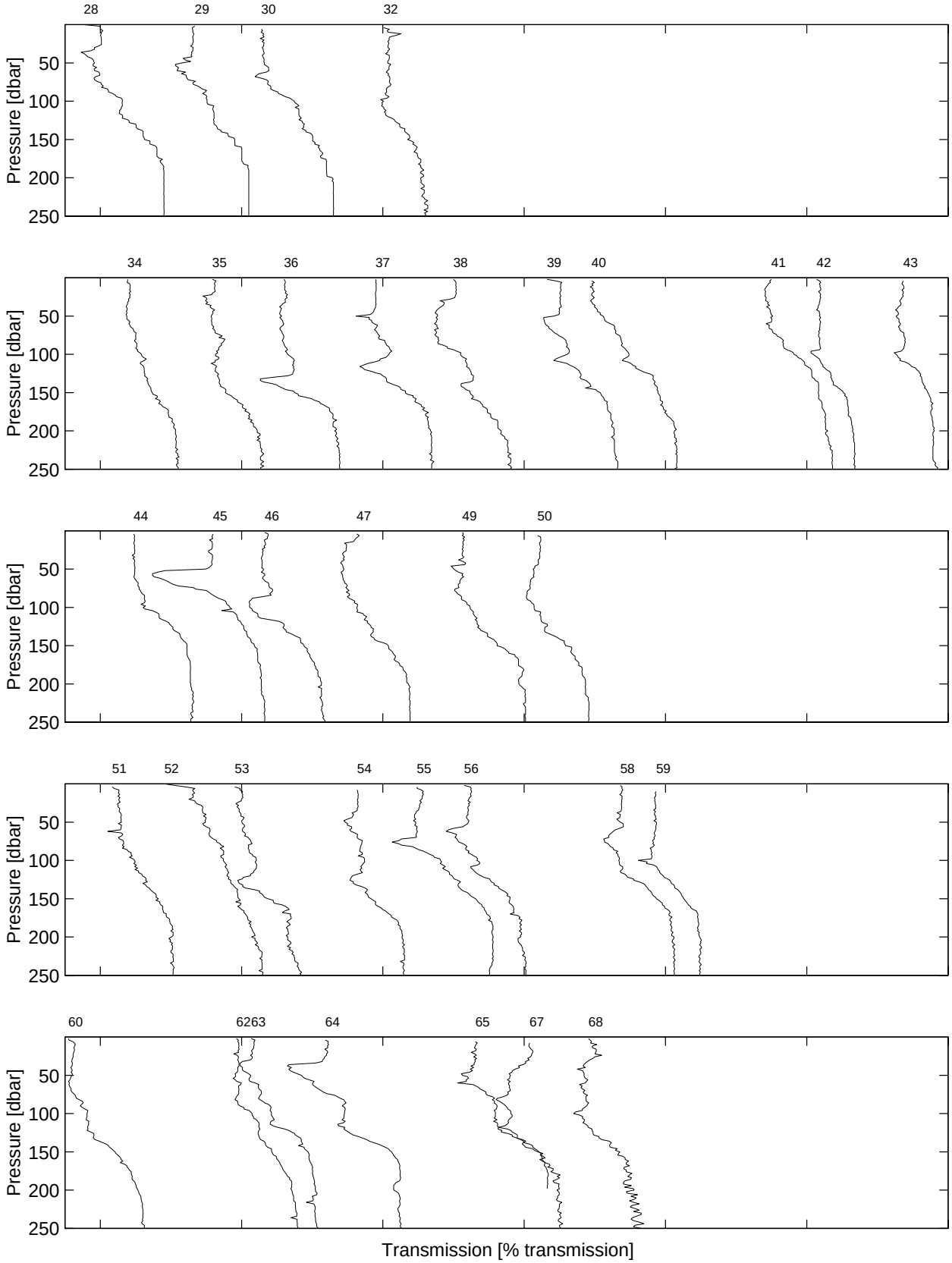
28
29
30
32
34
35
36
37
38
39
40
41
42
43
44
45
46
47
49
50
51
52
53
54
55
56
58
59
60
6263
64
65
67
68
Pressure [dbar]
50
100
150
200
250
Transmission [% transmission]

Figure 6.4.12

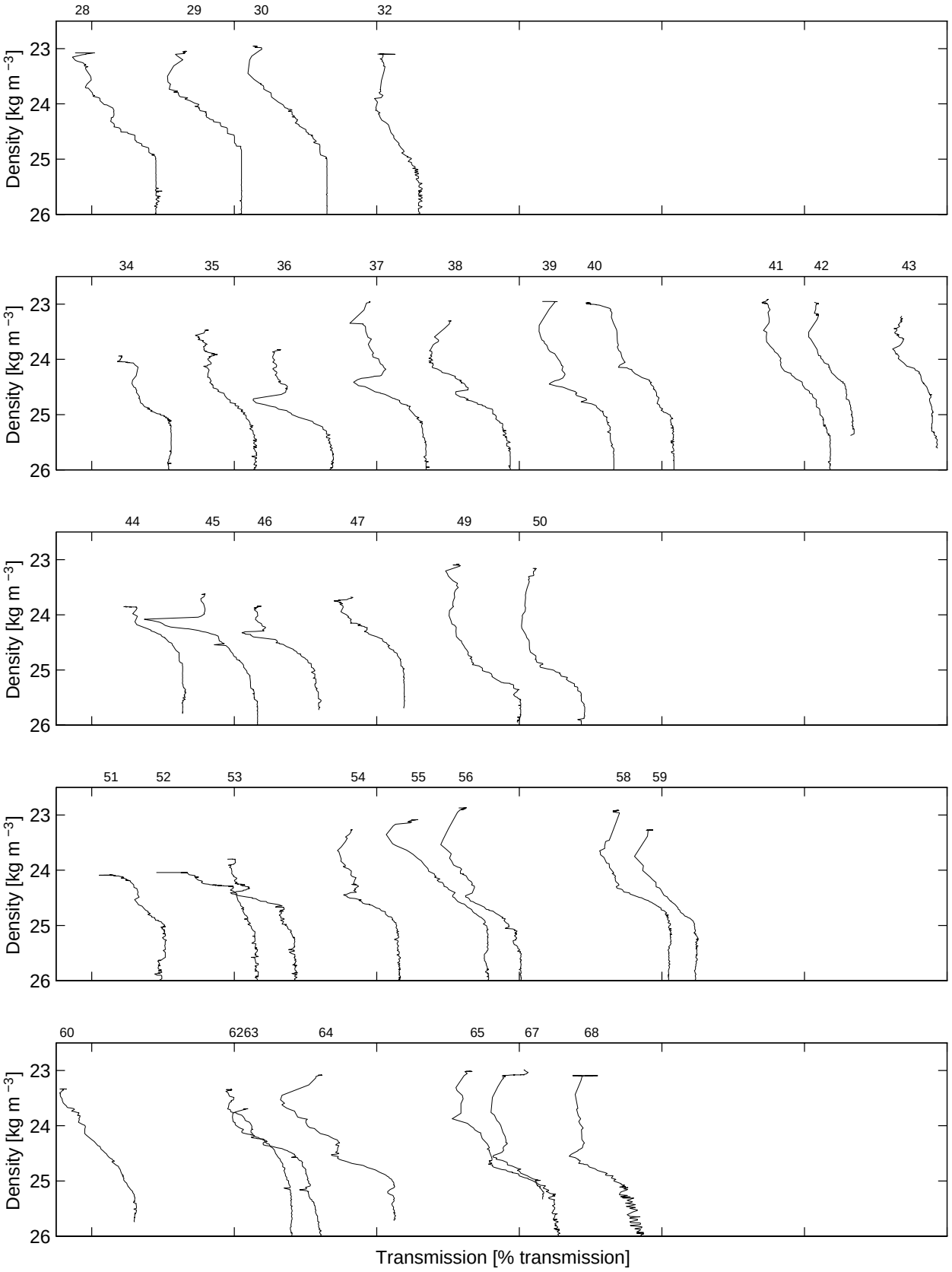
28
29
30
32
34
35
36
37
38
39
40
41
42
43
44
45
46
47
49
50
51
52
53
54
55
56
58
59
60
6263
64
65
67
68
Density [kg m −3]
23
24
25
26
Transmission [% transmission]

Figure 6.4.13

6.5. Biogeochemistry

Figure 6.5.1: Contoured time-series of DIC in the upper 1000 dbar at Station ALOHA normalized to 35 salinity. Location of bottle closure is indicated by solid circle.

Figure 6.5.2: Contoured time-series of titration alkalinity in the upper 1000 dbar at Station ALOHA normalized to 35 salinity. Location of bottle closure is indicated by solid circle.

Figure 6.5.3: Mean titration alkalinity and DIC in surface waters (0-50 dbars) at Station ALOHA. [Upper panel] Titration alkalinity plotted versus time for all HOT cruises. Error bars represent standard deviation of pooled samples collected between 0 and 50 dbar. [Lower panel] As in upper panel except for DIC.

Figure 6.5.4: Soluble reactive phosphorus measured by the MAGIC procedure in the upper 250 dbar at Station ALOHA in 1995.

Figure 6.5.5: [Nitrate+nitrite] measured by chemiluminescence in the upper 250 dbar at Station ALOHA in 1995.

Figure 6.5.6: Upper water column (0-100 m) depth-integrated [nitrate+nitrite] concentrations at Station ALOHA.

Figure 6.5.7: Upper water column (0-100 m) depth-integrated soluble reactive phosphorus as measured by both autoanalysis (solid line) and high-sensitivity MAGIC (dashed line) procedures at Station ALOHA. The solid line is a model I linear regression fit to the MAGIC data set.

Figure 6.5.8: Contoured time-series of fluorometric chlorophyll *a* in the upper 200 dbar for all HOT cruises.

Figure 6.5.9: Particulate carbon at Station ALOHA on all HOT cruises. [Upper panel] Mean particulate carbon concentration in the upper 50 dbar . Error bar represents the standard deviation of pooled samples collected between 0 and 50 dbar. [Lower panel] As in upper panel but for 50 to 100 dbar.

Figure 6.5.10: As in Figure 6.5.9 except for particulate nitrogen.

Figure 6.5.11: As in Figure 6.5.9 except for particulate phosphorus.

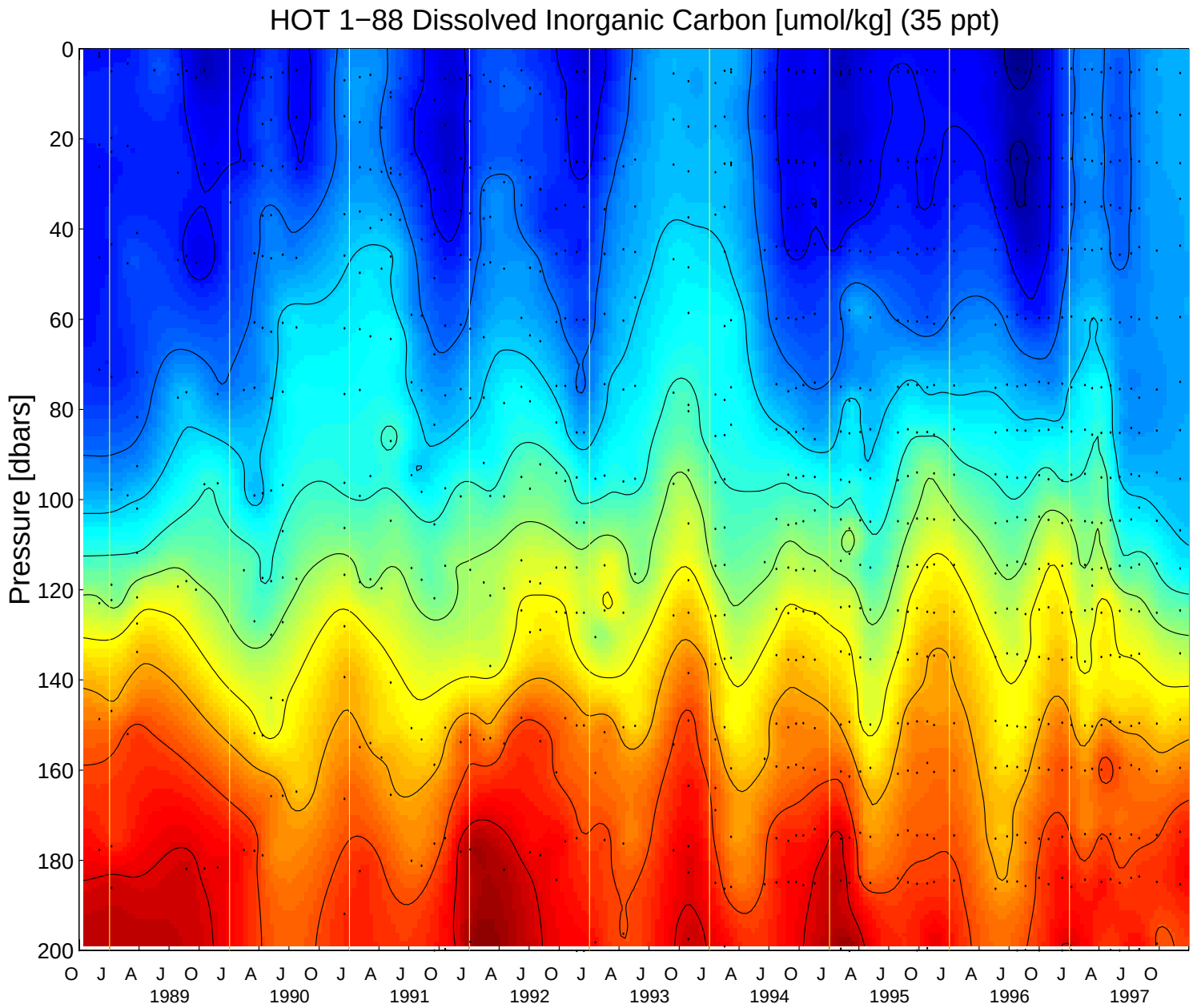
HOT 1−88 Dissolved Inorganic Carbon [umol/kg] (35 ppt)
Pressure [dbars]
0
20
40
60
80
100
120
140
160
180
200
O J A J O J A J O J A J O J A J O J A J O J A J O J A J O J A J O J A J O J A J O J A J O
1989
1990
1991
1992
1993
1994
1995
1996
1997

Figure 6.5.1

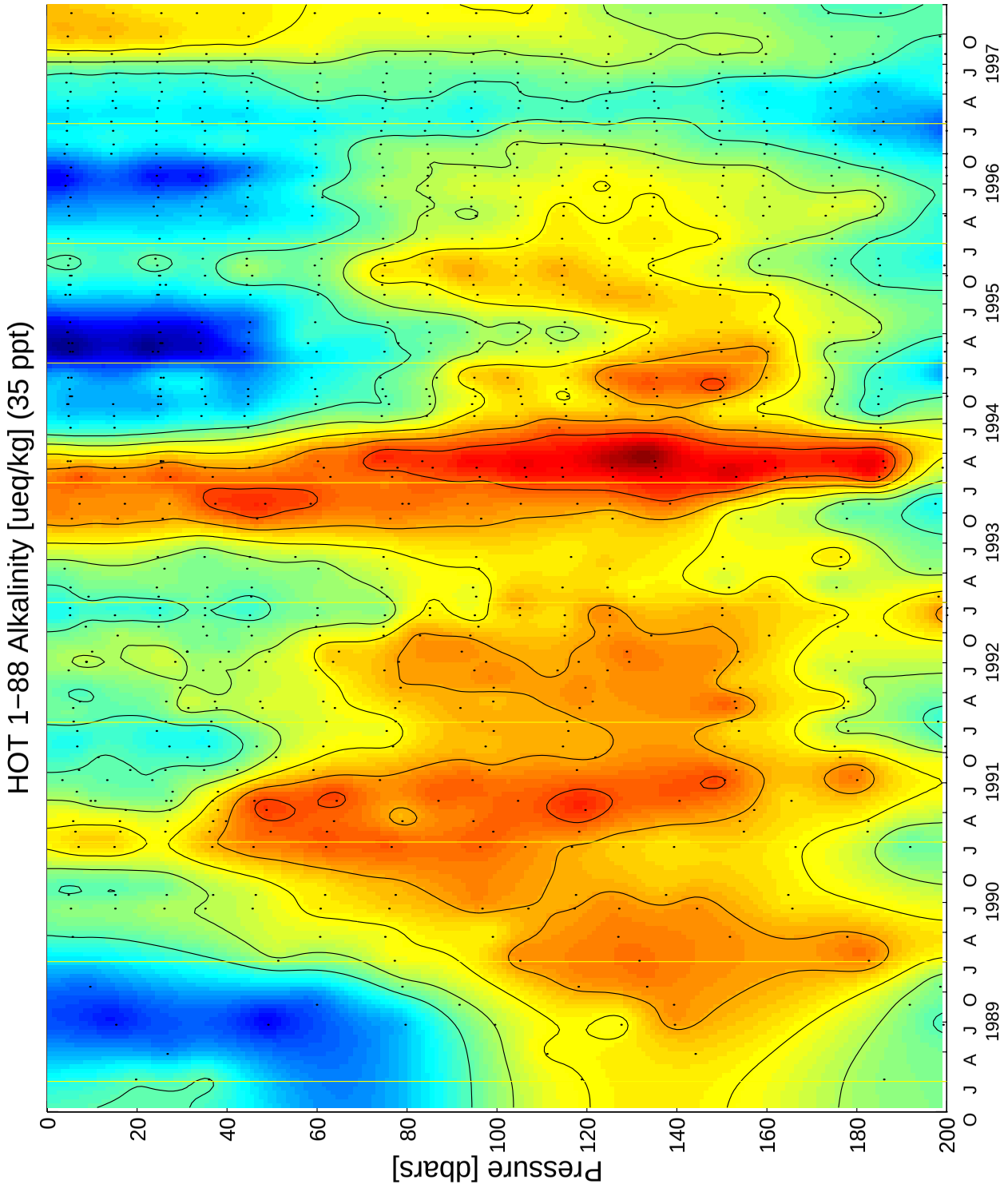
HOT 1−88 Alkalinity [ueq/kg] (35 ppt)
Pressure [dbars]
0
20
40
60
80
100
120
140
160
180
200
O J A J O J A J O J A J O J A J O J A J O J A J O J A J O J A J O J A J O J A J O
1989
1990
1991
1992
1993
1994
1995
1996
1997

Figure 6.5.2

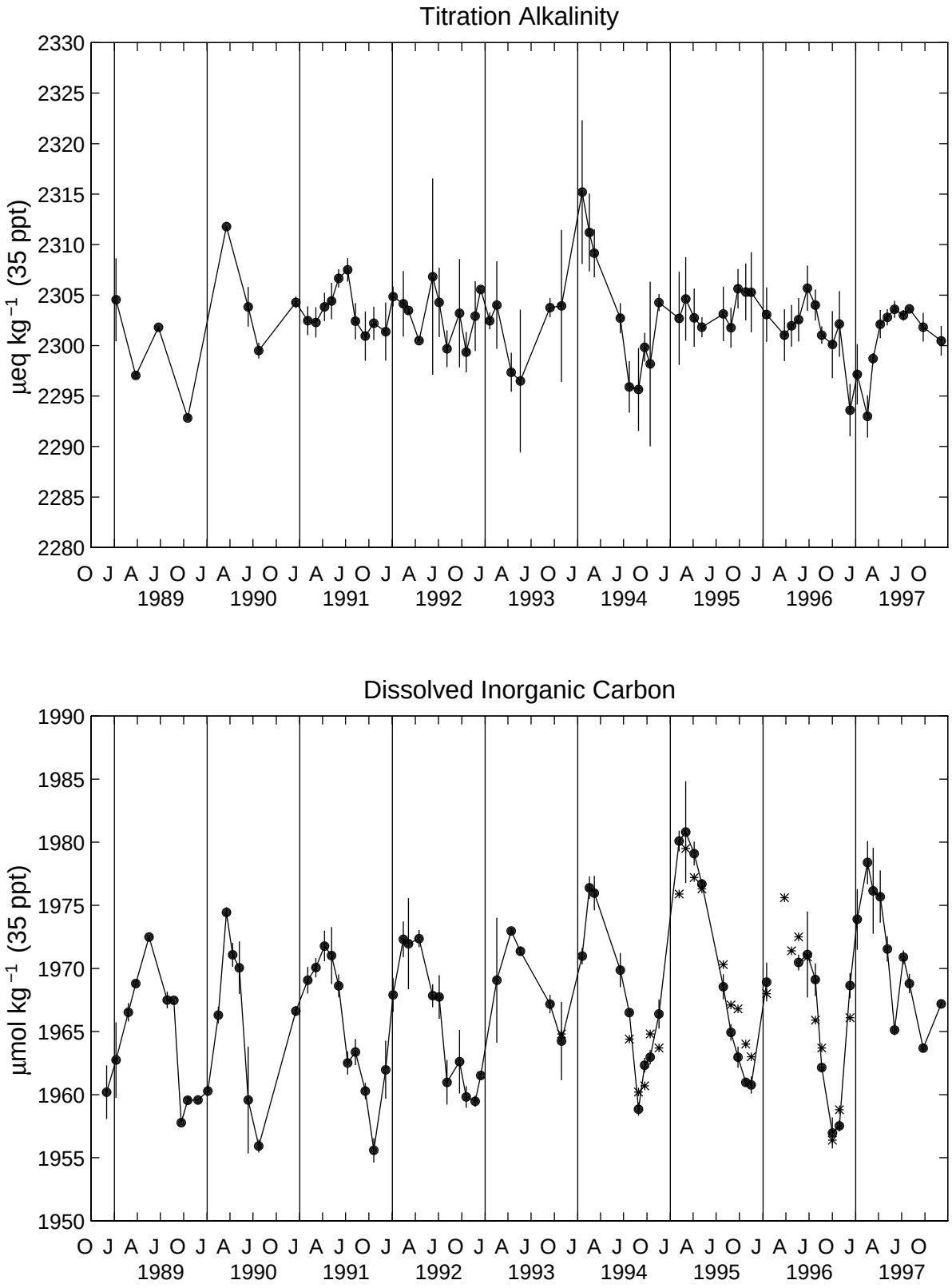
Titration Alkalinity
µeq kg⁻¹ (35 ppt)
2330
2325
2320
2315
2310
2305
2300
2295
2290
2285
2280
O J A J O J A J O J A J O J A J O J A J O J A J O J A J O J A J O J A J O J A J O
1989
1990
1991
1992
1993
1994
1995
1996
1997

Dissolved Inorganic Carbon
µmol kg⁻¹ (35 ppt)
1990
1985
1980
1975
1970
1965
1960
1955
1950
O J A J O J A J O J A J O J A J O J A J O J A J O J A J O J A J O J A J O J A J O
1989
1990
1991
1992
1993
1994
1995
1996
1997

Figure 6.5.3

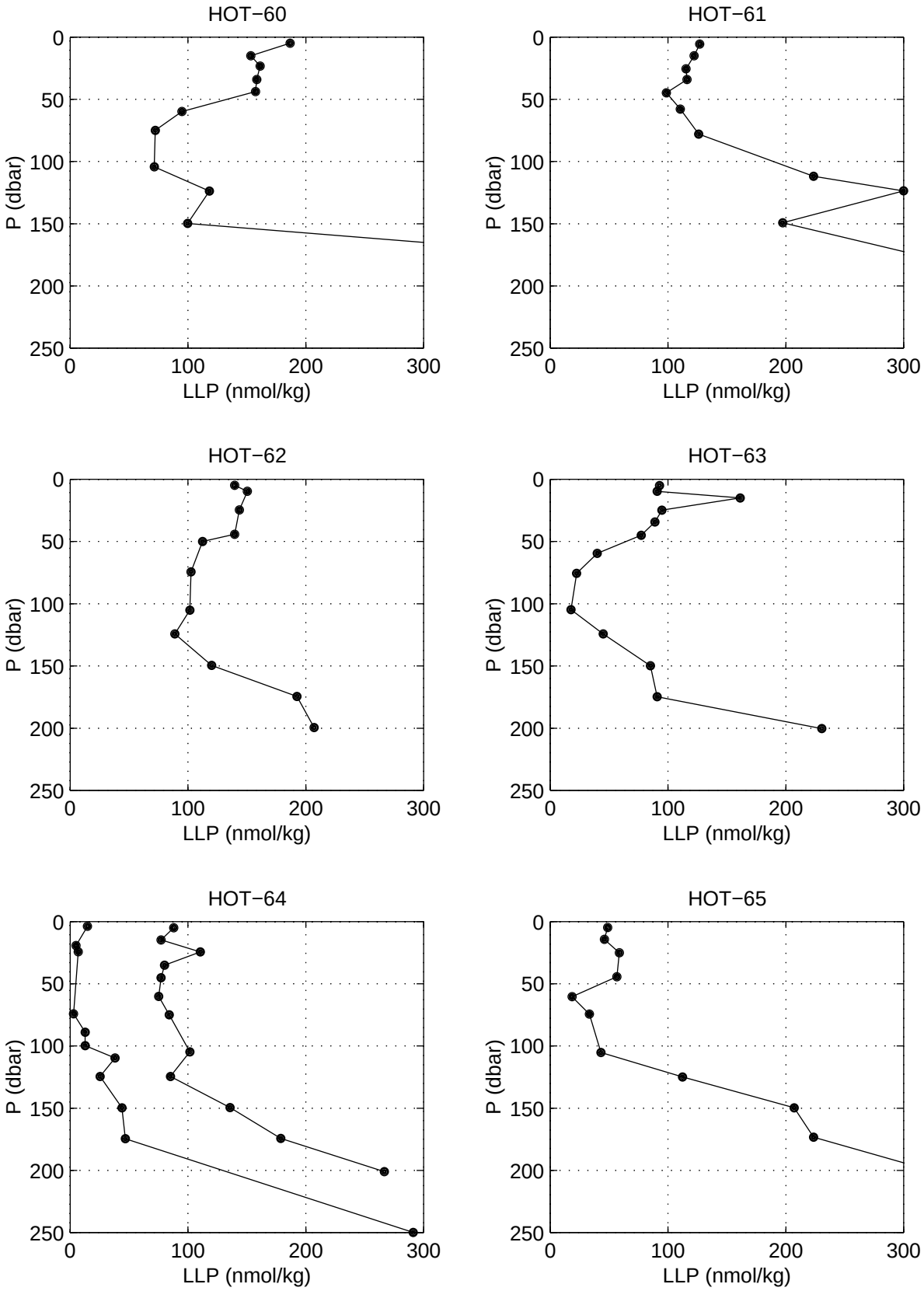
HOT−60
HOT−61
HOT−62
HOT−63
HOT−64
HOT−65
P (dbar)
LLP (nmol/kg)
0
50
100
150
200
250
300

Figure 6.5.4

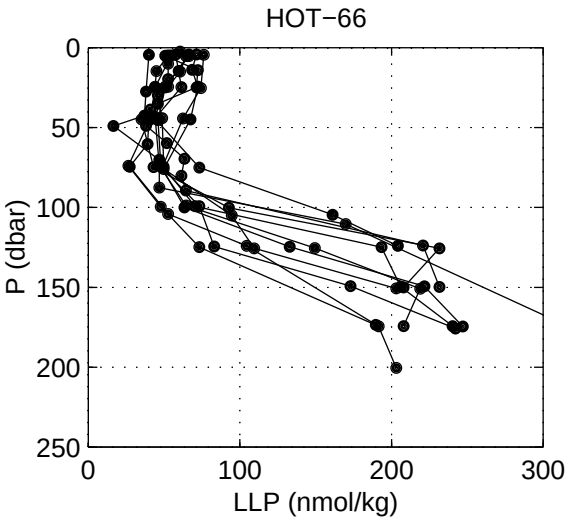

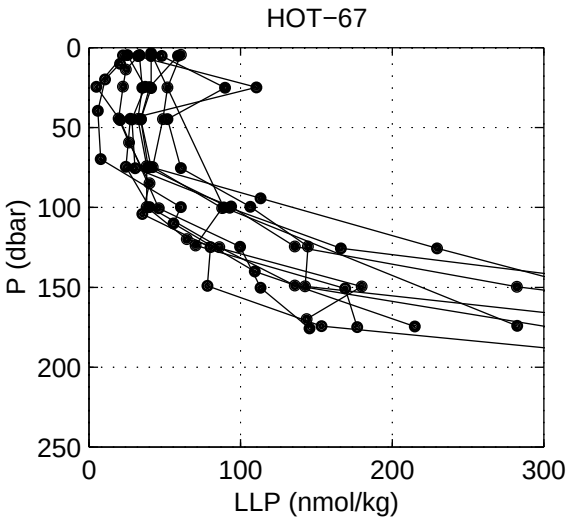

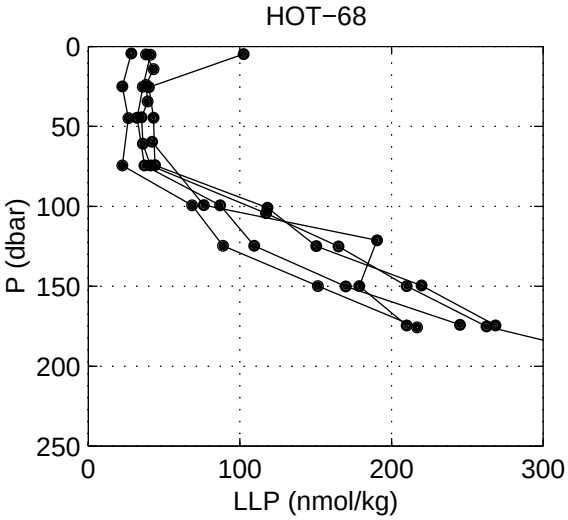

Figure 6.5.4 continued

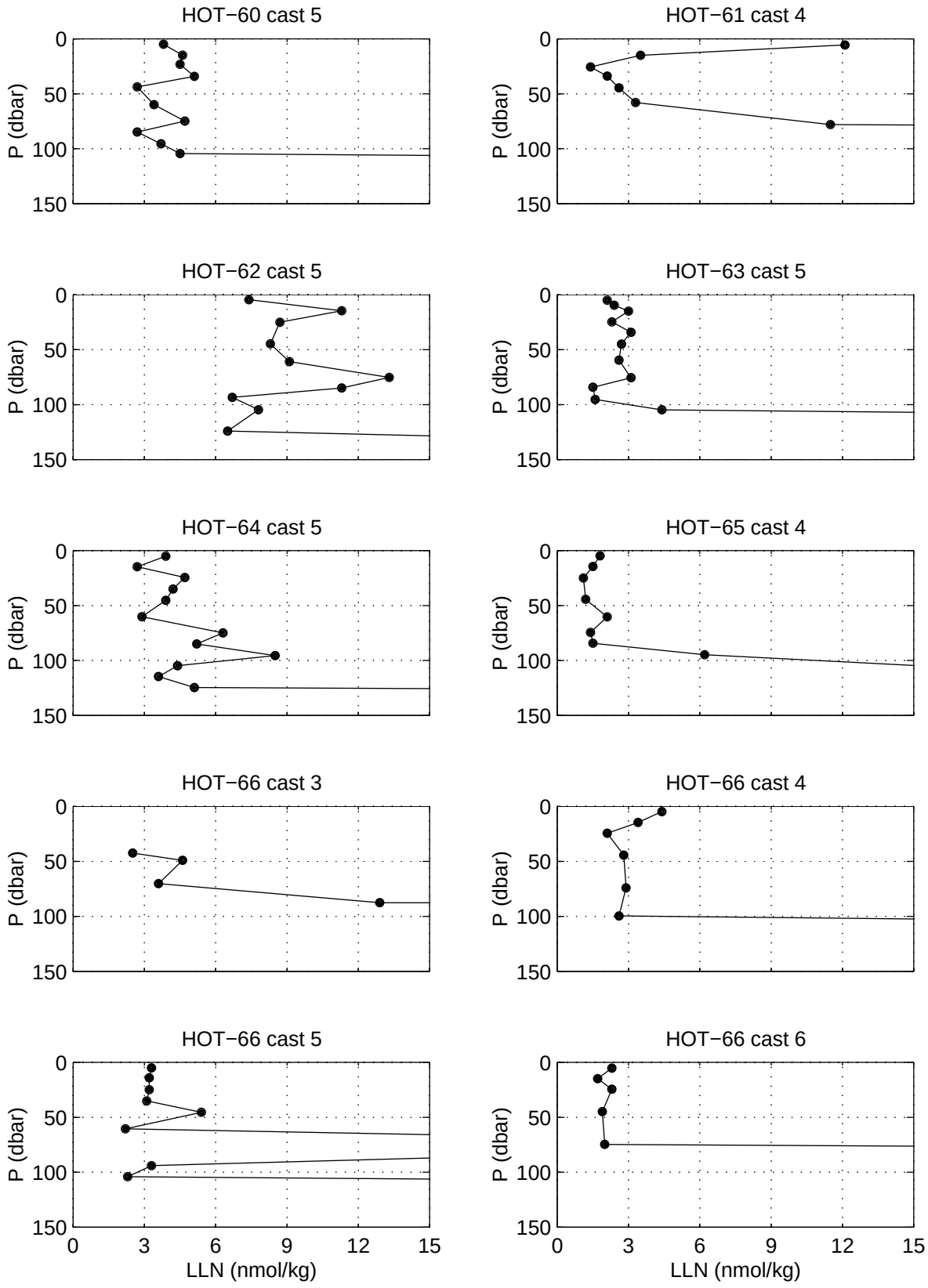
HOT−60 cast 5
HOT−61 cast 4
HOT−62 cast 5
HOT−63 cast 5
HOT−64 cast 5
HOT−65 cast 4
HOT−66 cast 3
HOT−66 cast 4
HOT−66 cast 5
HOT−66 cast 6
P (dbar)
0
50
100
150
0
3
6
9
12
15
LLN (nmol/kg)

Figure 6.5.5

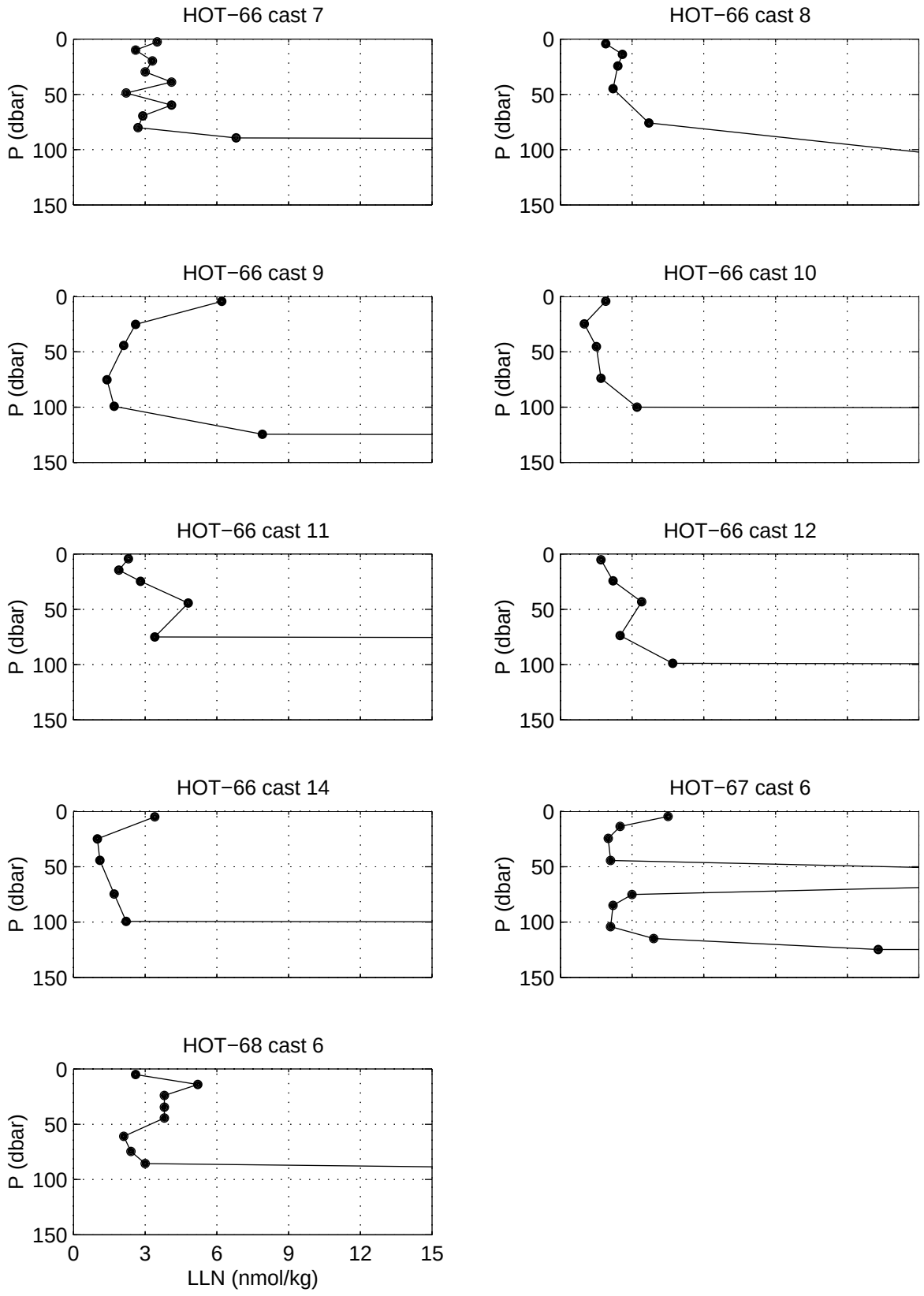

Figure 6.5.5 continued

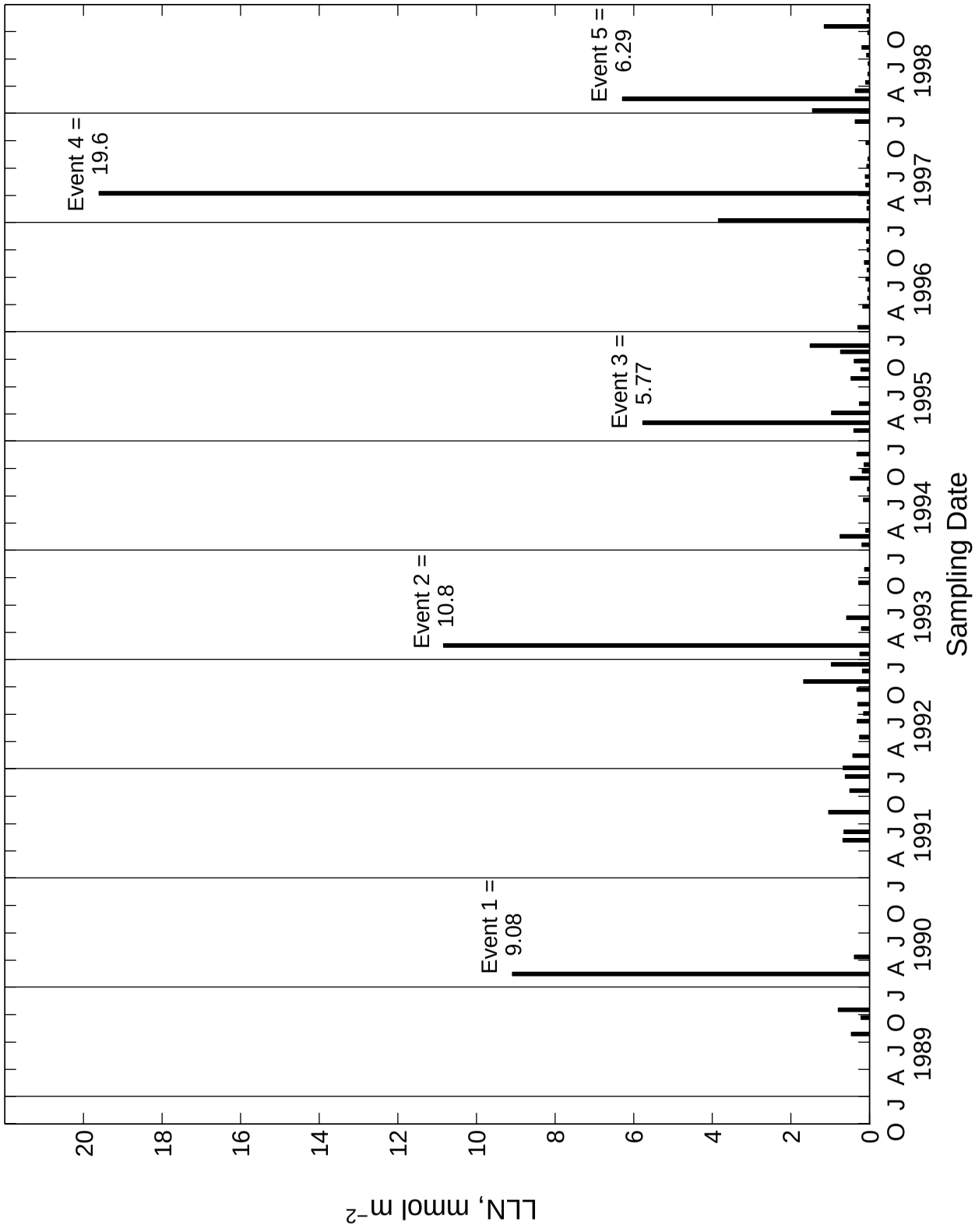
LLN, mmol m⁻²
0
2
4
6
8
10
12
14
16
18
20
O J A J O J A J O J A J O J A J O J A J O J A J O J A J O J A J O
1989
1990
1991
1992
1993
1994
1995
1996
1997
1998
Sampling Date
Event 1 = 9.08
Event 2 = 10.8
Event 3 = 5.77
Event 4 = 19.6
Event 5 = 6.29

Figure 6.5.6

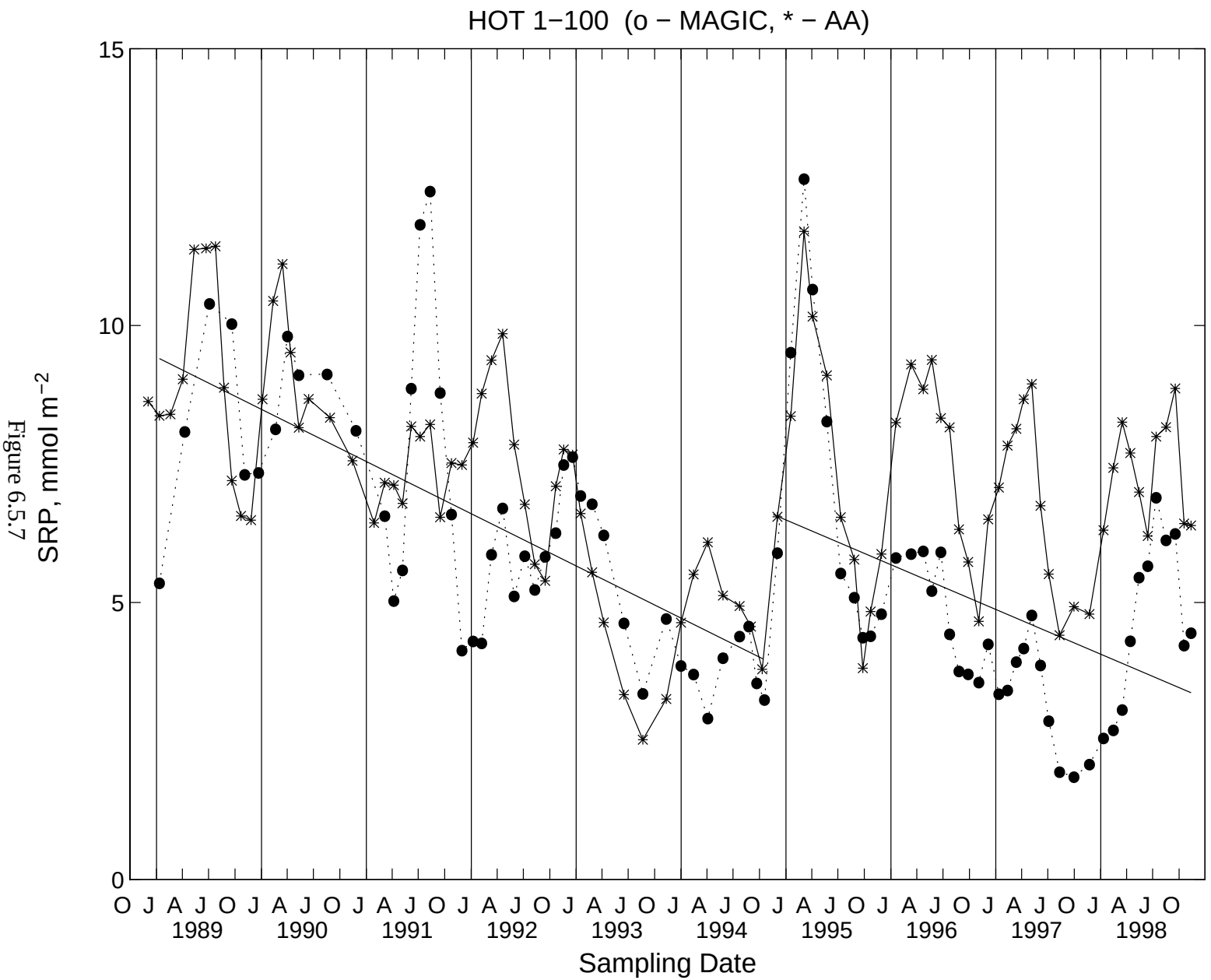
HOT 1−100 (o − MAGIC, * − AA)
SRP, mmol m^{-2}
15
10
5
0
O J A J O J A J O J A J O J A J O J A J O J A J O J A J O J A J O J A J O J A J O
1989
1990
1991
1992
1993
1994
1995
1996
1997
1998
Sampling Date

Figure 6.5.7

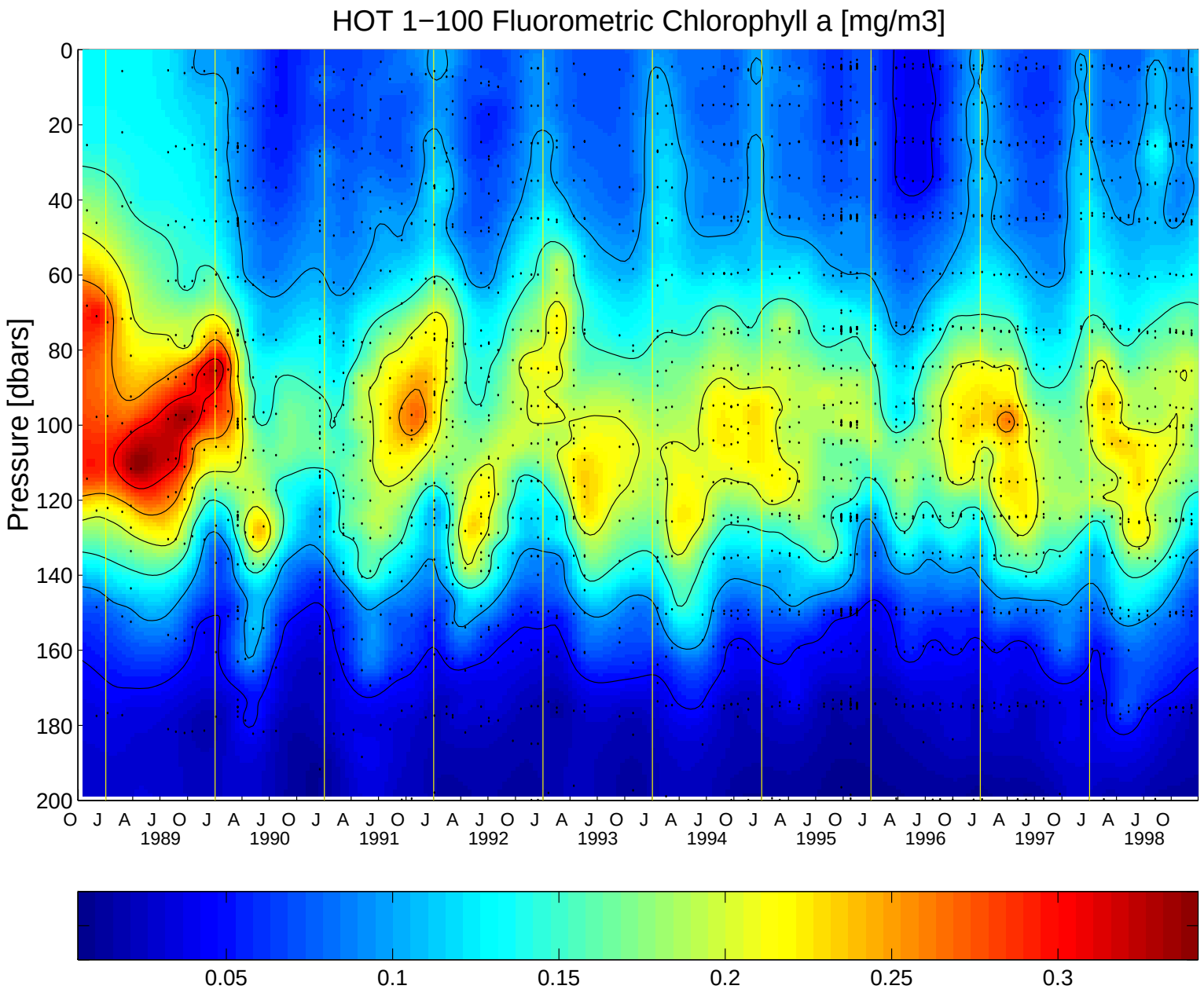
HOT 1−100 Fluorometric Chlorophyll a [mg/m3]
Pressure [dbars]
0
20
40
60
80
100
120
140
160
180
200
O J A J O J A J O J A J O J A J O J A J O J A J O J A J O J A J O J A J O J A J O J A J O J A J O J A J O
1989
1990
1991
1992
1993
1994
1995
1996
1997
1998
0.05
0.1
0.15
0.2
0.25
0.3

Figure 6.5.8

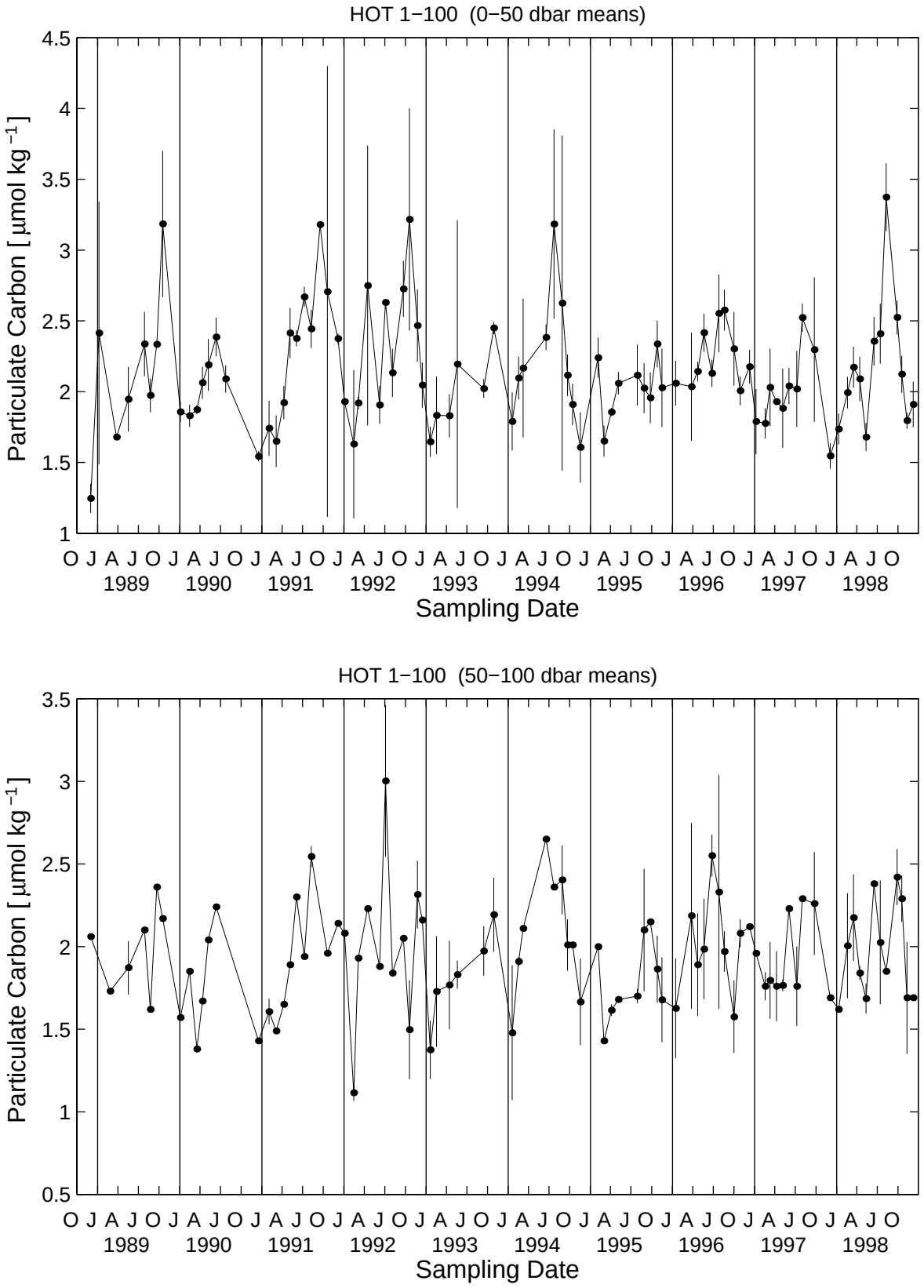
HOT 1−100 (0−50 dbar means)
Particulate Carbon [µmol kg −1]
4.5
4
3.5
3
2.5
2
1.5
1
O J A J O J A J O J A J O J A J O J A J O J A J O J A J O J A J O J A J O J A J O J A J O
1989
1990
1991
1992
1993
1994
1995
1996
1997
1998
Sampling Date
HOT 1−100 (50−100 dbar means)
Particulate Carbon [µmol kg −1]
3.5
3
2.5
2
1.5
1
0.5
O J A J O J A J O J A J O J A J O J A J O J A J O J A J O J A J O J A J O J A J O J A J O
1989
1990
1991
1992
1993
1994
1995
1996
1997
1998
Sampling Date

Figure 6.5.9

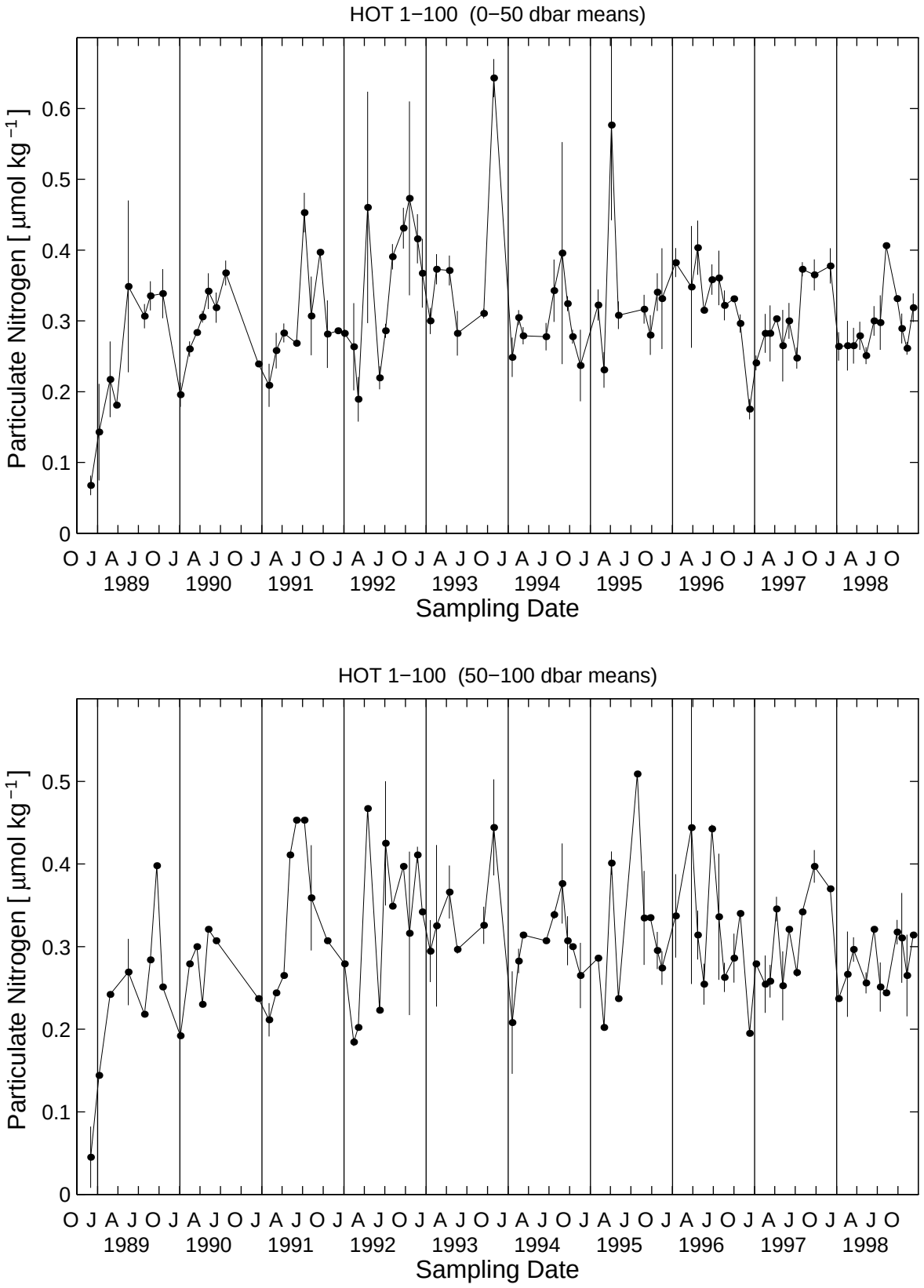
HOT 1−100 (0−50 dbar means)
Particulate Nitrogen [µmol kg −1]
0
0.1
0.2
0.3
0.4
0.5
0.6
O J A J O J A J O J A J O J A J O J A J O J A J O J A J O J A J O J A J O J A J O J A J O
1989
1990
1991
1992
1993
1994
1995
1996
1997
1998
Sampling Date
HOT 1−100 (50−100 dbar means)
Particulate Nitrogen [µmol kg −1]
0
0.1
0.2
0.3
0.4
0.5
O J A J O J A J O J A J O J A J O J A J O J A J O J A J O J A J O J A J O J A J O J A J O
1989
1990
1991
1992
1993
1994
1995
1996
1997
1998
Sampling Date

Figure 6.5.10

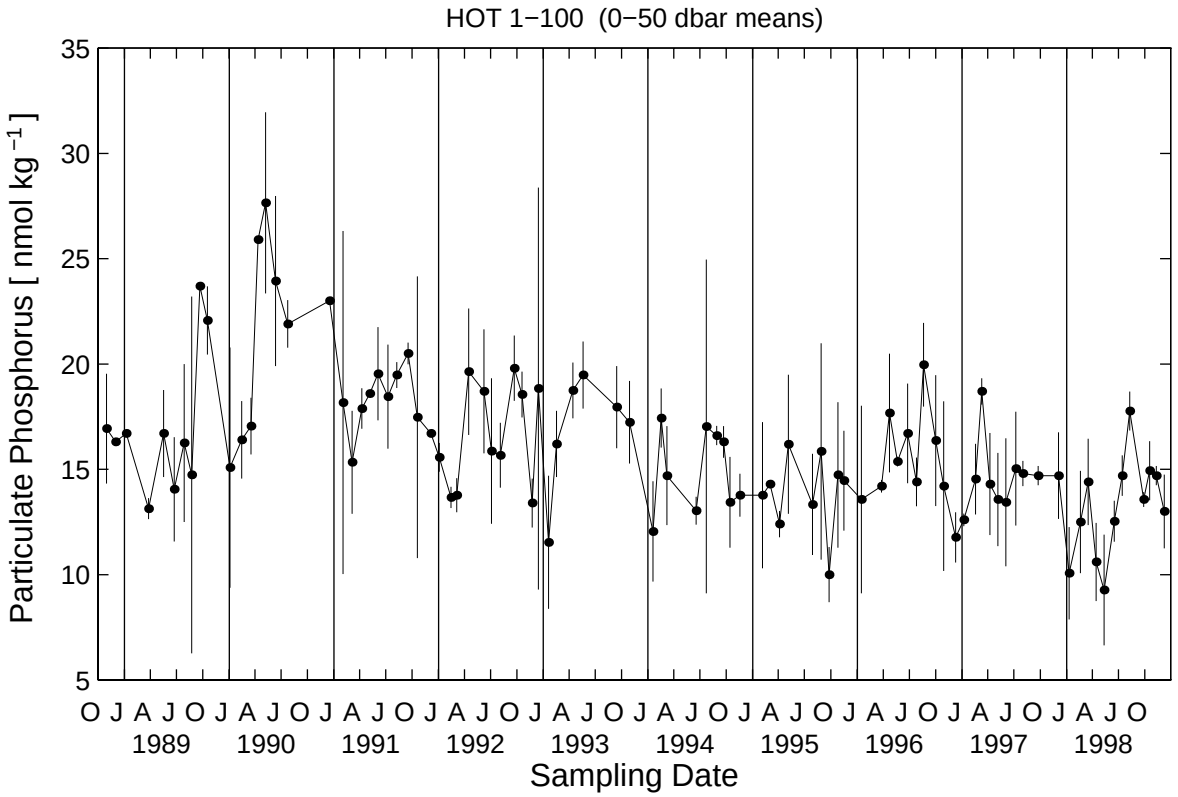
HOT 1−100 (0−50 dbar means)
Particulate Phosphorus [nmol kg −1]
35
30
25
20
15
10
5
O J A J O J A J O J A J O J A J O J A J O J A J O J A J O J A J O J A J O J A J O J A J O
1989
1990
1991
1992
1993
1994
1995
1996
1997
1998
Sampling Date

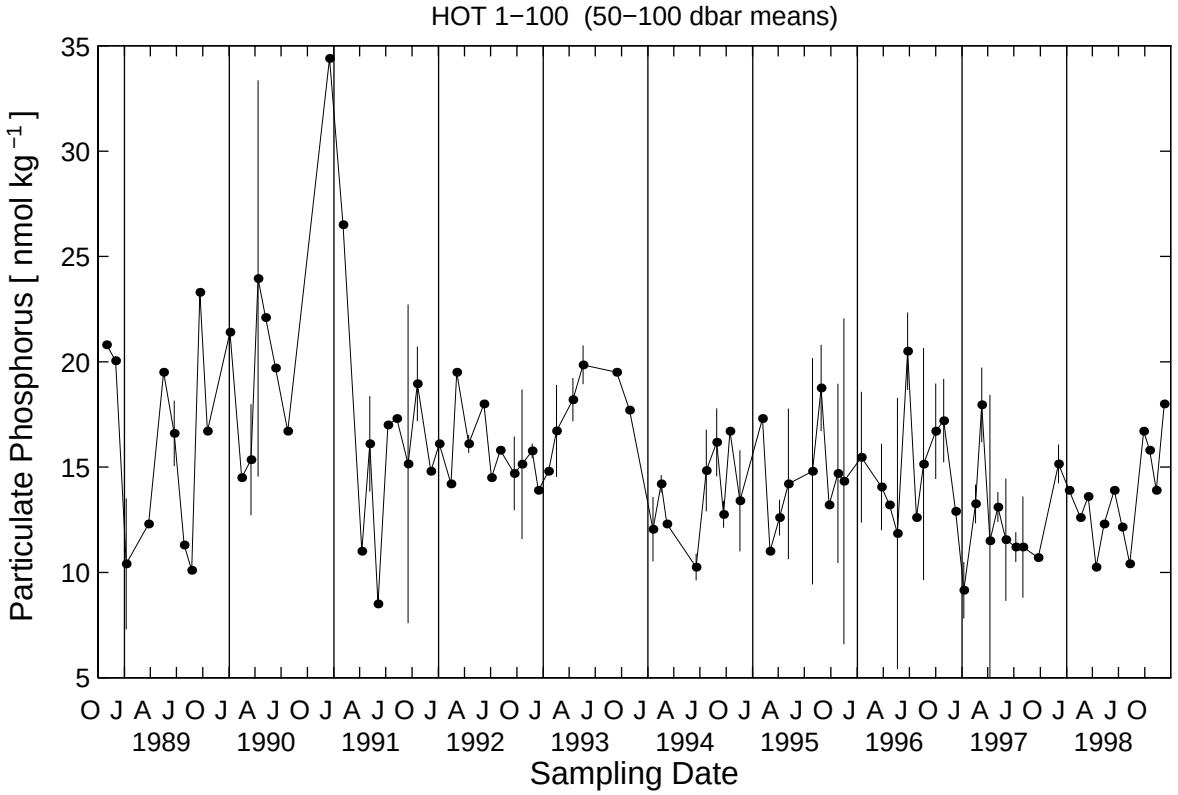
HOT 1−100 (50−100 dbar means)
Particulate Phosphorus [nmol kg −1]
35
30
25
20
15
10
5
O J A J O J A J O J A J O J A J O J A J O J A J O J A J O J A J O J A J O J A J O J A J O
1989
1990
1991
1992
1993
1994
1995
1996
1997
1998
Sampling Date

Figure 6.5.11

6.6. Primary Production and Particle Flux

Figure 6.6.1: Integrated (0-200 m) primary production rates measured on all HOT cruises. Data for both *in situ* and on-deck incubations are presented. On HOT-15 (March 1990) primary production was measured on three consecutive days.

Figure 6.6.2: Carbon flux at 150 m measured on all HOT cruises from 1988 through 1995. Error bars represent the standard deviation of replicate determinations.

Figure 6.6.3: Same as 6.6.2 but for nitrogen.

Figure 6.6.4: Same as 6.6.2 but for phosphorus.

Figure 6.6.5: Same as 6.6.2 but for total mass

.

Figure 6.6.6: Contour plot of carbon flux for all cruises from 1988 through 1995.

Figure 6.6.7: Same as 6.6.6 but for nitrogen.

Figure 6.6.8: Same as 6.6.6 but for phosphorus.

Figure 6.6.9: Same as 6.6.6 but for total mass.

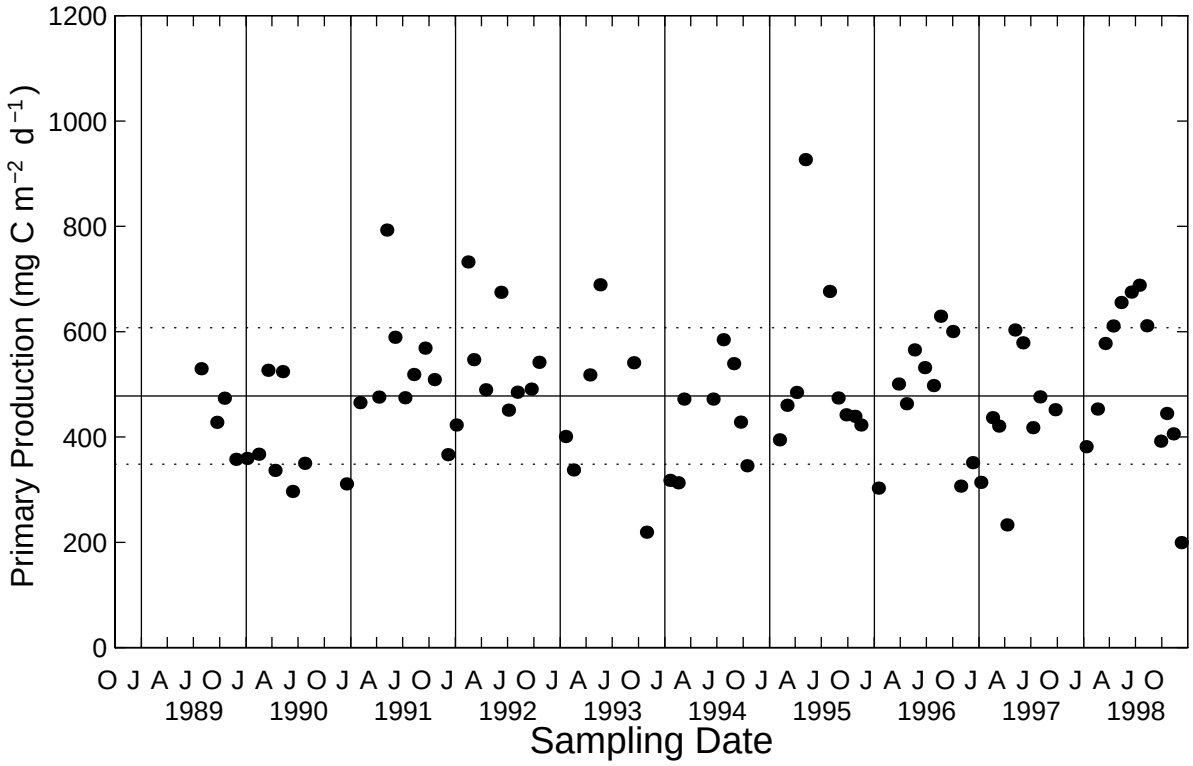
Primary Production (mg C m^{-2} d^{-1})
0
200
400
600
800
1000
1200
O J A J O J A J O J A J O J A J O J A J O J A J O J A J O J A J O J A J O J A J O J A J O
1989
1990
1991
1992
1993
1994
1995
1996
1997
1998
Sampling Date

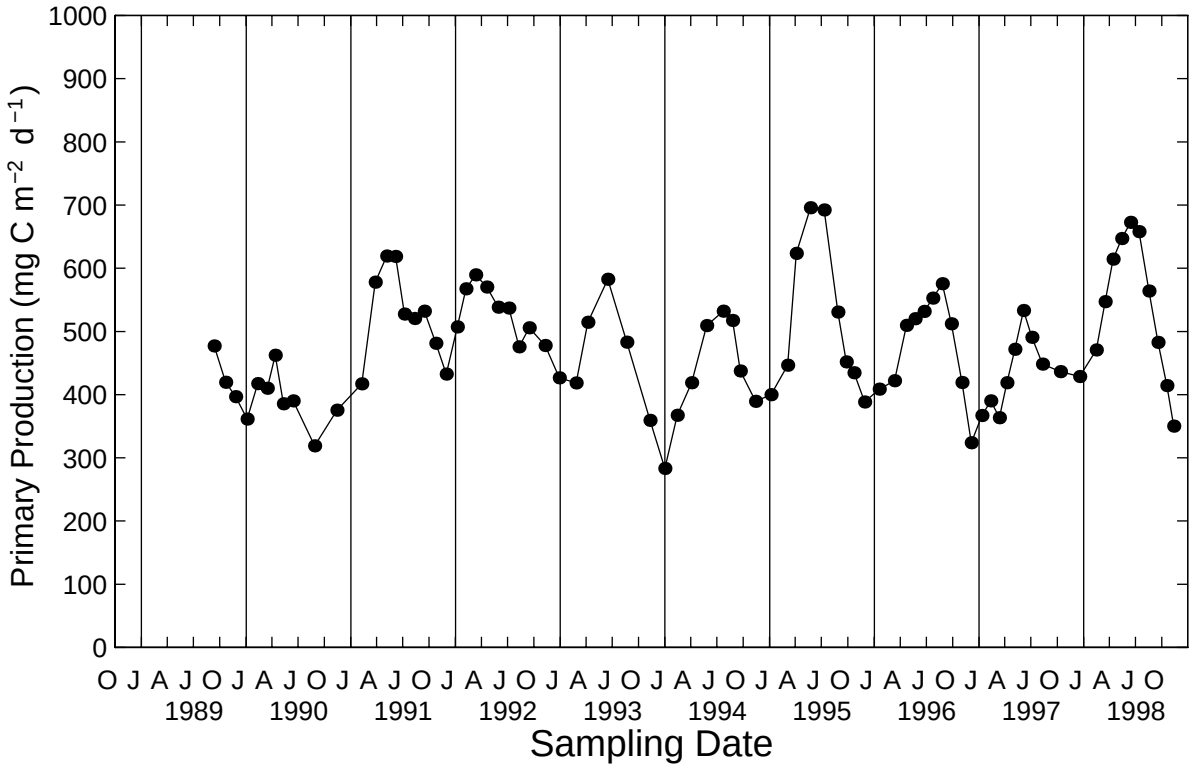
Primary Production (mg C m^{-2} d^{-1})
0
100
200
300
400
500
600
700
800
900
1000
O J A J O J A J O J A J O J A J O J A J O J A J O J A J O J A J O J A J O J A J O J A J O
1989
1990
1991
1992
1993
1994
1995
1996
1997
1998
Sampling Date

Figure 6.6.1

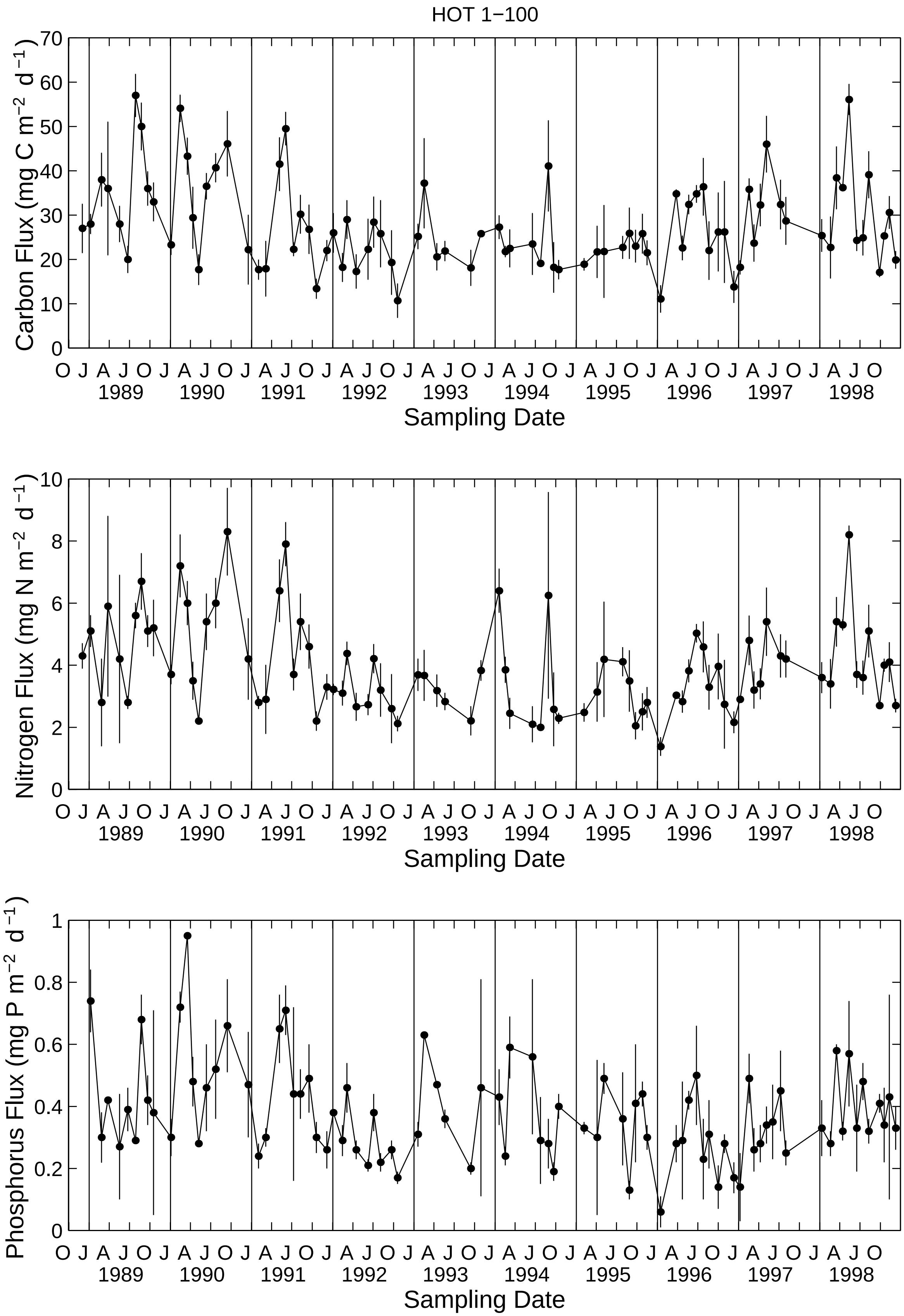

Figure 6.6.2, 6.6.3, 6.6.4

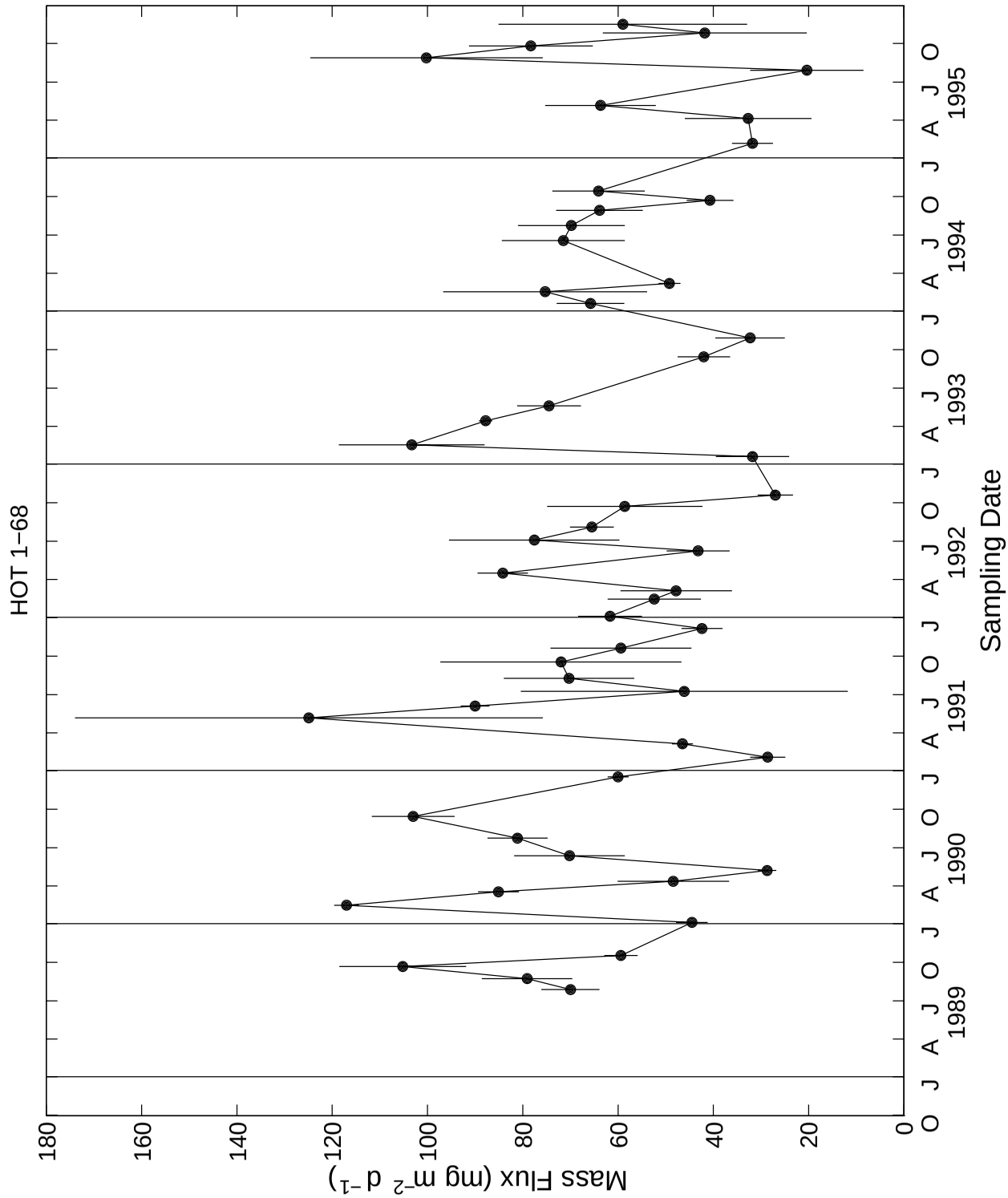
HOT 1−68
Mass Flux (mg m⁻² d⁻¹)
0
20
40
60
80
100
120
140
160
180
O J A J O J A J O J A J O J A J O J A J O
1989
1990
1991
1992
1993
1994
1995
Sampling Date

Figure 6.6.5

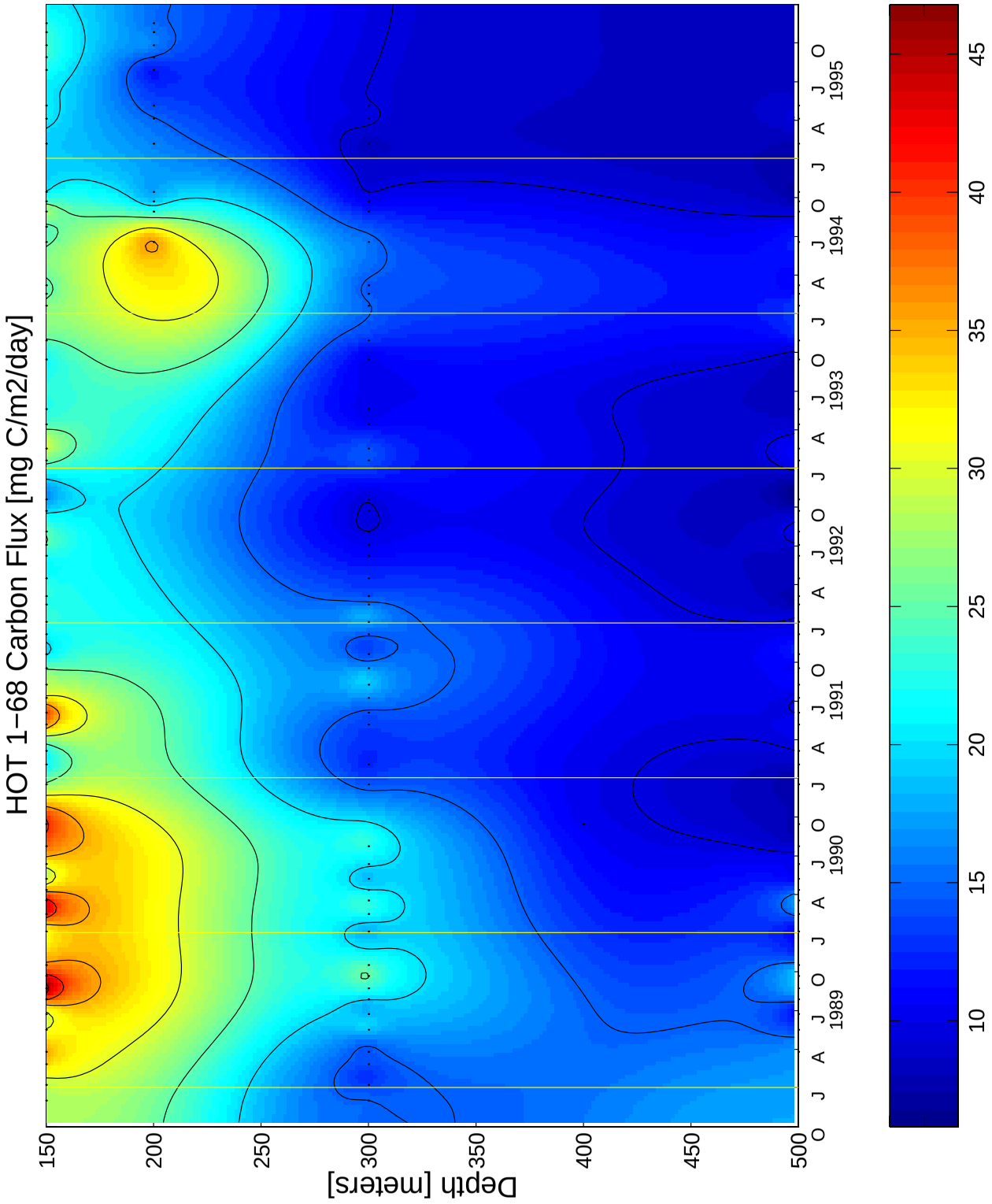
HOT 1−68 Carbon Flux [mg C/m2/day]
Depth [meters]
150
200
250
300
350
400
450
500
O J A J O J A J O J A J O J A J O J A J O
1989
1990
1991
1992
1993
1994
1995
10
15
20
25
30
35
40
45

Figure 6.6.6

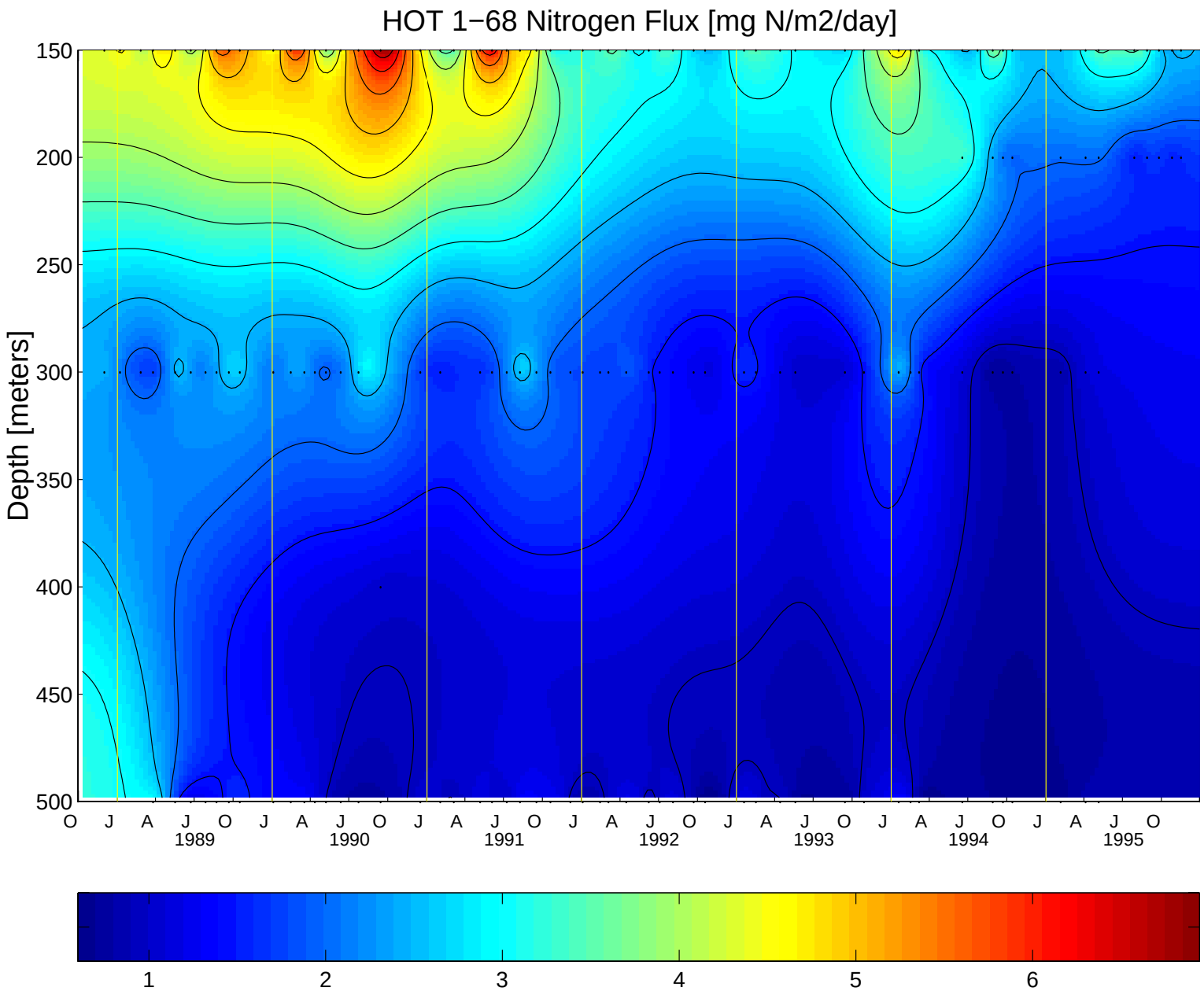
HOT 1−68 Nitrogen Flux [mg N/m2/day]
Depth [meters]
150
200
250
300
350
400
450
500
O J A J O J A J O J A J O J A J O J A J O J A J O J A J O
1989
1990
1991
1992
1993
1994
1995
1
2
3
4
5
6

Figure 6.6.7

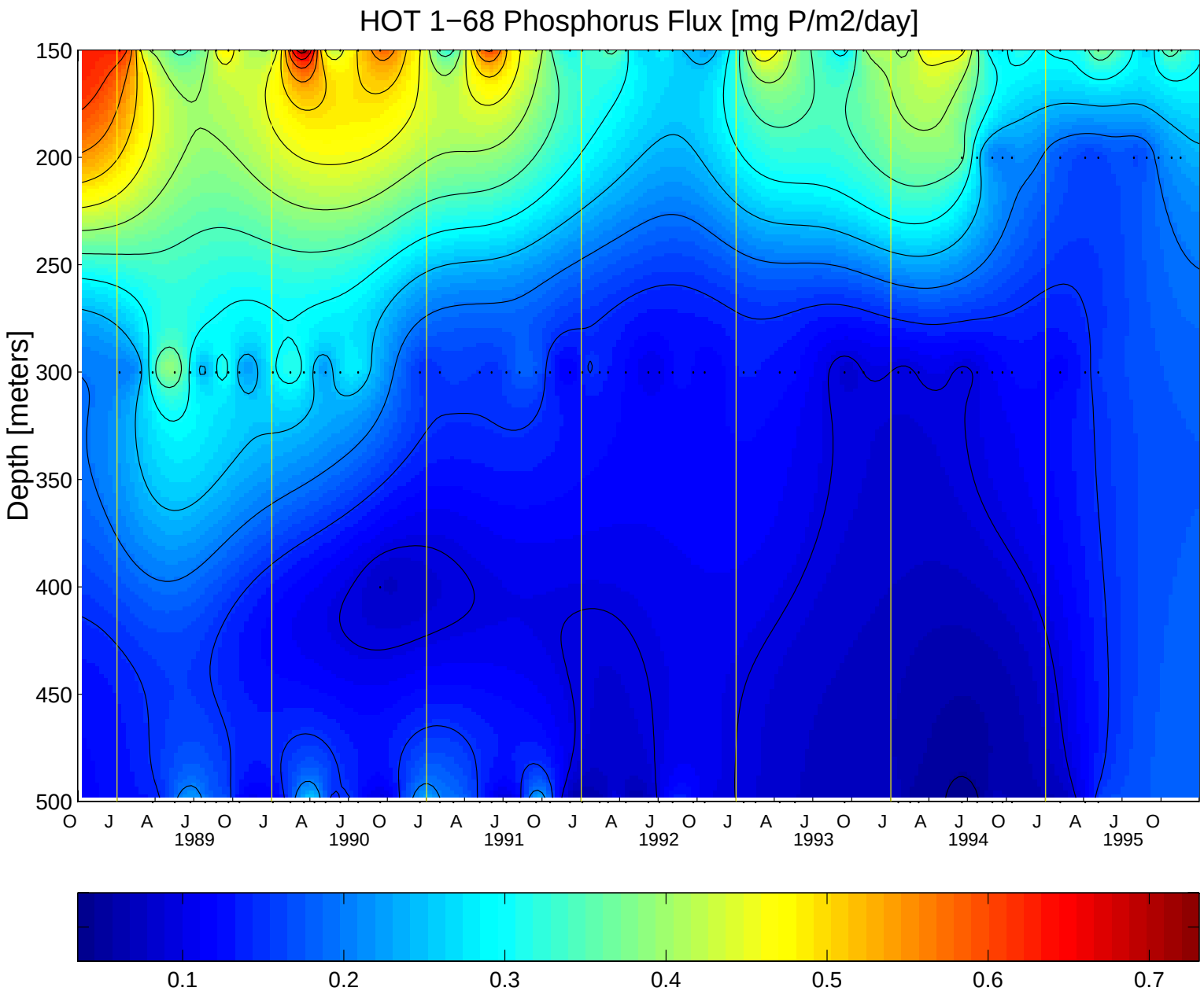
HOT 1−68 Phosphorus Flux [mg P/m2/day]
Depth [meters]
150
200
250
300
350
400
450
500
O J A J O J A J O J A J O J A J O J A J O J A J O J A J O J A J O
1989
1990
1991
1992
1993
1994
1995
0.1
0.2
0.3
0.4
0.5
0.6
0.7

Figure 6.6.8

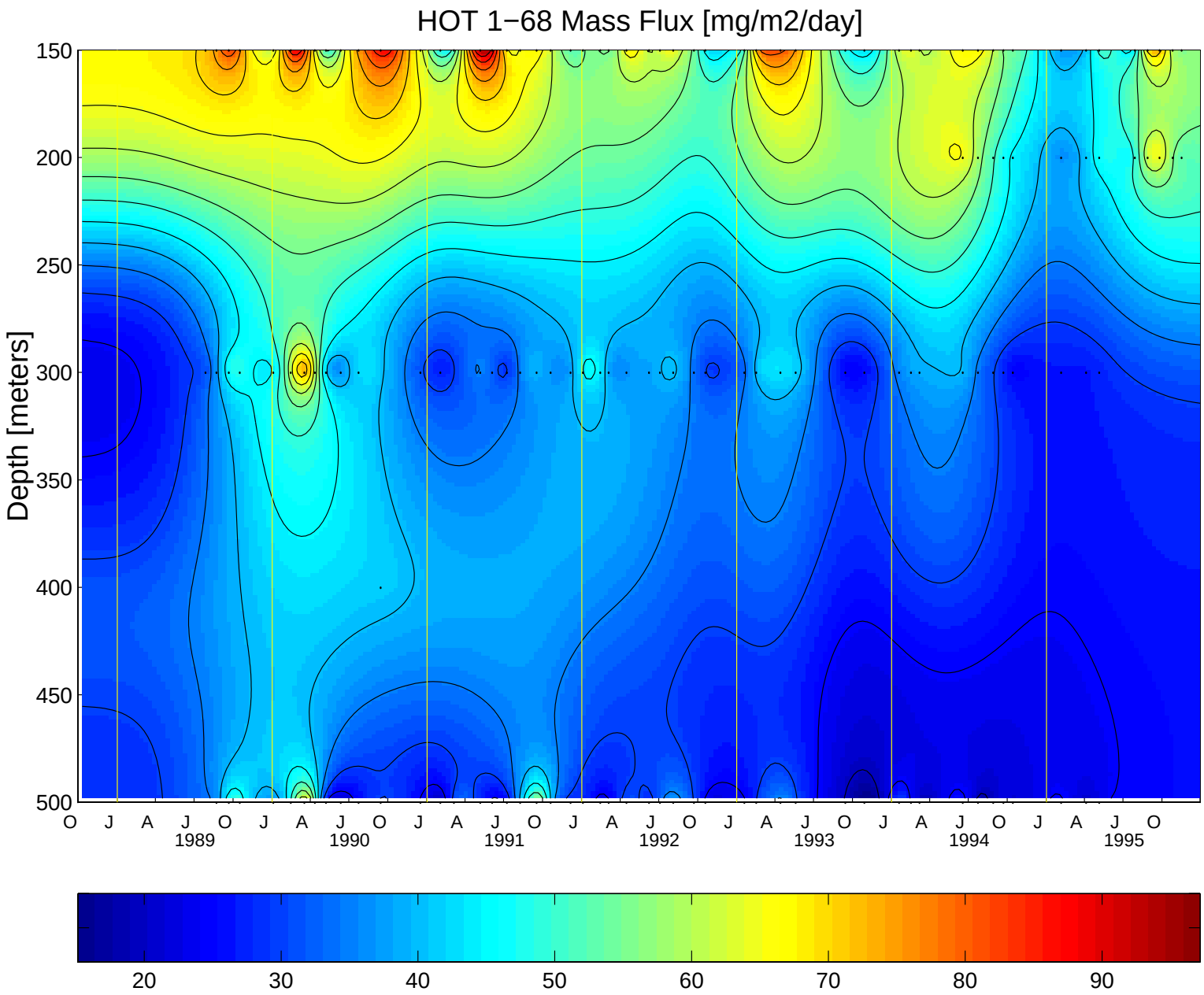
HOT 1−68 Mass Flux [mg/m2/day]
Depth [meters]
150
200
250
300
350
400
450
500
O J A J O J A J O J A J O J A J O J A J O J A J O J A J O
1989
1990
1991
1992
1993
1994
1995
20
30
40
50
60
70
80
90

Figure 6.6.9

6.7. ADCP Measurements

For each cruise with shipboard ADCP, the following figures are provided:

Figures 6.7.1a-i: Velocity fields at Station ALOHA. Top panel shows hourly averages at 20-m depth intervals while the ship was on station. The orientation of each stick gives the direction of the current: up is northward, to the right is eastward. The bottom panel shows the results of a least-squares fit of the hourly averages to a mean, trend, semidiurnal and diurnal tides and an inertial cycle. In the first column, the arrow shows the mean current, and the headless stick shows the sum of the mean plus the trend at the end of the station. For each harmonic, the current ellipse is shown in the first column. The orientation of the stick in the second column shows the direction of that harmonic component of the current at the beginning of the station, and the arrowhead at the end of the stick shows the direction of rotation of the current vector around the ellipse. The gap in the on-station data of HOT-60 is due to drift away from ALOHA during a period of equipment problems exacerbated by bad weather. Gaps in HOT-63 are due to excursions to retrieve the primary productivity array and the optical mooring buoy.

Figures 6.7.2a-i: Velocity field on the transits to and from the Station ALOHA and Station 3. Velocity is shown as a function of latitude, averaged in 10-minute time intervals. On the southward transit of HOT-63 the ship was diverted 100 km west of the normal track to assist a vessel in distress.

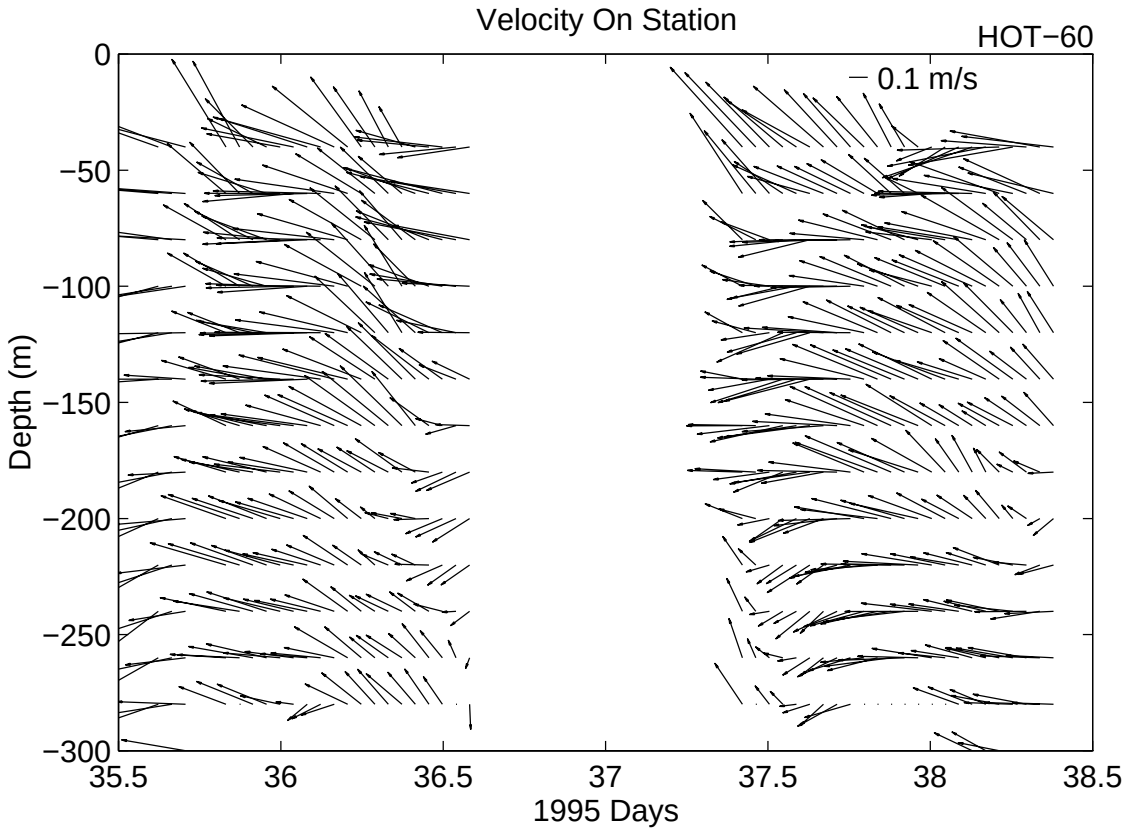
Velocity On Station
HOT−60
− 0.1 m/s
0
−50
−100
−150
−200
−250
−300
Depth (m)
35.5
36
36.5
37
37.5
38
38.5
1995 Days

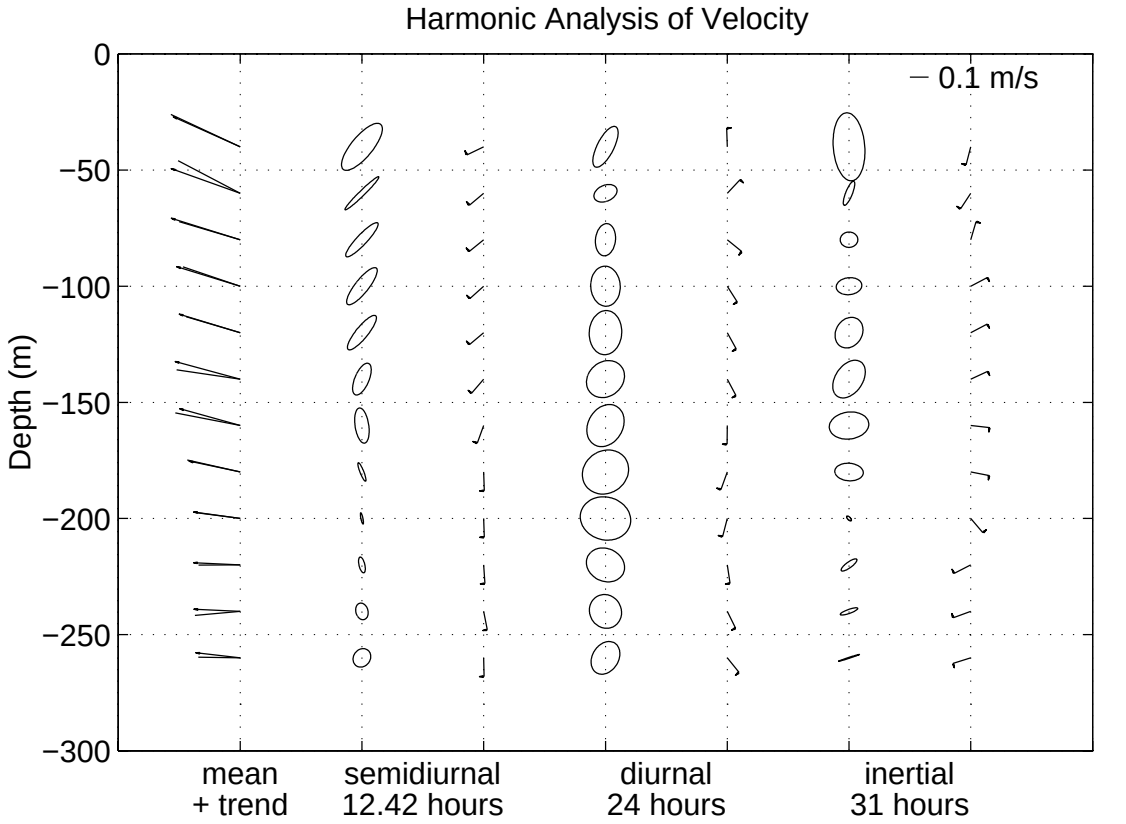
Harmonic Analysis of Velocity
− 0.1 m/s
0
−50
−100
−150
−200
−250
−300
Depth (m)
mean
+ trend
semidiurnal
12.42 hours
diurnal
24 hours
inertial
31 hours

Figure 6.7.1a

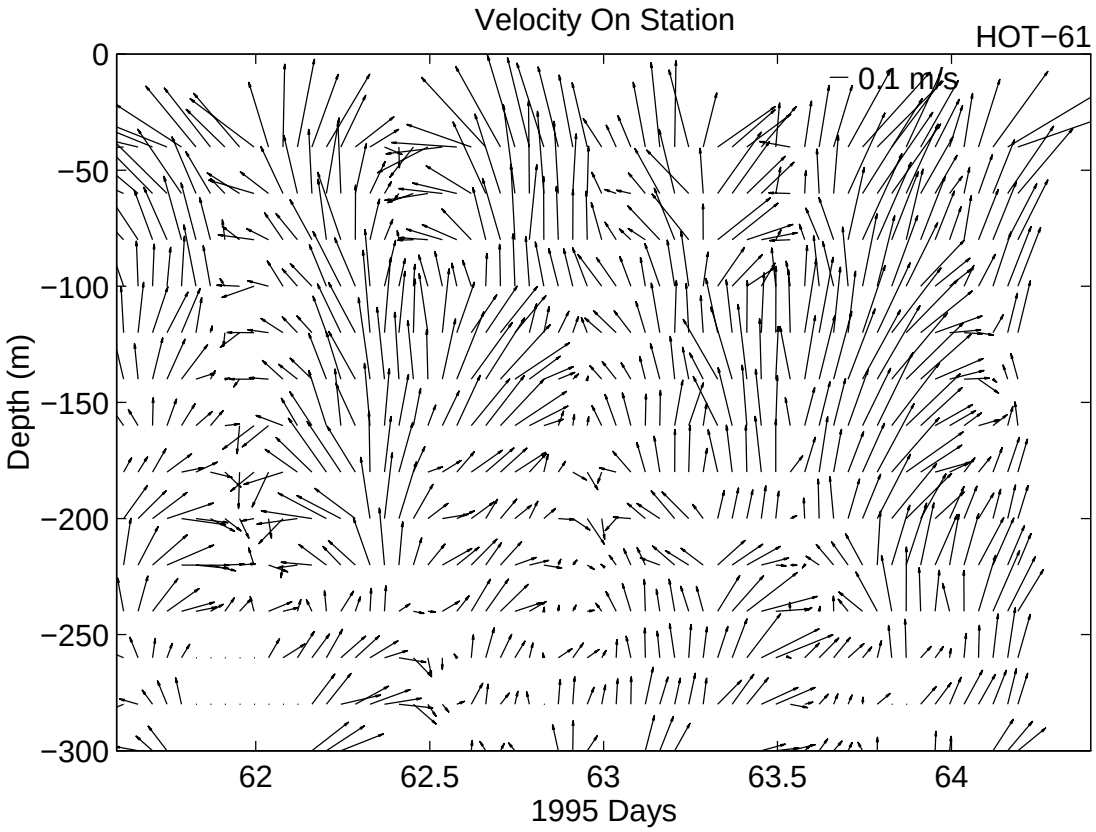
Velocity On Station
HOT−61
0.1 m/s
0
−50
−100
−150
−200
−250
−300
Depth (m)
62
62.5
63
63.5
64
1995 Days

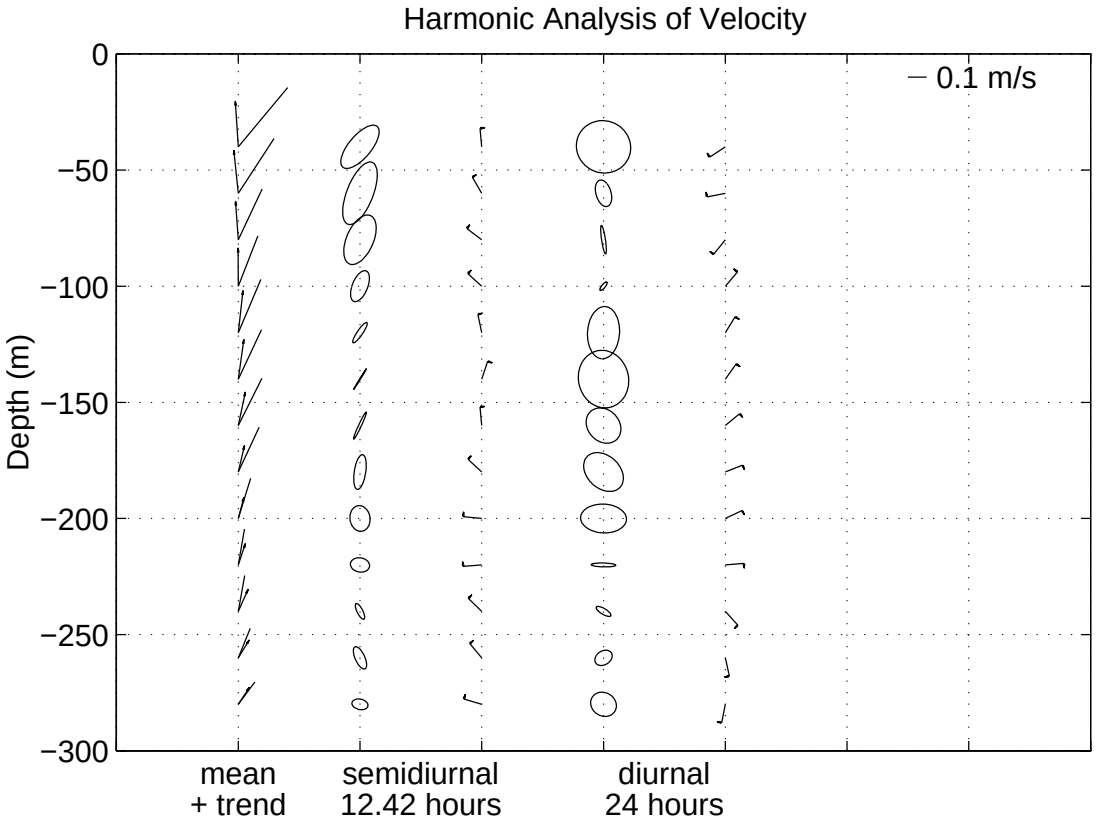
Harmonic Analysis of Velocity
0.1 m/s
0
−50
−100
−150
−200
−250
−300
Depth (m)
mean
+ trend
semidiurnal
12.42 hours
diurnal
24 hours

Figure 6.7.1b

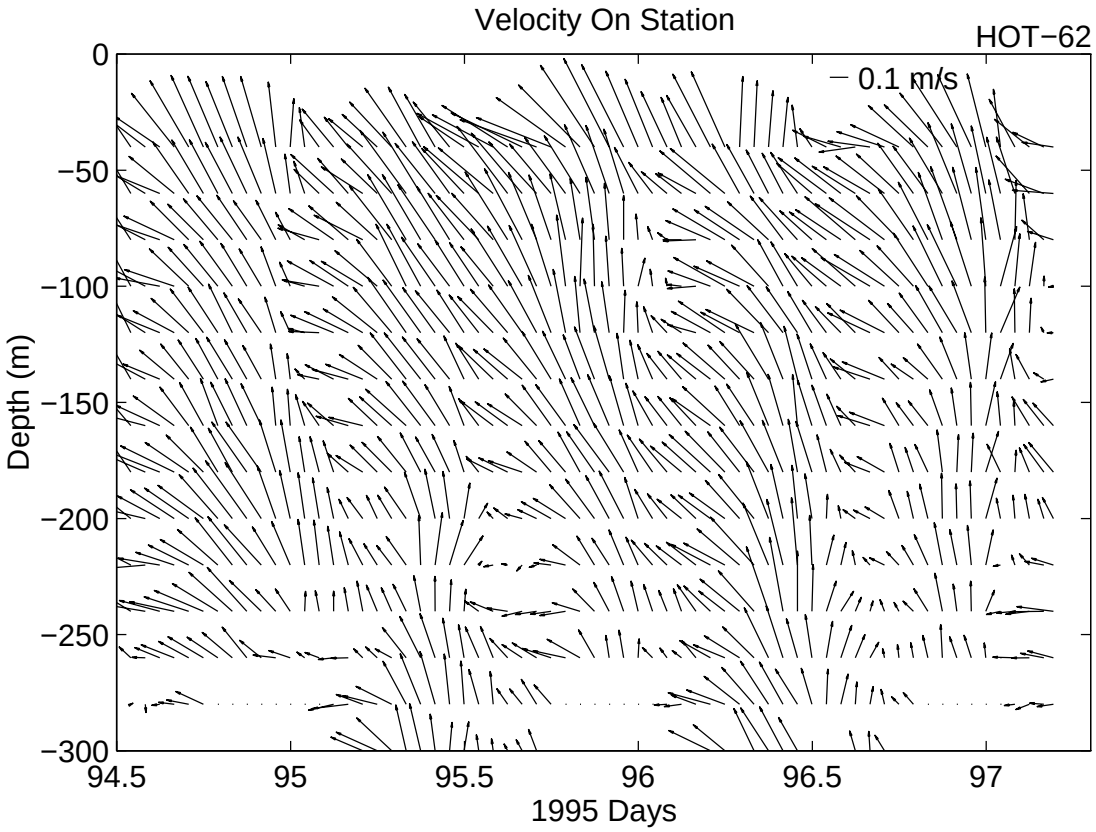
Velocity On Station
HOT−62
− 0.1 m/s
0
−50
−100
−150
−200
−250
−300
Depth (m)
94.5
95
95.5
96
96.5
97
1995 Days

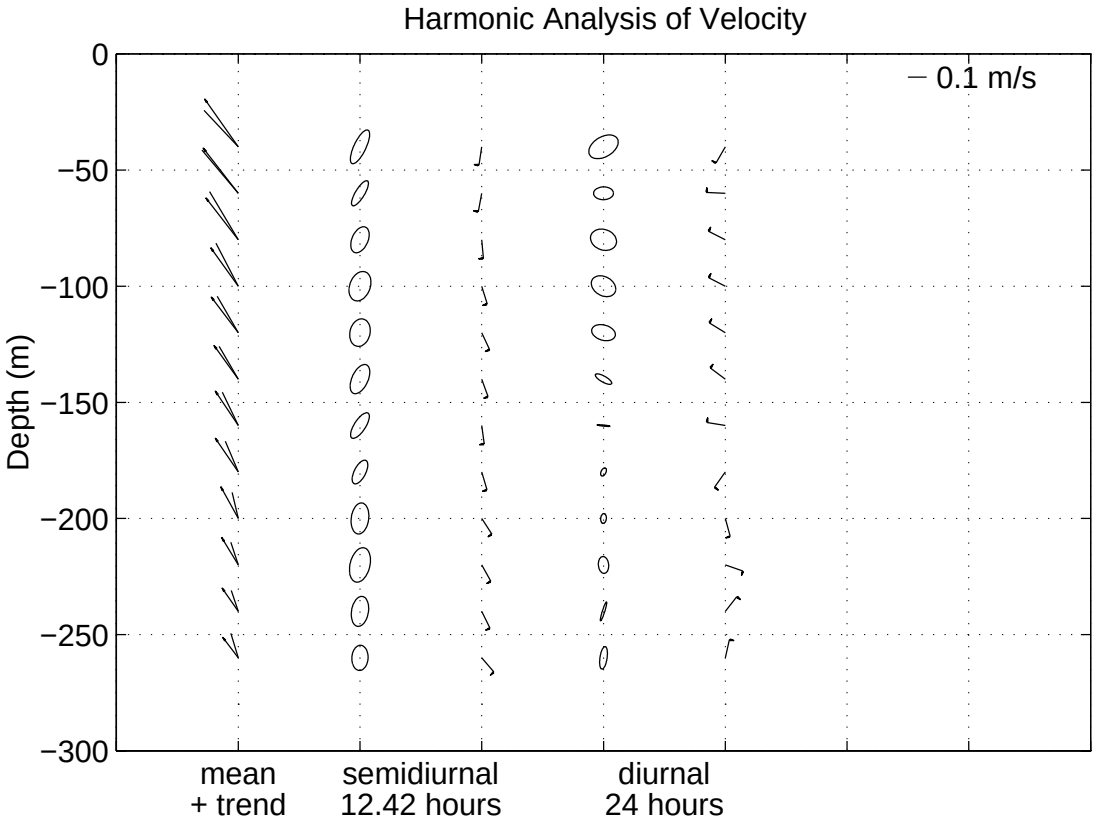
Harmonic Analysis of Velocity
− 0.1 m/s
0
−50
−100
−150
−200
−250
−300
Depth (m)
mean
+ trend
semidiurnal
12.42 hours
diurnal
24 hours

Figure 6.7.1c

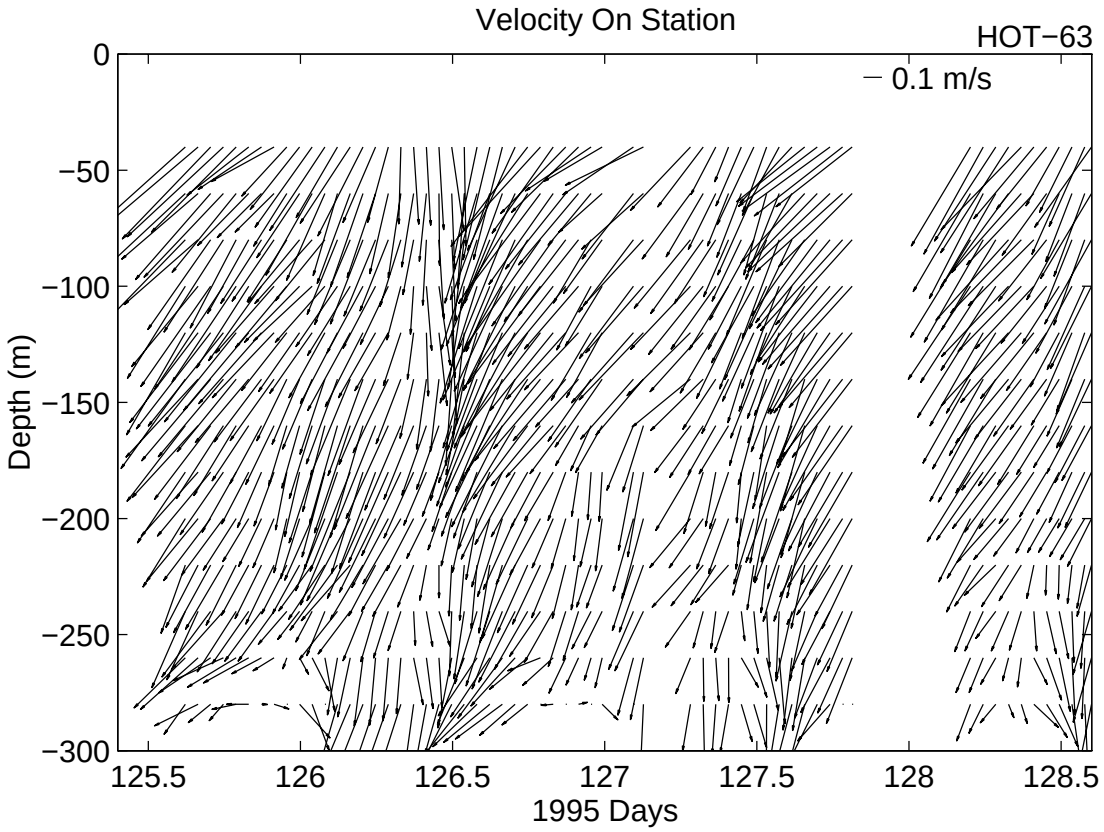
Velocity On Station
HOT−63
0.1 m/s
0
−50
−100
−150
−200
−250
−300
Depth (m)
125.5
126
126.5
127
127.5
128
128.5
1995 Days

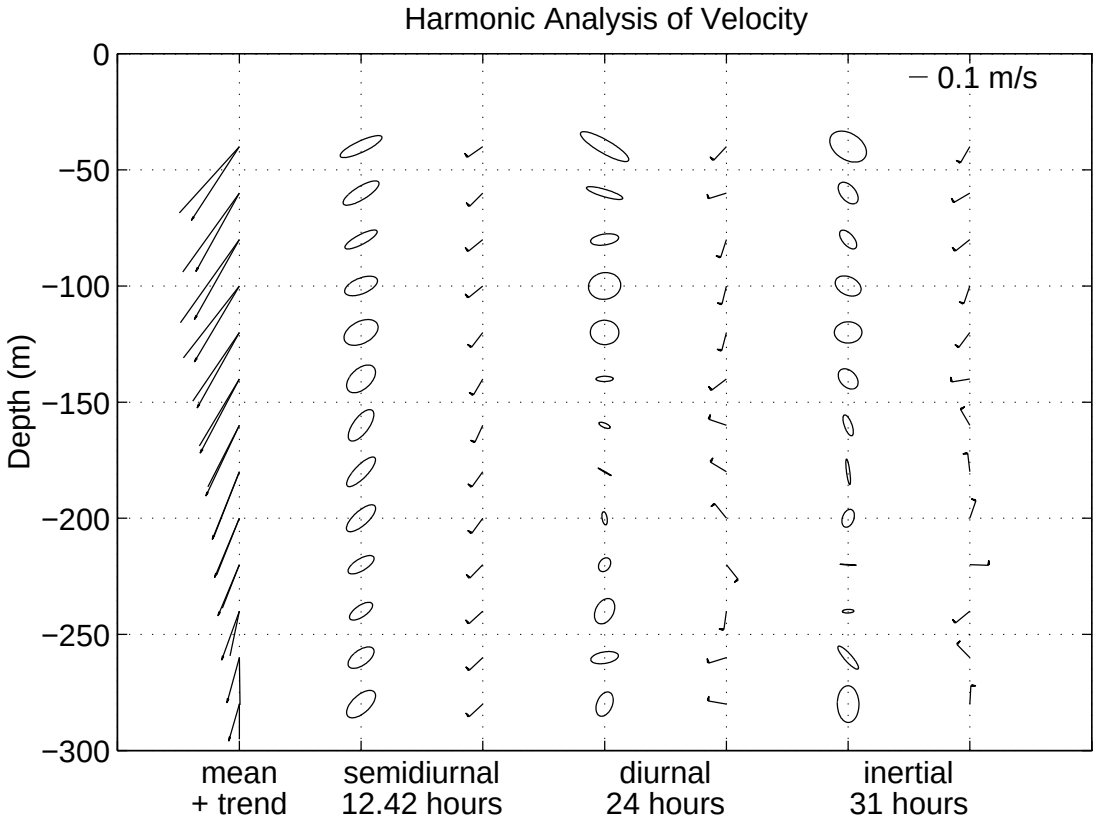
Harmonic Analysis of Velocity
0.1 m/s
0
−50
−100
−150
−200
−250
−300
Depth (m)
mean
+ trend
semidiurnal
12.42 hours
diurnal
24 hours
inertial
31 hours

Figure 6.7.1d

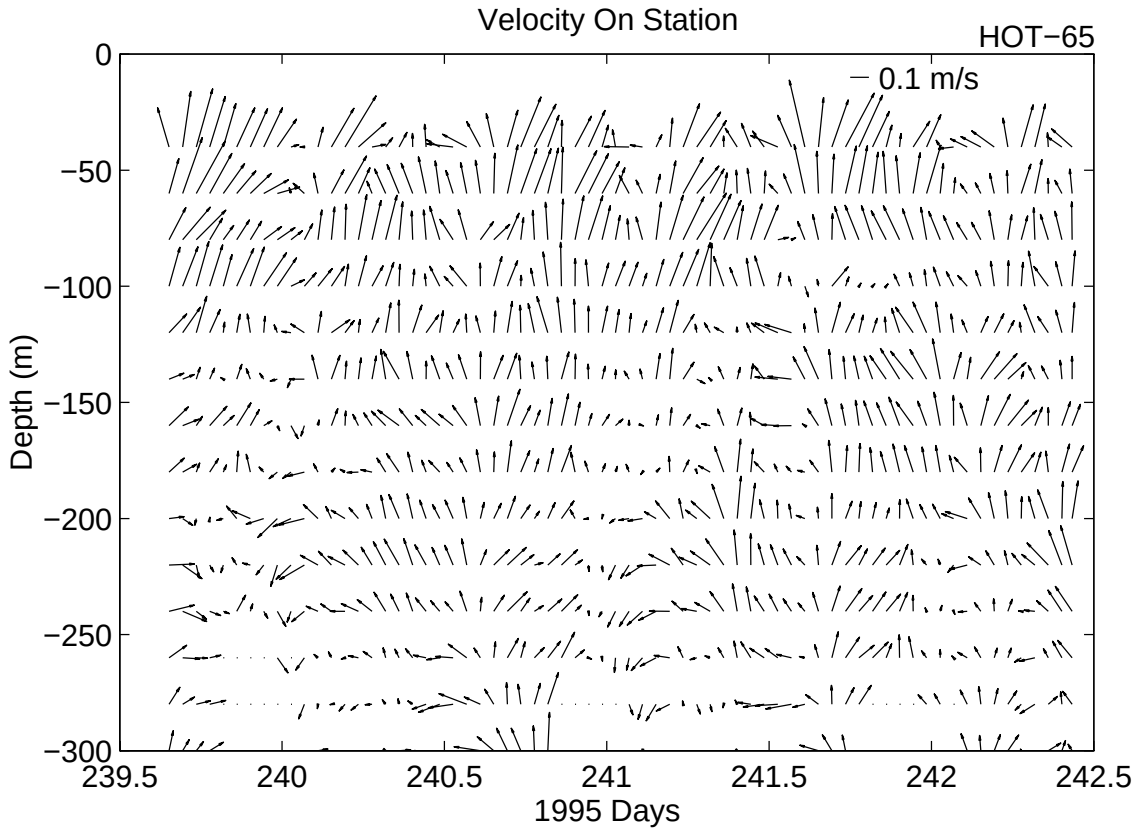
Velocity On Station
HOT−65
0.1 m/s
0
−50
−100
−150
−200
−250
−300
Depth (m)
239.5
240
240.5
241
241.5
242
242.5
1995 Days

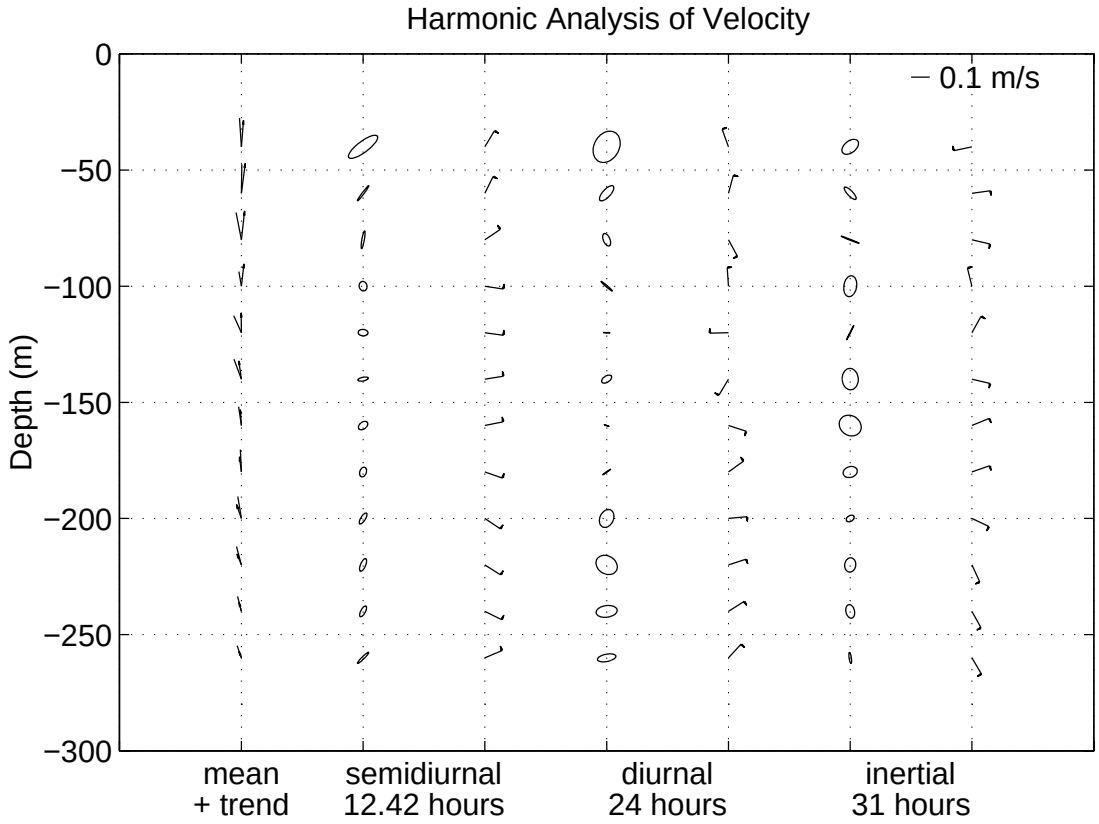
Harmonic Analysis of Velocity
0.1 m/s
0
−50
−100
−150
−200
−250
−300
Depth (m)
mean
+ trend
semidiurnal
12.42 hours
diurnal
24 hours
inertial
31 hours

Figure 6.7.1e

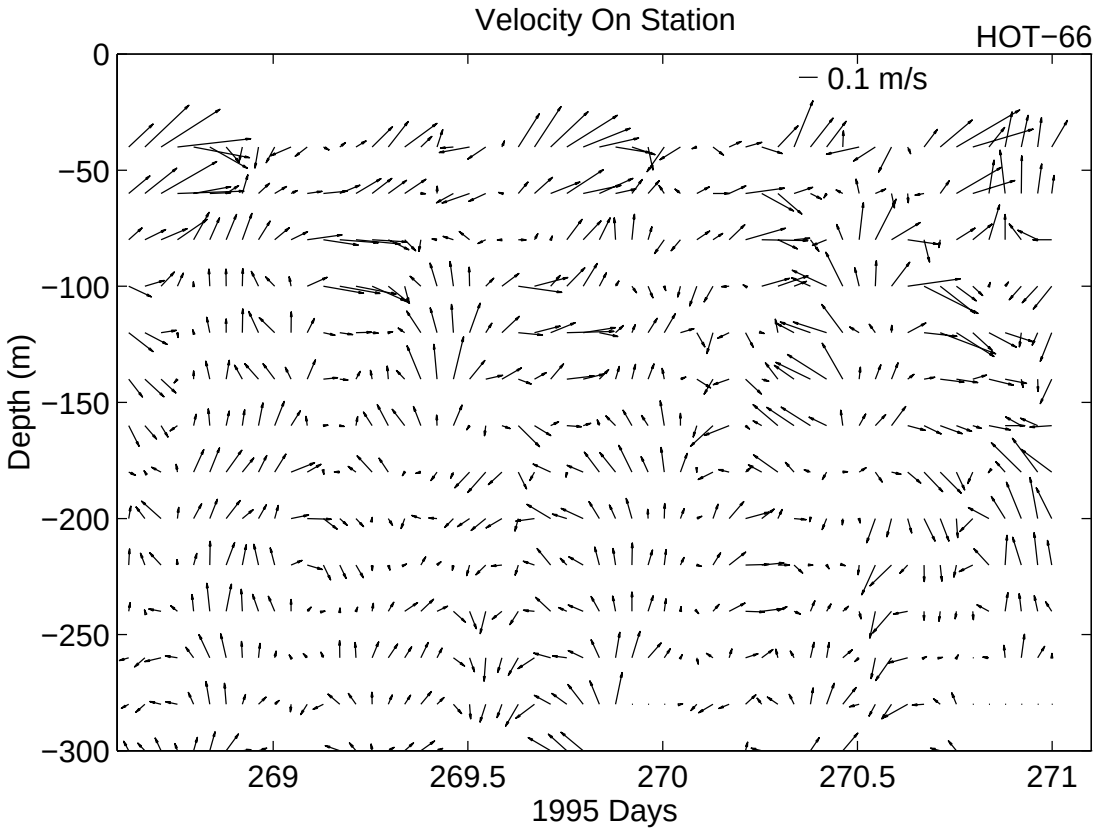
Velocity On Station
HOT−66
0.1 m/s
0
−50
−100
−150
−200
−250
−300
Depth (m)
269
269.5
270
270.5
271
1995 Days

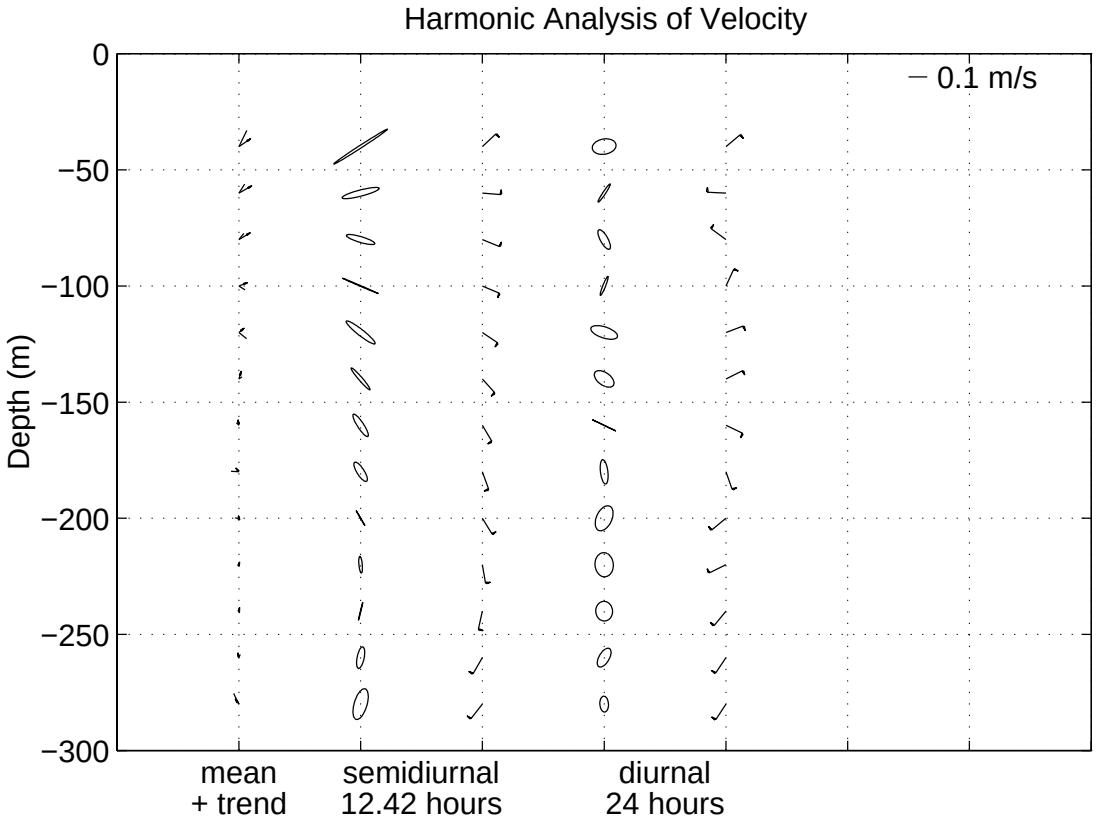
Harmonic Analysis of Velocity
0.1 m/s
0
−50
−100
−150
−200
−250
−300
Depth (m)
mean
+ trend
semidiurnal
12.42 hours
diurnal
24 hours

Figure 6.7.1f

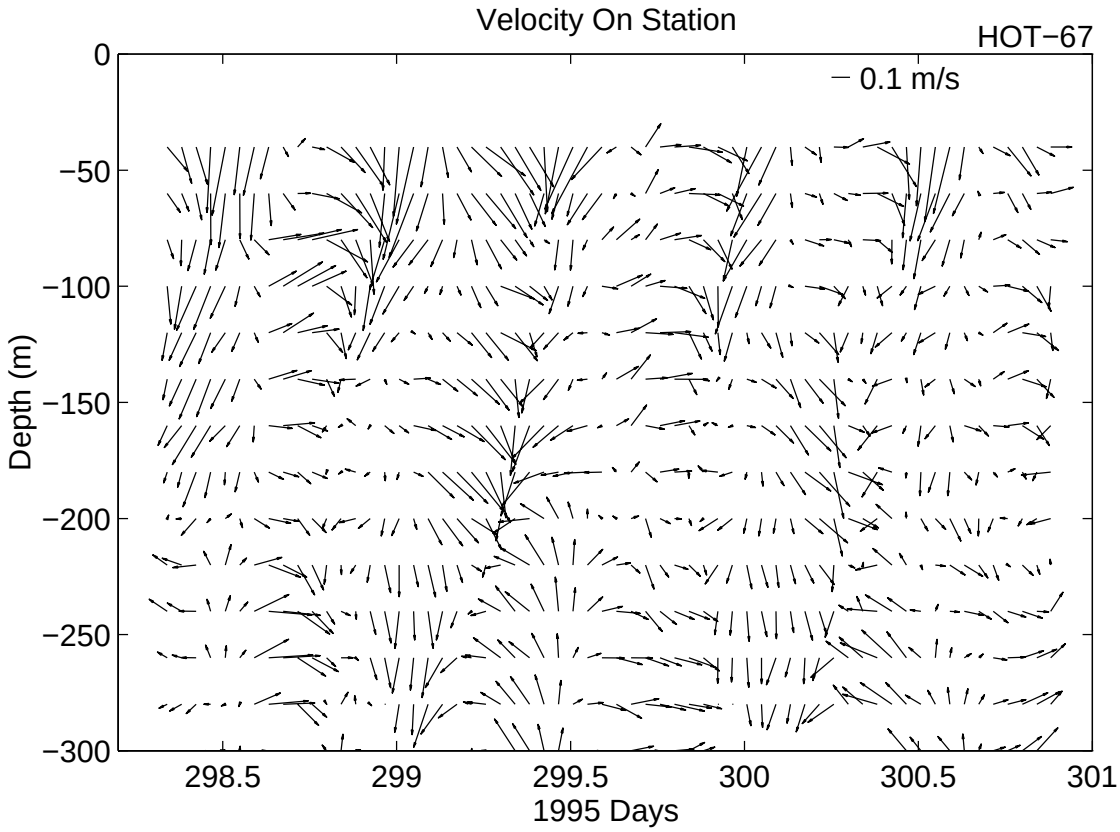
Velocity On Station
HOT−67
0.1 m/s
0
−50
−100
−150
−200
−250
−300
Depth (m)
298.5
299
299.5
300
300.5
301
1995 Days

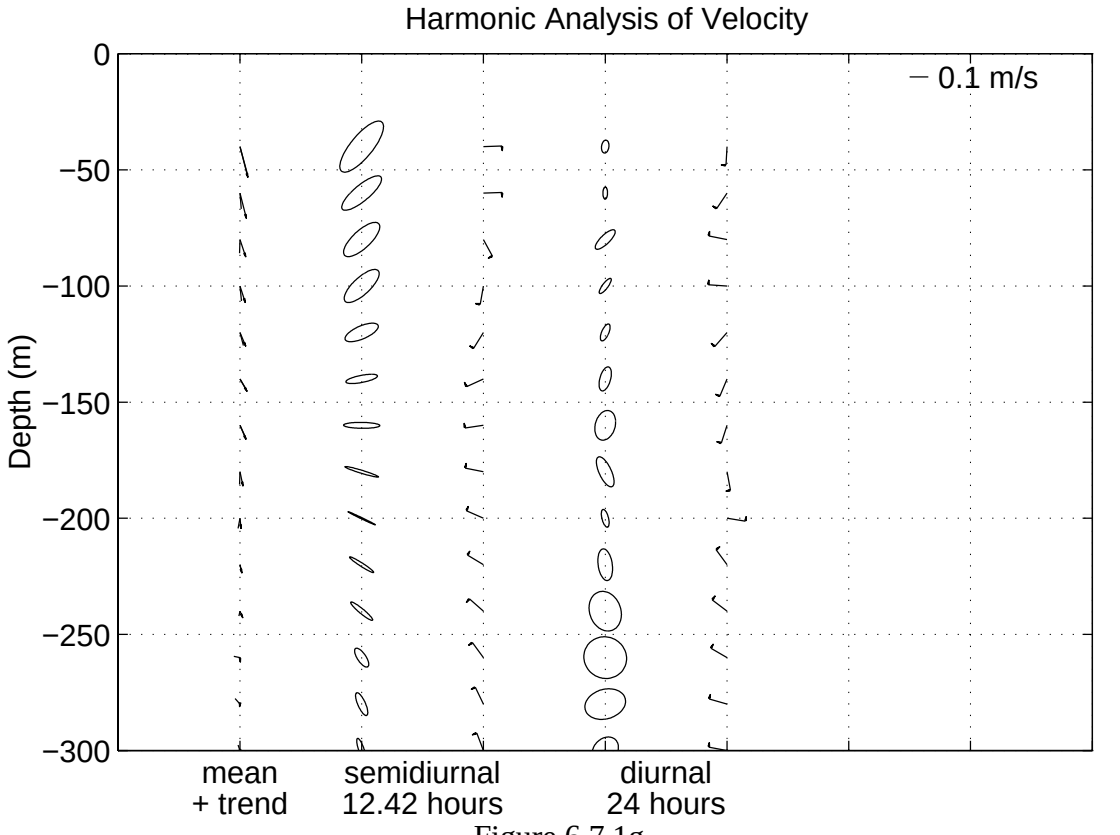
Harmonic Analysis of Velocity
0.1 m/s
0
−50
−100
−150
−200
−250
−300
Depth (m)
mean
+ trend
semidiurnal
12.42 hours
diurnal
24 hours

Figure 6.7.1g

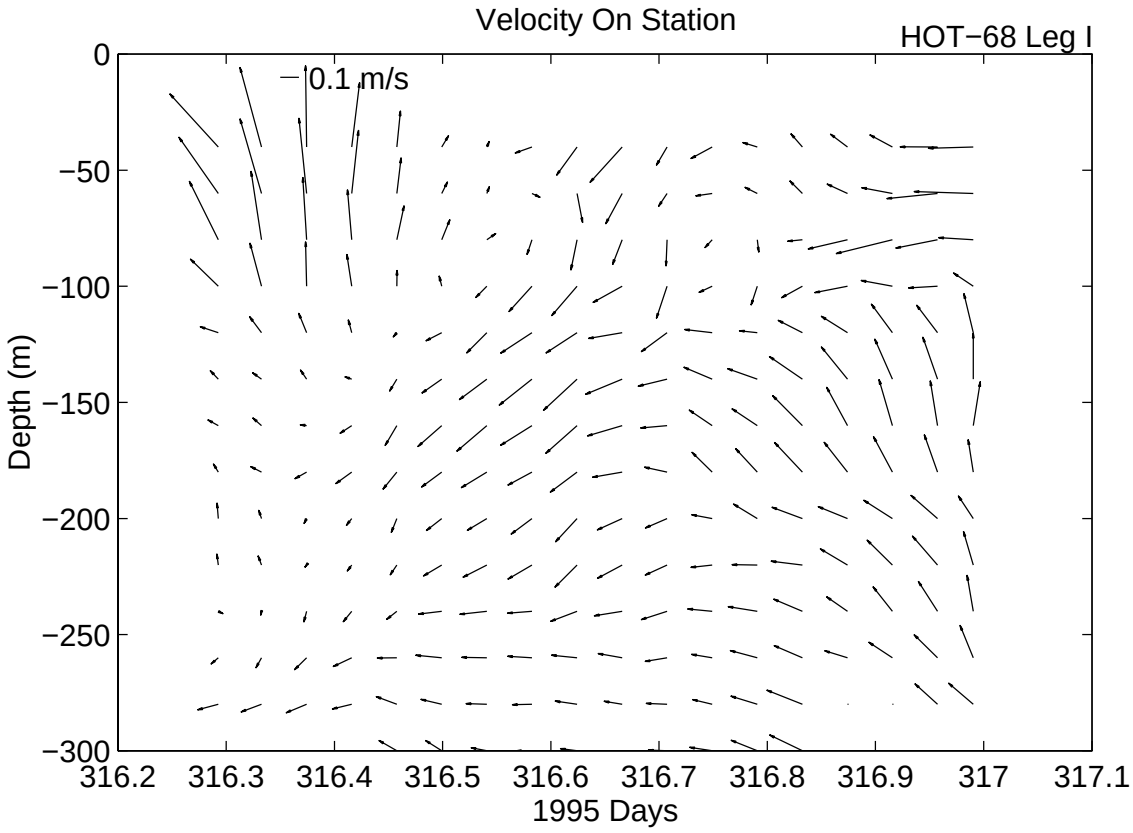
Velocity On Station
HOT−68 Leg I
0.1 m/s
Depth (m)
0
−50
−100
−150
−200
−250
−300
316.2
316.3
316.4
316.5
316.6
316.7
316.8
316.9
317
317.1
1995 Days

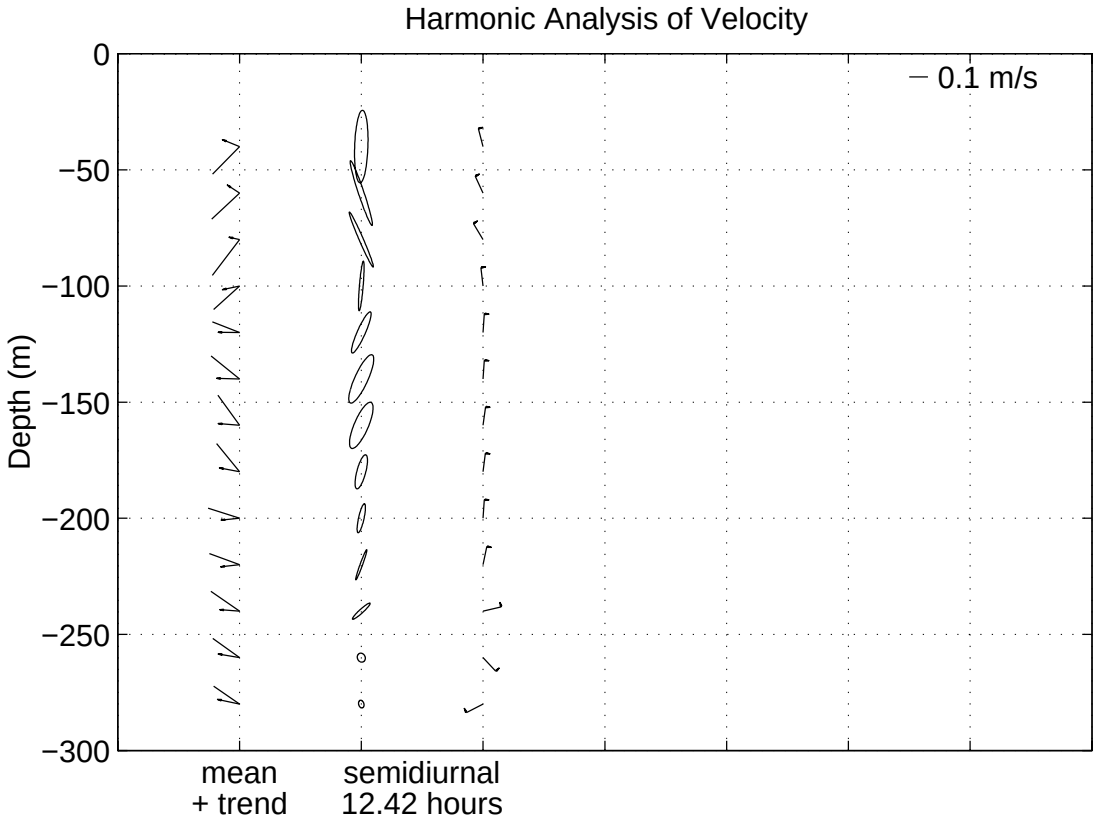
Harmonic Analysis of Velocity
0.1 m/s
Depth (m)
0
−50
−100
−150
−200
−250
−300
mean
+ trend
semidiurnal
12.42 hours

Figure 6.7.1h

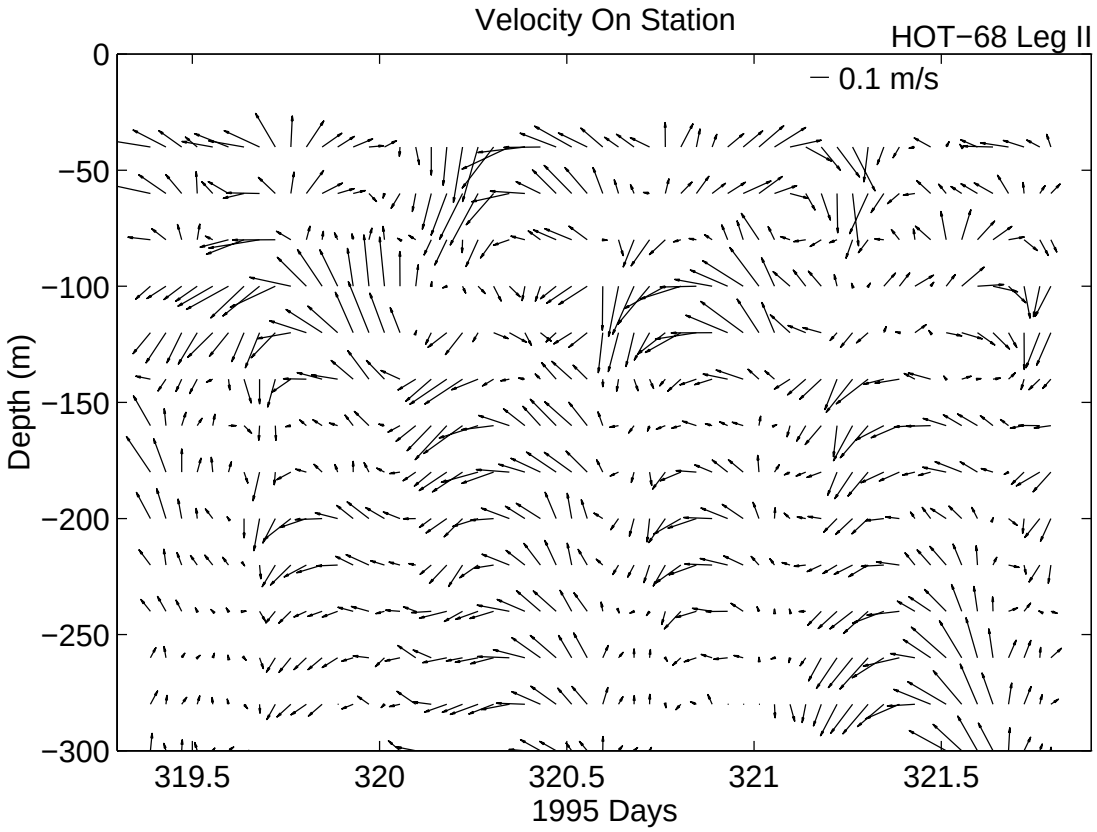
Velocity On Station
HOT−68 Leg II
− 0.1 m/s
0
−50
−100
−150
−200
−250
−300
Depth (m)
319.5
320
320.5
321
321.5
1995 Days

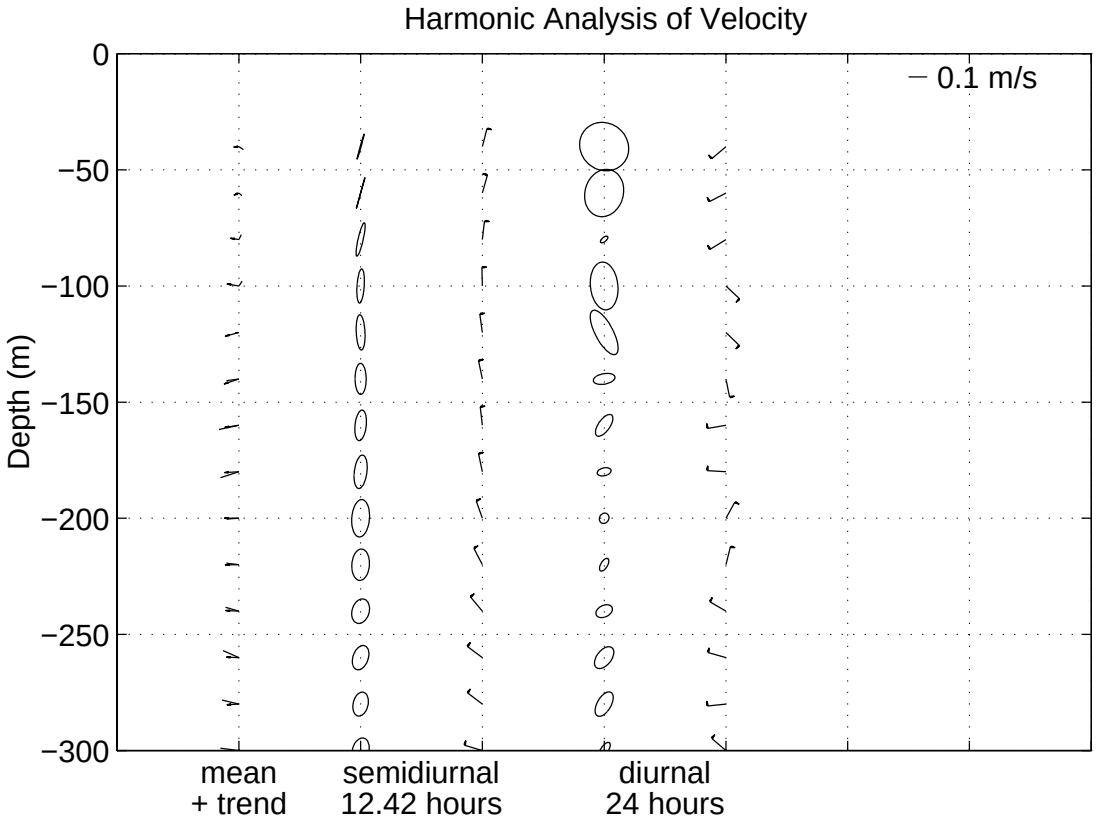
Harmonic Analysis of Velocity
− 0.1 m/s
0
−50
−100
−150
−200
−250
−300
Depth (m)
mean
+ trend
semidiurnal
12.42 hours
diurnal
24 hours

Figure 6.7.1i

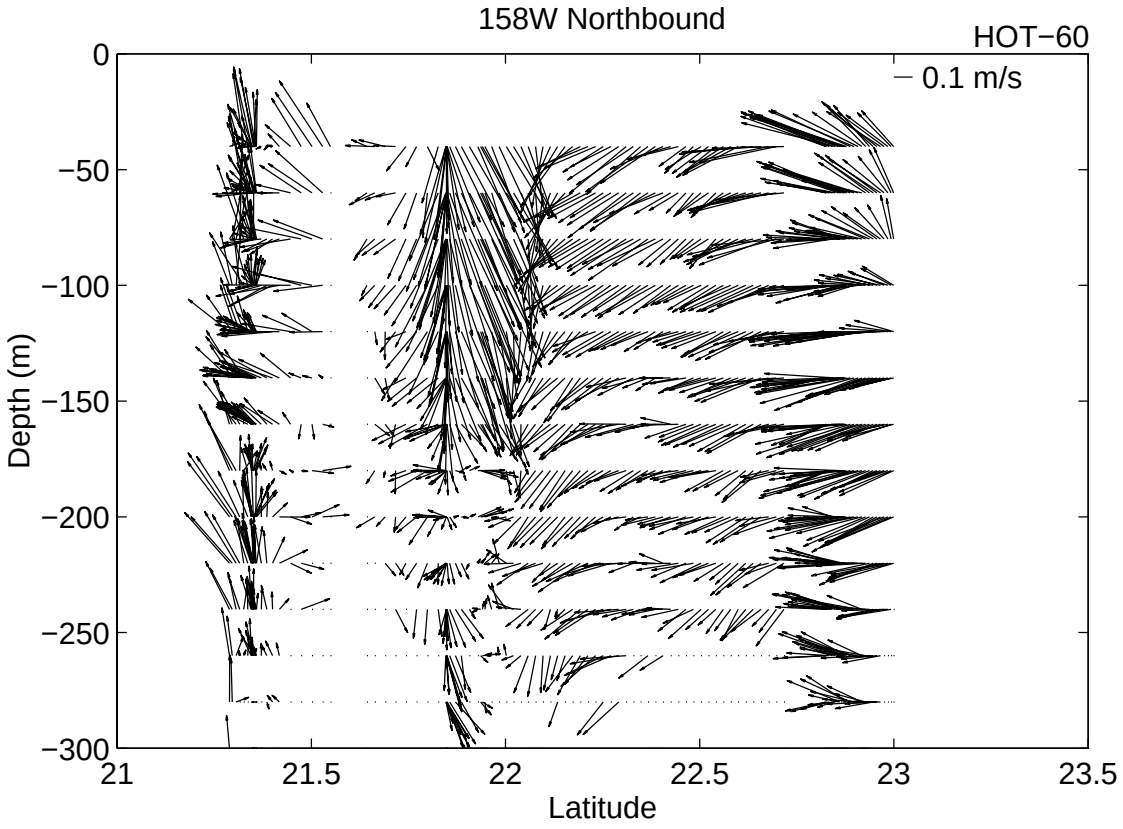
158W Northbound
HOT−60
0.1 m/s
0
−50
−100
−150
−200
−250
−300
Depth (m)
21
21.5
22
22.5
23
23.5
Latitude

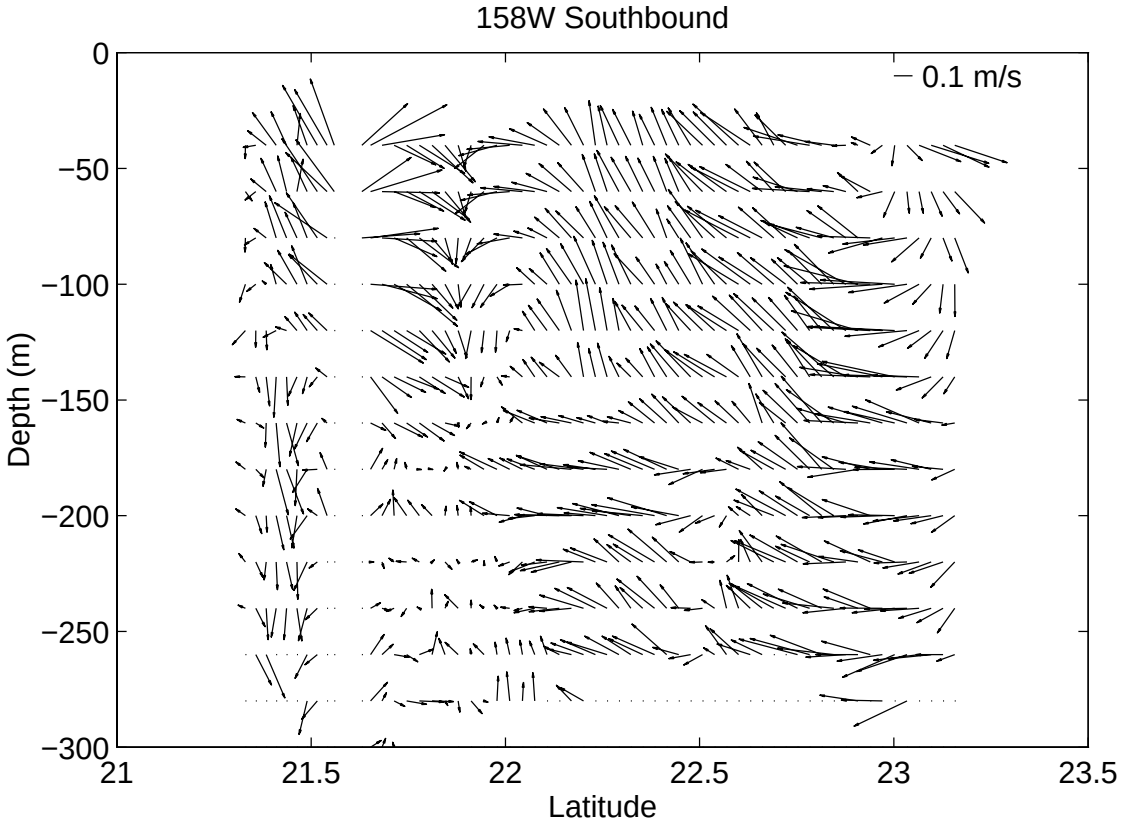
158W Southbound
0.1 m/s
0
−50
−100
−150
−200
−250
−300
Depth (m)
21
21.5
22
22.5
23
23.5
Latitude

Figure 6.7.2a

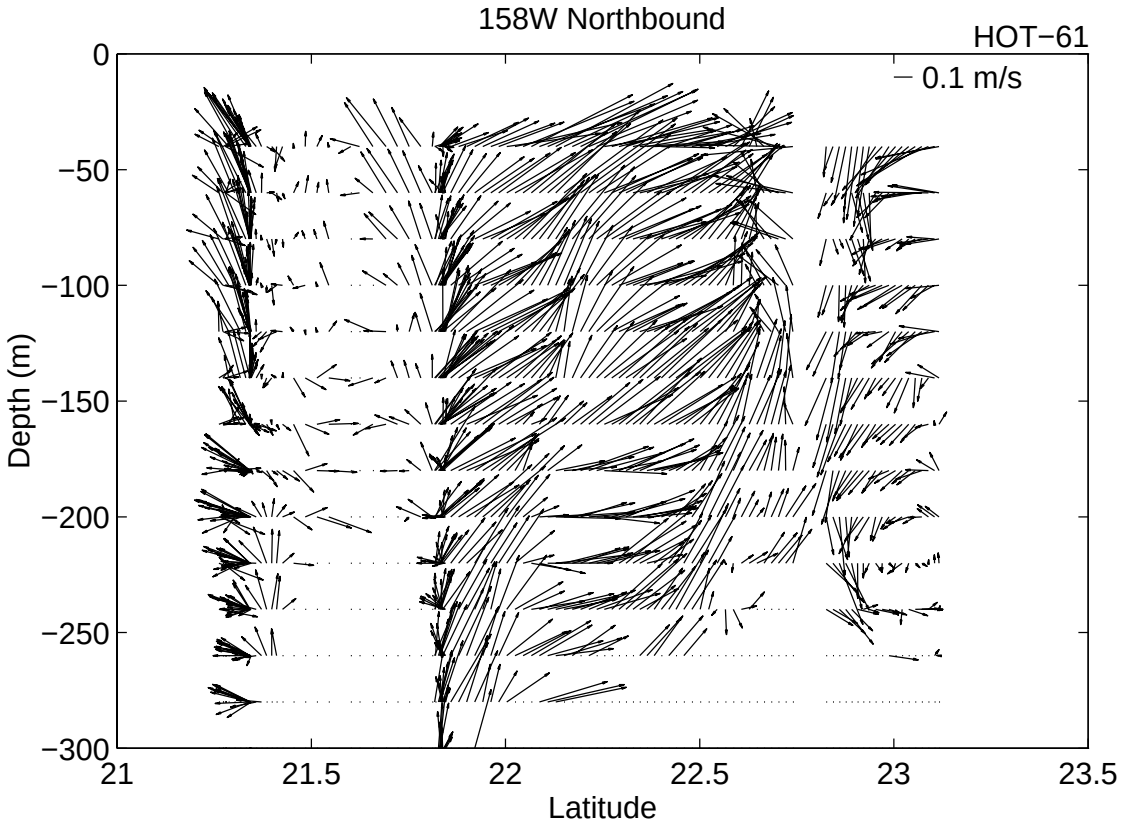
158W Northbound
HOT−61
0.1 m/s
0
−50
−100
−150
−200
−250
−300
Depth (m)
21
21.5
22
22.5
23
23.5
Latitude

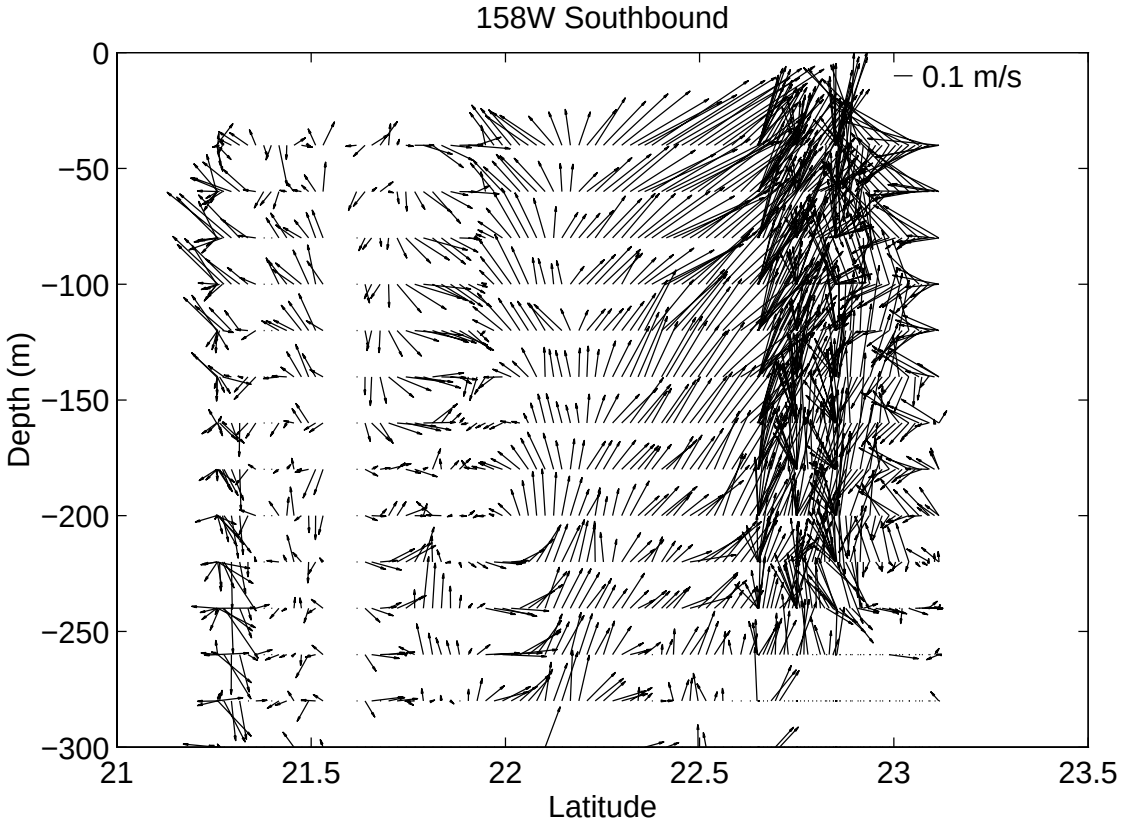
158W Southbound
0.1 m/s
0
−50
−100
−150
−200
−250
−300
Depth (m)
21
21.5
22
22.5
23
23.5
Latitude

Figure 6.7.2b

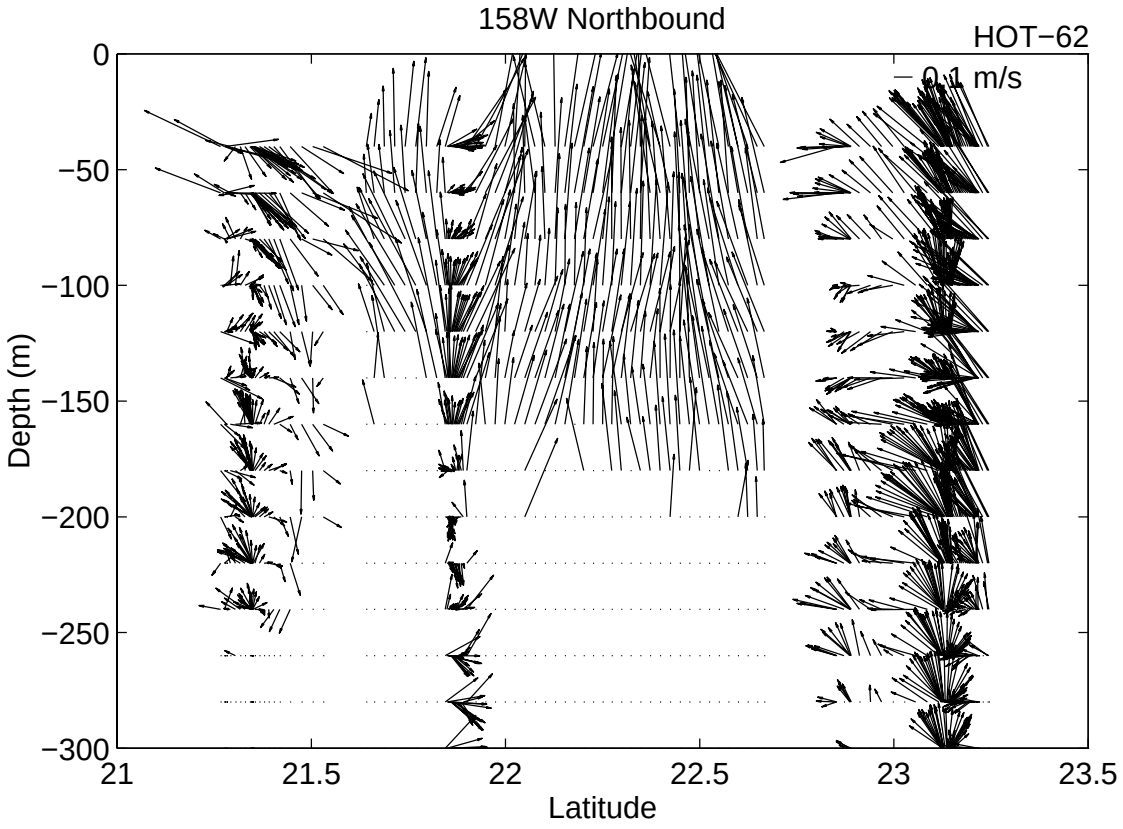
158W Northbound
HOT−62
− 0.1 m/s
0
−50
−100
−150
−200
−250
−300
Depth (m)
21
21.5
22
22.5
23
23.5
Latitude

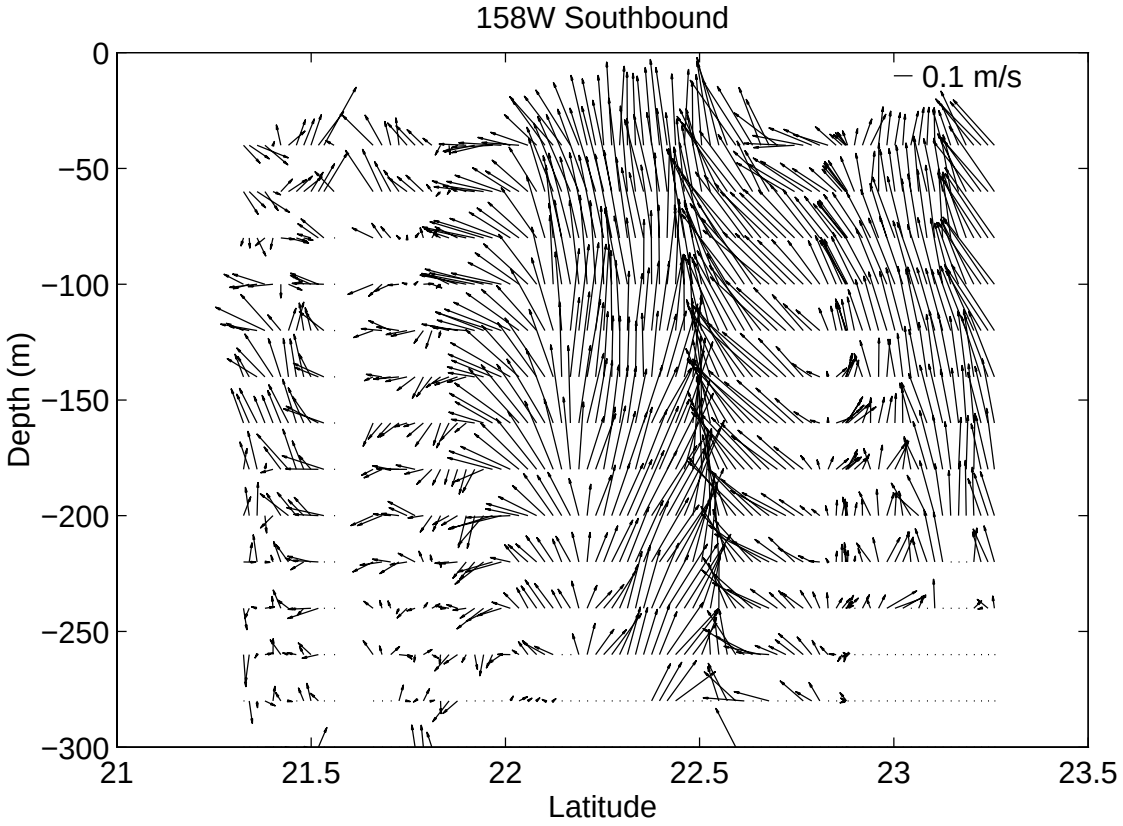
158W Southbound
− 0.1 m/s
0
−50
−100
−150
−200
−250
−300
Depth (m)
21
21.5
22
22.5
23
23.5
Latitude

Figure 6.7.2c

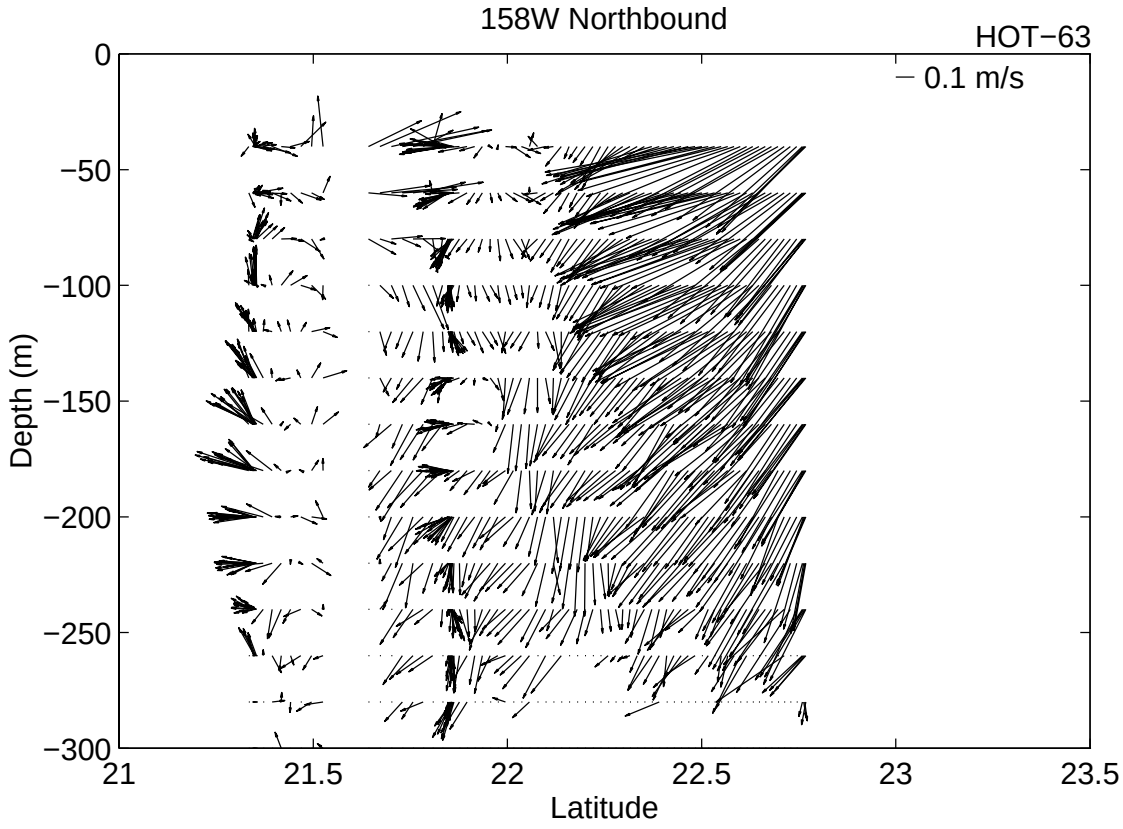
158W Northbound
HOT−63
0.1 m/s
0
−50
−100
−150
−200
−250
−300
Depth (m)
21
21.5
22
22.5
23
23.5
Latitude

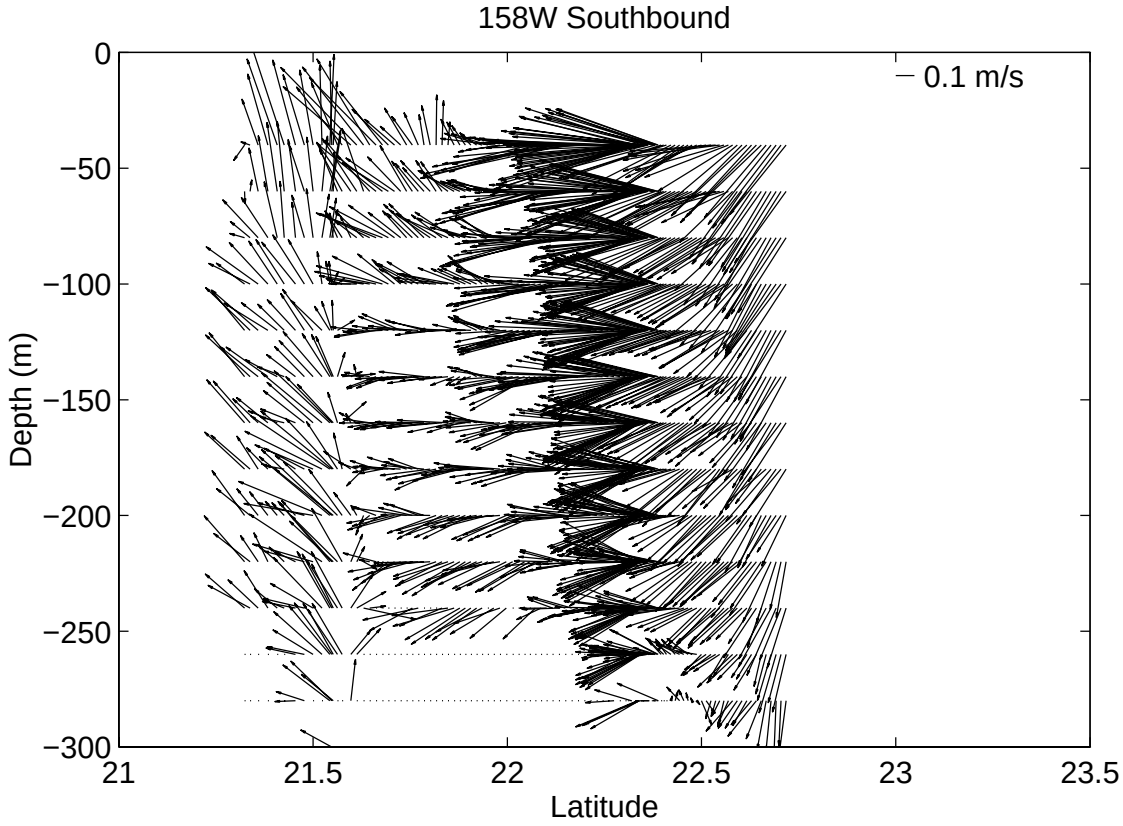
158W Southbound
0.1 m/s
0
−50
−100
−150
−200
−250
−300
Depth (m)
21
21.5
22
22.5
23
23.5
Latitude

Figure 6.7.2d

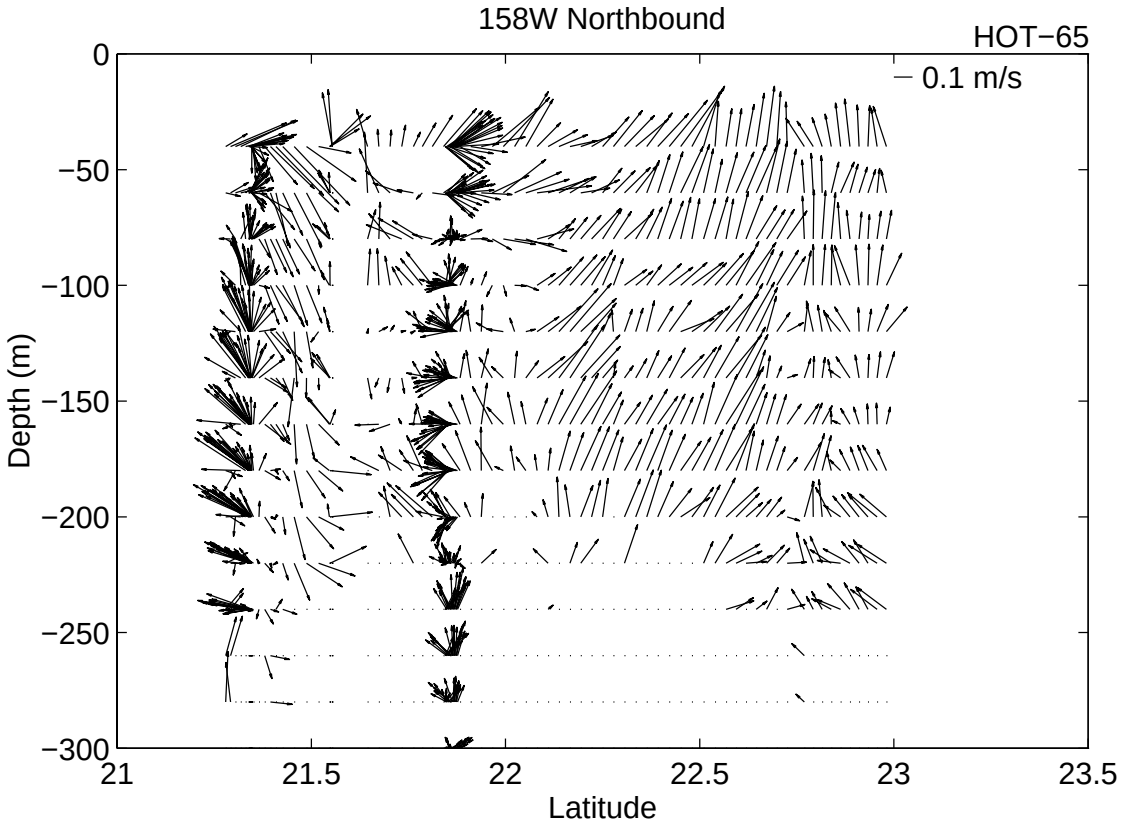
158W Northbound
HOT−65
0.1 m/s
0
−50
−100
−150
−200
−250
−300
Depth (m)
21
21.5
22
22.5
23
23.5
Latitude

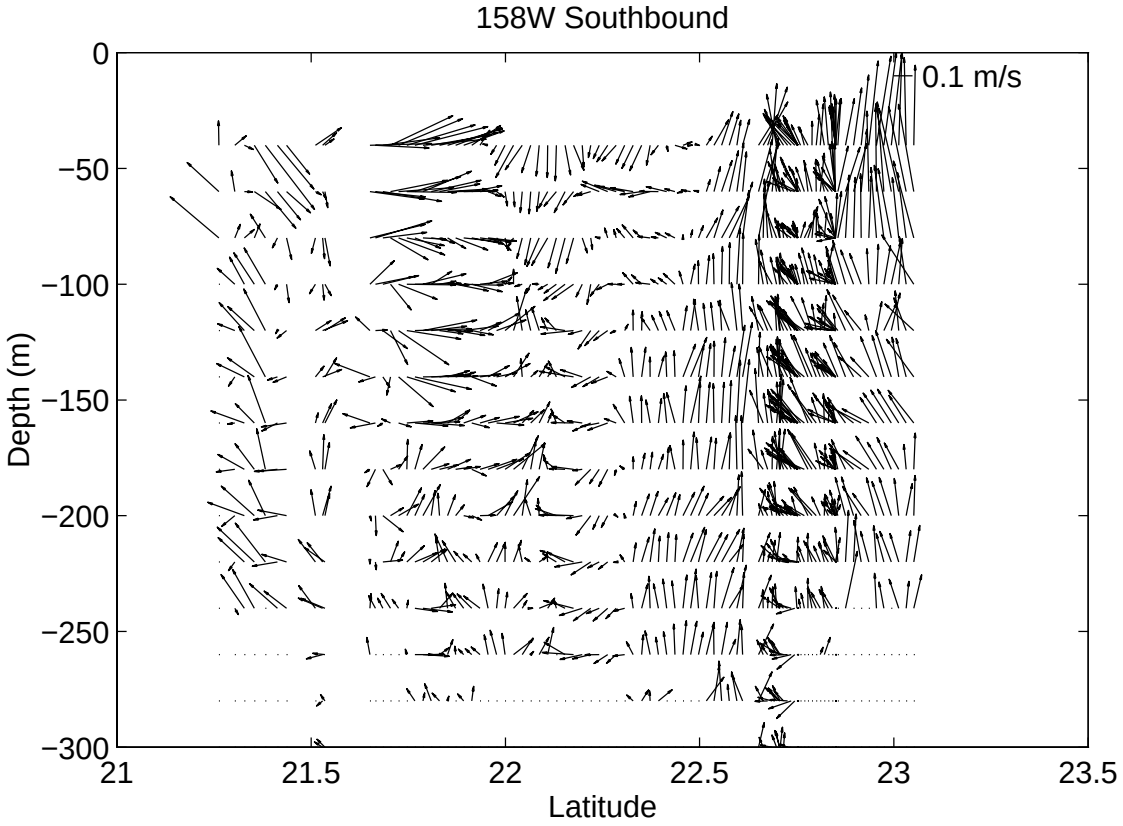
158W Southbound
0.1 m/s
0
−50
−100
−150
−200
−250
−300
Depth (m)
21
21.5
22
22.5
23
23.5
Latitude

Figure 6.7.2e

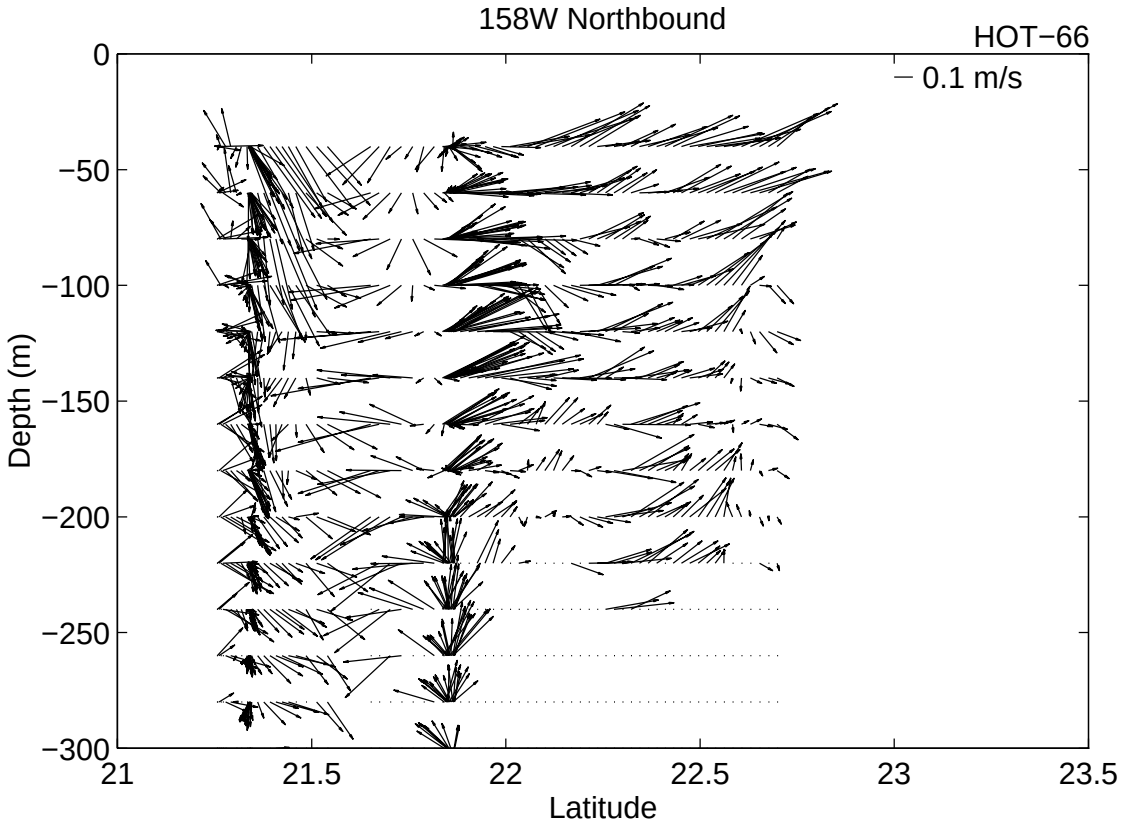
158W Northbound
HOT−66
0.1 m/s
0
−50
−100
−150
−200
−250
−300
Depth (m)
21
21.5
22
22.5
23
23.5
Latitude

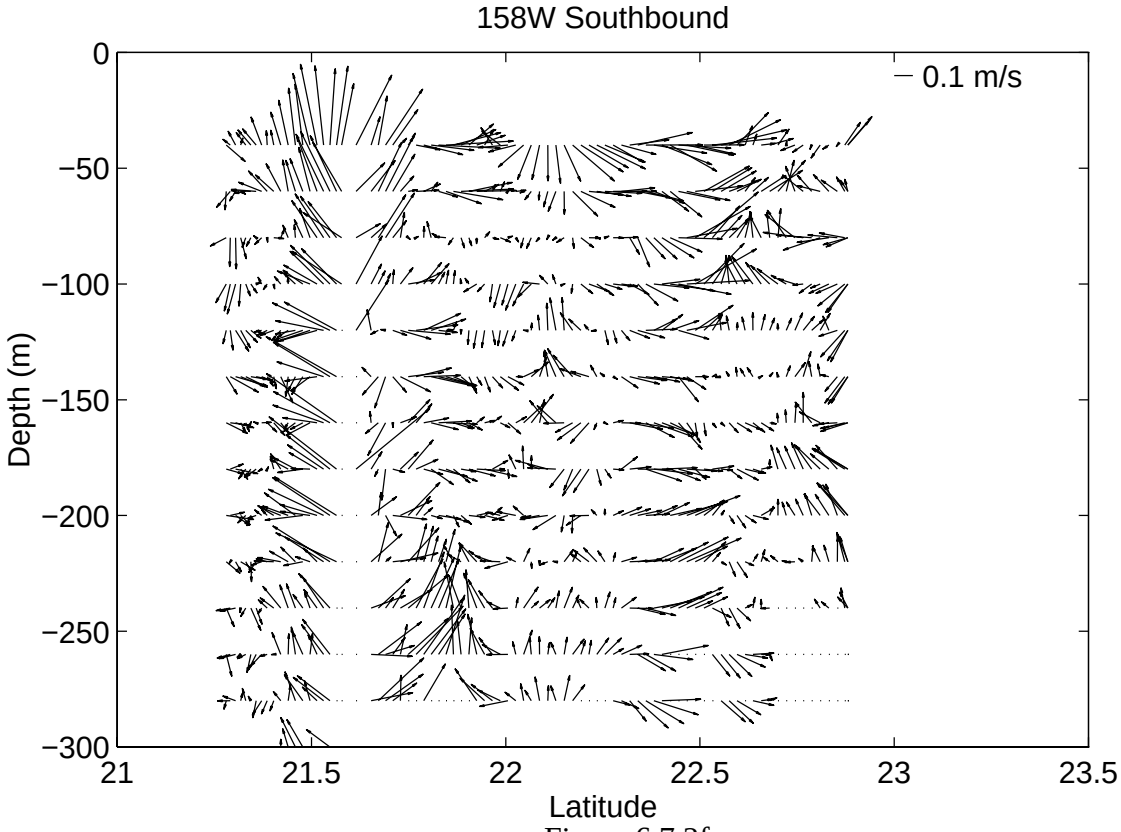
158W Southbound
0.1 m/s
0
−50
−100
−150
−200
−250
−300
Depth (m)
21
21.5
22
22.5
23
23.5
Latitude

Figure 6.7.2f

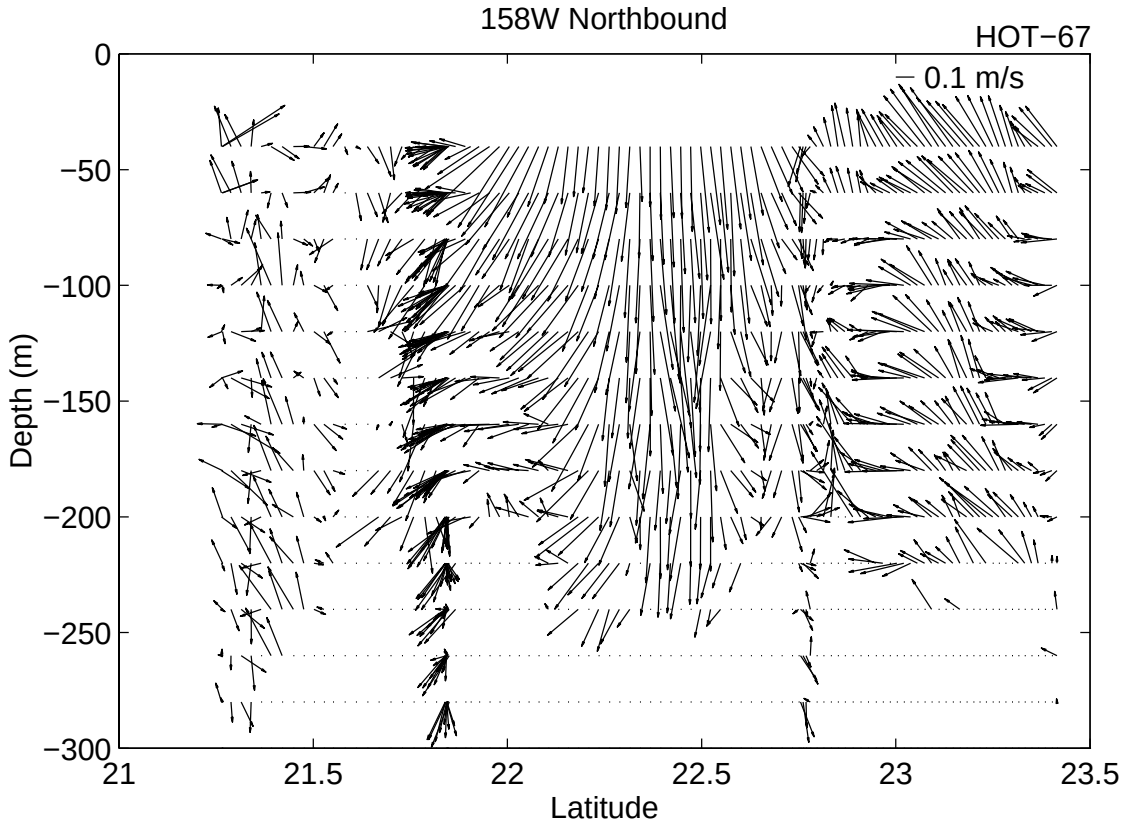
158W Northbound
HOT−67
0.1 m/s
0
−50
−100
−150
−200
−250
−300
Depth (m)
21
21.5
22
22.5
23
23.5
Latitude

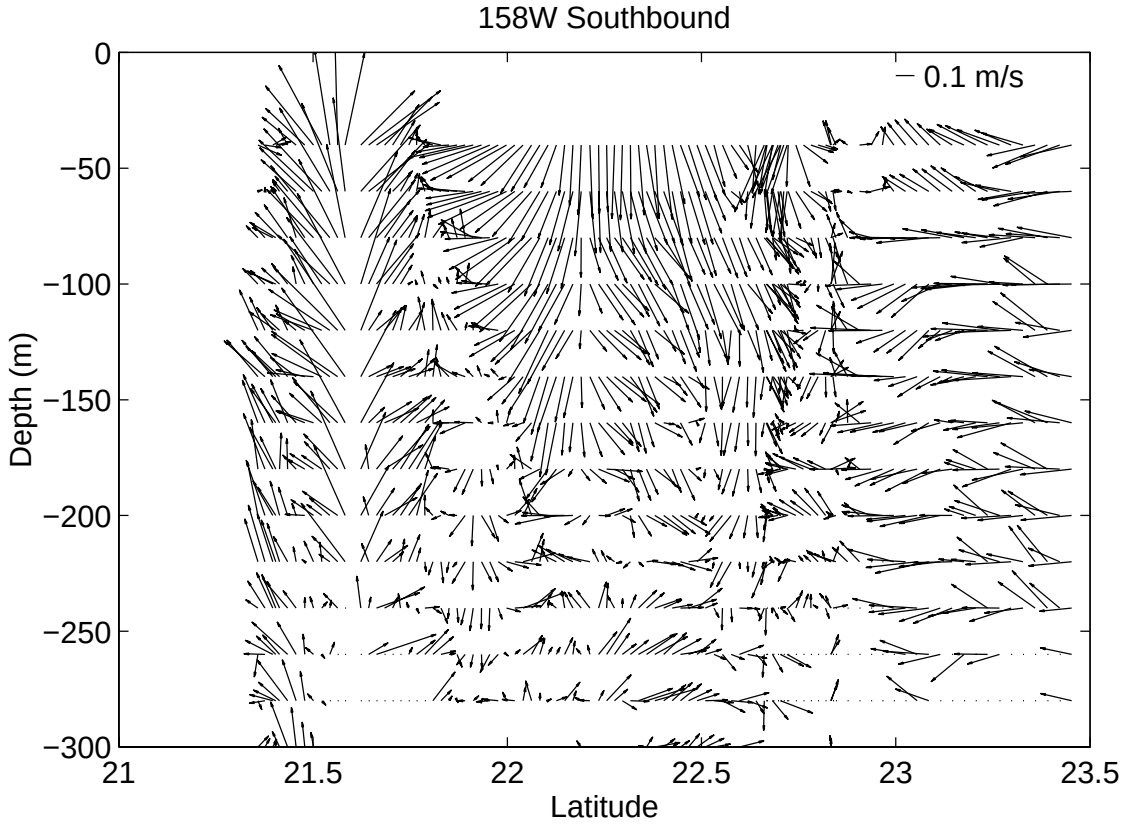
158W Southbound
0.1 m/s
0
−50
−100
−150
−200
−250
−300
Depth (m)
21
21.5
22
22.5
23
23.5
Latitude

Figure 6.7.2g

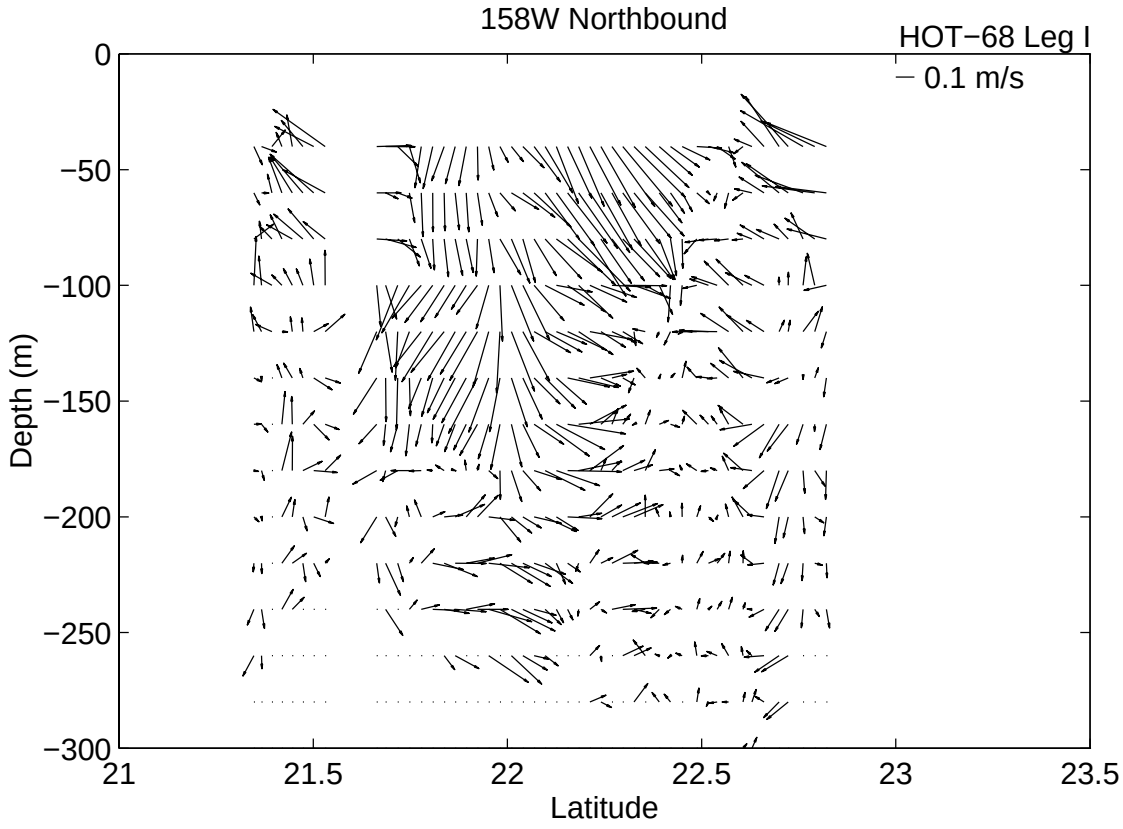
158W Northbound
HOT−68 Leg I
0.1 m/s
Depth (m)
0
−50
−100
−150
−200
−250
−300
21
21.5
22
22.5
23
23.5
Latitude

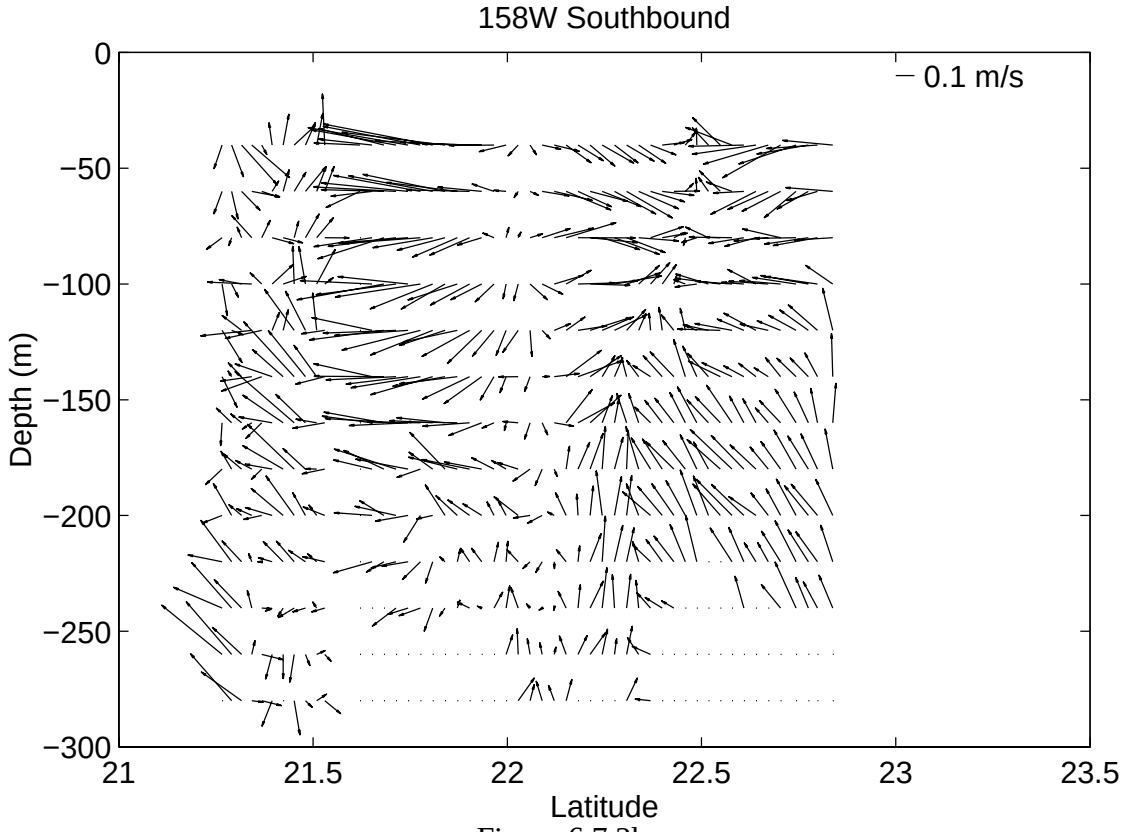
158W Southbound
0.1 m/s
Depth (m)
0
−50
−100
−150
−200
−250
−300
21
21.5
22
22.5
23
23.5
Latitude

Figure 6.7.2h

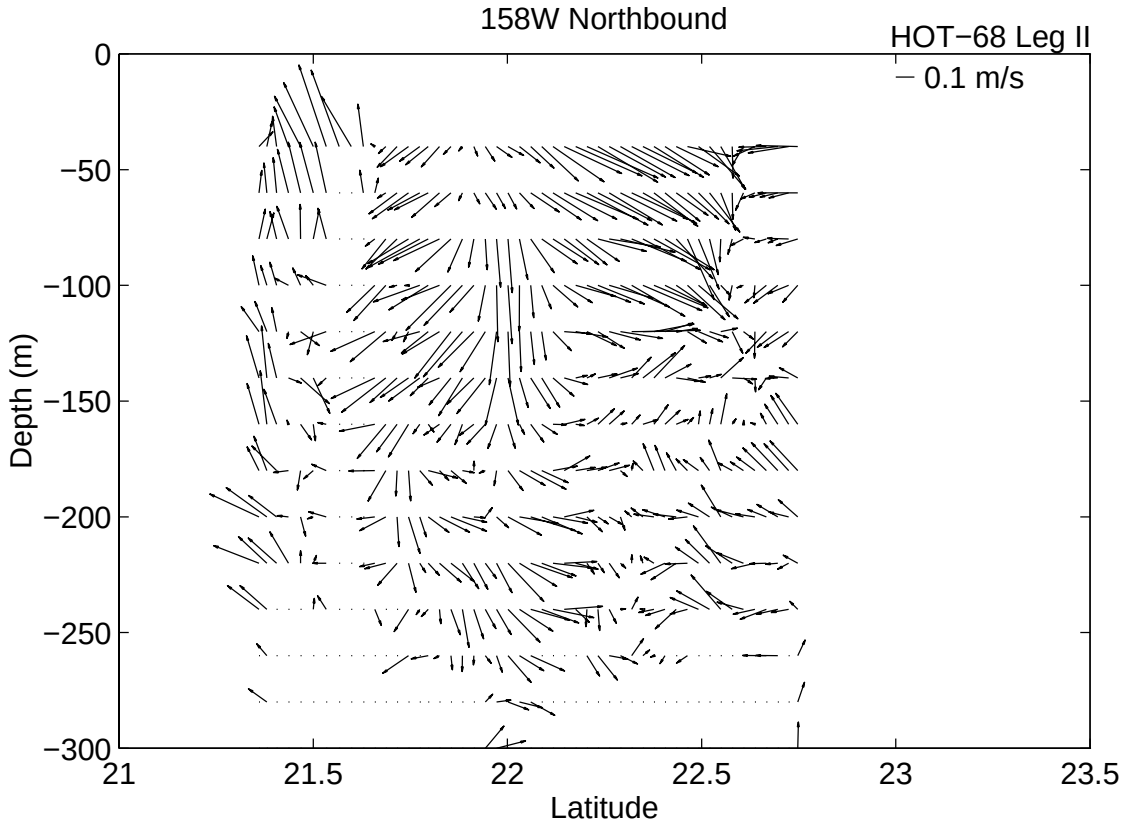
158W Northbound
HOT−68 Leg II
0.1 m/s
Depth (m)
0
−50
−100
−150
−200
−250
−300
21
21.5
22
22.5
23
23.5
Latitude

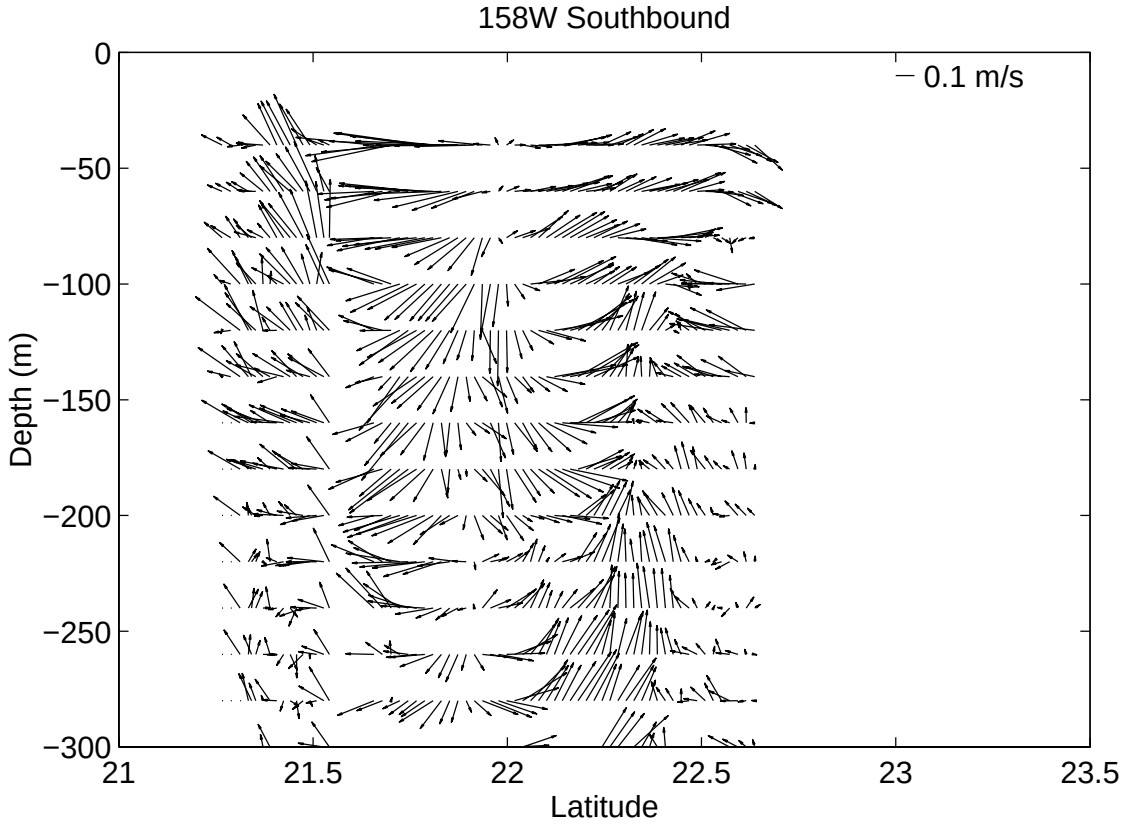
158W Southbound
0.1 m/s
Depth (m)
0
−50
−100
−150
−200
−250
−300
21
21.5
22
22.5
23
23.5
Latitude

Figure 6.7.2i

6.8. Meteorology

Figure 6.8.1: [Upper panel] Atmospheric pressure measured while at Station ALOHA during 1995. Open circles represent individual measurements. [Lower panel] Sea surface temperature measured from bucket sample while at Station ALOHA during 1995.

Figure 6.8.2: [Upper panel] Dry bulb air temperature measured while on station during 1995. [Lower panel] Wet bulb air temperature measure while at Station ALOHA during 1995.

Figure 6.8.3: [Upper panel] SST-dry air temperature measured at Station ALOHA during 1995. [Lower panel] Dry-wet air temperature measured at Station ALOHA during 1995.

Figure 6.8.4: [Upper panel] True winds collected by NDBC Buoy #51001 during HOT-60. [Middle panel] True winds measured at Station ALOHA during HOT-60. [Bottom panel] True winds collected by NDBC Buoy #51026 during HOT-60. The orientation of the arrows indicate the wind direction; up is northward, to the right is eastward.

Figure 6.8.5: As in Figure 6.8.4, except for HOT-61.

Figure 6.8.6: As in Figure 6.8.4, except for HOT-62

Figure 6.8.7: As in Figure 6.8.4, except for HOT-63.

Figure 6.8.8: As in Figure 6.8.4, except for HOT-64.

Figure 6.8.9: As in Figure 6.8 4, except for HOT-65.

Figure 6.8.10: As in Figure 6.8.4, except for HOT-66.

Figure 6.8.11: As in Figure 6.8.4, except for HOT-67.

Figure 6.8.12: As in Figure 6.8.4, except for HOT-68.

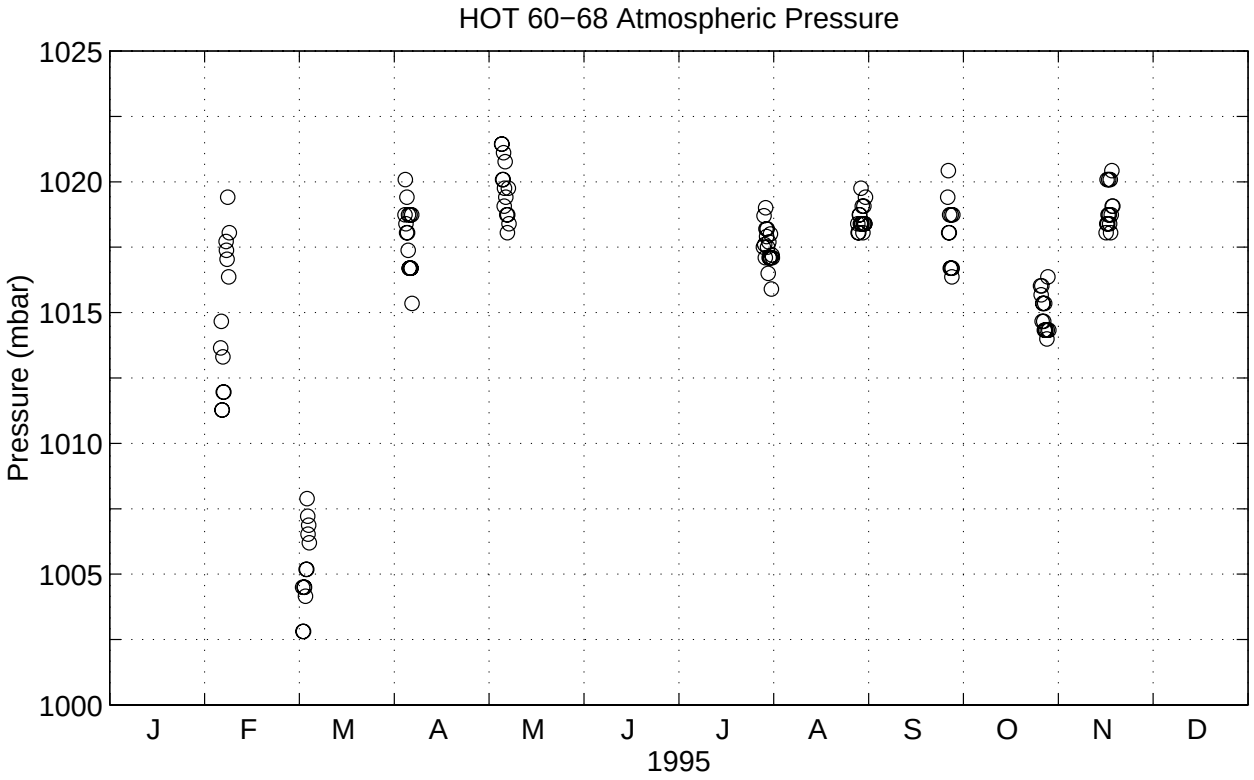
HOT 60−68 Atmospheric Pressure
Pressure (mbar)
1025
1020
1015
1010
1005
1000
J
F
M
A
M
J
J
A
S
O
N
D
1995

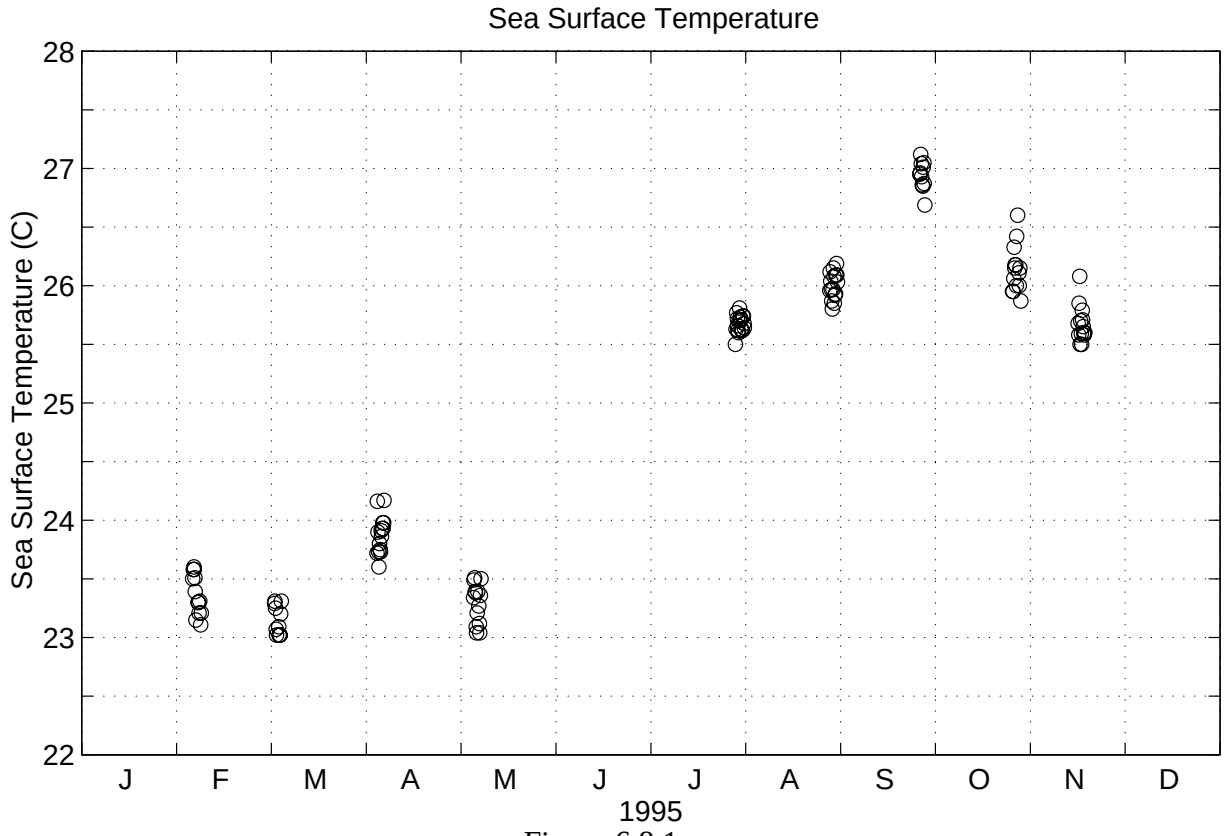
Sea Surface Temperature
Sea Surface Temperature (C)
28
27
26
25
24
23
22
J
F
M
A
M
J
J
A
S
O
N
D
1995

Figure 6.8.1

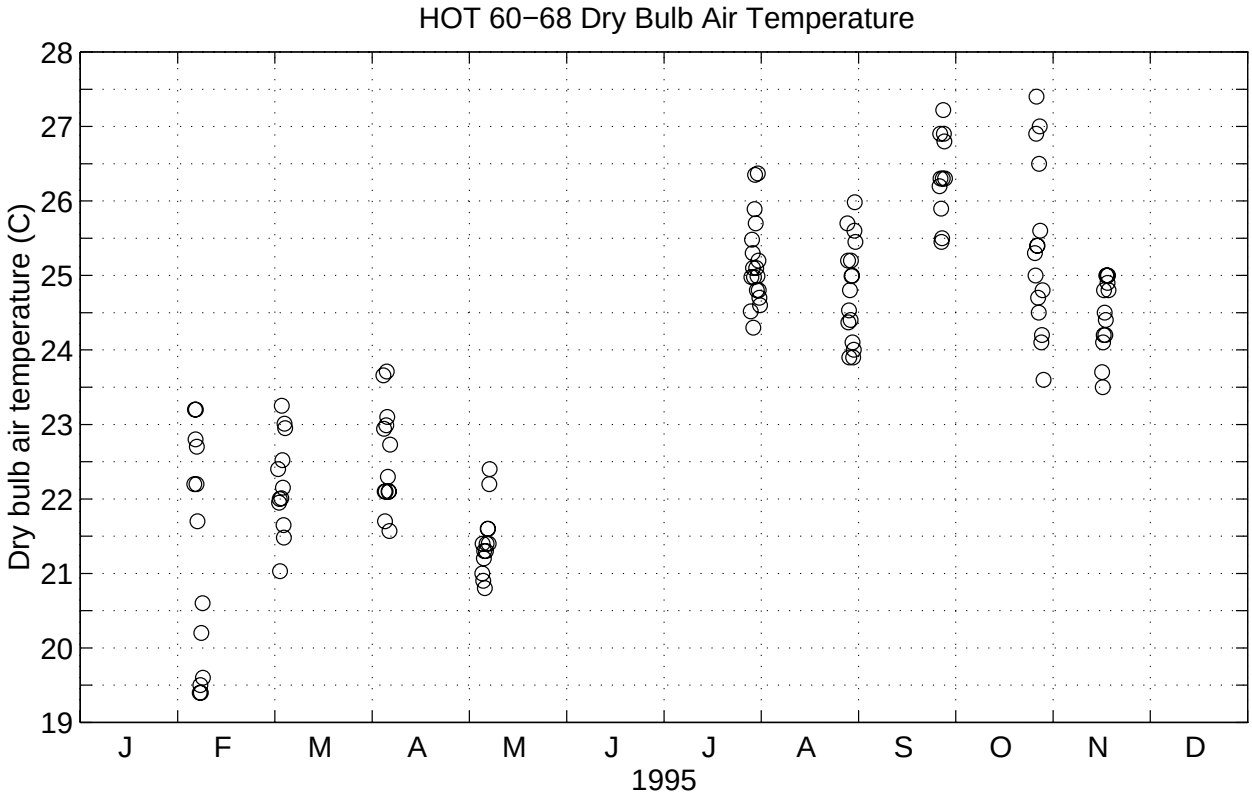
HOT 60−68 Dry Bulb Air Temperature
Dry bulb air temperature (C)
28
27
26
25
24
23
22
21
20
19
J
F
M
A
M
J
J
A
S
O
N
D
1995

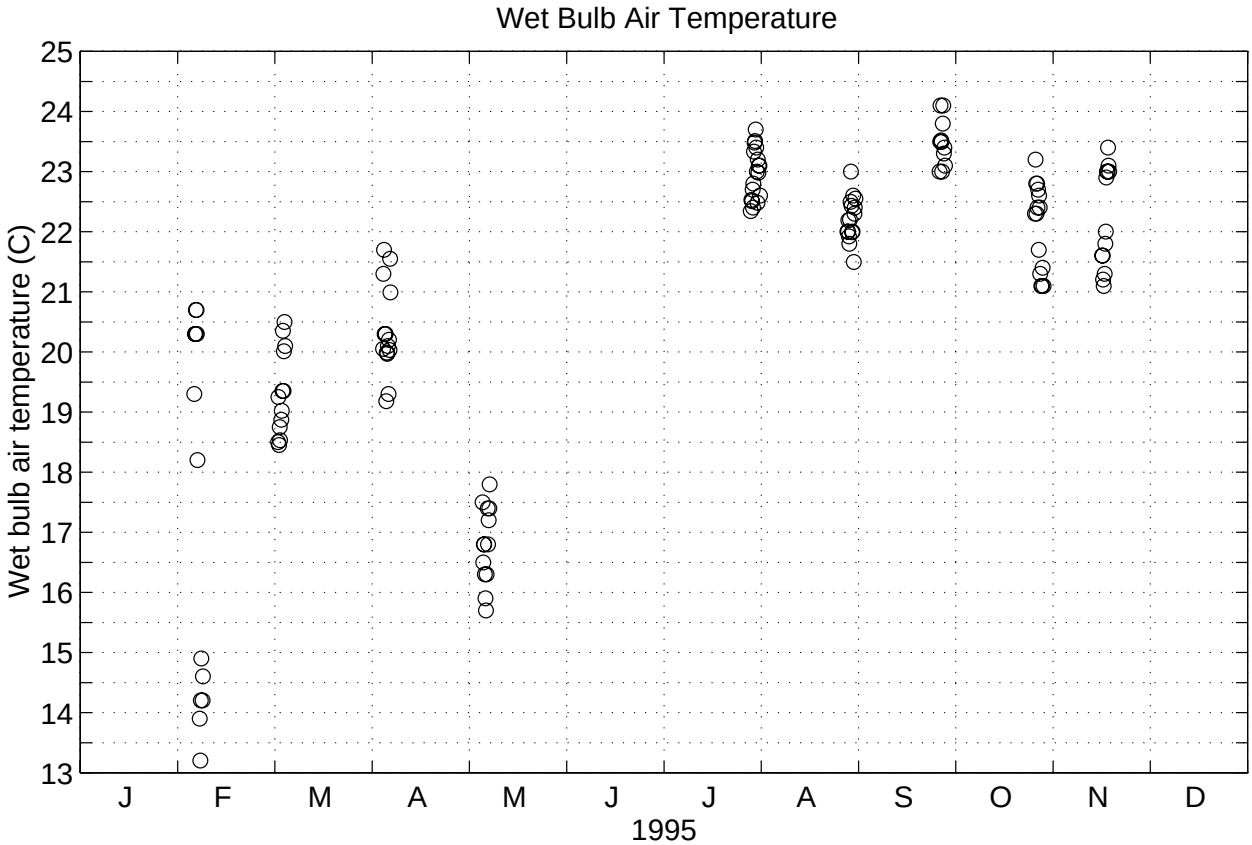
Wet Bulb Air Temperature
Wet bulb air temperature (C)
25
24
23
22
21
20
19
18
17
16
15
14
13
J
F
M
A
M
J
J
A
S
O
N
D
1995

Figure 6.8.2

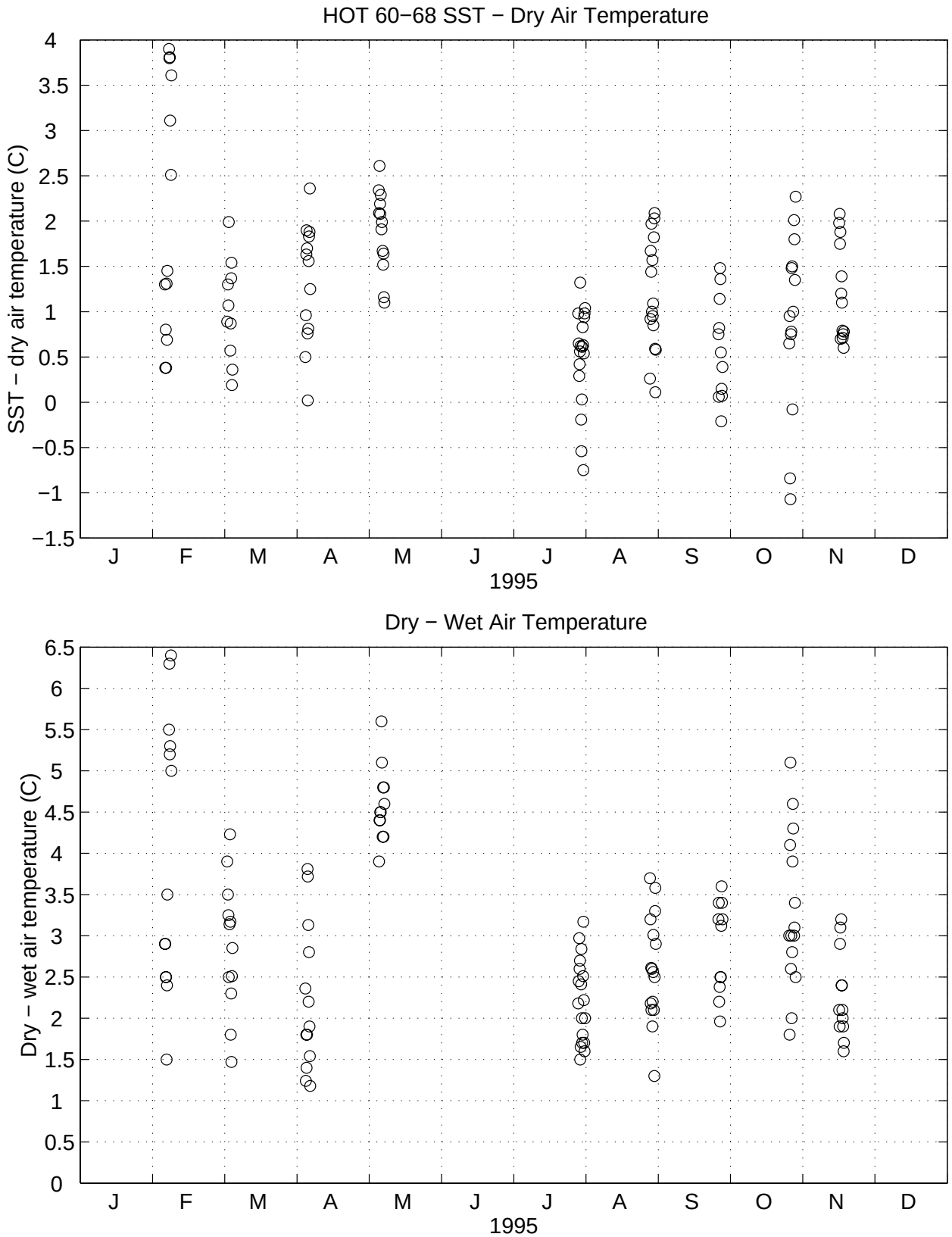
HOT 60−68 SST − Dry Air Temperature
SST − dry air temperature (C)
4
3.5
3
2.5
2
1.5
1
0.5
0
−0.5
−1
−1.5
J F M A M J J A S O N D
1995
Dry − Wet Air Temperature
Dry − wet air temperature (C)
6.5
6
5.5
5
4.5
4
3.5
3
2.5
2
1.5
1
0.5
0
J F M A M J J A S O N D
1995
Figure 6.8.3

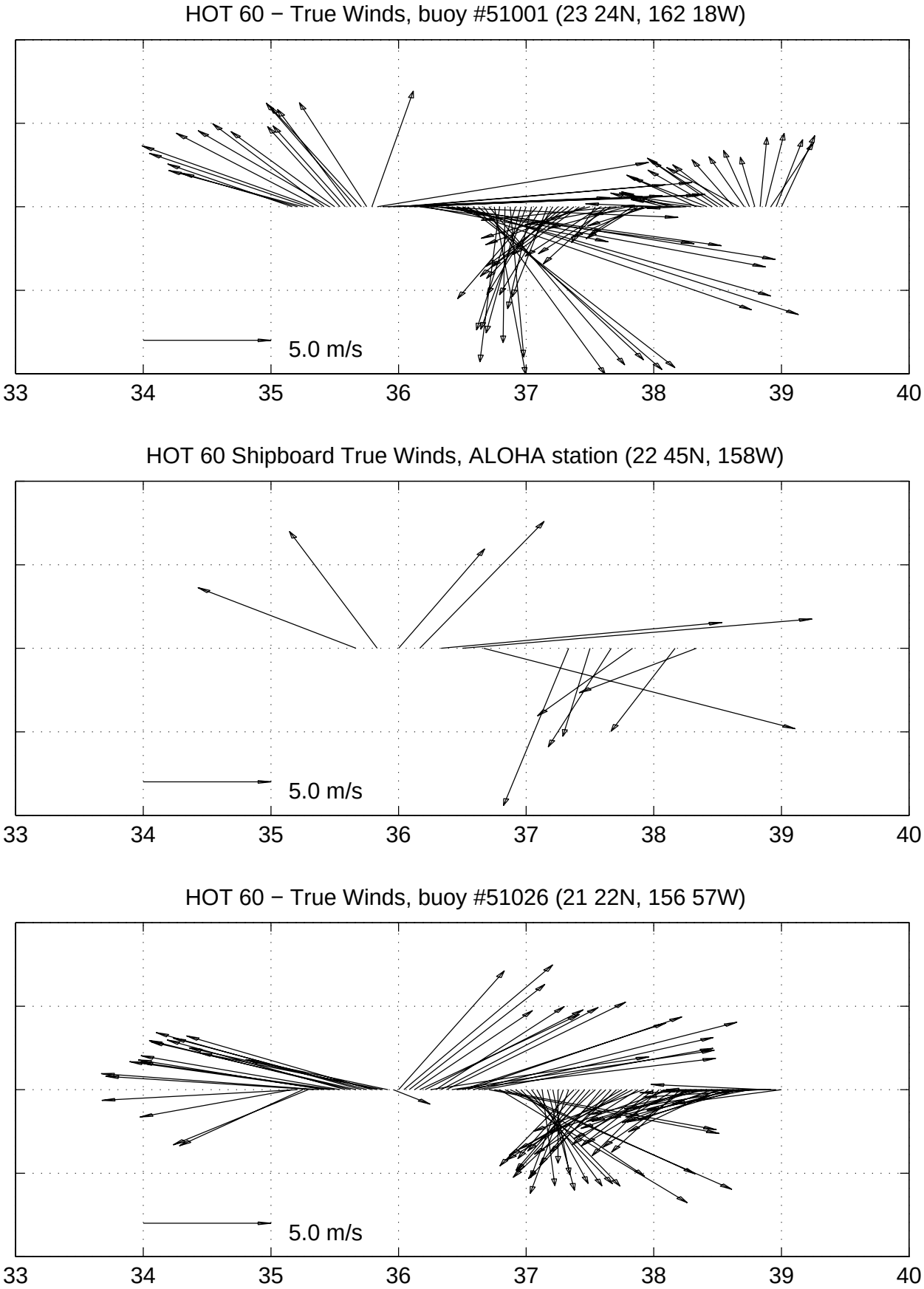
HOT 60 − True Winds, buoy #51001 (23 24N, 162 18W)
5.0 m/s
33
34
35
36
37
38
39
40
HOT 60 Shipboard True Winds, ALOHA station (22 45N, 158W)
5.0 m/s
33
34
35
36
37
38
39
40
HOT 60 − True Winds, buoy #51026 (21 22N, 156 57W)
5.0 m/s
33
34
35
36
37
38
39
40
Julian days from January 1, 1995

Figure 6.8.4

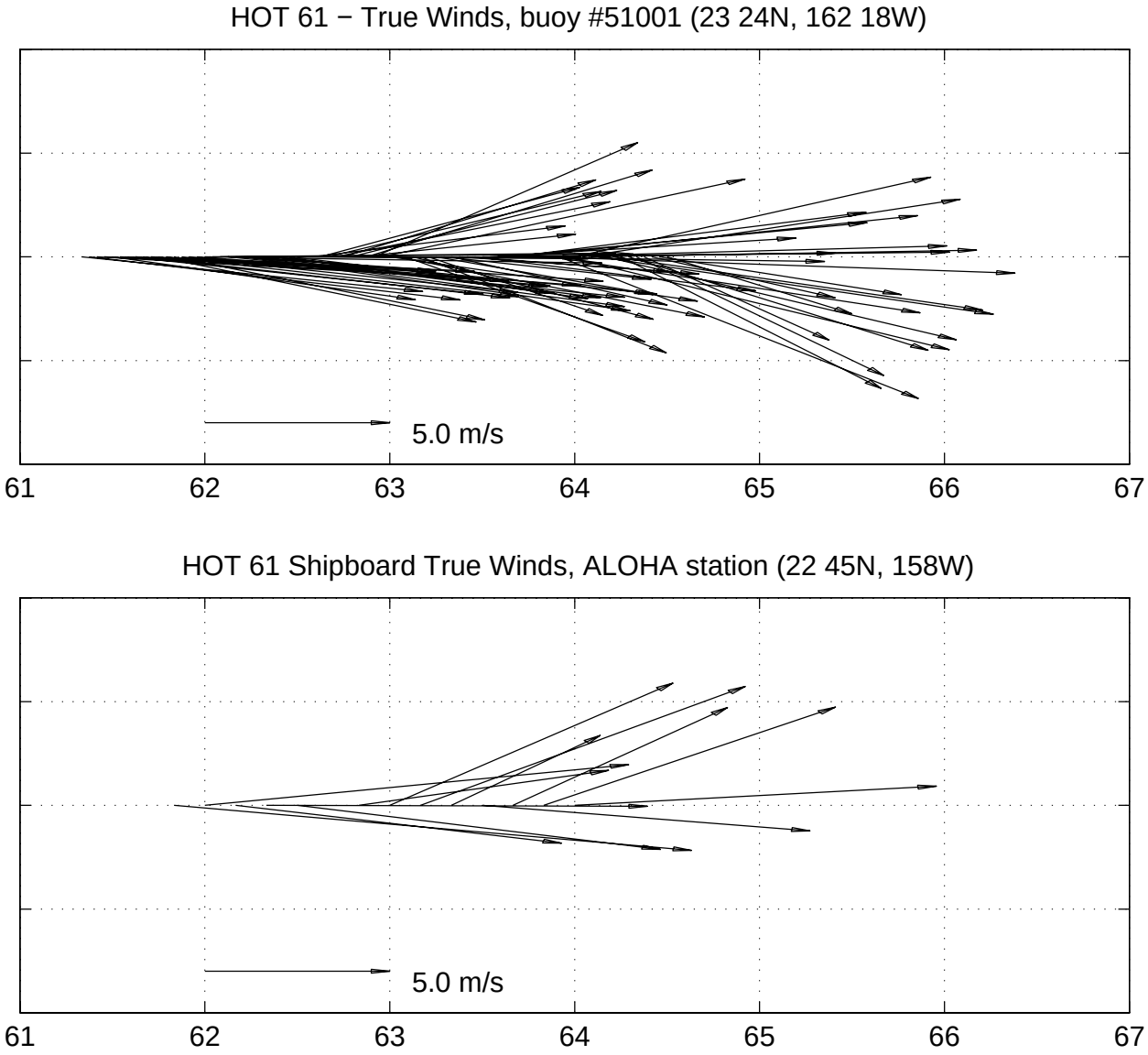
HOT 61 − True Winds, buoy #51001 (23 24N, 162 18W)
5.0 m/s
61
62
63
64
65
66
67
HOT 61 Shipboard True Winds, ALOHA station (22 45N, 158W)
5.0 m/s
61
62
63
64
65
66
67
HOT 61 − True Winds, buoy #51026 (21 22N, 156 57W)
5.0 m/s
61
62
63
64
65
66
67
Julian days from January 1, 1995

Figure 6.8.5

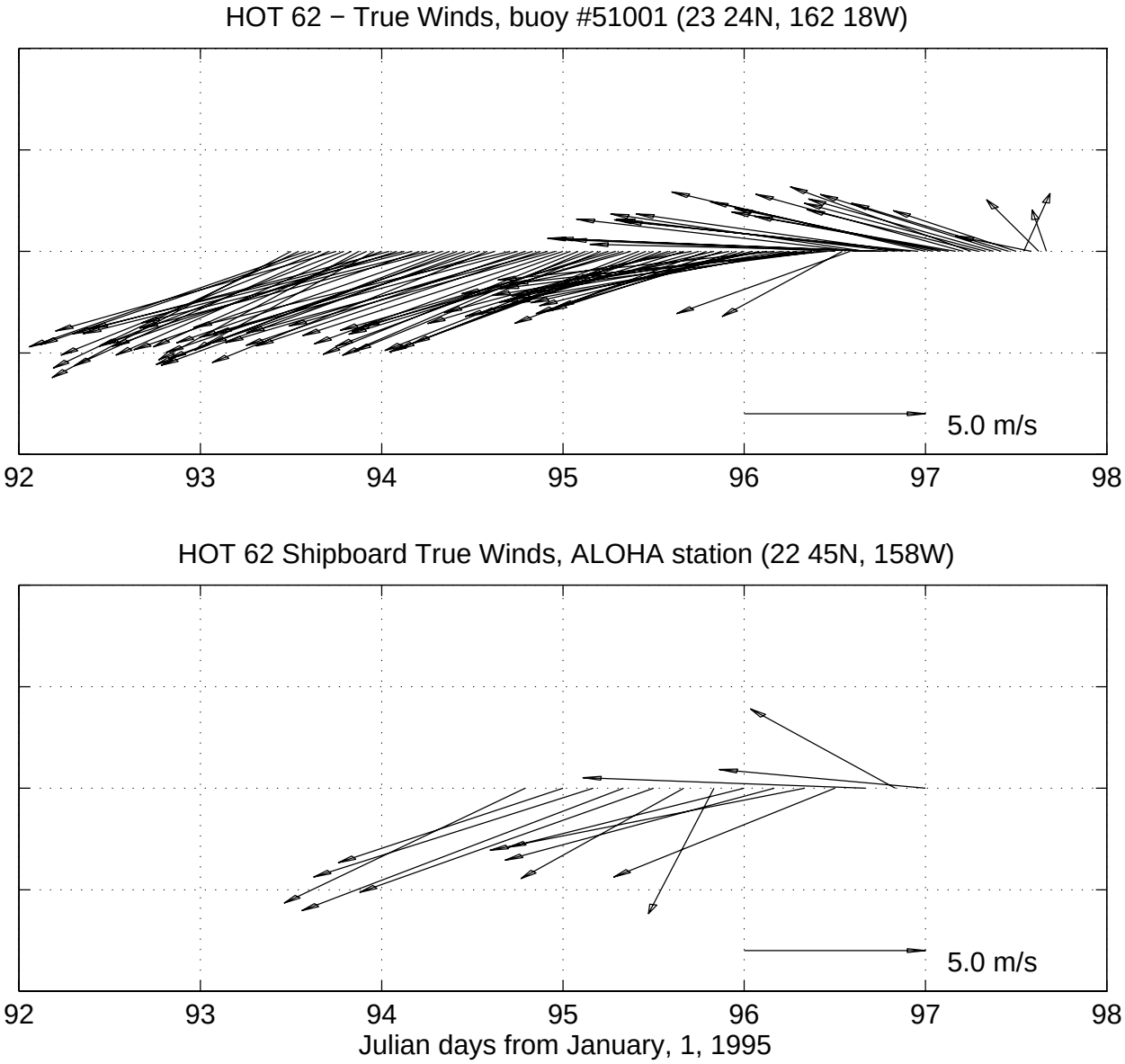
HOT 62 − True Winds, buoy #51001 (23 24N, 162 18W)
5.0 m/s
92
93
94
95
96
97
98
HOT 62 Shipboard True Winds, ALOHA station (22 45N, 158W)
5.0 m/s
92
93
94
95
96
97
98
Julian days from January, 1, 1995

Figure 6.8.6

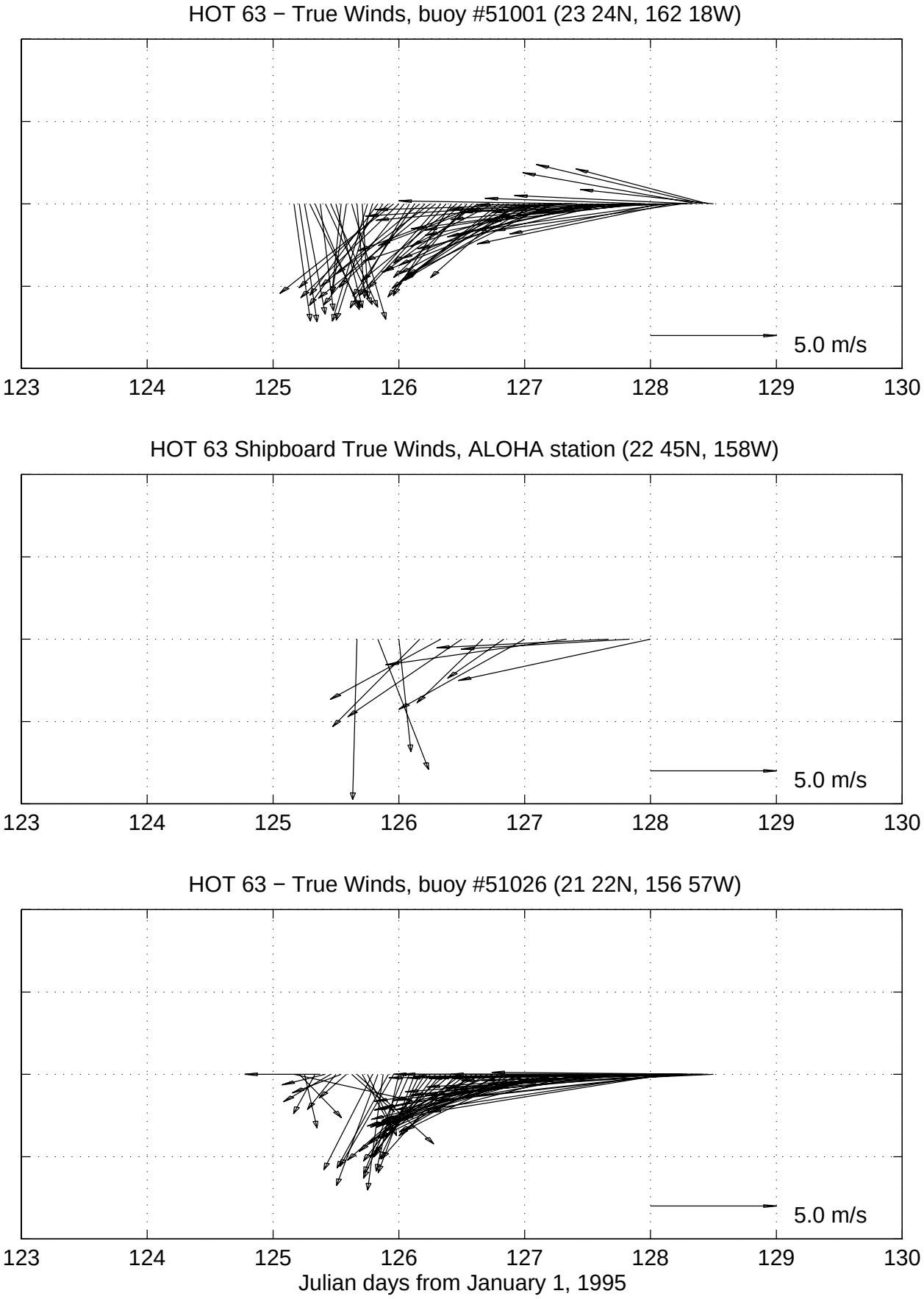
HOT 63 − True Winds, buoy #51001 (23 24N, 162 18W)
5.0 m/s
123
124
125
126
127
128
129
130
HOT 63 Shipboard True Winds, ALOHA station (22 45N, 158W)
5.0 m/s
123
124
125
126
127
128
129
130
HOT 63 − True Winds, buoy #51026 (21 22N, 156 57W)
5.0 m/s
123
124
125
126
127
128
129
130
Julian days from January 1, 1995

Figure 6.8.7

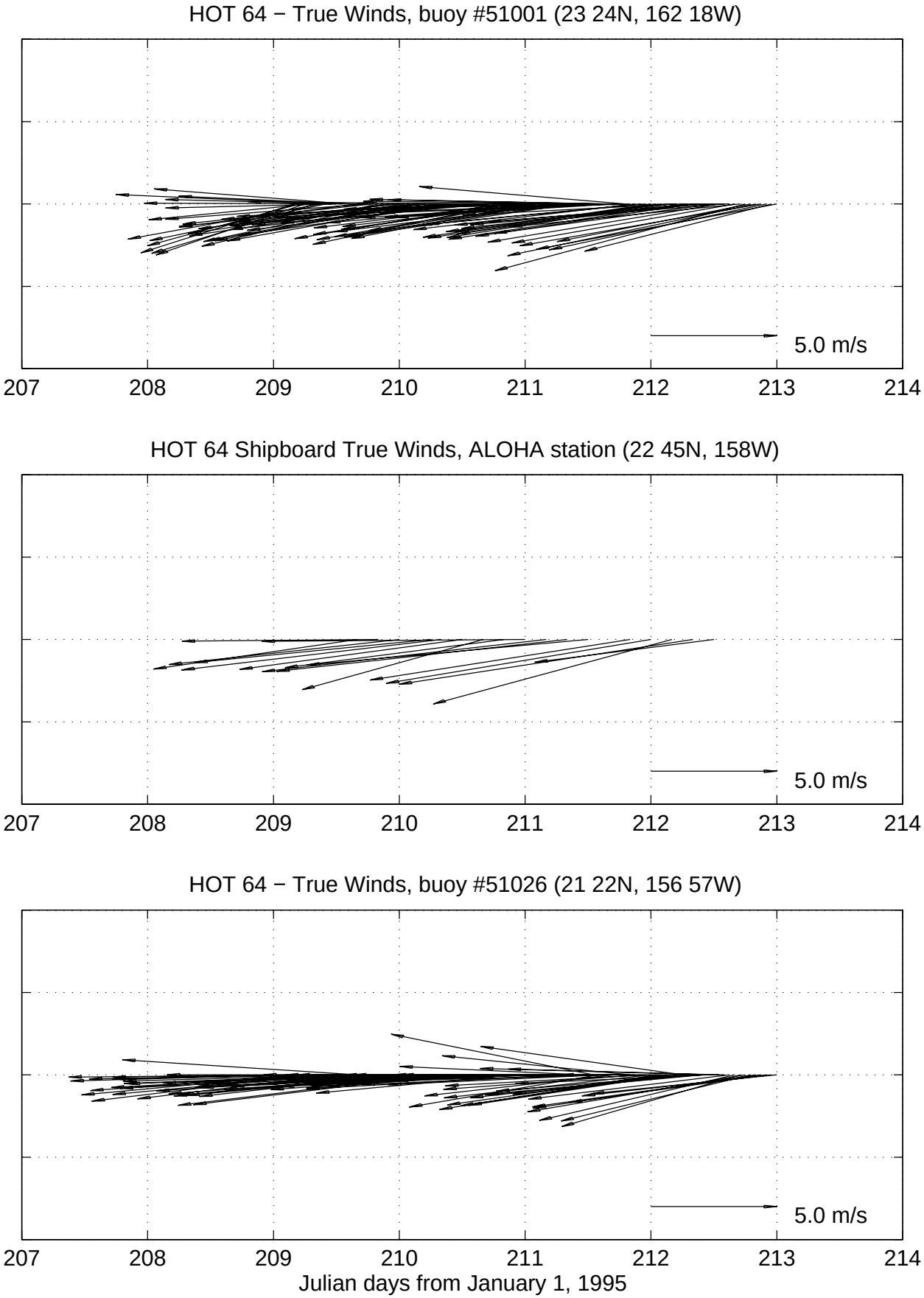
HOT 64 − True Winds, buoy #51001 (23 24N, 162 18W)
5.0 m/s
HOT 64 Shipboard True Winds, ALOHA station (22 45N, 158W)
5.0 m/s
HOT 64 − True Winds, buoy #51026 (21 22N, 156 57W)
5.0 m/s
207
208
209
210
211
212
213
214
Julian days from January 1, 1995

Figure 6.8.8

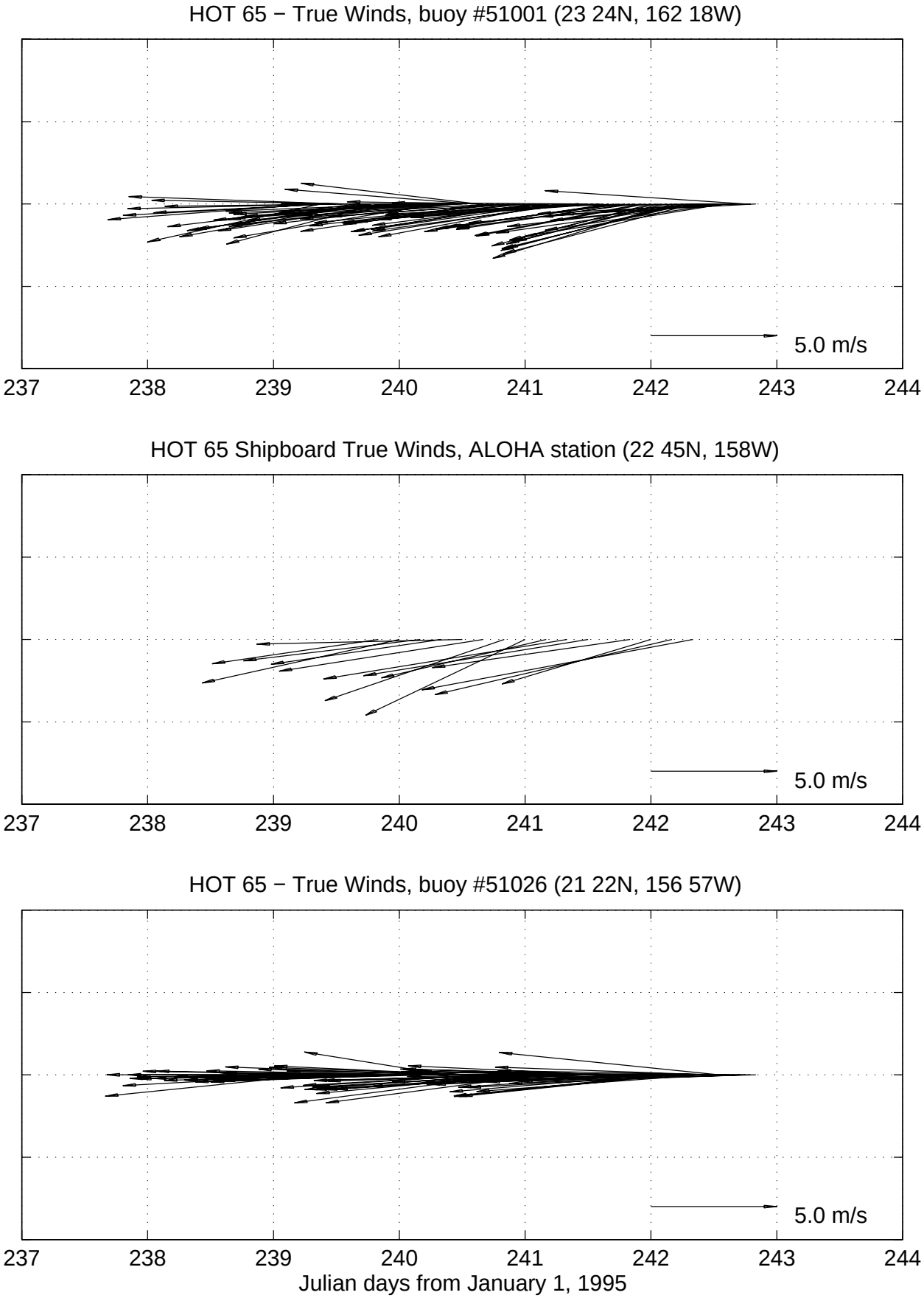
HOT 65 − True Winds, buoy #51001 (23 24N, 162 18W)
5.0 m/s
HOT 65 Shipboard True Winds, ALOHA station (22 45N, 158W)
5.0 m/s
HOT 65 − True Winds, buoy #51026 (21 22N, 156 57W)
5.0 m/s
237
238
239
240
241
242
243
244
Julian days from January 1, 1995

Figure 6.8.9

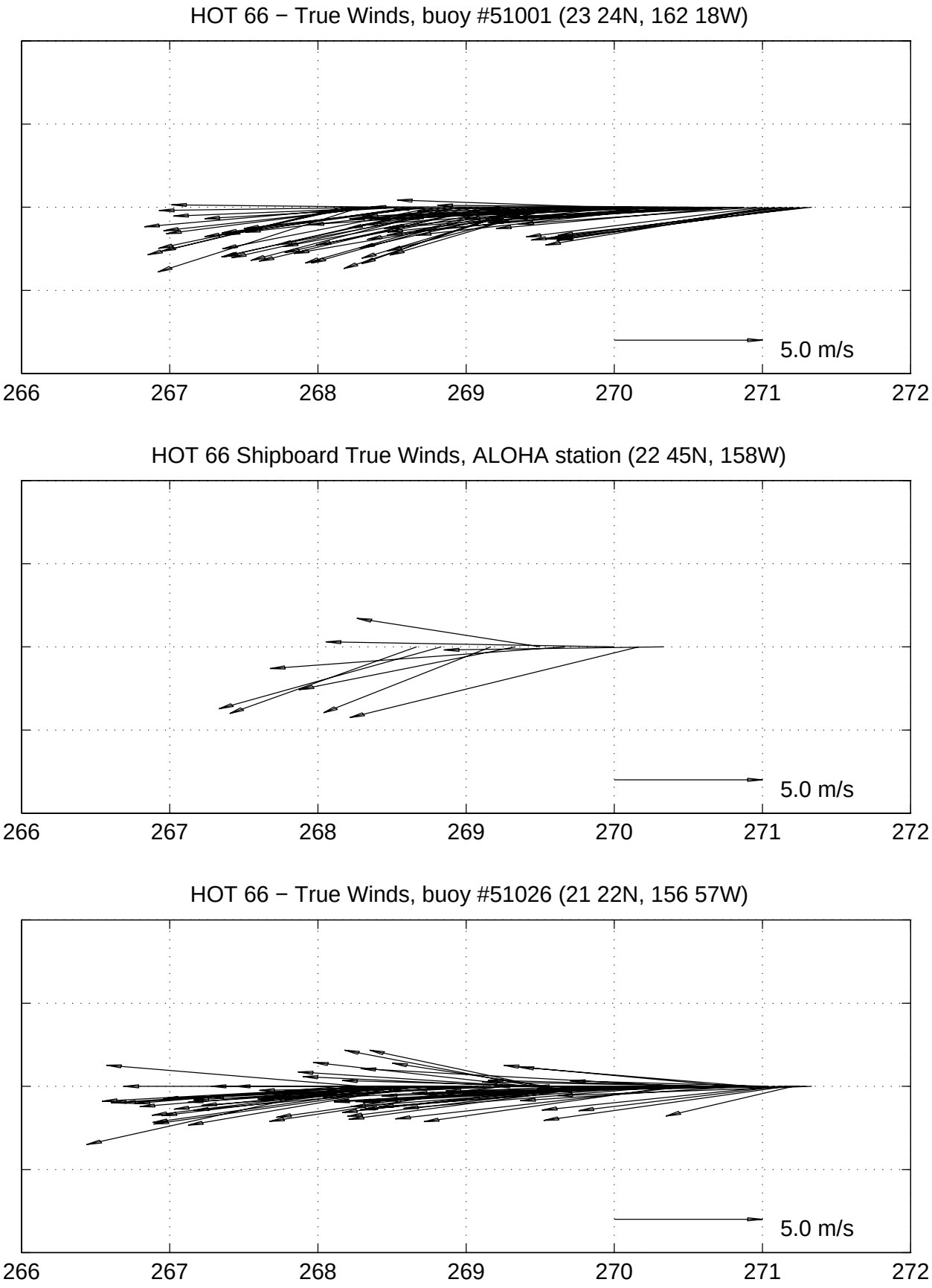
HOT 66 − True Winds, buoy #51001 (23 24N, 162 18W)
5.0 m/s
266
267
268
269
270
271
272
HOT 66 Shipboard True Winds, ALOHA station (22 45N, 158W)
5.0 m/s
266
267
268
269
270
271
272
HOT 66 − True Winds, buoy #51026 (21 22N, 156 57W)
5.0 m/s
266
267
268
269
270
271
272
Julian days from January 1, 1995

Figure 6.8.10

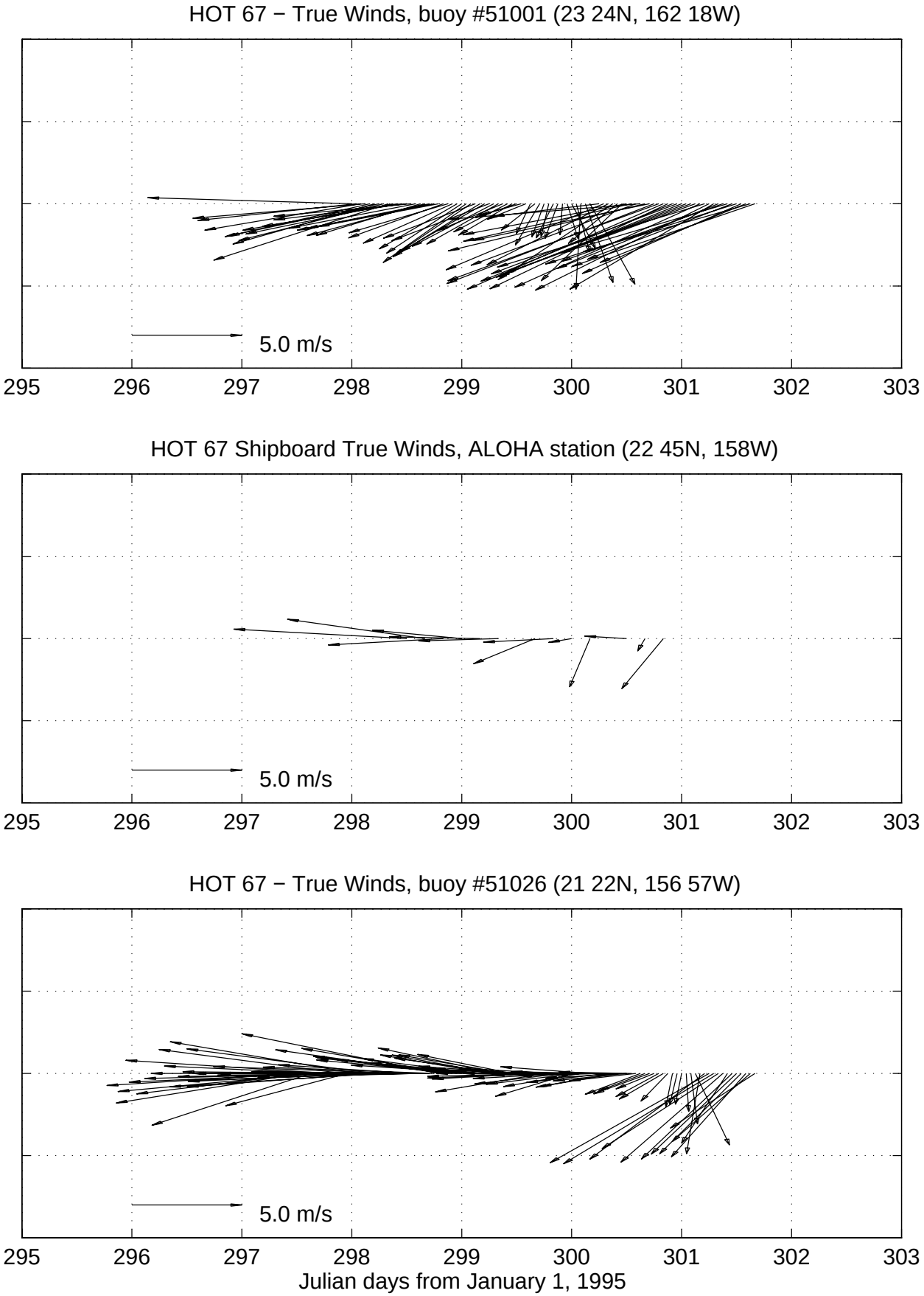
HOT 67 − True Winds, buoy #51001 (23 24N, 162 18W)
5.0 m/s
HOT 67 Shipboard True Winds, ALOHA station (22 45N, 158W)
5.0 m/s
HOT 67 − True Winds, buoy #51026 (21 22N, 156 57W)
5.0 m/s
295
296
297
298
299
300
301
302
303
Julian days from January 1, 1995
Figure 6.8.11

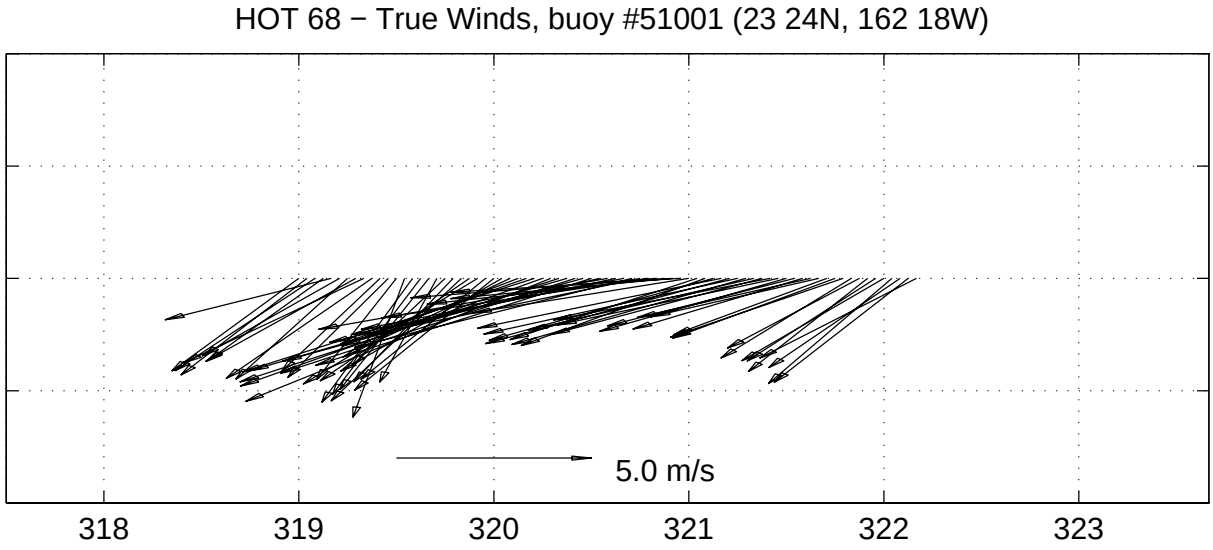
HOT 68 − True Winds, buoy #51001 (23 24N, 162 18W)
5.0 m/s
318
319
320
321
322
323

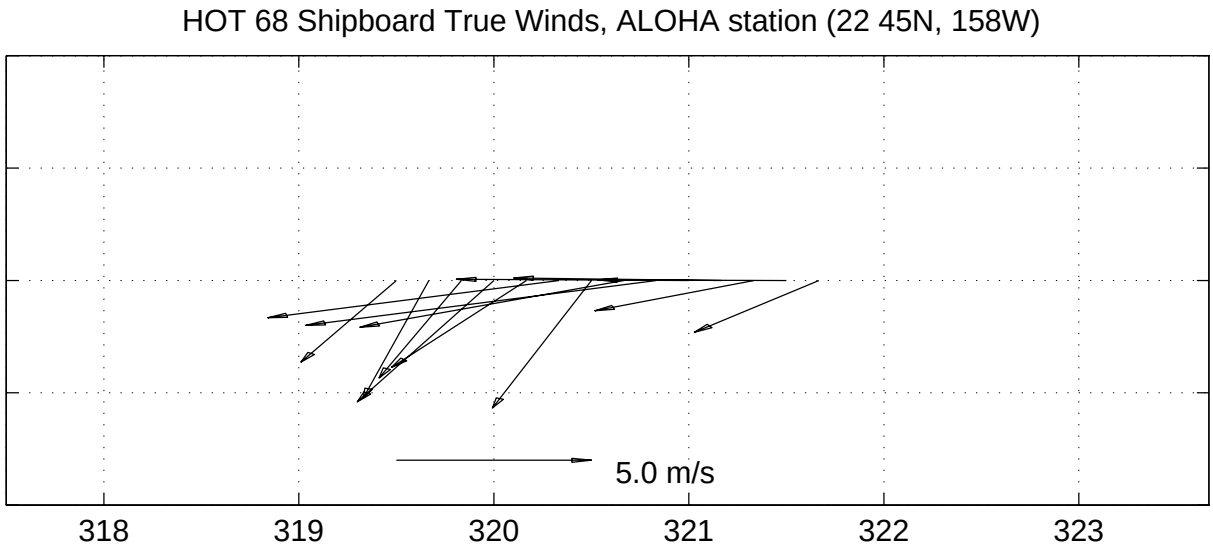
HOT 68 Shipboard True Winds, ALOHA station (22 45N, 158W)
5.0 m/s
318
319
320
321
322
323

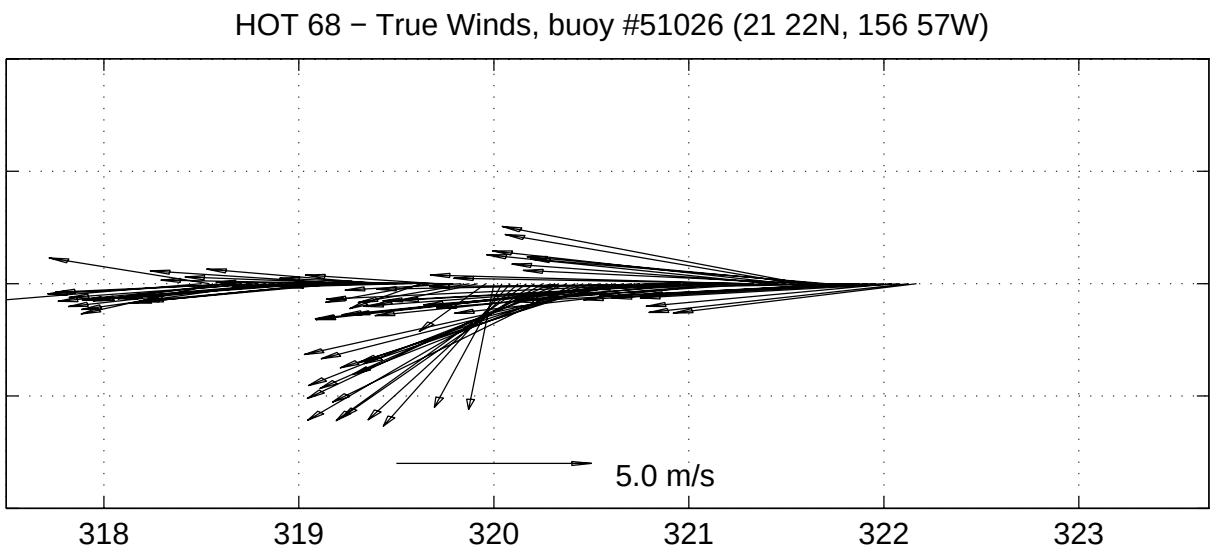
HOT 68 − True Winds, buoy #51026 (21 22N, 156 57W)
5.0 m/s
318
319
320
321
322
323
Julian days from January 1, 1995

Figure 6.8.12

6.9. Thermosalinograph

Figure 6.9.1: [Top] Time-series of the near surface temperature (NST), near surface salinity (NSS) and potential density measured by thermosalinograph during HOT-63. Circles indicate CTD data at 4 dbar and x's indicate the salinity from bottle samples. [Bottom] Navigation and ship speed during the cruise.

Figure 6.9.2: [Top] Time-series of the NST measured by thermosalinograph during HOT-66. Circles indicate CTD data at 4 dbar. [Bottom] Navigation and ship speed during the cruise.

Figure 6.9.3: [Top] Time-series of the NST measured by thermosalinograph during HOT-67. Circles indicate CTD data at 4 dbar. [Bottom] Navigation and ship speed during the cruise.

Figure 6.9.4: [Top] Time-series of the near surface temperature (NST), near surface salinity (NSS) and potential density measured by thermosalinograph during HOT-68. Circles indicate CTD data at 4 dbar and x's indicate the salinity from bottle samples. [Bottom] Navigation and ship speed during the cruise.

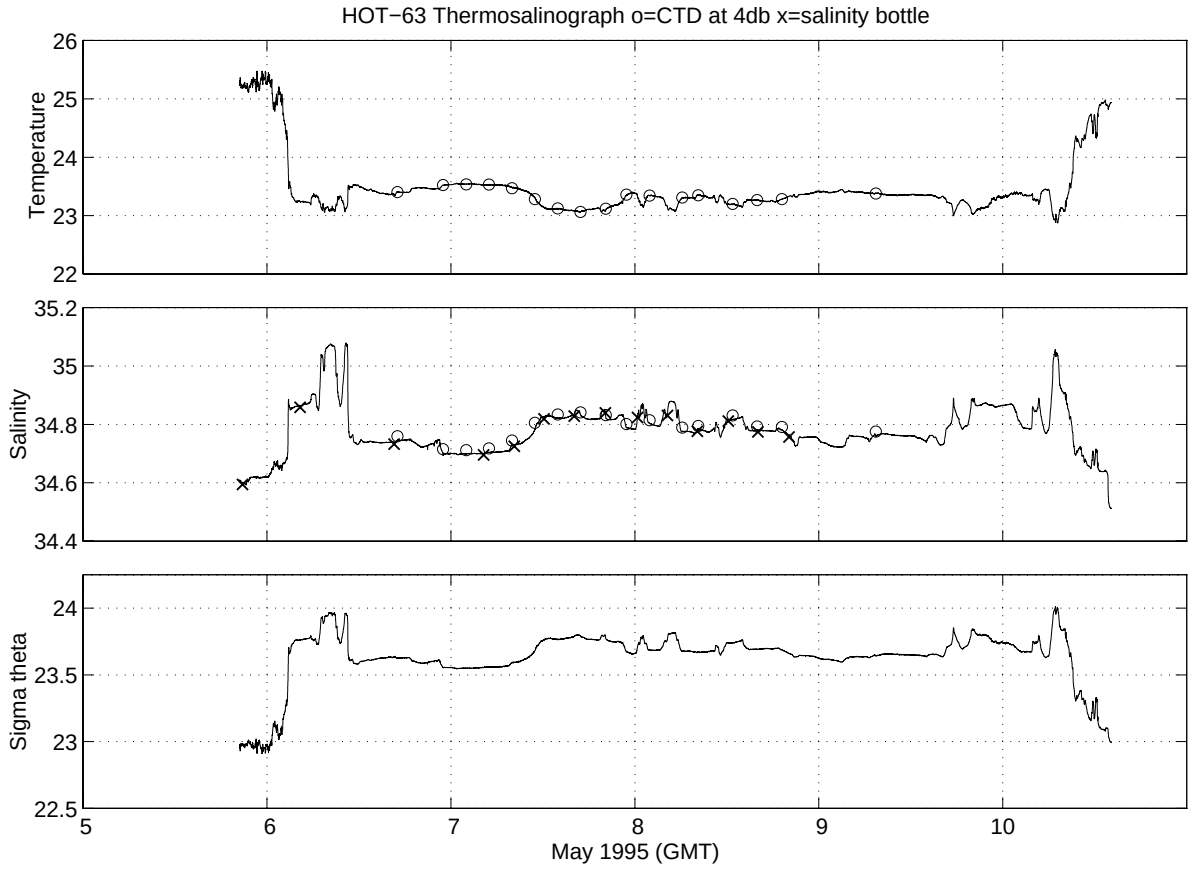
HOT−63 Thermosalinograph o=CTD at 4db x=salinity bottle
Temperature
Salinity
Sigma theta
May 1995 (GMT)

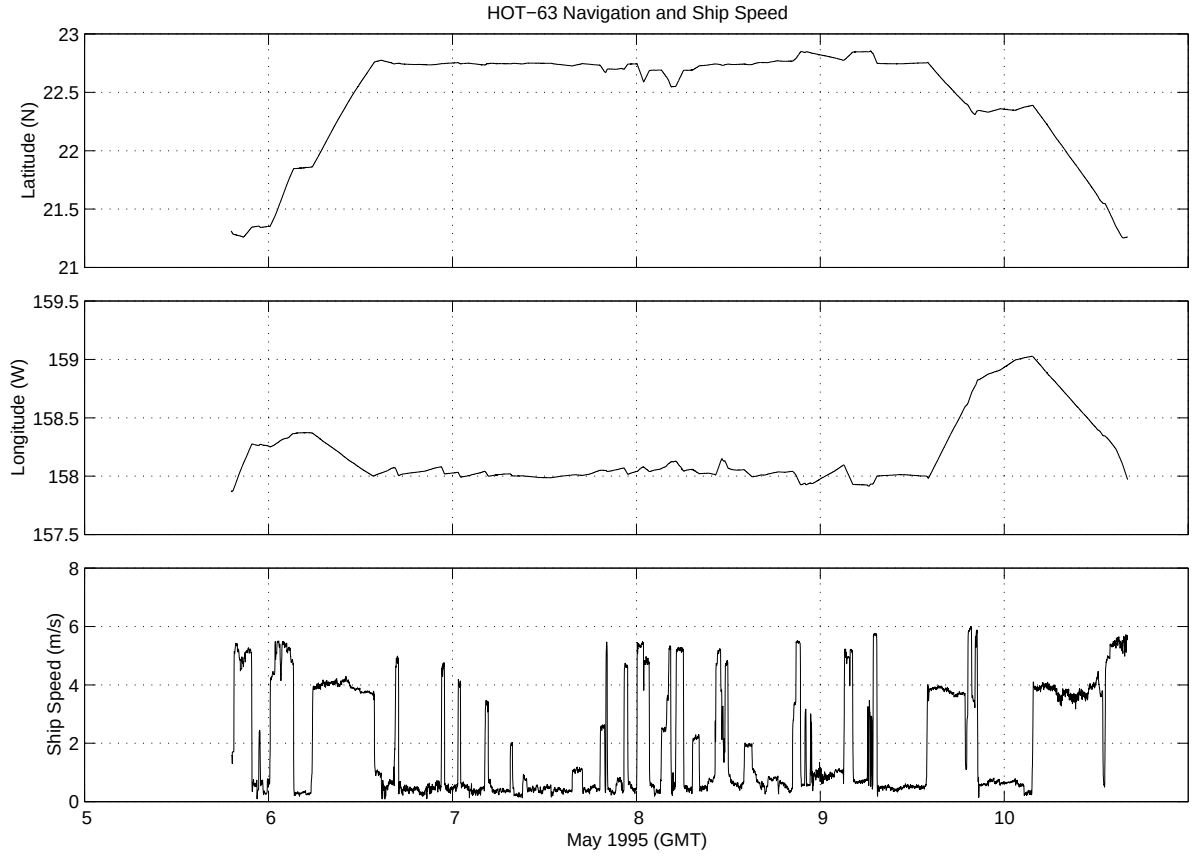
HOT−63 Navigation and Ship Speed
Latitude (N)
Longitude (W)
Ship Speed (m/s)
May 1995 (GMT)

Figure 6.9.1

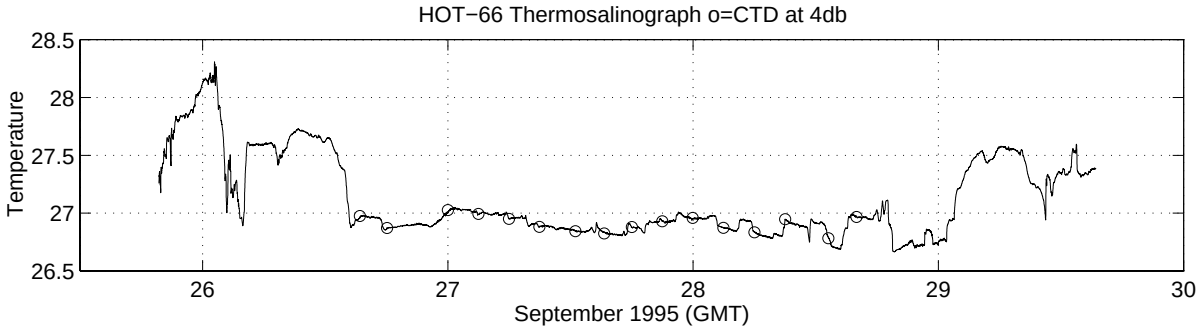
HOT−66 Thermosalinograph o=CTD at 4db
Temperature
28.5
28
27.5
27
26.5
26
27
28
29
30
September 1995 (GMT)

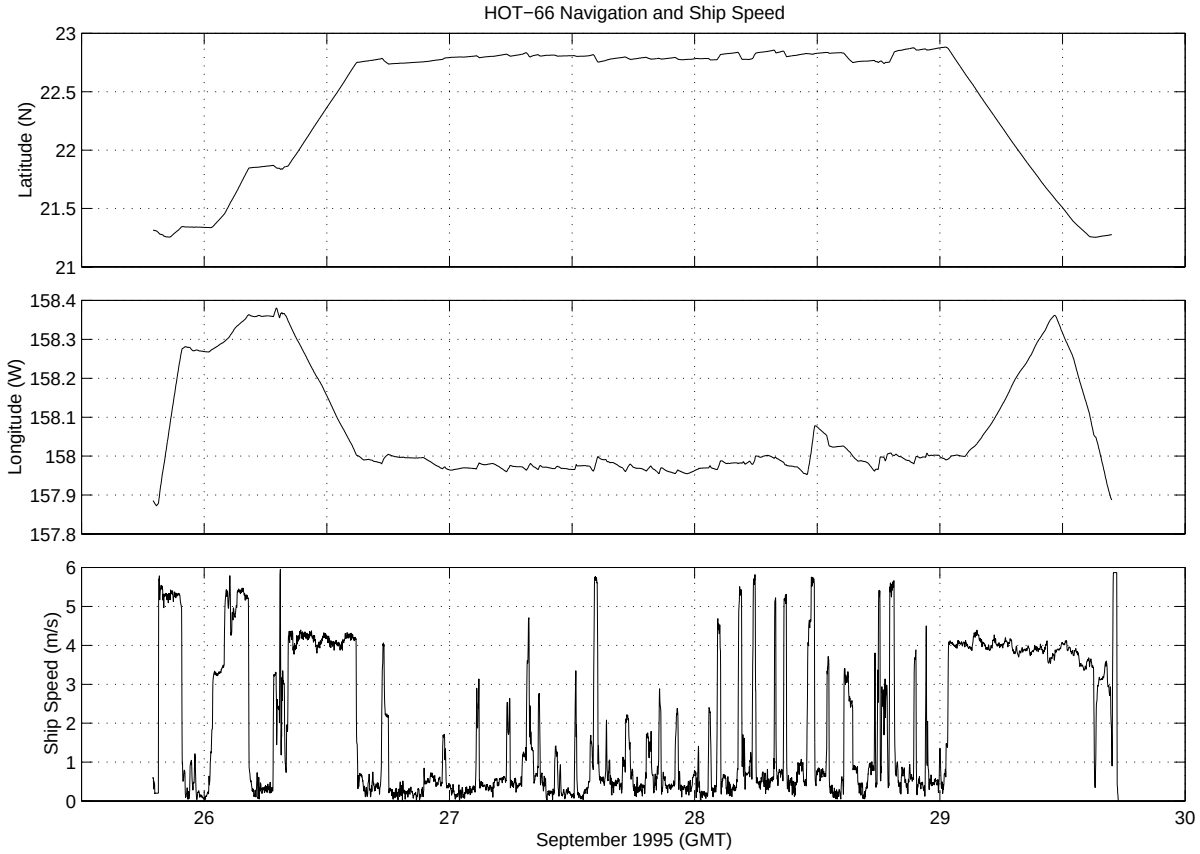
HOT−66 Navigation and Ship Speed
Latitude (N)
23
22.5
22
21.5
21
Longitude (W)
158.4
158.3
158.2
158.1
158
157.9
157.8
Ship Speed (m/s)
6
5
4
3
2
1
0
26
27
28
29
30
September 1995 (GMT)

Figure 6.9.2

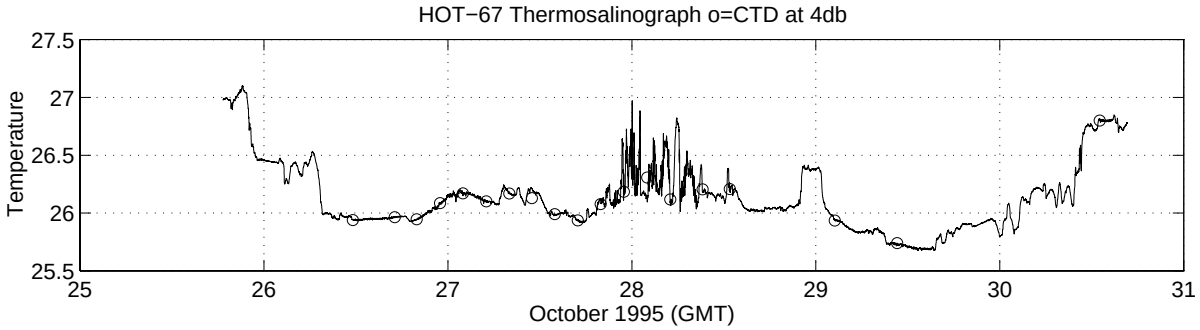
HOT−67 Thermosalinograph o=CTD at 4db
Temperature
27.5
27
26.5
26
25.5
25
26
27
28
29
30
31
October 1995 (GMT)

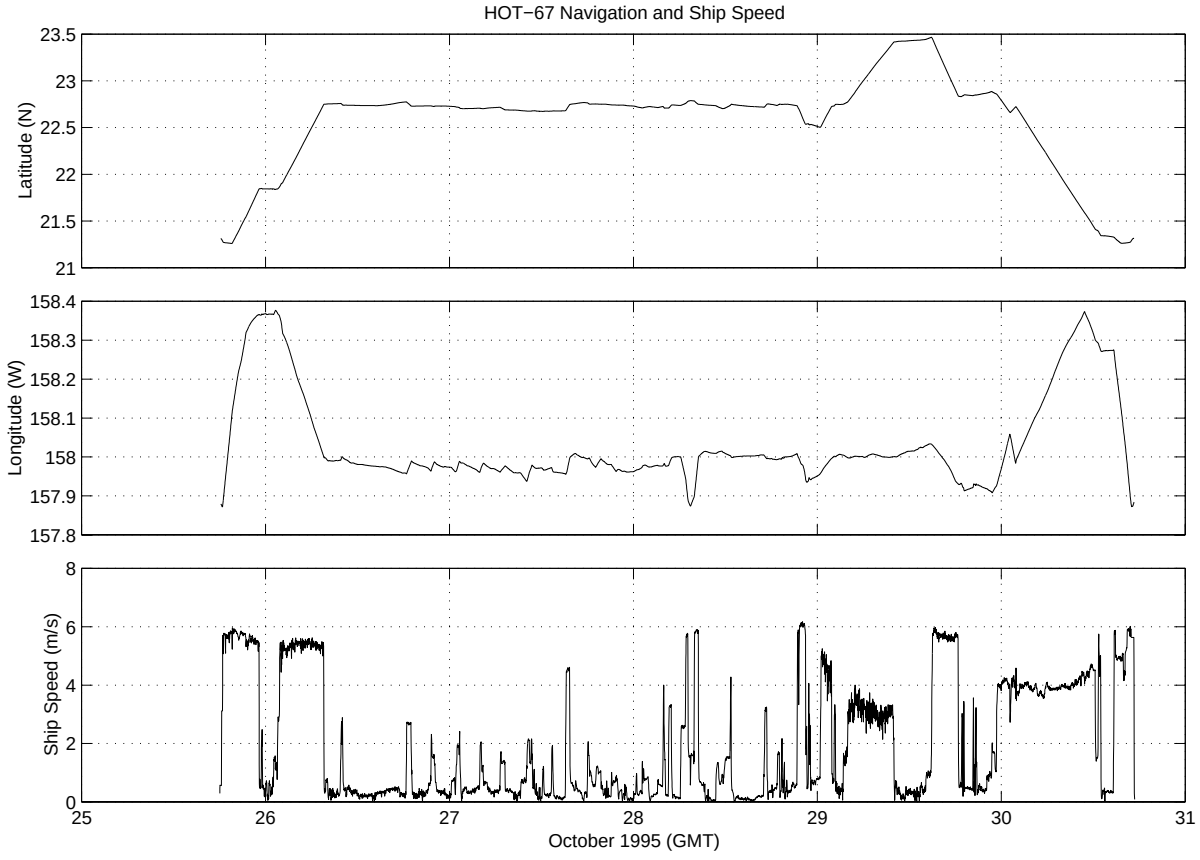
HOT−67 Navigation and Ship Speed
Latitude (N)
23.5
23
22.5
22
21.5
21
Longitude (W)
158.4
158.3
158.2
158.1
158
157.9
157.8
Ship Speed (m/s)
8
6
4
2
0
25
26
27
28
29
30
31
October 1995 (GMT)

Figure 6.9.3

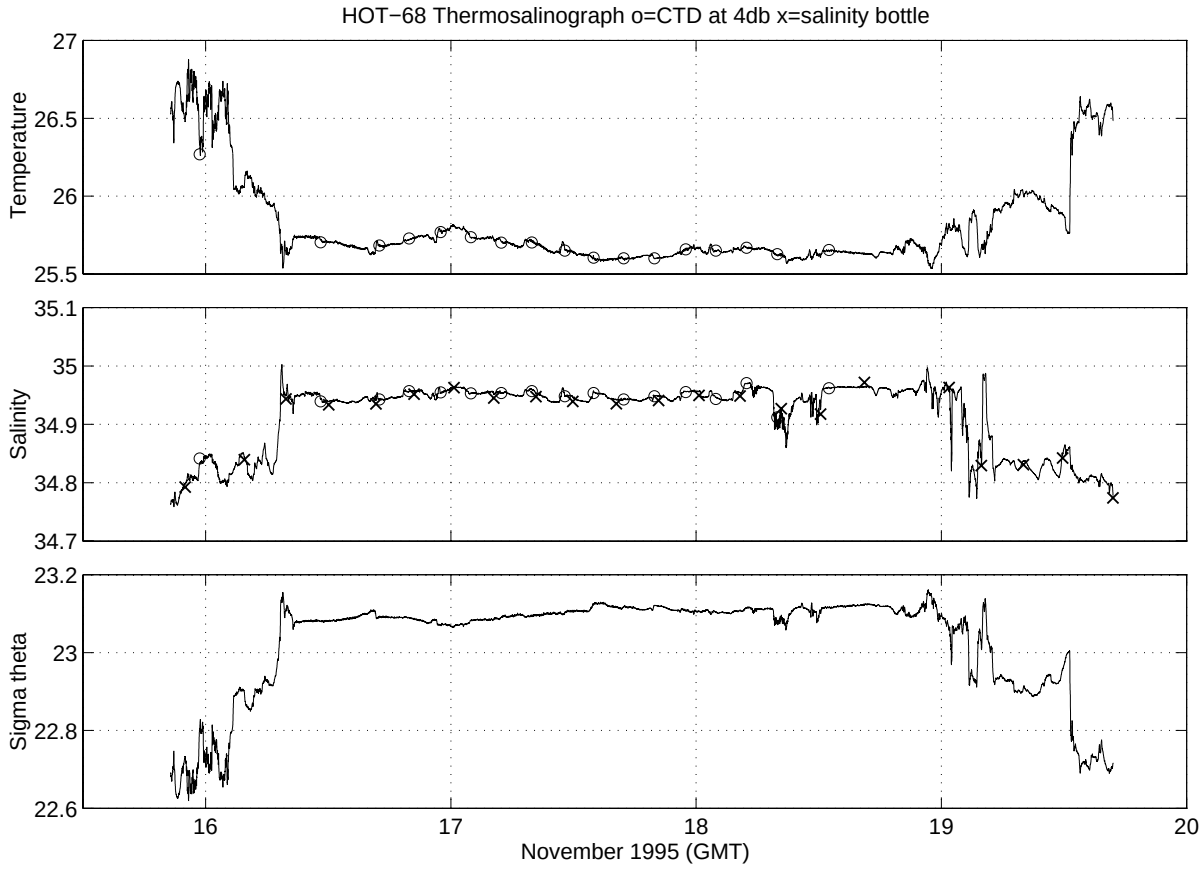
HOT−68 Thermosalinograph o=CTD at 4db x=salinity bottle
Temperature
27
26.5
26
25.5
Salinity
35.1
35
34.9
34.8
34.7
Sigma theta
23.2
23
22.8
22.6
16
17
18
19
20
November 1995 (GMT)

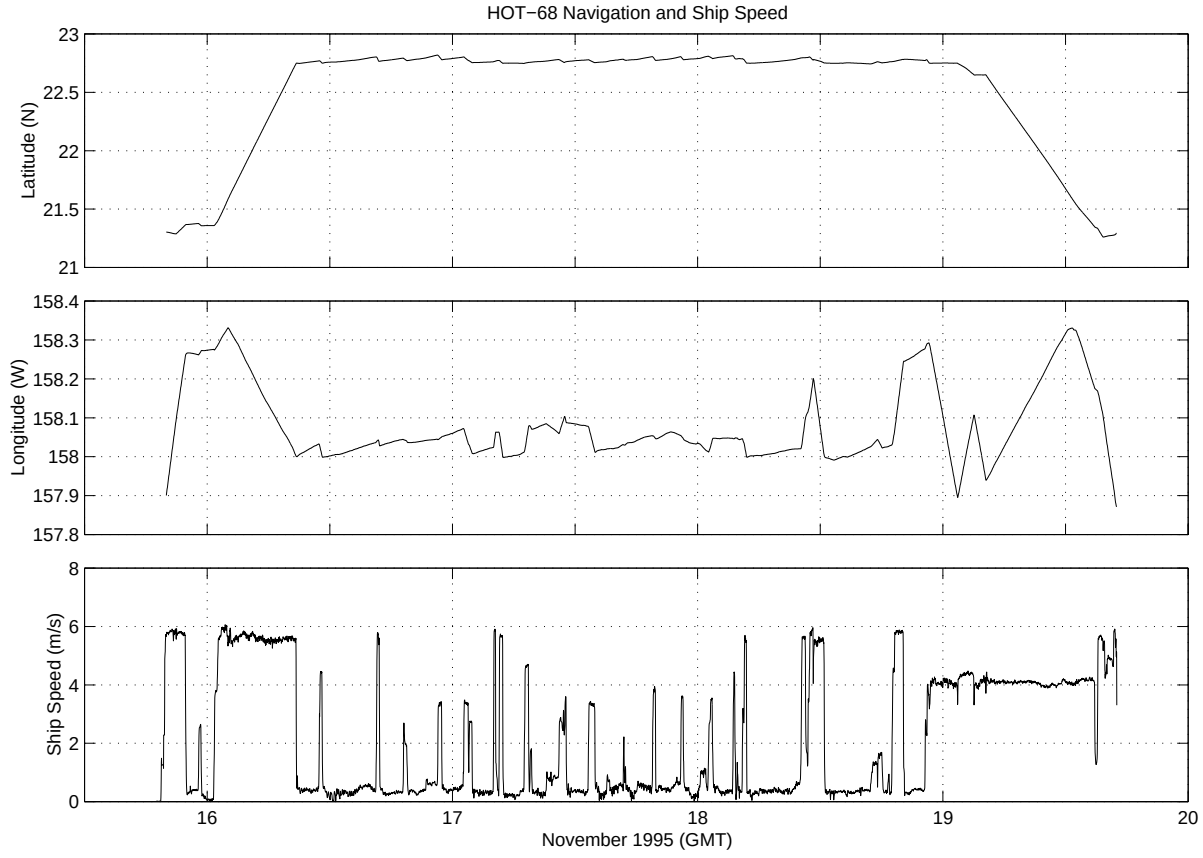
HOT−68 Navigation and Ship Speed
Latitude (N)
23
22.5
22
21.5
21
Longitude (W)
158.4
158.3
158.2
158.1
158
157.9
157.8
Ship Speed (m/s)
8
6
4
2
0
16
17
18
19
20
November 1995 (GMT)

Figure 6.9.4

7. HOT PROGRAM PRESENTATIONS AND PUBLICATIONS

I. Invited Presentations and Published Abstracts

I.1. 1988 Karl, D. NSF-sponsored symposium on Dissertations in Chemical Oceanography, "Research opportunities in Hawaiian waters", Honolulu, Hawaii, November 1988.

I.2. 1988 Karl, D. NSF/GOFS-sponsored workshop on sediment traps, "Determination of total C, N, P flux" and "Screens: A potential solution to the problem of swimmers", Gulf Coast Research Laboratory, Mississippi, November 1988.

I.3. 1989 Winn, C. D., S. Chiswell, D. M. Karl and R. Lukas. Long time-series research in the Central Pacific Ocean. The Oceanography Society 1st Annual Meeting, Monterey, California.

I.4. 1990 Karl, D., R. Letelier, D. Bird, D. Hebel, C. Sabine and C. Winn. An *Oscillatoria* bloom in the oligotrophic North Pacific Ocean near the GOFS station ALOHA. *EOS, Transactions of the American Geophysical Union* 71, 177-178.

I.5. 1990 Winn, C. D., D. Hebel, R. Letelier, D. Bird and D. Karl. Variability in biogeochemical fluxes in the oligotrophic central Pacific: Results of the Hawaii Ocean Time- Series Program. *EOS, Transactions of the American Geophysical Union* 71, 190.

I.6. 1990 Chiswell, S. M. and R. Lukas. The Hawaii Ocean Time-series (HOT). *EOS, Transactions of the American Geophysical Union* 71, 1397.

I.7. 1990 Karl, D. "JGOFS time-series programs," San Francisco, California, December 1990.

I.8. 1991 Winn, C., C. Sabine, D. Hebel, F. Mackenzie and D. M. Karl. Inorganic carbon system dynamics in the central Pacific Ocean: Results of the Hawaii Ocean Time-series program. *EOS, Transactions of the American Geophysical Union* 72, 70.

I.9. 1991 Lukas, R. Water mass variability observed in the Hawaii Ocean Time Series. *EOS, Transactions of the American Geophysical Union* 72, 70.

I.10. 1991 Letelier, R., D. Karl, R. Bidigare, J. Christian, J. Dore, D. Hebel and C. Winn. Temporal variability of phytoplankton pigments at the U.S.-JGOFS station ALOHA (22°45'N, 158°W). *EOS, Transactions of the American Geophysical Union* 72, 74.

I.11. 1991 Karl, D. "The Hawaii Ocean Time-series program: Carbon production and particle flux", The Oceanography Society 2nd Annual Meeting, St. Petersburg, Florida, March 1991.

I.12. 1991 Karl, D. NATO symposium on Biology and Ecology of Diazotrophic Marine Organisms, "*Trichodesmium* blooms and new nitrogen in the North Pacific gyre", Bamberg, Germany, May 1991.

I.13. 1992 Anbar, A. D. Rhenium in seawater: Confirmation of generally conservative behavior. *EOS, Transactions of the American Geophysical Union* 73, 278.

I.14. 1992 Schudlich, R. and S. R. Emerson. Modelling dissolved gases in the subtropical upper ocean: JGOFS/WOCE Hawaiian Ocean Time-series. *EOS, Transactions of the American Geophysical Union* 73, 287.

I.15. 1992 Tupas, L. M., B. N. Popp and D. M. Karl. Dissolved organic carbon in oligotrophic waters: experiments on sample preservation, storage and analysis. *EOS, Transactions of the American Geophysical Union* 73, 287.

I.16. 1992 Karl, D., C. Winn, D. Hebel, R. Letelier, J. Dore and J. Christian. The U.S.-JGOFS Hawaii Ocean Time-Series (HOT) program. American Society for Limnology and Oceanography Aquatic Sciences Meeting, Santa Fe, NM, February 1992.

I.17. 1992 Campbell, L., R. R. Bidigare, R. Letelier, M. Ondrusek, S. Hall, B. Tsai and C. Winn. Phytoplankton population structure at the Hawaii Ocean Time-series station. American Society for Limnology and Oceanography Aquatic Sciences Meeting, Santa Fe, NM, February 1992.

I.18. 1992 Karl, D. NSF-sponsored GLOBEC scientific steering committee meeting, "Hawaii Ocean Time-series (HOT) program: A GLOBEC 'Blue Water' initiative", Honolulu, Hawaii, March 1992.

I.19. 1992 Karl, D. IGBP International Symposium on Global Change, "Oceanic ecosystem variability: Initial results from the JGOFS Hawaii Ocean Time-series (HOT) experiment", Tokyo, Japan, March 1992.

I.20. 1992 Karl, D. Conoco HOT Topics Seminar Series, "The U.S.-JGOFS Hawaii Ocean Time- Series (HOT) Program: Biogeochemical Vignettes from the Oligotrophic North Pacific Ocean" and "Temporal Variability in Bioelement Flux at Station ALOHA (22°45'N, 158°W)", Woods Hole, Massachusetts, May 1992

I.21. 1992 Bidigare, R. R., L. Campbell, M. Ondrusek, R. Letelier and D. Vaulot. Characterization of picophytoplankton at Station ALOHA (22°45'N, 158°W) using HPLC, flow cytometry and immunofluorescence techniques. PACON 1992 Meeting, June 1992.

I.22. 1992 Winn, C. D., D. Hebel, R. Letelier, J. Christian, J. Dore, R. Lukas and D. M. Karl. Long time-series measurements in the central North Pacific: Results of the Hawaii Ocean Time-series program. PACON conference, Kona, Hawaii, June 1992.

I.23. 1993 Atkinson, M. J. A potentiometric solid state sensor for oceanic CTDs, Abstract of The Oceanography Society Annual Meeting, Seattle, Washington, April 1993.

I.24. 1993 Campbell, L., H. A. Nolla and D. Vaulot. Microbial biomass in the subtropical central North Pacific Ocean (Station ALOHA): The importance of Prochlorococcus, Abstract of The Oceanography Society Annual Meeting, Seattle, Washington, April 1993.

I.25. 1993 Emerson, S., P. Quay, C. Stump, D. Wilbur and R. Schudlich. Oxygen cycles and productivity in the oligotrophic subtropical Pacific Ocean. Abstract of The Oceanography Society Annual Meeting, Seattle, Washington, April 1993.

I.26. 1993 Sharp, J. H., R. Benner, L. Bennett, C. A. Carlson, S. E. Fitzwater, E. T. Peltzer, and L. Tupas. Dissolved organic carbon: Intercalibration of analyses with equatorial Pacific samples. Abstract of The Oceanography Society Annual Meeting, Seattle, Washington, April 1993.

I.27. 1993 Winn, C. D., C. J. Carrillo, F. T. Mackenzie and D. M. Karl. Variability in the inorganic carbon system parameters in the North Pacific subtropical gyre. Abstract of The Oceanography Society Annual Meeting, Seattle, Washington, April 1993.

I.28. 1993 Yanagi, K. and D. M. Karl. Note on the fractional determination of TDP in seawater by an UV-irradiation method combined with the MAGIC procedure. Abstract of the Oceanography Society of Japan annual meeting, Tokyo, Japan, April 1993.

I.29. 1993 Campbell, L., H. Liu, R. R. Bidigare and D. Vaulot. Immunochemical characterization of *Prochlorococcus*. Abstract of the American Society of Limnology and Oceanography 1993 Annual Meeting, Edmonton, Alberta, Canada, May 1993.

I.30. 1993 Christian, J. R. and D. M. Karl. Bacterial exoenzymes in marine waters: Implications for global biogeochemical cycles. Abstract of the American Society of Limnology and Oceanography 1993 Annual Meeting, Edmonton, Alberta, Canada, May 1993.

I.31. 1993 Moyer, C. L., L. Campbell, D. M. Karl and J. Wilcox. Restriction fragment length polymorphism (RFLP) and DNA sequence analysis of PCR-generated clones to assess diversity of picoeukaryotic algae in the subtropical central North Pacific Ocean (Station ALOHA). Abstract of the American Society of Limnology and Oceanography 1993 Annual Meeting, Edmonton, Alberta, Canada, May 1993.

I.32. 1993 Sharp, J. H., R. Benner, L. Bennett, C. A. Carlson, S. E. Fitzwater and L. Tupas. The equatorial Pacific intercalibration analyses of dissolved organic carbon in seawater. Abstract of the American Society of Limnology and Oceanography 1993 Annual Meeting, Edmonton, Alberta, Canada, May 1993.

I.33. 1994 Yuan, J., C. I. Measures and J. A. Resing. Rapid determination of iron in seawater: In-line preconcentration flow injection analysis with spectrophotometric detection. *EOS, Transactions of the American Geophysical Union* 75, 25.

I.34. 1994 Smith, C. R., S. Garner, D. Hoover and R. Pope. Macrobenthos, mechanisms of bioturbation and carbon flux proxies at the abyssal seafloor along the JGOFS Equatorial Pacific Transect. *EOS, Transactions of the American Geophysical Union* 75, 70.

I.35. 1994 Farrenkopf, A. M., G. W. Luther, III and C. H. Van Der Weijden. Vertical distribution of dissolved iodine species in the northwest Indian Ocean. *EOS, Transactions of the American Geophysical Union* 75, 78.

I.36. 1994 Campbell, L., C. D. Winn, R. Letelier, D. Hebel and D. M. Karl. Temporal variability in phytoplankton fluorescence at Station ALOHA. *EOS, Transactions of the American Geophysical Union* 75, 100.

I.37. 1994 Winn, C., F. T. Mackenzie, C. Carrillo, T. Westby and D. M. Karl. Air-sea carbon dioxide exchange at Station ALOHA. *EOS, Transactions of the American Geophysical Union* 75, 112.

I.38. 1994 Lukas, R., F. Bingham and A. Mantyla. An anomalous cold event in the bottom water observed north of Oahu. *EOS, Transactions of the American Geophysical Union* 75, 205.

I.39. 1994 Tupas, L. M., B. N. Popp and D. M. Karl. Dissolved organic carbon in oligotrophic waters; experiments on sample preservation, storage and analysis. *EOS, Transactions of the American Geophysical Union* 75, 287.

I.40. 1994 Bingham, F.M. Drifter observations of the North Hawaiian Ridge Current. *EOS, Transactions of the American Geophysical Union* 75, 307.

I.41. 1994 HOT Program P.I.s, staff and students. The Hawaii Ocean Time-series (HOT) program: The first five years, p. 59. Abstract of The Oceanography Society Pacific Basin Meeting, Honolulu, Hawaii, July 1994.

I.42. 1994 HOT Program P.I.s, staff and students. HOT: a time-series study of carbon cycling in the oligotrophic North Pacific, p. 24. Abstract of The Oceanography Society Pacific Basin Meeting, Honolulu, Hawaii, July 1994.

I.43. 1994 Bidigare, R. R., L. Campbell, M. E. Ondrusek, R. Letelier, D. Vaulot and D. M. Karl. Phytoplankton community structure at station ALOHA (22°45'N, 158°W) during fall 1991, p. 58. Abstract of The Oceanography Society Pacific Basin Meeting, Honolulu, Hawaii, July 1994.

I.44. 1994 Bingham, F. M. and B. Qiu. Interannual varibility of surface and mixed layer properties observed in the Hawaii Ocean Time-series, p. 89. Abstract of The Oceanography Society Pacific Basin Meeting, Honolulu, Hawaii, July 1994.

I.45. 1994 Bingham, F. M. and R. Lukas. Seasonal cycles of temperature, salinity and dissolved oxygen observed in the Hawaii Ocean Time-series, p. 90. Abstract of The Oceanography Society Pacific Basin Meeting, Honolulu, Hawaii, July 1994.

I.46. 1994 Christian, J. Vertical fluxes of carbon and nitrogen at Station ALOHA, p. 61. Abstract of The Oceanography Society Pacific Basin Meeting, Honolulu, Hawaii, July 1994.

I.47. 1994 Dore, J. E. and D. M. Karl. Nitrite distributions and dynamics at Station ALOHA, p. 60. Abstract of The Oceanography Society Pacific Basin Meeting, Honolulu, Hawaii, July 1994.

I.48. 1994 Firing, E. Currents observed north of Oahu during the first five years of HOT, p. 90. Abstract of The Oceanography Society Pacific Basin Meeting, Honolulu, Hawaii, July 1994.

I.49. 1994 Fujieki, L. A., D. V. Hebel, L. M. Tupas and D. M. Karl. Hawaii Ocean Time-series Data Organization and Graphical System (HOT-DOGS), p. 61. Abstract of The Oceanography Society Pacific Basin Meeting, Honolulu, Hawaii, July 1994.

I.50. 1994 Hebel, D. V., F. P. Chavez, K. R. Buck, R. R. Bidigare, D. M. Karl, M. Latasa, M. E. Ondrusek, L. Campbell and J. Newton. Do GF/F filters underestimate particulate chlorophyll *a* and primary production in the oligotrophic ocean?, p. 62. Abstract of The Oceanography Society Pacific Basin Meeting, Honolulu, Hawaii, July 1994.

I.51. 1994 Houlihan, T., J. E. Dore, L. Tupas, D. V. Hebel, G. Tien and D. M. Karl. Freezing as a method of preservation for seawater dissolved nutrient and organic carbon samples, p. 62. Abstract of The Oceanography Society Pacific Basin Meeting, Honolulu, Hawaii, July 1994.

I.52. 1994 Kennan, S. C. and R. Lukas. Saline intrusions in the intermediate waters north of Oahu, p. 91. Abstract of The Oceanography Society Pacific Basin Meeting, Honolulu, Hawaii, July 1994.

I.53. 1994 Letelier, R. M., J. Dore, C. D. Winn and D. M. Karl. Temporal variations in photosynthetic carbon assimilation efficiencies at Station ALOHA (22°45'N; 158°00'W), p. 60. Abstract of The Oceanography Society Pacific Basin Meeting, Honolulu, Hawaii, July 1994.

I.54. 1994 Liu, H. and L. Campbell. Growth and grazing rates of *Prochlorococcus* and *Synechococcus* at Station ALOHA measured by the selective inhibitor technique, p. 59. Abstract of The Oceanography Society Pacific Basin Meeting, Honolulu, Hawaii, July 1994.

I.55. 1994 Lukas, R. Interannual variability of Pacific deep and bottom waters observed in the Hawaii Ocean Time-series, p. 91. Abstract of The Oceanography Society Pacific Basin Meeting, Honolulu, Hawaii, July 1994.

I.56. 1994 Lukas, R., F. Bingham and E. Firing. Seasonal-to-interannual variability observed in the Hawaii Ocean Time-series, p. 28. Abstract of The Oceanography Society Pacific Basin Meeting, Honolulu, Hawaii, July 1994.

I.57. 1994 Tupas, L. M., B. N. Popp, D. V. Hebel, G. Tien and D. M. Karl. Dissolved organic carbon measurements at Station ALOHA measured by high temperature catalytic oxidation: Characteristics and variation in the water column, p. 63. Abstract of The Oceanography Society Pacific Basin Meeting, Honolulu, Hawaii, July 1994.

I.58. 1994 Winn, C. D., F. T. Mackenzie, C. Carrillo and D. M. Karl. Air-sea carbon dioxide exchange at Station ALOHA, p. 58. Abstract of The Oceanography Society Pacific Basin Meeting, Honolulu, Hawaii, July 1994.

I.59. 1994 Liu, H. and L. Campbell. Measurement of growth and mortality rate of *Prochloroccus* and *Synechococcus* at Station ALOHA using a new selective inhibitor technique. Fifth International Phycological Congress, Qingdao, China, July 1994.

I.60. 1994 Winn, C., F. T. Mackenzie, C. Carrillo, T. Westby and D. M. Karl. Air-sea carbon dioxide exchange at Station ALOHA, p. 112. Abstract of the American Society of Limnology and Oceanography 1994 Ocean Sciences Meeting, San Diego, California.

I.61. 1994 Measures, C. I., J. Yuan and J. A. Resing. The rapid determination of iron in seawater at sub-nanomolar concentrations using in-line preconcentration and spectrophotometric detection. Sixth Winter Conference on Flow Injection Analysis, San Diego, CA.

I.62. 1994 Measures, C. I., J. Yuan and J. A. Resing. Determination of iron in seawater using in-line preconcentration and spectrophotometric detection. Workshop on Iron Speciation and its Biological Activity, Bermuda Biological Station for Research, Bermuda.

I.63. 1995 Cortés, M. Y. and H. R. Thierstein. Coccolithophore dynamics during 1994 at the JGOFS time series Station ALOHA, Hawaii. 5th International Conference on Paleoceanography, Halifax, Canada, Abstract, p. 121.

I.64. 1995 Campos, M. L. A. M., T. D. Jickells, A. M. Farrenkopf and G. W. Luther, III. A comparison of dissolved iodine cycling at the Bermuda Atlantic Time Series station and Hawaii Ocean Time-series station. *EOS, Transactions of the American Geophysical Union* 76, S175.

I.65. 1995 Yuan, J. Collecting iron samples from well mounted on CTD rosette. *EOS, Transactions of the American Geophysical Union* 76, S175.

I.66. 1995 Michaels, A. F., D. Karl and A. H. Knap. Insights on ocean variability from the JGOFS time-series stations. Invited plenary lecture, The Oceanography Society Biennial Meeting, April 1995.

I.67. 1995 Emerson, S., P. Quay, L. Tupas and D. Karl. Chemical tracers of productivity and respiration in the upper ocean at U.S. JGOFS station ALOHA, 10th Anniversary JGOFS Science Conference, Villefranche, France, May 1995.

I.68. 1995 Michaels, A. F., D. Karl and A. H. Knap. Insights on ocean variability from the JGOFS time-series stations. Invited lecture, 10th Anniversary JGOFS Science Conference, Villefranche, France, May 1995.

I.69. 1995 Karl, D. M. Oceanic carbon cycle and global environmental change: A microbiological perspective. Invited plenary talk, 7th International Symposium on Microbial Ecology, Santos, Brazil, August 1995.

I.70. 1995 Winn, C., D. Sadler and D. M. Karl. Carbon dioxide dynamics at the Hawaii JGOFS/WOCE time-series station. International Association for the Physical Sciences of the Oceans, Honolulu, Hawaii, August 1995.

I.71. 1996 Campbell, L., H. Liu and H. A. Nolla. Picophytoplankton population dynamics at Station ALOHA, p. OS65. AGU-ASLO Ocean Sciences Meeting, San Diego, CA, February 1996.

I.72. 1996 Christian, J. R., J. E. Dore and D. M. Karl. Mixing and nutrient fluxes at the US-JGOFS Station ALOHA ((22°45'N, 158°00'W), p. OS65. AGU-ASLO Ocean Sciences Meeting, San Diego, CA, February 1996.

I.73. 1996 Dulaney, T. S. and L. R. Sautter. Sedimentation of planktonic foraminifera: Seasonal changes in shell flux north of Oahu, Hawaii, p. OS85. AGU-ASLO Ocean Sciences Meeting, San Diego, CA, February 1996.

I.74. 1996 Emerson, S. Chemical tracers of biological processes: O_2, Ar and N_2 mass balance in the subtropical Pacific at the HOT station, p. OS85. AGU-ASLO Ocean Sciences Meeting, San Diego, CA, February 1996.

I.75. 1996 Hebel, D. V., D. M. Karl, J. R. Christian, J. E. Dore, R. M. Letelier, L. M. Tupas and C. D. Winn. Seasonal and interannual variability in primary production and particle flux at Station ALOHA, p. OS85. AGU-ASLO Ocean Sciences Meeting, San Diego, CA, February 1996.

I.76. 1996 Karl, D. M.. Alternation of N and P control of new and export production in the North Pacific gyre: A hypothesis based on the HOT program data set, p. OS86. AGU-ASLO Ocean Sciences Meeting, San Diego, CA, February 1996.

I.77. 1996 Lawson, L. M. and E. E. Hofmann. Time series sampling and data assimilation in a simple marine ecosystem model, p. OS86. AGU-ASLO Ocean Sciences Meeting, San Diego, CA, February 1996.

I.78. 1996 Lopez, M. D. G., Y. Zhu and M. E. Huntley. Space-time variability of zooplankton-sized particle concentrations at the Hawaii Ocean Time-series station (Station ALOHA), p. OS85. AGU-ASLO Ocean Sciences Meeting, San Diego, CA, February 1996.

I.79. 1996 Quay, P. D. and H. Anderson. Organic carbon export rates in the subtropical N. Pacific, p. OS85. AGU-ASLO Ocean Sciences Meeting, San Diego, CA, February 1996.

I.80. 1996 Richman, J. G., R. M. Letelier, M. R. Abbott and D. Pillsbury. Expandable optical mooring test at Station ALOHA (22°45'N; 158°00'W), p. OS64. AGU-ASLO Ocean Sciences Meeting, San Diego, CA, February 1996.

I.81. 1996 Scharek, R., M. Latasa, D. M. Karl and R. R. Bidigare Diatom abundance and vertical flux at the US-JGOFS/WOCE Station "ALOHA" in the oligotrophic North Pacific gyre, p. OS85. AGU-ASLO Ocean Sciences Meeting, San Diego, CA, February 1996.

I.82. 1996 Selph, K. E., M. R. Landry, R. J. Miller and H. A. Al-Mutairi. Temporal variability in the mesozooplankton community at ocean Station ALOHA, p. OS85. AGU-ASLO Ocean Sciences Meeting, San Diego, CA, February 1996.

I.83. 1996 Tersol, V., S. Vink, J. Yuan and C. I. Measures. Variations in iron, aluminium and berylium concentrations in surface waters at Station ALOHA, p. OS65. AGU-ASLO Ocean Sciences Meeting, San Diego, CA, February 1996.

I.84. 1996 Tupas, L. M., M P. Sampson and D. M. Karl. Stable nitrogen isotopic analysis of sinking particulate matter at the Hawaii Ocean Time-series site, p. OS86. AGU-ASLO Ocean Sciences Meeting, San Diego, CA, February 1996.

I.85. 1996 Venrick, E. L.. A comparison between the phytoplankton species from Station ALOHA and from the Climax region, p. OS65. AGU-ASLO Ocean Sciences Meeting, San Diego, CA, February 1996.

I.86. 1996 Winn, C. D. Carbon dioxide dynamics at the Hawaii JGOFS/WOCE time-series station: Annual and interannual variability, p. OS64. AGU-ASLO Ocean Sciences Meeting, San Diego, CA, February 1996.

II. Invited/Contributed Book Chapters and Refereed Publications

II.1. 1990 Firing, E. and R. L. Gordon. Deep ocean acoustic Doppler current profiling. In: G. F. Appell and T. B. Curtin (eds.), *Proceedings of the Fourth IEEE Working Conference on Current Measurements*, pp. 192-201. IEEE, New York.

II.2. 1990 Giovannoni, S. J., E. F. DeLong, T. M. Schmidt and N. R. Pace. Tangential flow filtration and preliminary phylogenetic analysis of marine picoplankton. *Applied and Environmental Microbiology*, 56, 2572-2575.

II.3. 1991 Chiswell, S. M. Dynamic response of CTD pressure sensors to temperature. *Journal of Atmospheric and Oceanic Technology* 8, 659-668.

II.4 1991 Karl, D. M., J. E. Dore, D. V. Hebel and C. Winn. Procedures for particulate carbon, nitrogen, phosphorus and total mass analyses used in the US-JGOFS Hawaii Ocean Time- Series Program. In: D. Spencer and D. Hurd (eds.), *Marine Particles: Analysis and Characterization*, pp. 71-77. American Geophysical Union, Geophysical Monograph 63.

II.5. 1991 Karl, D. M., W. G. Harrison, J. Dore et al. Chapter 3. Major bioelements workshop report. In: D. C. Hurd and D. W. Spencer (eds.), *Marine Particles: Analysis*

and Characterization, pp. 33-42. American Geophysical Union, Geophysical Monograph 63.

II.6. 1991 Karl, D. M. and C. D. Winn. A sea of change: Monitoring the oceans' carbon cycle. *Environmental Science & Technology* 25, 1976-1981.

II.7. 1991 Laws, E. A. Photosynthetic quotients, new production and net community production in the open ocean. *Deep-Sea Research* 38, 143-167.

II.8. 1991 Sabine, C. L. and F. T. Mackenzie. Oceanic sinks for anthropogenic CO_2. *International Journal of Energy, Environment, Economics* 1, 119-127.

II.9. 1991 Schmidt, T. M., E. F. DeLong and N. R. Pace. Analysis of a marine picoplankton community by 16S rRNA gene cloning and sequencing. *Journal of Bacteriology* 173, 4371- 4378.

II.10. 1992 Benner, R., J. D. Pakulski, M. McCarthy, J. I. Hedges and P. G. Hatcher. Bulk chemical characteristics of dissolved organic matter in the ocean. *Science* 255, 1561-1564.

II.11. 1992 Chen, R. F. and J. L. Bada. The fluorescence of dissolved organic matter in seawater. *Marine Chemistry* 37, 191-221.

II.12. 1992 Karl, D. M. The oceanic carbon cycle: Primary production and carbon flux in the oligotrophic North Pacific Ocean. In: Y. Oshima (ed.), *Proceedings of the IGBP Symposium on Global Change*, pp. 203-219. Japan National Committee for the IGBP, Waseda University, Tokyo, Japan.

II.13. 1992 Karl, D. M., R. Letelier, D. V. Hebel, D. F. Bird and C. D. Winn. *Trichodesmium* blooms and new nitrogen in the North Pacific gyre. In: E. J. Carpenter et al. (eds.), *Marine Pelagic Cyanobacteria: Trichodesmium and Other Diazotrophs*, pp. 219-237. Kluwer Academic Publishers, Netherlands.

II.14. 1992 Karl, D. M. and G. Tien. MAGIC: A sensitive and precise method for measuring dissolved phosphorus in aquatic environments. *Limnology and Oceanography* 37, 105-116.

II.15. 1992 Quay, P.D., B. Tilbrook and C. S. Wong. Oceanic uptake of fossil fuel CO_2: Carbon- 13 evidence. *Science* 256, 74-78.

II.16. 1993 Anbar, A. D., R. A. Creaser, D. A. Papanastassiou and G. J. Wasserburg. Rhenium in seawater: Confirmation of generally conservative behavior. *Geochimica et Cosmochimica Acta* 56, 4099-4103.

II.17. 1993 Campbell, L. and D. Vaulot. Photosynthetic picoplankton community structure in the subtropical North Pacific Ocean near Hawaii (station ALOHA). *Deep-Sea Research* 40, 2043- 2060.

II.18. 1993 Coble, P. G., C. A. Schultz and K. Mopper. Fluorescence contouring analysis of DOC intercalibration experiment samples: a comparison of techniques. *Marine Chemistry* 41, 173-178.

II.19. 1993 Emerson, S., P. Quay, C. Stump, D. Wilbur and R. Schudlich. Determining primary production from the mesoscale oxygen field. *ICES Marine Science Symposium* 197, 196-206.

II.20. 1993 Hedges, J. I., B. A. Bergamaschi and R. Benner. Comparative analyses of DOC and DON in natural waters. *Marine Chemistry* 41, 121-134.

II.21. 1993 Karl, D. M. Total microbial biomass estimation derived from the measurement of particulate adenosine-5'-triphosphate. In: P. F. Kemp, B. F. Sherr, E. B. Sherr and J. J. Cole (eds.), *Current Methods in Aquatic Microbial Ecology*, pp. 359-368. Lewis Publishers, Boca Raton.

II.22. 1993 Karl, D. M., G. Tien, J. Dore and C. D. Winn. Total dissolved nitrogen and phosphorus concentrations at US-JGOFS Station ALOHA: Redfield reconciliation. *Marine Chemistry* 41, 203-208.

II.23. 1993 Keeling, C. D. Lecture 2: Surface ocean CO_2. *NATO ASI Series* I(15), 413-429.

II.24. 1993 Letelier, R. M., R. R. Bidigare, D. V. Hebel, C. D. Winn and D. M. Karl. Temporal variability study of the phytoplankton community structure at the US-JGOFS Time-series Station ALOHA (22°45'N, 158°00'W) based on pigment analyses. *Limnology and Oceanography* 38, 1420-1437.

II.25. 1993 Mopper, K. and C. A. Schultz. Fluorescence as a possible tool for studying the nature and water column distribution of DOC components. *Marine Chemistry* 41, 229-238.

II.26. 1993 Selph, K. E., D. M. Karl and M. R. Landry. Quantification of chemiluminescent DNA probes using liquid scintillation counting. *Analytical Biochemistry* 210, 394-401.

II.27. 1993 Sharp, J. H., E. T. Peltzer, M. J. Alperin, G. Cauwet, J. W. Farrington, B. Fry, D. M. Karl, J. H. Martin, A. Spitzy, S. Tugrul and C. A. Carlson. Procedures subgroup report. *Marine Chemistry* 41, 37-49.

II.28. 1993 Winn, C. D., R. Lukas, D. Hebel, C. Carrillo, R. Letelier and D. M. Karl. The Hawaii Ocean Time-series program: Resolving variability in the North Pacific. In: N. Saxena (ed.), *Recent Advances in Marine Science and Technology*, pp. 139-150. Proceedings of the Pacific Ocean Congress (PACON).

II.29. 1994 Baines, S. B., M. L. Pace and D. M. Karl. Why does the relationship between sinking flux and planktonic primary production differ between lakes and ocean? *Limnology and Oceanography* 39, 213-226.

II.30. 1994 Björkman, K. and D. M. Karl. Bioavailability of inorganic and organic phosphorus compounds to natural assemblages of microorganisms in Hawaiian coastal waters. *Marine Ecology Progress Series*, 111, 265-273.

II.31. 1994 Campbell, L., H. A. Nolla and D. Vaulot. The importance of photosynthetic prokaryote biomass in the subtropical central North Pacific Ocean (Station ALOHA). *Limnology and Oceanography*, 39, 954-961.

II.32. 1994 Campbell, L., L. P.Shapiro and E. M. Haugen. Immunochemical characterization of the eukaryotic ultraplankton in the Atlantic and Pacific Oceans. *Journal of Plankton Research* 16, 35-51.

II.33. 1994 Christian, J. R. and D. M. Karl. Microbial community structure at the U.S.-Joint Global Ocean Flux Study Station ALOHA: Inverse methods for estimating biochemical indicator ratios. *Journal of Geophysical Research* 99, 14,269-14,276.

II.34. 1994 Karl, D. M. Accurate estimation of microbial loop processes and rates. *Microbial Ecology*, 28, 147-150.

II.35. 1994 Karl, D. M. and B. D. Tilbrook. Production and transport of methane in oceanic particulate organic matter. *Nature* 368, 732-734.

II.36. 1994 Tupas, L. M., B. N. Popp and D. M. Karl. Dissolved organic carbon in oligotrophic waters: experiments on sample preservation, storage and analysis. *Marine Chemistry* 45, 207- 216.

II.37. 1994 Winn, C. D., F. T. Mackenzie, C. J. Carrillo, C. L. Sabine and D. M. Karl. Air-sea carbon dioxide exchange in the North Pacific subtropical gyre: Implications for the global carbon budget. *Global Biogeochemical Cycles* 8, 157-163.

II.38. 1995 Atkinson, M. A., F. I. M. Thomas, N. Larson, E. Terrill, K. Morita and C. Liu. A micro-hole potentiostatic oxygen sensor for oceanic CTDs. *Deep-Sea Research* 42, 761-771.

II.39. 1995 Chavez, F. P., K. R. Buck, R. R. Bidigare, D. M. Karl, D. Hebel, M. Latasa, M. E. Ondrusek, L. Campbell and J. Newton. On the chlorophyll *a* retention properties of glass- fiber GF/F filters. *Limnology and Oceanography*, 40, 428-433.

II.40. 1995 Christian, J. R. and D. M. Karl. Bacterial exocellular enzymes in marine waters: activity ratios and temperature kinetics in three oceanographic provinces. *Limnology and Oceanography* 40, 1042-1049.

II.41. 1995 Christian, J. R. and D. M. Karl. Measuring bacterial ectoenzyme activities in marine waters using mercuric chloride as a preservative and a control. *Marine Ecology Progress Series*, 123, 217-224.

II.42. 1995 Emerson, S., P. D. Quay, C. Stump, D. Wilbur and R. Schudlich. Chemical tracers of productivity and respiration in the subtropical Pacific Ocean. *Journal of Geophysical Research,* 100, 15,873-15,887.

II.43. 1995 Jones, D. R., D. M. Karl and E. A. Laws. DNA:ATP ratios in marine microalgae and bacteria: Implications for growth rate estimates based on rates of DNA synthesis. *Journal of Phycology,* 31, 215-223.

II.44. 1995 Karl, D. M. A reply to a comment by J. A. McGowan "HOT and the North Pacific gyre." *Nature* 378, 21-22.

II.45. 1995 Karl, D. M., R. Letelier, D. Hebel, L. Tupas, J. Dore, J. Christian and C. Winn. Ecosystem changes in the North Pacific subtropical gyre attributed to the 1991-92 El Niño. *Nature,* 373, 230-234.

II.46. 1995 Liu, H., L. Campbell and M. R. Landry. Growth and mortality rates of *Prochlorococcus* and *Synechococcus* measured with a selective inhibitor technique. *Marine Ecology Progress Series* 116, 277-287.

II.47. 1995 Maranger, R. and D. F. Bird. Viral abundance in aquatic systems: a comparison between marine and fresh waters. *Marine Ecology Progress Series* 121, 217-226.

II.48. 1995 Sabine, C. L. and F. T. Mackenzie. Bank-derived carbonate sediment transport and dissolution in the Hawaiian Archipelago. *Aquatic Geochemistry,* 1, 189-230.

II.49. 1995 Sabine, C. L., F. T. Mackenzie, C. Winn and D. M. Karl. Geochemistry of particulate and dissolved inorganic carbon at the Hawaii Ocean Time-series station, ALOHA. *Journal of Biogeochemical Cycles* 9, 637-651.

II.50. 1995 Sharp, J. H., R. Benner, L. Bennett, C. A. Carlson, S. E. Fitzwater, E. T. Peltzer and L. M. Tupas. Analyses of dissolved organic carbon in seawater: the JGOFS EqPac methods comparison. *Marine Chemistry,* 48, 91-108.

II.51. 1995 Thomas, F. I. M. and M. J. Atkinson. Field calibration of a microhole potentiostatic oxygen sensor for oceanic CTDs. *Journal of Atmospheric and Oceanic Technology* 12, 390-394.

II.52. 1995 Thomas, F. I. M., S. A. McCarthy, J. Bower, S. Krothapalli, M. J. Atkinson and P. Flament. Response characteristics of two oxygen sensors for oceanic CTDs. *Journal of Atmospheric and Oceanic Technology* 12, 687-690.

II.53. 1995 Tilbrook, B. D. and D. M. Karl. Methane sources, distributions and sinks from California coastal waters to the oligotrophic North Pacific gyre. *Marine Chemistry* 49, 51-64.

II.54. 1995 Winn, C. D., L. Campbell, R. Letelier, D. Hebel, L. Fujieki and D. M. Karl. Seasonal variability in chlorophyll concentrations in the North Pacific subtropical gyre. *Global Biogeochemical Cycles,* 9, 605-620.

II.55. 1996 Andersen, R., R. Bidigare, M. Keller and M. Latasa. A comparison of HPLC pigment signatures and electron microscopic observations for oligotrophic waters of the North Atlantic and Pacific Oceans. *Deep-Sea Research* 43, 517-537.

II.56. 1996 Atkinson, M., F. Thomas and N. Larson. Effects of pressure on oxygen sensors. *Journal of Atmospheric and Oceanic Technology*, in press.

II.57. 1996 Bingham, F. and R. Lukas Seasonal cycles of temperature, salinity and dissolved oxygen observed in the Hawaii Ocean Time-series. *Deep-Sea Research* 43, 199-213.

II.58. 1996 Campos, M. L., A. Farrenkopf, T. Jickells and G. Luther. A comparison of dissolved iodine cycling at the Bermuda Atlantic Time-series Study station and Hawaii Ocean Time-series station. *Deep-Sea Research* 43, 455-466.

II.59. 1996 Chiswell, S. Intraseasonal oscillations at Station ALOHA, north of Oahu, Hawaii. *Deep-Sea Research* 43, 305-319.

II.60. 1996 Chiswell, S. Using an array of inverted echo sounders to measure dynamic height and geostrophic current in the North Pacific subtropical gyre. *Journal of Atmospheric and Oceanic Technology*, in press.

II.61. 1996 Dore, J. E., T. Houlihan, D. V. Hebel, G. Tien, L. M. Tupas and D. M. Karl. Freezing as a method of seawater preservation for the analysis of dissolved inorganic nutrients in seawater. *Marine Chemistry*, 53, 173-185.

II.62. 1996 Dore, J. E. and D. M. Karl. Nitrification in the euphotic zone as a source for nitrite, nitrate and nitrous oxide at Station ALOHA. *Limnology and Oceanography*, in press.

II.63. 1996 Dore, J. E. and D. M. Karl. Nitrite distributions and dynamics at Station ALOHA. *Deep-Sea Research* 43, 385-402.

II.64. 1996 Feller, R. J. and D. M. Karl. The National Association of Marine Laboratories: A connected web for studying long-term changes in U.S. coastal and marine waters. *Biological Bulletin*, 190, 269-277.

II.65. 1996 Firing, E. Currents observed north of Oahu during the first 5 years of HOT. *Deep-Sea Research* 43, 281-303.

II.66. 1996 Jones, D. R., D. M. Karl and E. A. Laws. Growth rates and production of heterotrophic bacteria and phytoplankton in the North Pacific subtropical gyre. *Deep-Sea Research*, in press.

II.67. 1996 Karl, D. M. Oceanic carbon cycle and global environmental change: A microbiological perspective. In: M. T. Martins (ed.), *Global Aspects of Microbial Ecology*, in press.

II.68. 1996 Karl, D. M., J. R. Christian, J. E. Dore, D. V. Hebel, R. M Letelier, L. M. Tupas and C. D. Winn. Seasonal and interannual variability in primary production and particle flux at Station ALOHA. *Deep-Sea Research* 43, 539-568.

II.69. 1996 Karl, D. M. and F. C. Dobbs. Molecular approaches to microbial biomass estimation in the sea. *Molecular Approaches to the Study of the Ocean (K. E. Cooksey, Ed.),* in press.

II.70. 1996 Karl, D. M. and R. Lukas. The Hawaii Ocean Time-series (HOT) program: Background, rationale and field implementation. *Deep-Sea Research* 43, 129-156.

II.71. 1996 Karl, D. M. and G. Tien. Temporal variability in dissolved phosphorus concentrations at Station ALOHA (22°45'N, 158°W). *Marine Chemistry*, in press.

II.72. 1996 Kennan, S. C. and R. Lukas. Saline intrusions in the intermediate waters north of Oahu, Hawaii. *Deep-Sea Research* 43, 215-241.

II.73. 1996 Latasa, M., R. R. Bidigare, M. E. Ondrusek and M. C. Kennicutt II. HPLC analysis of algal pigments: a comparison exercise among laboratories and recommendations for improved analytical performance. *Marine Chemistry* 51, 315-324.

II.74. 1996 Lawson, L., Y. Spitz and E. Hofmann. Time series sampling and data assimilation in a simple marine ecosystem model. *Deep-Sea Research* 43, 625-651.

II.75. 1996 Letelier, R. M., J. E. Dore, C. D. Winn and D. M. Karl. Temporal variations in photosynthetic carbon assimilation efficiencies at Station ALOHA. *Deep-Sea Research* 43, 467-490.

II.76. 1996 Letelier, R. M. and D. M. Karl. The role of *Trichodesmium* spp. in the productivity of the subtropical North Pacific Ocean. *Marine Ecology Progress Series* 133, 263-273.

II.77. 1996 Lukas, R. and F. Santiago-Mandujano. Interannual variability of Pacific deep and bottom waters observed in the Hawaii Ocean Time-series. *Deep-Sea Research* 43, 243-255.

II.78. 1996 Mitchum, G. On using satellite altimetric heights to provide a spatial context for the Hawaii Ocean Time-series measurements. *Deep-Sea Research* 43, 257-280.

II.79. 1996 Moyer, C. L., J. M. Tiedje, F. C. Dobbs and D. M. Karl. A computer-simulated restriction fragment length polymorphism analysis of bacterial small-subunit rRNA genes: Efficacy of selected tetrameric restriction enzymes for studies of microbial diversity in nature. *Applied and Environmental Microbiology* 62, 2501-2507.

II.80 1996 Roy-Barman, M., J. H. Chen and G. J. Wasserburg. ^{230}Th-^{232}Th systematics in the central Pacific Ocean: The sources and the fates of thorium. *Earth and Planetary Science Letters* 139, 351-363.

II.81. 1996 Schudlich, R. and S. Emerson. Gas saturation in the surface ocean: The roles of heat flux, gas exchange and bubbles. *Deep-Sea Research* 43, 569-589.

III. Submitted Papers

III.1. 1996 Campbell, L., H. Liu and H. A. Nolla. Picophytoplankton population dynamics in the subtropical North Pacific Ocean. Submitted to *Deep-Sea Research*.

III.2. 1996 Liu, H., L. Campbell and H. A. Nolla. *Prochlorococcus* growth rate and contribution to primary production in the equatorial and subtropical North Pacific Ocean. Submitted to *Limnology and Oceanography*.

III.3. 1996 Winn, C. D., Y. H. Li, F. T. Mackenzie and D. M. Karl. Rising surface ocean total dissolved inorganic carbon at the Hawaii Ocean Time-series site. Submitted to *Marine Chemistry*.

III.4. 1996 Karl, D. M. and K. Yanagi. Partial characterization of the dissolved organic phosphorus pool in the oligotrophic North Pacific Ocean. Submitted to *Limnology and Oceanography*.

III.5. 1996 Christian, J. R., M. R. Lewis and D. M. Karl. Vertical fluxes of carbon, nitrogen and phosphorus in the North Pacific subtropical gyre. Submitted to *Journal of Geophysical Research*.

IV. Theses and Dissertations

IV.1. 1992 Sabine, C. L. Geochemistry of particulate and dissolved inorganic carbon in the central North Pacific. Ph.D. Dissertation, May 1992

IV.2. 1993 Kennan, S. Variability of the intermediate water north of Oahu. M.S. Thesis, December 1993.

IV.3. 1994 Letelier, R. M. Studies on the ecology of *Trichodesmium* spp. (*Cyanophyceae*) in the central North Pacific gyre. Ph.D. Dissertation, April 1994.

IV.4. 1994 Liu, H. B. Growth and mortality rates of *Prochlorococcus* and *Synechococcus* measured by a selective inhibitor technique. M.S. Thesis, May 1994.

IV.5. 1995 Dore, J. E. Microbial nitrification in the marine euphotic zone: Rates and relationships with nitrite distributions, recycled production and nitrous oxide generation. Ph.D. Dissertation, May 1995.

IV.6. 1995 Christian, J. R. Biochemical mechanisms of bacterial utilization of dissolved and particulate organic matter in the upper ocean. Ph.D. Dissertation, December 1995.

V. Data Reports and Manuals

V.1. 1990 Karl, D. M., C. D. Winn, D. V. W. Hebel and R. Letelier. Hawaii Ocean Time-series Program Field and Laboratory Protocols, September 1990. School of Ocean and Earth Science and Technology, Univ. of Hawaii, Honolulu, HI, 72 pp.

V.2. 1990 Collins, D. J., W. J. Rhea and A. van Tran. Bio-optical profile data report: HOT-3. National Aeronautics and Space Administration JPL Publ. #90-36.

V.3. 1990 Chiswell, S., E. Firing, D. Karl, R. Lukas and C. Winn. Hawaii Ocean Time-series Program Data Report 1, 1988-1989. SOEST Tech. Rept. #1, School of Ocean and Earth Science and Technology, Univ. of Hawaii, Honolulu, HI, 269 pp.

V.4. 1992 Winn, C., S. Chiswell, E. Firing, D. Karl and R. Lukas. Hawaii Ocean Time-series Program Data Report 2, 1990. SOEST Tech. Rept. 92-1, School of Ocean and Earth Science and Technology, Univ. of Hawaii, Honolulu, HI, 175 pp.

V.5. 1993 Winn, C., R. Lukas, D. Karl and E. Firing. Hawaii Ocean Time-series Program Data Report 3, 1991. SOEST Tech. Report 93-3, School of Ocean and Earth Science and Technology, Univ. of Hawaii, Honolulu, HI, 228 pp.

V.6. 1993 Tupas, L., F. Santiago-Mandujano, D. Hebel, R. Lukas, D. Karl and E. Firing. Hawaii Ocean Time-series Program Data Report 4, 1992. SOEST Tech. Report 93-14, School of Ocean and Earth Science and Technology, Univ. of Hawaii, Honolulu, HI, 248 pp.

V.7. 1994 Tupas, L., F. Santiago-Mandujano, D. Hebel, E. Firing, F. Bingham, R. Lukas and D. Karl. Hawaii Ocean Time-series Program Data Report 5, 1993. SOEST Tech. Report 94-5, School of Ocean and Earth Science and Technology, Univ. of Hawaii, Honolulu, HI, 156 pp.

V.8. 1994 Voss, C. I. and W. W. Wood Synthesis of geochemical, isotopic and groundwater modelling analysis to explain regional flow in a coastal aquifer of Southern Oahu, Hawaii. In: *Mathematical Models and Their Applications to Isotope Studies in Groundwater Hydrology*, pp. 147-178, International Atomic Energy Agency, Vienna, Austria.

V.9. 1995 Tupas, L., F. Santiago-Mandujano, D. Hebel, E. Firing, R. Lukas and D. Karl. Hawaii Ocean Time-series Program Data Report 6, 1994. SOEST Tech. Report 95-6, School of Ocean and Earth Science and Technology, Univ. of Hawaii, Honolulu, HI, in press.

VI. Newsletters

VI.1. 1989 Karl, D. M. Hawaiian Ocean Time-series program: It's HOT. *GOFS Newsletter* 1(2), 1-3.

VI.2. 1990 Karl, D. M. HOT Stuff: An update on the Hawaiian Ocean Time-series program. *U.S. JGOFS Newsletter* 2(1), 6,9.

VI.3. 1990 Karl, David M. HOT Stuff: Rescue at sea. *U.S. JGOFS Newsletter* 2(2), 8.

VI.4. 1991 Karl, D. M. HOT Stuff: Retrospect and prospect. *U.S. JGOFS Newsletter* 2(3), 10.

VI.5. 1991 Karl, D. M. HOT Stuff: Hectic spring schedule keeps HOT team hustling. *U.S. JGOFS Newsletter* 2(4), 9-10.

VI.6. 1991 Lukas, R. and S. Chiswell. Submesoscale water mass variations in the salinity minimum of the North Pacific. *WOCE Notes*, 3(1), 6-8.

VI.7. 1992 Karl, D. M. Hawaii Time-series program: Progress and prospects. *U.S. JGOFS Newsletter* 3(4), 1,15.

VI.8. 1992 Michaels, A. F. Time-series programs compare results, methods and plans for future. *U.S. JGOFS Newsletter* 4(1), 7,9.

VI.9. 1992 Winn, C. W. HOT program builds time-series set of carbon measurements for central Pacific. *U.S. JGOFS Newsletter* 4(2), 7.

VI.10. 1992 Dickey, T. D. Oversight committee reviews time-series programs, issues recommendations. *U.S. JGOFS Newsletter* 4(2), 14-15.

VI.11. 1992 Firing, E. and P. Hacker. ADCP results from WHP P16/P17. *WOCE Notes*, 4(3), 6- 12.

VI.12. 1992 Chiswell, S. Inverted echo sounders at the WOCE deep-water station. *WOCE Notes*, 4(4), 1, 3-6.

VI.13. 1993 Karl, D. M. HOT Stuff: The five-year perspective. *U.S. JGOFS Newsletter* 5(1), 6,15.

VI.14. 1994 Karl, D. M. HOT Stuff: Surprises emerging from five years' worth of data. *U.S. JGOFS Newsletter* 5(4), 9-10.

VI.15. 1994 Tupas, L. M. Euphotic zone nitrate variability in the central North Pacific gyre at the Hawaii Ocean Time-series Station ALOHA. *International WOCE Newsletter* 17, 21-23.

VI.16. 1994 Lukas, R. HOT results show interannual variability of Pacific Deep and Bottom waters. *WOCE Notes* 6(2), 1, 3, 14-15.

VI.17. 1995 Karl, D. M. HOT and COLD: A trapper's tale of two oceans. *U.S. JGOFS Newsletter* 6(2): 7, 15.

VI.18. 1995 Karl, D. M. HOT Stuff: New hypotheses and projects evolve from growing data set. *U.S. JGOFS Newsletter* 7(1): 11.

VI.19. 1996 Winn, C.D. and P. G. Driscoll. Hawaii Time-series data reveal rising ocean CO_2 levels. *U.S. JGOFS Newsletter* 7(4): 7-8.

VI.20. 1996 Karl, D. M. The Hawaii Ocean Time-series study: Still HOT at 75. *U.S. JGOFS Newsletter* 7(4): 8-9.

VII. Other

VII.1. Presentations from the "HOT Program: Progress and Prospectus" symposium, 3-4 June 1992, East-West Center, Honolulu, HI

Campbell, L. Bacterial numbers by flow cytometry: A new approach
Chiswell, S. Results from the inverted echo sounder network
Christian, J. Biomass closure in the epipelagic zone
Christian, J. Exoenzymatic hydrolysis of high molecular weight organic matter
Dore, J. Annual and short-term variability in the distribution of nitrite at the US-JGOFS time-series station ALOHA
Dore, J. and D. Hebel. Low-level nitrate and nitrite above the nutricline at Station ALOHA
Firing, E. Ocean currents near ALOHA
Hebel, D., R. Letelier and J. Dore. Evaluation of the depth dependence and temporal variability of primary production at Station ALOHA
Hebel, D., R. Letelier and J. Dore. Past and present dissolved oxygen trends, methodology, and quality control during the Hawaii Ocean Time series
Hebel, D. and U. Magaard. Structure and temporal variability in biomass estimates at Station ALOHA
Houlihan, T. and D. Hebel. Organic and inorganic nutrients: Water column structure and usefulness in time-series analysis
Karl, D. Carbon utilization in the mesopelagic zone: AOU-DOC relationships
Karl, D. HOT/JGOFS program objectives: A brief overview
Karl, D. P-control of N_2 fixation: An ecosystem model
Karl, D. Primary production and particle flux
Karl, D. et al. Review and re-assessment of core measurements: Suggestions for refinement and improvement
Karl, D. and G. Tien. Low-level SRP above the nutricline at Station ALOHA
Karl, D., L. Tupas, G. Tien and B. Popp. "High-temperature" DOC: Pools and implications
Karl, D., K. Yanagi and K. Bjorkman. Composition and turnover of oceanic DOP
Letelier, R. Temporal variability of algal accessory pigments at Station ALOHA: What does it tell about the phytoplankton community structure at the DCML?
Letelier, R. and D. Hebel. Evaluation of fluorometric and HPLC chlorophyll *a* measurements at Station ALOHA
Letelier, R. and F. Santiago-Mandujano. Wind, sea surface temperature and significant wave height records from NDBC buoy #51001 compared to ship observations at Station ALOHA
Lukas, R. Water mass variability observed in the Hawaii Ocean Time-series
Sadler, D., C. Winn and C. Carrillo. Time-series measurements of pH: A new approach for HOT

Schudlich, R. Upper ocean gas modelling at Station ALOHA
Winn, C. DIC variability
Winn, C. and C. Carrillo. DIC and alkalinity profiles and elemental ratios

VII.2. Presentations from the "HOT Golden Anniversary Science Symposium," 16 November 1993, East-West Center, Honolulu, HI

Bingham, F. M. The oceanographic context of HOT
Campbell, L., H. Nolla, H. Liu and D. Vaulot. Phytoplankton population dynamics at the Hawaii Ocean Time series Station ALOHA
Campbell, L., H. Nolla and D. Vaulot. The importance of *Prochlorococcus* to community structure in the central North Pacific Ocean
Christian, J. Vertical fluxes of carbon and nitrogen at Station ALOHA
Dore, J. Nitrate diffusive flux cannot support new production during quiescent periods at Station ALOHA
Dore, J. Nitrification in lower euphotic zone at Station ALOHA: Patterns and significance
Firing, E. The north Hawaiian ridge current and other flows near ALOHA
Hebel, D. Temporal distribution, abundance and variability of suspended particualte matter (particulate carbon, nitrogen and phosphorus) at Station ALOHA -- Observations of a seasonal cycle
Karl, D., D. Hebel, L. Tupas, J. Dore and C. Winn. Station ALOHA particle fluxes and estimates of export production
Karl, D. M., R. Letelier, L. Tupas, J. Dore, D. Hebel and C. Winn. N_2 fixation as a contributor to new production at Station ALOHA
Karl, D. M., G. Tien and K. Yanagi. Phosphorus dynamics at Station ALOHA
Kennan, S. C. Possibilities for stirring along the Hawaiian ridge
Krothapalli, S., Y. H. Li and F. T. Mackenzie. What controls the temporal variability of carbon flux at Station ALOHA?
Letelier, R. M. Inorganic carbon assimilation at Station ALOHA: Possible evidence of a change in carbon fluxes
Letelier, R. M. Spatial and temporal distribution of *Trichodesmium* sp. at Station ALOHA: How important are they?
Liu, H. and L. Campbell. Measurement of growth and mortality rates of *Prochlorococcus* and *Synechococcus* at Station ALOHA using a new selective inhibitor technique
Lukas, R. and F. Bingham. Annual and interannual variations of hydrographic properties observed in the Hawaii Ocean Time-series (HOT)
Lukas, R., F. M. Bingham and A. Mantyla An anomalous cold event in the bottom water observed at Station ALOHA
Moyer, C. L., L. Campbell, D. M. Karl and J. Wilcox. Restriction fragment length polymorphism (RFLP) and DNA sequence analysis of PCR-generated clones to assess diversity of picoeukaryotic algae in the subtropical central North Pacific Ocean (Station ALOHA)
Polovina, J. J. and D. R. Kobayashi. HOT and Hawaii's fisheries landings: Complementary or independent time-series?
Sadler, D. Time series measurement of pH at Station ALOHA

Smith, C. R., D. J. DeMaster, R. H. Pope, S. P. Garner, D. J. Hoover and S. E. Doan. Seabed radionuclides, bioturbation and benthic community structure at the Hawaii Ocean Time-series Station ALOHA

Tupas, L. M., B. N. Popp and D. M. Karl. Dissolved organic carbon in oligotrophic waters: Experiments on sample preservation, storage and analysis

Winn, C. D. Air-sea carbon dioxide exchange at Station ALOHA

Yuan, J.and C. I. Measures. Sampling and analysis of dissolved iron

VII.3. Presentations from the "HOT-75 Commemorative Science Symposium," 9 September 1996, East-West Center, Honolulu, HI

Atkinson, M. A Potentiostatic, Solid-state Oxygen Sensor for Oceanic CTDs

Bidigare, R., M. Latasa, R. Andersen and M. Keller. A Comparison of HPLC Pigment Signatures and Electron Microscopic Observations for Oligotrophic Waters of the North Atlantic and North Pacific Oceans

Campbell, L., H. Liu, H. Nolla and D. Vaulot. Annual Variability of Phytoplankton and Bacteria in the Subtropical North Pacific Ocean at Station ALOHA during the 1991-1994 ENSO Event

Christian, J., M. Lewis and D. Karl. Vertical Fluxes of Carbon, Nitrogen and Phosphorus at the US-JGOFS Time-Series Station ALOHA

Dore, J. and D. Karl. Nitrification, New Production and Nitrous Oxide at Station ALOHA

Ducklow, H. Joint Global Ocean Flux Study -- Vision and Progress

Emerson, S., C. Stump and D. Wilber. Inert Gases as Tracers of Diapycnal Mixing in the Upper Ocean

Firing, E. Currents in the Vicinity of Station ALOHA: An Update

Fujieki, L. HOTDOGS: A New Tool for HOT Program Data Base Analysis and Presentation

Hebel, D., L. Tupas and D. Karl. The Importance of Organic Exudates in the Measurement of Oligotrophic Ocean Primary Productivity

Karl, D., D. Hebel and L. Tupas. Regionalization of Station ALOHA

Karl, D., G. Tien, K. Björkman, K. Yanagi, R.Letelier, A. Colman and A. Thomson. The "Forgotten" Open Ocean P-Cycle

Karl, D., L. Tupas, D. Hebel, R. Letelier, J. Christian and J. Dore. Station ALOHA N-Cycle: The Case for N2 Fixation

Landry, M., K. Selph and H. Al-Mutairi. Seasonal and Diurnal Variability of the Mesozooplankton Community at Ocean Station ALOHA

Letelier, R. and M. Abbott. Effects of a Subsurface *Trichodesmium* spp. Bloom on the Optical Reflectance Measured in the Upper 150 m of the Water Column in the North Pacific Subtropical Gyre

Liu, H., L. Campbell and H. Nolla. *Prochlorococcus* Growth Rate and Daily Variability at Station ALOHA

Lopez, M. and M. Huntley. Particle Concentrations at the Hawaii Ocean Time-series Station (Station ALOHA) Measured with an Optical Plankton Counter

Michaels, A. and A. Knap. The Bermuda Atlantic Time-Series Study (BATS): A View from the "Other" Ocean

Nolla, H., J. Kirshtein, M. Landry, D. Karl, L. Campbell and D. Pence. Flow Cytometry Correction Factors for Enumeration of Heterotrophic Bacteria and Phytoplankton

Quay, P. and H. Anderson. A Dissolved Inorganic Carbon Budget at Station ALOHA

Santiago-Mandujano, F. and R. Lukas. Cold Bottom Water Events Observed in the Hawaii Ocean Time-Series: Modelling and Implications for Vertical Mixing

Scharek, R., M. Latasa, D. Karl and R. Bidigare. Vertical Flux of Diatoms at the JGOFS/WOCE Station ALOHA

Smith, C., R. Miller, R. Pope and D. DeMaster. Seafloor Inventories of Pb-210, Th-234 and Benthic Biomass as Proxies for Deep POC Flux: Placing Export Production at the HOT Station in a General Oceanic Context

Tien, G., D. Pence and D. Karl. Hydrogen Peroxide Measurements at Station ALOHA

Tupas, L., G. Tien, D. Hebel and D. Karl. Dissolved Organic Carbon Dynamics in the Upper Water Column at Station ALOHA

Vink, S., K. Falkner, V. Tersol, J. Yuan and C. Measures. Variations in Iron, Aluminum, Beryllium and Barium Concentrations in Surface Waters at Station ALOHA

Winn, C. Secular Changes in Inorganic Carbon Parameters at HOT and BATS

8. DATA AVAILABILITY AND DISTRIBUTION

Data collected by HOT program scientists are made available to the oceanographic community as soon after processing as possible. In order to provide easy access to our data, we have provided summaries of our CTD and water column chemistry data on the enclosed IBM PC 3.5" high-density floppy diskette. CTD data at NODC standard pressures for temperature, potential temperature, salinity, oxygen and potential density are provided in ASCII files; water column chemistry data are provided in Lotus 1-2-3™ files. The pressure and temperature reported for each water column sample are derived from CTD temperature and pressure readings at the time of bottle trip. Densities are calculated from calibrated CTD temperature, pressure and salinity values. These densities are used, where appropriate, to express chemical concentrations on a per kilogram basis. With the exception of the results of replicate analysis, all water column chemical data collected during 1995 are given in these data sets.

The data included in the Lotus 1-2-3™ files have been quality controlled and the flags associated with each value indicate our estimate of the quality of each value. The text file readme.txt gives a description of data formats and quality flags.

A more complete data set, containing data collected since year 1 of the HOT program (1988), as well as 2 dbar averaged CTD data, are available from two sources. The first is through NODC in the normal manner. The second source is via self-service computer access. The measurements reside in a data base on a workstation at the University of Hawaii, and may be accessed using anonymous ftp on Internet or the World Wide Web (www). The www address is ***http://hahana.soest.hawaii.edu***. Access via ftp is described in more detail below. An overview of the HOT-WOCE program including selected results and the current status of the HOT database is available at http://www.soest.hawaii.edu/HOT_WOCE in the www.

In order to maximize ease of access, the data are in ASCII files. File names are chosen so that they may be copied to DOS machines without ambiguity. (DOS users should be aware that Unix is case-sensitive, and Unix extensions may be longer than 3 characters.)

The data are in a subdirectory called ***/pub/hot***. More information about the data base is given in several files called ***Readme.**** at this level. The file ***Readme.first*** gives general information on the data base; we encourage users to read it first.

The following is an example of how to use ftp to obtain HOT data. The user's command are denoted by bold italicized text. The workstation's Internet address is ***mana.soest.hawaii.edu***, or ***128.171.154.9*** (either address should work). All information except optical data reside on this address. Optical data are stored at ***hahana.soest.hawaii.edu***, or ***128. 171. 154. 13***.

1. At the Prompt >, type ***ftp 128.171.154.9*** or ***ftp mana.soest.hawaii.edu.***

2. When asked for your login name, type ***anonymous***.

3. When asked for a password, type ***your email address***.

4. To change to the HOT database, type ***cd /pub/hot***. To view files type ls. A directory of files and subdirectories will appear.

4a. To obtain a list of publications, type ***cd publication-list*** then ***get hotpub.lis***.

4b. To obtain the HOT Field and Laboratory Protocols manual, type ***cd protocols*** then ***get 1142.asc***.

4c. To obtain water column data, type ***cd water***, then ***get <filename>*** where the filename is hot#.gof (JGOFS data) or hot#.sea (WOCE data) and # is the HOT cruise of interest.

5. To obtain further information about the database type ***get Readme.first***. This will transfer an ASCII file to your system. Use any text editor to view it.

6. To exit type ***bye***.

7. Data on optical parameters are located on another server. To obtain light data, at the prompt type ***ftp 128.171.154.13*** or ***ftp hahana.soest.hawaii.edu*** then follow steps 2 to 4.